

**ALKANE FLUIDS CONFINED AND COMPRESSED BY
TWO SMOOTH CRYSTALLINE GOLD SURFACES:
PURE LIQUIDS AND MIXTURES**

A Thesis
Presented to
The Academic Faculty

by

Lina P. Merchan Alvarez

In Partial Fulfillment
of the Requirements for the Degree
Doctor of Philosophy in the
School of Physics

Georgia Institute of Technology
May 2012

**ALKANE FLUIDS CONFINED AND COMPRESSED BY
TWO SMOOTH CRYSTALLINE GOLD SURFACES:
PURE LIQUIDS AND MIXTURES**

Approved by:

Professor Uzi Landman,
Committee Chair
School of Physics
Georgia Institute of Technology

Professor Uzi Landman, Advisor
School of Physics
Georgia Institute of Technology

Doctor Jianping Gao
School of Physics
Georgia Institute of Technology

Professor Michael Schatz
School of Physics
Georgia Institute of Technology

Professor Mostafa A. El-Sayed
School of Chemistry
Georgia Institute of Technology

Professor Brian Kennedy
School of Physics
Georgia Institute of Technology

Professor Elisa Riedo
School of Physics
Georgia Institute of Technology

Date Approved: 12 January 2012

To the Holy Spirit.

ACKNOWLEDGEMENTS

I want to thank God for giving me the strength to persevere until today in pursue of this degree. Thank you for allowing me to live my life to the fullest while pursuing this PhD.

I want to thank Prof. Uzi Landman for his support from the very beginning of my work with him. Thank you for guiding me and, at the same time, giving me independence to work on my own. I have learned immensely from you about starting from basic physical principles when exploring an idea or verifying results. I also learned how to present my work such that people would enjoy and remember my contribution. Thank you for being the type of scientist, I hope to emulate one day.

I want to thank Dr. Jianping Gao for his constant help. Thank you for always answering my questions with so much kindness and patience. Thank you for teaching me so much and for sometimes doubting my ideas because you made look for stronger arguments.

I want to thank my beloved husband, Jorge, who has walked with me this journey, and from now on I want to be encourage you in your own path. I believe in your great potential.

I wish to thank my little ones for their laughter and the joy they have brought to my life. Now that I'm done with my book, we will have more time for your books.

Thank you to my parents because my dad was a model to follow academically and my mom a model to follow in my personal life.

Thank you to all the friends I've made in this long journey, including my sister, because your encouragement and friendship have meant a lot to me.

Thank you.

TABLE OF CONTENTS

DEDICATION	iii
ACKNOWLEDGEMENTS	iv
LIST OF FIGURES	viii
SUMMARY	xiii
I INTRODUCTION	1
II HISTORICAL BACKGROUND	4
III MOLECULAR DYNAMICS	12
3.1 Alkanes	13
3.2 Hexane	15
3.3 Hexadecane	16
3.4 Phytane	16
3.5 Interaction Force	17
3.6 Method	19
IV STRUCTURE OF PURE SYSTEMS	29
4.1 Density Profile	32
4.1.1 Molecular Density	36
4.1.2 Segmental Density	38
4.1.3 Densities during transition from 4 to 3 layers, and from 3 to 2 layers	46
4.1.4 Phytane's Branched Density	54
4.2 End-to-end distance	59
4.3 Molecule Orientation	64
4.4 Configuration plots during compression	69
4.5 Number of confined molecules during compression	74
4.5.1 Hexane	74
4.5.2 Hexadecane	75

4.5.3	Phytane	76
4.6	Distribution of surface molecules during compression	80
4.6.1	Hexane	80
4.6.2	Hexadecane	80
4.6.3	Phytane	86
4.7	In-layer alignment during compression	88
4.8	Solvation Force during compression	93
4.9	Diffusion during compression	99
4.9.1	Hexane	102
4.9.2	Hexadecane	103
4.9.3	Phytane	105
4.10	Comparison on the three pure systems	107
V	STRUCTURE OF MIXED SYSTEMS	111
5.1	Density Profile	114
5.1.1	Molecular density	115
5.1.2	Segmental density	119
5.1.3	Molar fraction	122
5.1.4	Densities during transition from 4 to 3 layers, and from 3 to 2 layers	125
5.1.5	Phytane's Branched Density in the C20&C16 mixture	131
5.2	End-to-end distance	135
5.3	Molecular Orientation	140
5.4	Configuration plots during compression	147
5.5	Number of confined molecules during compression	150
5.6	Molar fraction during compression	154
5.7	Distribution of surface molecules during compression	158
5.7.1	Hexane-Hexadecane	158
5.7.2	Phytane-Hexadecane	166
5.8	In-layer alignment during compression	169

5.9	Solvation force during compression	174
5.10	Diffusion during compression	180
5.11	Comparison on the two mixed systems	184
VI	CONCLUSIONS	187
	REFERENCES	188

LIST OF FIGURES

1	Computational cell dimensions	12
2	Side view of staggered and eclipsed conformation of a C-C bond. . . .	14
3	Dihedral angle corresponding to staggered and eclipsed conformations.	15
4	Periodic Boundaries	19
5	Computational cell dimensions	27
6	C6: Side view of gap size 14.7Å, and its segmental density profile. . .	35
7	C16: Side view of gap size 26Å, and its segmental density profile. . .	35
8	C20: Side view of gap size 14.2Å, and its segmental density profile. .	35
9	Hexane molecular density inside well formed gaps	39
10	Hexadecane molecular density inside well formed gaps	40
11	Phytane molecular density inside well formed gaps	41
12	Hexane segmental density inside well formed gaps	43
13	Hexadecane segmental density inside well formed gaps	44
14	Phytane segmental density inside well formed gaps	45
15	C6 segmental density during transition between well-formed gaps . .	48
16	C6 molecular density during transition between well-formed gaps . . .	49
17	C16 segmental density during transition between well-formed gaps . .	50
18	C16 molecular density during transition between well-formed gaps . .	51
19	C20 segmental density during transition between well-formed gaps . .	52
20	C20 molecular density during transition between well-formed gaps . .	53
21	C20 Segmental and branched densities inside well formed gaps	56
22	C20 Segmental and branched densities during transition	57
23	Distribution of phytane branches during the transition	58
24	Diagram showing the dimensions of an alkane backbone	59
25	C6 Length and segmental density inside well-formed gaps	61
26	C16 Length and segmental density inside well-formed gaps	62
27	C20 Length and segmental density inside well-formed gaps	63

28	Intralayer ordering measured with angle θ	64
29	C6 intralayer-orientation and segmental density inside well-formed gaps	66
30	C16 Length and intralayer-orientation inside well-formed gaps	67
31	C20 Length and intralayer-orientation inside well-formed gaps	68
32	C6: Side view of the confinement for various well formed gaps	71
33	C6: Side view of the confinement for various well formed gaps	72
34	C20: Side view of the confinement for various well formed gaps	73
35	Number of confined hexane molecules versus gap size	77
36	Number of confined hexadecane molecules versus gap size	78
37	Number of confined phytane molecules versus gap size	79
38	Alignment of Hexane molecules on surface layer	81
39	Top view of the bottom C6 surface layer for well formed gaps	82
40	Top view of the bottom C16 surface layer for well formed gaps	84
41	Intralayer ordering in between hexadecane layers	85
42	Distribution of phytane molecules on surface layer	86
43	Top view of the bottom C20 surface layer for well formed gaps	87
44	ϕ is the angle that measures inlayer alignment.	88
45	$\cos^2(\phi)$ for perfectly aligned molecules or in random order.	88
46	Inlayer orientation in pure hexane: $\cos^2(\phi)$ versus gap size.	90
47	Inlayer orientation in pure hexadecane: $\cos^2(\phi)$ versus gap size.	91
48	Inlayer orientation in pure hexane: $\cos^2(\phi)$ versus gap size.	92
49	Solvation force for pure hexane. Top inset: Vertical zoom after 18Å.	93
50	Solvation force for hexadecane. Top inset: Vertical zoom after 20Å.	94
51	Solvation force for phytane. Top inset: Vertical zoom after 15Å.	95
52	Side view of the reservoir region in between two consecutive confinements.	100
53	Hexane coefficient of Diffusion versus gap size	102
54	Hexane coefficient of Diffusion versus gap size in logarithmic scale	102
55	Hexadecane coefficient of diffusion versus gap size	103
56	Hexadecane coefficient of diffusion versus gap size, in logarithmic scale.	104

57	Phytane coefficient of diffusion versus gap size.	105
58	Phytane coefficient of diffusion versus gap size, in logarithmic scale. .	106
59	Comparison of solvation force, number of confined molecules and diffusion for C6, C16 and C20.	109
60	Molecular density inside well-formed gaps for C6&C16 mixture. . . .	117
61	Molecular density inside well-formed gaps for C20&C16 mixture. . . .	118
62	Segmental density inside well-formed gaps C20&C16	120
63	Segmental density inside well-formed gaps for C20&C16 mixture. . .	121
64	Molar fraction inside well-formed gaps for C6&C16 mixture.	123
65	Molar fraction inside well-formed gaps for C20&C16 mixture.	124
66	Segmental density inside well-formed gaps during transition from 4 to 2 layers for mixture C6&C16	126
67	Molecular density inside well-formed gaps during transition from 4 to 2 layers for mixture C6&C16	127
68	Segmental density inside well-formed gaps during transition from 4 to 2 layers for mixture C20&C16	128
69	Molecular density inside well-formed gaps during transition from 4 to 2 layers for mixture C20&C16	129
70	Phytane's Branched density inside well formed gaps when part of the C20&C16 mixture.	132
71	Phytane's Branched density inside well formed gaps when part of the C20&C16 mixture during transition from 4 to 2 layers.	133
72	C6 Relative end-to-end distance and density inside well ordered gaps in the mixture C6&C16.	136
73	C16 Relative end-to-end distance and density inside well ordered gaps in the mixture C6&C16.	137
74	C20 Relative end-to-end distance and density inside well ordered gaps in the mixture C20&C16.	138
75	C20 Relative end-to-end distance and density inside well ordered gaps in the mixture C20&C16.	139
76	Intralayer ordering measured with angle θ	140
77	C6&C16: Density and intralayer-orientation of C6 inside well-formed gaps	143

78	C6&C16: Density and intralayer-orientation of C16 inside well-formed gaps	144
79	C20&C16: Density and intralayer-orientation of C20 inside well-formed gaps	145
80	C20&C16: Density and intralayer-orientation of C16 inside well-formed gaps	146
81	Side view of the confinement for various well formed gaps of C20&C16	148
82	Side view of the confinement for various well formed gaps of C20&C16	149
83	Number of confined hexane and hexadecane molecules versus gap size	152
84	Number of confined phytane and hexadecane molecules versus gap size	153
85	C6&C16: Molar fraction versus gap size	156
86	C20&C16: Molar fraction versus gap size	157
87	Initial surface layer for pure hexadecane (left) and when mixed with hexane(right)	158
88	Speed gradient diagram	160
89	Surface layer when there are 3 layers in the confinement, for pure hexadecane (left) and when hexadecane is mixed with hexane(right) . . .	161
90	Top and bottom layer when there are only 2 layers inside de confinement	162
91	Top and middle layer when there are 3 layers inside de confinement .	162
92	C6&C16: Top view of the surface layer for well formed gaps	164
93	C6&C16: Top view of the second surface layer for well formed gaps .	165
94	Top and middle layers, when there are 3 layers inside the confinement, D=14Å.	166
95	C20&C16: Top view of the surface layer for well formed gaps	167
96	C20&C16: Top view of the second surface layer for well formed gaps .	168
97	Average value of $\cos^2(\phi)$ versus gap size in the C6&C16 mixture . . .	172
98	Average value of $\cos^2(\phi)$ versus gap size in the C6&C16 mixture . . .	173
99	Solvation force versus gap size for mixtures C6&16 and C20C16 . . .	175
100	Comparison of solvation forces for C16, C6&16 and C6	177
101	Comparison of solvation forces for C16, C20&C16 and C20	178
102	Diffusion coefficient for the mixture of C6&C16 versus gap size. . . .	181

103	Diffusion coefficient for the mixture of C6&C16 versus gap size, in logarithmic scale.	181
104	Diffusion coefficient for the mixture of C20&C16 versus gap size. . . .	182
105	Diffusion coefficient for the mixture of C20&C16 versus gap size, in logarithmic scale.	183
106	Comparison of force, confined molecules and density for C16, C6&C16 and C6	185
107	Comparison of force, confined molecules and density for C16, C20&C16 and C6	186

SUMMARY

With the use of grand canonical molecular dynamics, we studied the slow compression (0.01 m/s) of very thin liquid films made of equimolar mixtures of short and long alkane chains (hexane and hexadecane), and branched and unbranched alkanes (phytane and hexadecane). Besides comparing how these mixtures behave under constant speed compression, we will compare their properties with the behavior and structure of the pure systems undergoing the same type of slow compression. To understand the arrangement of the molecules inside the confinement, we present segmental and molecular density profiles, average length and orientation of the molecules inside well formed gaps. To observe the effects of the compression on the fluids, we present the number of confined molecules, the inlayer orientation, the solvation force and the inlayer diffusion coefficient, versus the thickness of the gap. We observe that pure hexadecane, although liquid at this temperature, starts presenting strong solid-like behavior when it is compressed to thicknesses under 30 Å, while pure hexane and pure phytane continue to behave liquid-like except at 13 Å when they show some weak solid-like features. When hexadecane is mixed with the short straight hexane, it remains liquid down to 28 Å at which point this mixture behaves solid-like with an enhanced alignment of the long molecules not seen in its pure form; but when hexadecane is mixed with the branched phytane the system does not present the solid-like features seen when hexadecane is compressed pure.

CHAPTER I

INTRODUCTION

It has been observed experimentally, and through computer simulations that some substances, such as water and, in the present case, oil, can have a different structure and behavior when they are confined to nanometer gaps. This means that either the structure of the molecules and how they interact between them, can be considerably differently than what is normally observed in the bulk. AFM experiments done in E.Riedo's lab showed that a molecularly thin film of water can be as viscous as honey, even at room temperature, and able to withstand pressure, which is not the case in bulk water[16]. We have now observed that an oily substance can experience a similar change as its confinement is reduced down to nanometer scale.

With the present advances in engineering, the spacing in between machinery parts has decreased considerably and hence it is possible for lubricants or oils to be confined down to thicknesses of the order or several molecular layers. Some of short and medium length alkanes are used as additives to motor oil and as lubricants components, so it is necessary to know if molecules that aid in the viscosity of a lubricant in the bulk are fulfilling their intended purpose when they are compressed to nanometer gaps. An alkane liquid that is very fluid in the bulk, might not behave the same way if it is compressed in a particular way, possibly even solidifying, preventing it from fulfilling its intended lubricity. It is for this reason that we find it important to study the behaviour of alkane systems under confinement. We have found that some alkanes tend to crystallize under certain conditions, but that the addition of particular alkanes can hinder or enhance this from happening.

We model an oily substance as a fluid made of one-component or two-components

of alkanes. We study three alkanes: hexane, unbranched linear alkane with 6 carbons in the backbone; hexadecane, unbranched linear alkane with 16 carbons in its backbone; and phytane, a branched alkane with 4 branches on one side of the backbone, composed of 16 carbons. In chapter 4, we present the behaviour of each of the three systems, as a pure fluid, and how their behaviour changes as they are compressed by 2 smooth parallel gold surfaces. Then in the following chapter, we present our findings when we studied the compression of two mixed systems: an equimolar mixture of hexane and hexadecane, and an equimolar mixture of hexadecane and phytane. We wanted to compare the behavior of each pure system with their behaviour when mixed, in the first mixture we compared small or short hexane with long or big hexadecane; in the second mixture, we wanted to compare same backbone length of branched phytane, and unbranched hexadecane.

We chose a temperature at which the 3 pure systems would be in liquid form in the bulk, 315K. The initial separation of the confining surfaces was chosen such that the fluid inside the confining gap would behave almost as in the bulk with no apparent structure, and that a computer simulation at that size would take a reasonable time. The gap size was 36.67\AA , and from the density profiles it can be seen that very little ordering is found at this separation for all systems, whether pure or mixed. The confinement region is connected to a reservoir kept at constant pressure, constant temperature, and equal molarity, in the case of the mixed system. From the initial separation, each system is compressed at a constant speed down to 6.7\AA , where only one layer of molecules can be accommodated.

We observe that depending on the length of the carbon chains and whether they are linear or branched, the fluid can arrange itself in layers, and in some cases, even present in-layer ordering. When we study the two component systems, we observe segregation and separation of the components, and in some circumstances the system appears to crystallize. This is very interesting because we are looking at substances

that at room temperature in the bulk are liquids, but when confined to small gaps might have a crystalline structure and a mobility that is significantly less.

We also observe that the level of crystallization of these fluids depended on the type of molecules that were combined. We observe that when mixing linear chains, the short molecules behaved as a solvent that allowed the longer molecules to attain high order; but when mixing linear and branched molecules of similar weight, neither type of molecule was able to crystallize. This information could give the oil industry some insight on which types of alkane mixtures to use to ensure a fluid is lubricant at nanometer scale.

CHAPTER II

HISTORICAL BACKGROUND

The structure of alkane fluids has been studied theoretically [24, 15, 30, 13], experimentally [31, 11, 29, 17, 28, 23] and computationally [20, 27, 26, 25, 18, 9, 10]. One phenomenon that is very interesting is the ability of thinly compressed liquids to withhold weight or sustain pressure. This can be seen by measuring the force exerted by the fluid on the confining surfaces while the system is being compressed. For large confinements, the force is merely the pressure in the bulk liquid times the surface. But as the distance between the confining surfaces decreases to less than 7 segmental diameters of the liquid molecules, oscillations in the force can be observed in some liquids[9, 32, 16]. As the fluid is compressed, the force increases until the liquid yields and some molecules leave the confinement, and then the force drops until the liquid compacts into well ordered layers again.

For the past 30 years, the force measurements of a variety of liquids in between smooth surfaces have been obtained through experiments and computer simulations. The solvation force between neutral confining surfaces, separated more than 10 segmental diameters, tends to be equal to the pressure times surface area. At smaller separations, oscillations tend to be present, with the spacing in between the peaks giving information on the structure of the compressed fluid. For simple molecules, it was observed in 1982 by Christenson, et al. that the molecules tend to organize in layers close to the surface and that this ordering continues as the surfaces are brought together[3].

A few years later in 1987, Israelachvili, et al.[2], addressed the question of how short alkane chains would behave under compression with the use of a surface force

apparatus. They studied hexane, octane, decane, dodecane, tetradecane and hexadecane. For hexane, they observed 4 minima, with a spacing of 0.5nm between them, while for hexadecane they observed 5 minima, with a 0.4 to 0.5 spacing. For all the alkanes, they were able to measure the minima, but had great difficulty with the maxima. From our molecular dynamics simulation we will see that the peaks of the force are approximately 1\AA wide, while the minima are about 3\AA wide. In their experiments, their precision was in the order of angstroms, which meant that they might not have been able to detect the maxima. From their measurements, they observe that the periodicity of the force for the different alkanes is the same. This is due to the fact that they couldn't differentiate between a periodicity of 4.5 or 5 due to their accuracy. In our simulations, our accuracy is in the order of 0.05 angstroms, so we can differentiate the periodicity of the different alkanes. From the average spacing, they concluded that the periodicity is related to the thickness of the layers inside the confinement. We also observe the same, but our precision allows us to say which liquids produce well defined layers and which don't.

One interesting idea they tried to address with the information they had at hand was the inlayer and intralayer ordering. They observe that alkanes are flexible and randomly oriented in the bulk, and it seems hard to believe that the chain molecules would all lay down as pencils. They do concede that the surface does orient the molecules to some extent. They estimate that there could be 3 layers parallel to the surface. They predict a series of 6 alternating maxima and minima, whose magnitude decreases as the film thickness increases, and spaced by the width of a linear hydrocarbon chain. We observe this phenomena in all the systems we study, although in some cases we are able to measure a seventh peak.

They discuss the possibility that short range order in the bulk could be enhanced by presence of the confining surfaces, resulting in a long range two-dimensional ordering parallel to the surface and short range ordering perpendicular to the surface. In

our study, we observed that the different systems do arrange in layers, and intra-layer ordering is possible in some cases.

They also briefly discuss an issue that we encountered, the speed at which the confining surfaces approach each other. They mention that, specifically with hexadecane, there seems to be a difference with the number of maxima that can be detected if the speed of approach changes. They infer that if the speed of approach is too high, the long chain molecules would find it hard to leave the confinement. We found that when the compression speed was high, the system seemed to be in a glassy state, and the strength of the seventh peak in the solvation force curve was smaller.

They compare their results with Flory’s rotational state (RIS) model[8], but their experimental results don’t agree with this model. They explain that the model has several short comings which might explain the discrepancy. The model assumes a uniform density inside the gap, and ignores the interaction of the alkane chains with the surface and among themselves, elements that in our study we will see that are very influential to the inner structure of the fluid in the confinement.

Since the experimental observations hinted at the alkane chains laying parallel to the surfaces, the behavior of hexadecane near a single smooth surface was later studied through molecular dynamics simulations by Uzi Landman, et al[27]. They observed an oscillatory segmental density with its amplitude decreasing as the distance to the surface increased. The range of the oscillations extended up to almost 20Å, which was the range at which the experimental oscillations in the force were observed.

In their simulation of hexadecane in the presence of a single gold surface, the C_{16} molecules can be seen to be forming domains of intermolecular orientational order. In our study of pure hexadecane compressed by 2 gold surfaces, we also observe this ordering inside the layers, but our domains are larger. Our intra-layer ordering is enhanced by the presence of a flow of molecules leaving the confinement while the system is slowly being compressed and the existence of a preferred direction, which

was not the case for a single surface where the system is isotropic above the surface.

Following their study, came the desire to know if this surface ordering by domains would also be present if the hexadecane molecules were mixed with short hexane molecules in the presence of a smooth surface[25]. When the long and short chains were mixed by equal weight, the hexadecane chains showed preferential adsorption by means of reptation-like penetration into the mixed surface. It should be mentioned that the strength of the interaction of an alkane segment with gold was 3 times larger than the interaction between segments of the same molecule or of a different molecule. They also observed that the first and second layer from the surface started disordered but, after running 8ns, attained a high degree of intermolecular order in domains. They conclude that the preferential parallel alignment of the molecules in the surface layer results in a stronger interaction with the surface and compensates for the loss in configurational entropy. In our studies of equimolar hexane-hexadecane, we have also observed that the presence of the small molecules enhances the intra-layer ordering during compression and after further equilibration. In their simulations, the diffusion of the hexadecane molecules on the surface is almost none existent but increases as the distance to the surface increases.

In the case of an alkane fluid in the presence of a single solid surface, there is the solid-liquid interface as well as the liquid-vapor interface. It is interesting to see how the alkane chains organize themselves in the various regions [26]. The arrangement of the molecules in parallel layers close to the surface had been observed through scanning tunneling microscopy (STM), atomic force microscopy (AFM), surface force apparatus (SFA), surface tension measurements, x-ray reflectivity (XR), and grazing-incidence diffraction (GID). The structure of the alkane fluid in the presence of only one surface had been observed through XR, GID and surface tension measurements. In this study of pure hexadecane and pure n-heptadecane, with twice as many hexadecane molecules as in Ref.[25] it was observed that on top of the 4 layers parallel to

the surface, a different ordering takes place with a large domain of molecules ordering almost normal to the surface at the interface liquid-vapor. From order parameter and pair-distribution studies, they observe hexagonal ordering in the top layer. This crystallization takes place at 288K, below the melting temperature of 291.32 K for hexadecane. From other simulations, they infer the melting point seems to be around 295K. Our simulations take place at 315K, and we observe crystalline ordering in some of our confined fluids. In our simulations of compressed pure hexadecane, we also observe hexagonal ordering of the molecules parallel to the gold surfaces.

Up to this point, alkane chains were known, either through experiments or simulations, to be layered parallel to the surface, and to attain ordering normal to the surface in the liquid-vapor interface. The next step was to understand the structure and dynamics of these molecules in the presence of 2 surfaces. Molecular dynamics and Monte Carlo simulations were done by several groups to study these properties as well as the solvation force between the surfaces. Mondello and Grest in 1995, introduced the united atom of n-alkanes to investigate the liquid state of branched alkanes, in particular squalane. They compare their results with simulations for n-decane and n-tetracosane.

In 1997, Landman, Gao and Luedtke did a review of this field of research and one of the things they observed was that the layering of the molecules and the oscillation in solvation forces were related, but even with the presence of layering the strength of the force peaks could be small[10, 9]. This seemed to be due to the type of layers, liquid-like or solid-like. When the layers behaved liquid-like, the fluid drained continuously from the confinement as the system was under compression, while in the case of solid-like layers, whole layers were expelled abruptly when the system was compressed.

The experimental setups used to study the properties of confined liquids, such as AFM, consisted of a liquid adsorbed on a surface and interacting with a nanoscale

tip while in contact with a surrounding bulk fluid. But the computer simulations at the time, they noted, either molecular dynamics or Monte Carlo, simulated an infinite fluid extended over an infinite surface. Landman, Gao and Luedtke devised molecular dynamics simulations in the grand canonical ensemble that modeled a confined fluid in contact with a constant chemical potential μ , constant pressure P , and constant temperature T [9]. This meant that a computational cell would contain a fluid, confined in between 2 atomically structured solid surfaces, in contact with a reservoir of bulk fluid. This allowed a free exchange of molecules between the confinement and the bulk, until an equilibrium was reached.

With this Grand Canonical Molecular Dynamics simulations they studied the relationship between structure inside the confinement and the shape of the solvation force by simulating spherical molecules, short and long linear chains and branched alkane chains, each of them in pure form. In our present case, we study the equimolar mixtures of hexane-hexadecane and phytane-hexadecane, and each of the 3 pure systems for comparison purposes.

When they compared the linear chained hexadecane with the branched squalane, they observed through the density profiles, that the layers of linear chains are better defined than the ones of branched chains, and there were more layers in the same gap thickness. In both cases, they observed that the narrowing of the gap led to molecules leaving the confinement, and rearranging to a smaller number of layers. In the solvation force curves, oscillations were observed in both cases, but the strength of the force peaks and the depth of the valleys were larger in the case of hexadecane. This was understood by inspection of the number of confined molecules versus the distance between the surfaces. This distance is normally known as gap size. For hexadecane molecules, this curve varies in a step-like manner with sharp drops when groups of molecules are expelled, while in the case of squalane the number of confined segments is almost a smooth curve, which means that when the fluid is compressed

the molecules leave the gap continuously. The oscillations in the solvation force for squalane were seen experimentally, among others, by Zhu and Granick when they did Surface Force Apparatus experiments on the compression on squalane[32].

After several studies done on pure alkanes, the attention was turned to mixed systems and their structure and behavior. Kioupis and Maginn did Equilibrium Molecular Dynamics(EMD) and Non-Equilibrium Molecular Dynamics (NEMD) to study the Rheology, dynamics and structure of an unconfined mixture of hexane and hexadecane at different compositions. They said:”It is clear that upon mixing, the rotational dynamics of the long chains speed up, whereas the dynamics of the short chains slow down. The longer chains when dissolved in the matrix of short chains are able to move and rotate easier, resulting in faster relaxation rates. The short chains act as a plasticizer or solvent for the long chains”[14]. We also observed this phenomenon and concluded that the presence of the small chains allows the longer molecules to attain a higher degree of crystallization than when pure.

The effect of branches in the structure of a confined alkane system was studied in 2001 by Cui, Cummings and Cochran[4]. They did molecular dynamics simulations of pure hexadecane and pure 2,6,11,15-tetramethylhexadecane in a confinement where 6 layers were possible. This branched alkane also has 4 methyl groups as phytane, but positioned differently. Their simulations were on a much smaller scale with only 128 molecules and without the presence of a reservoir. As in our case, they observe that hexadecane behaves solid-like and the branched alkane behaves liquid-like. They also see the independent layers of hexadecane parallel to the surface and the non-independent layers of phytane. In their case, the lack of a reservoir region means that the molecules leaving the confinement through one side enter through the opposite of the computational box.

They studied structural properties of the pure systems at one gap size, while in our case, we study the properties for 30 or 40 gap sizes to help us understand the evolution

of the system as it undergoes a slow compression. Besides structural properties, we look into the changes in the number of confined molecules, in the solvation force, and the coefficient of diffusion as the system is compressed by smooth surfaces. The presence of reservoirs on either side of our confinement allows the molecules to leave the gap to allow the system to equilibrate at its desired density and pressure.

Other types of confinements besides, parallel smooth surfaces, have been studied with molecular dynamics are zeolites. The diffusion of linear and branched alkanes is modeled as different types of alkanes diffuse through these pore networks.,[19, 7, 5, 6].

In our case, we study mixed alkane fluids, short with long and linear with brached, and pure alkane fluids, as they are confined between two smooth parallel gold surfaces in the presence of reservoirs on both sides of the confinement. The presence . to gain more information about the relationship between structure and solvation force, to observe if a combination of alkane molecules facilitates the mobility or crystallization of the mixtures under compression. We have observed that mixtures behave very differently from pure systems and in the following chapters I will present our results.

CHAPTER III

MOLECULAR DYNAMICS

In classical mechanics, if we know the interaction potential between 2 point particles and their initial conditions, we are able to predict the future state of our particle of interest, given by position and velocity after a certain time interval. With a known interaction potential, we can obtain the force through $\vec{F} = -dV/dr$, and in turn the acceleration from $\vec{a} = \vec{F}/m$. Once we have the acceleration \vec{a} , initial velocity \vec{v}_o and a desired time interval δt , we can calculate the final velocity \vec{v}_f and in turn the final position \vec{r}_f of our point particle. But if we are dealing with molecules that have shape, such as an elongated branched chain, we have to take into account the interaction of the segments within the molecule, plus the interaction of the segments with foreign bodies to our molecule. We can choose to model all the atoms of a organic molecule, such as all the hydrogen atoms, but in previous research it has already been considered whether this level of complication adds information needed to address the question we are asking about our molecule and

If our molecule of interest is part of a fluid and simultaneously interacts with

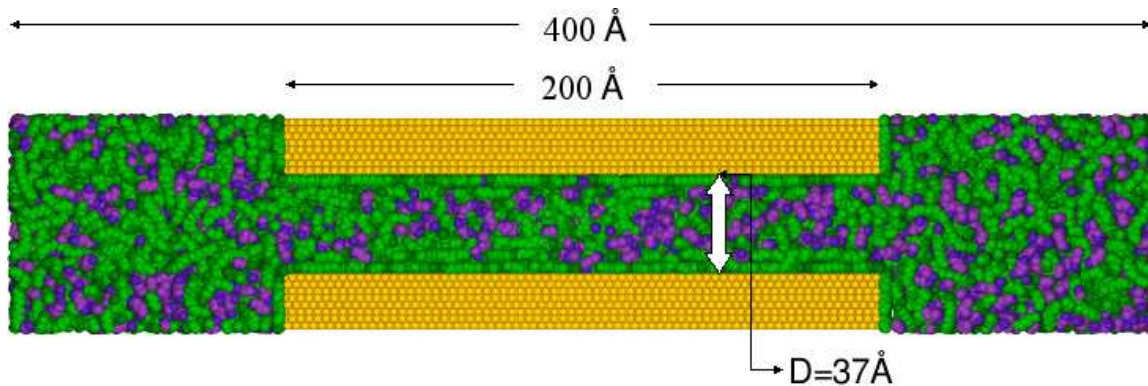


Figure 1: Dimensions of the computatioanl cell

hundreds of thousands of molecules with a similar level of complexity and all of them as mobile as our chosen molecule, then the task of calculating the force field that our molecule, and all the others, are experiencing becomes a daunting task. If on top of calculating the force, we need the accelerations, velocities and final positions of all the molecules of the fluid after just a small time step, usually on the order of 10^{-12} s, then the need to write a very efficient parallel program is necessary.

The level of detail and the interaction potentials used in a simulation uses valuable information learned from people that have worked in this field for decades. Past research has shown what type of detail is necessary to study certain properties, and what type of information can be disregarded in some cases and still be able to gain new insight into a particular phenomenon. In the following sections, I'll mention the model for alkane molecules and the potentials used to model their interactions.

3.1 Alkanes

Alkanes are hydrocarbons containing $C - C$ and $C - H_n$ bonds. They are considered saturated hydrocarbons because each carbon has the maximum number of hydrogens allowed. There are cyclic and acyclic alkanes. In our study, we will only discuss acyclic alkanes which can be described with a molecular formula C_nH_{2n+1} for the case of the unbranched alkanes. The carbon atoms in an alkane are surrounded by 4 groups, making it tetrahedral. The three groups in one plane are at an angle of 109.5° , and the fourth one is out the plane. Which is less than the 120° if the 4 atoms were in the same plane, 3 equidistant on a circle and the fourth one in the center. When referring to hexane or hexadecane, we refer to the straight chain isomers. Even having the molecular formula of an alkane and knowing the atoms are connected in a linear chain, doesn't give us all the information on the conformation of an alkane molecule, because rotations are allowed around $C - C$ bonds. Molecules that can go from one arrangement to another by rotating about a carbon bond are

called conformers. If we look at a 2 carbon molecule, the way the hydrogens in

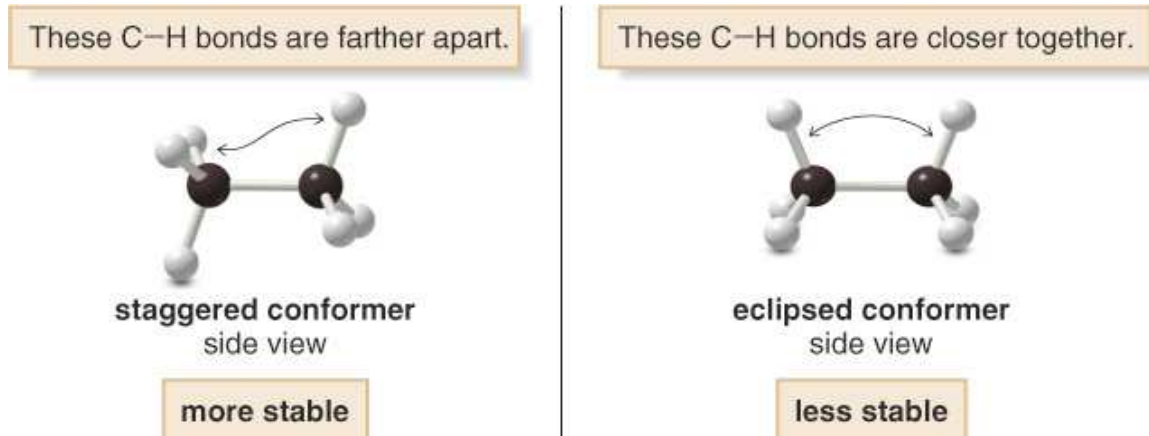


Figure 2: Side view of staggered and eclipsed conformation of a C-C bond.

one carbon are aligned with respect to the hydrogens in the adjacent carbon give rise to different configurations. If these hydrogens are aligned, the conformation is called eclipse, if there is an angle it is called staggered. Among the staggered conformations, an angle of 60° is called gauche, and an angle of 180° is called anti or trans. [[http : //www.uiowa.edu/ c004121/notes/ch043.pdf](http://www.uiowa.edu/~c004121/notes/ch043.pdf)] In the following figure, we can see the ball-and-stick models and the Newman projections for the staggered and eclipsed conformations for ethane. By a 180° rotation around the C-C bond the ethane molecule can go from one conformation to the other. In the model on the left, the staggered conformation resembles a trans because the hydrogens are rotated 180° from the eclipsed version.

In the trans conformation, or also known as antiperiplanar or anti, the hydrogens or methyls are farther apart so the energy is lower than in the eclipsed conformation where the clouds of electrons in the hydrogens repel each other. The lowest energy in a linear-chain alkane is obtained when all the groups are in a staggered conformation, preferably anti, which resembles a zigzag.

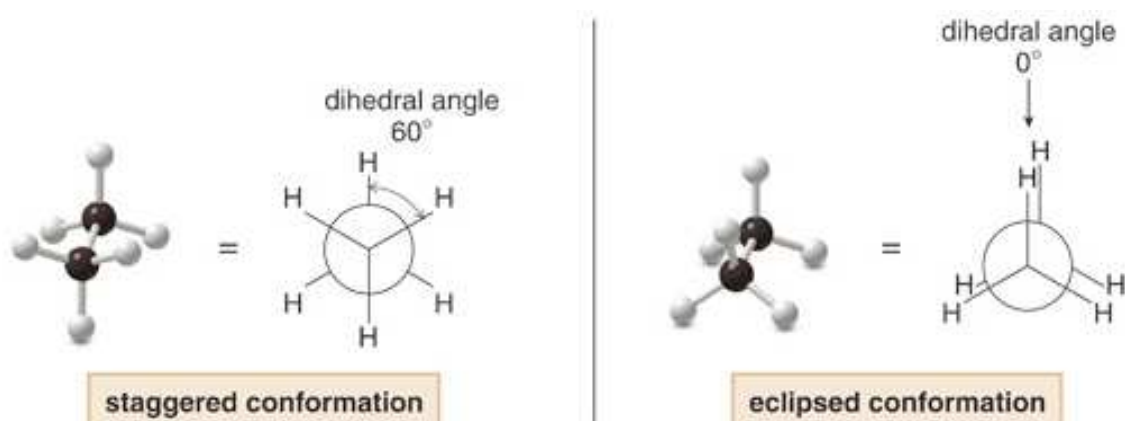


Figure 3: Dihedral angle corresponding to staggered and eclipsed conformations.

3.2 *Hexane*

Hexane is a small alkane. n-Hexane is a chemical made from crude oil. In bulk form, it is a colorless liquid with a slightly unpleasant odor. It evaporates very easily into the air and doesn't dissolve well with water. Hexane is highly flammable, and its vapors can be explosive.

In our study, we want to study the structure of a liquid sample of hexane as it is increasingly confined in between two gold surfaces. Hexane doesn't interact chemically with the gold. Some physical characteristics of hexane are as follows:

Molecular formula	C_6H_{14}
Molar mass	86.18 g mol^{-1}
Density	0.6548 g/mL
Melting point	178 K
Boiling point	342 K

According to the Agency for Toxic Substances and Disease Registry United States Public Health Service which produced a Toxicological Profile for Hexane in 1999: "Pure hexane is used in laboratories. Most of the hexane used in industry is mixed with similar chemicals in products known as solvents. Several hundred million pounds of hexane are produced in the United States each year in the form of these solvents.

The major use for solvents containing hexane is to extract vegetable oils from crops such as soybeans. They are also used as cleaning agents in the printing, textile, furniture and shoemaking industries. Certain kinds of special glues used in the roofing and the shoe and leather industries also contain hexane. Several consumer products contain hexane. For example, gasoline contains about 1 – 3% hexane.”

3.3 *Hexadecane*

”Hexadecane (also called cetane) is an alkane hydrocarbon with the chemical formula $C_{16}H_{34}$. Hexadecane consists of a chain of 16 carbon atoms, with three hydrogen atoms bonded to the two end carbon atoms, and two hydrogens bonded to each of the 14 other carbon atoms. It has 10,359 constitutional isomers.” In our study, we model the linear chain, with no branches.

We modeled 8000 hexadecane molecules in a computational box the same initial size as the one we used for hexane. They also don’t interact chemically with the gold. For consistency, we do the molecular dynamics simulation at the same temperature as in the case of hexane at 315K. At this temperature, it is in the liquid regime, even though it is relatively close to the melting point temperature.

Molecular formula	$C_{16}H_{34}$
Molar mass	$226.44 g mol^{-1}$
Density	g/mL
Melting point	$291K$
Boiling point	$560K$

3.4 *Phytane*

Phytane is a naturally occurring alkane produced by the alga *Spirogyra* and is a constituent of petroleum. The IUPAC name for phytane is 2,6,10,14-tetramethylhexadecane. Phytane is a branched alkane with molecular formula $C_{20}H_{42}$ and 366,319 isomers.

We model the alkane with a backbone of 16 carbons similar to hexadecane and with 4 methyl groups at the 2,6,10,14 carbons along the backbone. It can assume many conformatio and can go from one to another by rotation about different bonds. Some physics properties, obtained from ChemSpider, showing it having a high boiling point due in part to the number of bonds.

Molecular formula	$C_{20}H_{42}$
Molar mass	$282.55g$
Density	$0.791g/mLat20C$
Melting point	$22.17C, 295K$
Boiling point	$301.41C, 574K$

3.5 *Interaction Force*

In our case, the hydrogen atoms are not simulated, but a distinction is done between CH , CH_2 and CH_3 in terms of their mass, radius and the strength of the interactions between them and the gold atoms. They are all called united atoms, and they interact through bounded and nonbonded forces with each other. There are 2 models, model A (UA) and model B (UB). In model A (which is used in our simulations), the interaction site is at the center of mass of the carbon atom, while in model B, the interaction site is slightly shifted to approximate the true center of mass of the segment CH_n . The united atoms are also called pseudoatoms.

For the nonbonded segments, which can be in different molecules or in the same chained molecule but more than 3 segments in distance, the interaction used is Lennard Jones $V_{LJ} = 4\epsilon[(\sigma/r)^{12} - (\sigma/r)^6]$ which has a minimum at $r_0 = 2^{1/6}\sigma$. For the bonded segments that are nearest neighbors in a chain, there are bond forces that keep the intramolecular nearest neighbors at a fixed distance, for segments that are 1 segment from each other there is a bending term $V_b(\theta) = -(k_b/2)(\theta - \theta_b)^2$ where θ_b is the equilibrium angle between successive bonds, and for segments separated by

2 segments there is a torsional term $V_t(\phi) = \sum_i a_i [\cos(\phi)]^i$ characterizing preferred orientations and rotational barriers around all nonterminal (single) bonds. Since the minimum of the potential is $r_m = 2^{1/6}\sigma = 1.12\sigma$, σ gives an indication of size. For distances smaller than σ other molecules feel a repulsive force, but at $r = \sigma$ the force is a minimum.

For our model, the parameters σ and ϵ for n-alkanes were taken from Ref.[21, 22] and the values for CH and torsional potentials were taken from Ref.[12]. The matrix for σ is

$$\sigma = \begin{pmatrix} 2.637000 & 3.283500 & 2.637000 & 3.283500 & 3.223500 \\ 3.283500 & 3.930000 & 3.283500 & 3.930000 & 3.870000 \\ 2.637000 & 3.283500 & 2.637000 & 3.283500 & 3.223500 \\ 3.283500 & 3.930000 & 3.283500 & 3.930000 & 3.870000 \\ 3.223500 & 3.870000 & 3.223500 & 3.870000 & 3.810000 \end{pmatrix} \quad (1)$$

where type 2 is CH_2 , type 1 and type 3 represent Au , type 4 is CH_3 , and type 5 is CH . In the case of the interaction between gold molecules and CH_2 and CH_3 , where $\sigma_{Au-CH_2} = \sigma_{Au-CH_3} = 3.2835$, $r_m = 3.6856$. At this distance, the alkane segments are neither attracted nor repelled by the surface. From our density profile, we see that this is the distance between the center of the gold atoms and the surface layer.

Epsilon ϵ is related to the strength of the interaction, and as in the case of the σ there is a value depending on the interacting segments. The matrix for ϵ is

$$\epsilon = \begin{pmatrix} 0.055810 & 0.015002 & 0.055810 & 0.023439 & 0.013810 \\ 0.015002 & 0.004033 & 0.015002 & 0.006301 & 0.003740 \\ 0.055810 & 0.015002 & 0.055810 & 0.023439 & 0.013913 \\ 0.023439 & 0.006301 & 0.023439 & 0.009844 & 0.005843 \\ 0.013810 & 0.003740 & 0.013913 & 0.005843 & 0.003468 \end{pmatrix} \quad (2)$$

The values for σ and ϵ for individual atoms where obtained from reference , and with

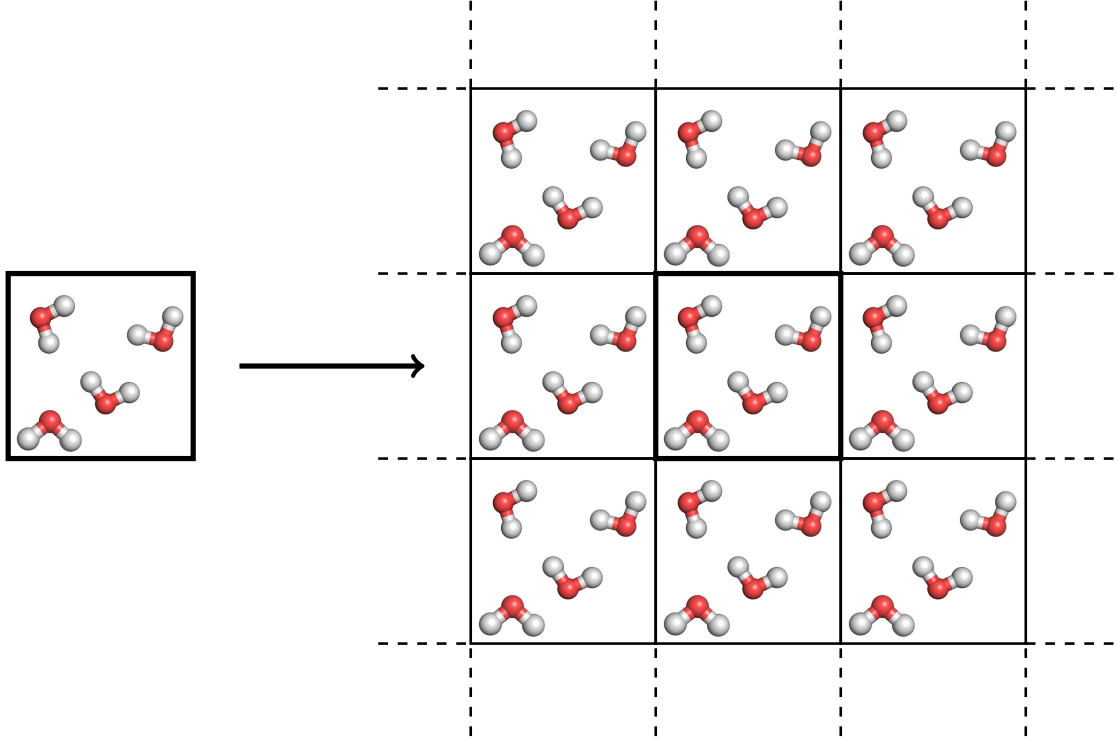


Figure 4: Computational cell with water molecules (on the left) and how periodic boundaries are used to simulate an infinite system (on the right).

rules of addition the parameters for interaction were obtained.

$$\begin{aligned}
 \epsilon_{a,b} &= \sqrt{\epsilon_{a,a} * \epsilon_{b,b}} \\
 \sigma_{a,b} &= \frac{\sigma_{a,a} + \sigma_{b,b}}{2}
 \end{aligned} \tag{3}$$

3.6 Method

We computed macroscopic scale properties such as diffusion, density, solvation force, among others, with a molecular dynamics simulation. With our present resources we can model around 10,000 chained molecules in a computational box, which is far from being macroscopic, so we used periodic boundaries to simulate an infinite system.

Periodic boundaries are used to give the illusion of infinite range along one or more dimensions. A molecule interacts, up to a chosen distance called the cutoff, with all the molecules in the original computational box in addition to the images

of the molecules in the surrounding boxes. In our case, the boxes have the same dimensions as our real computational cell and has 26 contiguous neighboring boxes.

When a molecule leaves the computational cell through one boundary, it enters through the opposite side. This allows for continuity in the movement of the molecules, there is no artificial insertion or deletion of molecules as in Monte Carlo simulations. We were mindful of the periodic boundaries when dealing with chained molecules that were crossing a boundary, both when calculating their center of mass and when calculating their displacement.

The range of the Lennard-Jones potential is infinite, but is usually considered to be short ranged, because the bulk of the interaction is dominated by interaction with molecules that are near. Computationally, it is not feasible to extend all the interaction to infinity, so the potential is usually truncated and shifted beyond a certain cutoff distance r_c . The error in disregarding some interactions, is decreased by choosing an appropriate cutoff distance. In our case, previous studies have concluded that a $r_{cutoff} = 2.5\sigma_{LJ}$ is appropriate for alkane systems. Since σ depends on the type of atoms interacting, the same is true for the cutoff distance, which means that the cutoff varies a few Å depending on whether the interacting pseudoatoms are gold atoms, or any of the other carbon segments.

Using a longer r_c wouldn't improve our statistics considerably, but it would extend the length of our simulations tremendously. One way to correct for this, which is what we do, is to shift the potential energy by a constant value such that the potential is zero at the cutoff. This adds a small discontinuity of the force, but we have confirmed that the system does conserve energy up to a small fraction of a percentage. Whenever we study a new type of molecule, we do trial runs of constant energy, volume and number of molecules and observe the total energy of the system. This assures up that the dynamics of the system are correct.

In single particle Lennard Jones systems, reduced units are commonly used to

simplify the computations, such as scaling the lengths with σ and the energy with ϵ to make them unitless. In our case where we have multiple σ 's and ϵ 's, we use a different approach to scaling of the variables into unitless. We scale the positions with 1\AA and the energy is transformed from international units to eV . Since the energy and length were transformed, then the time and force also have scaling factors that have to be computed from these ones. To calculate the force factor, we write the force in terms of the other variables:

$$\begin{aligned}
[Force] &= \frac{[Energy]}{[Length]} \\
&= \frac{eV}{\text{\AA}} \\
&= \frac{1.60217 * 10^{-19} kgm^2/s^2}{10^{-10}m} \\
&= 1.60217 nN
\end{aligned} \tag{4}$$

and the time factor is given by

$$\begin{aligned}
[Energy] &= \frac{[Mass][Length]^2}{[Time]^2} \\
[Time] &= \sqrt{\frac{[Mass][Length]^2}{[Energy]}} \\
&= \sqrt{\frac{(1.6605 * 10^{-27} kg)(10^{-20} m^2)}{1.60217 * 10^{-19} kgm^2/s^2}} \\
&= 0.01078 ps
\end{aligned} \tag{5}$$

The Lennard Jones potential in our case, with multiple types of atoms, is given by

$$V_{a,b}(r) = 4\epsilon_{a,b} \left[\left(\frac{\sigma_{a,b}}{r} \right)^{12} - \left(\frac{\sigma_{a,b}}{r} \right)^6 \right] \tag{6}$$

where a and b can be any of 4 types of molecules that we model in our system: CH , CH_2 , CH_3 or Au . Our model has a different σ and ϵ for the 2 types of atoms interacting, as we have seen before. With this in mind, the potential energy between any pair of atoms has a different cutoff, and hence the energy value that has to be

substracted is different:

$$E_{a,b} = 4\epsilon_{a,b} \left[\left(\frac{\sigma_{a,b}}{r_c} \right)^{12} - \left(\frac{\sigma_{a,b}}{r_c} \right)^6 \right] \quad (7)$$

By substracting a constant energy value $E_{a,b}$, the potential curve is shifted upward so that the potential is zero at the cutoff radius, and it is set to zero for distances greater than this. Which means that the range of interaction is limited, and each pseudoatom a interacts with all other pseudoatoms b up to a distance, r_c .

This constant value substracted from the potential energy doesn't affect our force calculations, because the force is the gradient of the potential, in particular the x component of the force is given by

$$\begin{aligned} f_x(r) &= -\frac{\delta V(r)}{\delta x} \\ &= -\left(\frac{x}{r}\right) \left(\frac{\delta V(r)}{\delta r}\right) \end{aligned} \quad (8)$$

where $r^2 = x^2 + y^2 + z^2$ and $(\frac{\delta r}{\delta x}) = (\frac{x}{r})$. The Lennard Jones force is

$$f_{a,b}(r) = \frac{48x\epsilon_{a,b}}{r^2} \left[\left(\frac{\sigma_{a,b}}{r} \right)^{12} - 0.5 \left(\frac{\sigma_{a,b}}{r} \right)^6 \right] \quad (9)$$

Once we have the Lennard Jones force, we can integrate the equations of motion to find the dynamics of the molecules. One of the best and most reliable methods used for this is called the Verlet algorithm. To derive the new position, we start with a Taylor expansion of the coordinates around a time t

$$r(t + \Delta t) = r(t) + v(t)\Delta t + \frac{f(t)}{2m}\Delta t^2 + \frac{\Delta t^3}{3!}r''' + O(\Delta^4) \quad (10)$$

where r''' stands for the triple time derivative of the position. in the same way

$$r(t - \Delta t) = r(t) - v(t)\Delta t + \frac{f(t)}{2m}\Delta t^2 - \frac{\Delta t^3}{3!}r''' + O(\Delta^4) \quad (11)$$

Adding both equations, gives

$$r(t + \Delta t) - r(t - \Delta t) = 2r(t) + \frac{f(t)}{2m}\Delta t^2 + O(\Delta^4) \quad (12)$$

or

$$r(t + \Delta t) \simeq 2r(t) + \frac{f(t)}{2m}\Delta t^2 \quad (13)$$

The new position has an error that is of the order of Δt^4 where Δt is the time step in our molecular dynamics simulations. The smaller the time step the smaller the error, but longer the computation time, so it has to be chosen in such a way as to obtain good statistical averages in reasonable computation time. For single atom Lennard Jones simulations, a time step of $10fs$ is common, but in our simulations where we are dealing with complex intramolecular potentials a $\Delta t = 3fs$ was the best given the size and complexity of our system. It should be mentioned that in molecular dynamics simulations, using a smaller time step does not give a more precise trajectory for each molecule, because of the Lyapunov instability two trajectories who start with 2 initial conditions slightly different will give completely different trajectories. Our aim is not to predict the final position of each individual molecule in our fluid, but to obtain statistical averages of the ensemble by taking into account the forces and other external constraints affecting the system.

Note that the calculation of the new position relies in current position and force, and the position at the previous time step. The velocity can be calculated from the new position.

$$v(t) = \frac{r(t + \Delta t) - r(t - \Delta t)}{2\Delta} + O(\Delta t^2) \quad (14)$$

One of the advantages of using the Verlet algorithm is that even though the short term energy conservation is moderate, the long term energy drift is small. Since we are dealing with systems that need long time intervals to equilibrate in the order of tens of nanoseconds this was an important factor. The speed of computation is fast for this algorithm and considering the time it takes to compute all the forces associated with each alkane chain, being able to produce the new positions and velocities fast for all the molecules is optimum. It requires little memory compared to other algorithms that require higher order derivatives to be saved, and when dealing with an order of

100,000 pseudoatoms less memory space needed is very practical. (We model 16000 hexane molecules, each with 6 segments).

With the new positions and velocities, properties of the system can be calculated, such as total energy, total force, and temperature. We study the dynamics of all the molecules inside the computational box in a NPT statistical ensemble. The number of molecules is constant, or almost constant. In the case of the mixed system, we keep the molarity in the bulk region at 50:50, by randomly removing molecules from the reservoir, but this number is so small that the number of molecules can be regarded as constant. Every 900 ps , we would remove approximately 10 to 20 molecules out of the more than 10,000 molecules that we simulate in our mixtures of hexane and hexadecane, for example. The pressure is held at 1 atm , by allowing the size variation of the box along the x -axis through constant pressure molecular dynamics.

The temperature in the reservoir was held constant by a velocity scaling method explained in the Ref. [1], while the molecules in the confinement reached the desired temperature through thermodynamical equilibrium with the reservoir. The approach of the aforementioned method is a weak coupling to an external heat bath at the desired temperature T_0 .

The Langevin equation of motion, including friction and stochastic terms, is given by

$$m_i v'_i = F_i - m_i \gamma_i v_i + R_i(t) \quad (15)$$

where F is the force, γ determines the strength of the coupling, and $R_i(t)$ is a Gaussian stochastic variable with intensity

$$\langle R_i(t) R_j(t + \tau) \rangle = 2 m_i \gamma_i k_B T_o \delta(\tau) \delta_{ij} \quad (16)$$

After the time dependence of the temperature T is obtained from the derivative of the total kinetic energy, they arrive at the modified equation of motion.

$$m_i v'_i = F_i + m_i \gamma \left(\frac{T_o}{T} - 1 \right) v_i \quad (17)$$

Which models a proportional scaling per time step, in which the $v_{N+1} = \lambda v_N$ where λ is

$$\lambda = \sqrt{1 + \frac{\Delta t}{\tau_T} \left(\frac{T_o}{T} - 1 \right)} \quad (18)$$

and $\tau = (2\gamma)^{-1}$.

It should also be mentioned that the code we use, makes use of parallel programming to deal with the numerous computations required to compute the evolution of the system. The program was written in Fortran 90 and uses MPI (Multi-Processor Interface) libraries. There are different ways to distribute the work among the processors, and in our case we use a spatial decomposition. Our computational cell is usually distributed among 16 to 64 processors, depending on the need and availability of resources. Considering that the gold atoms in the confining surfaces are static, the optimum spatial decomposition requires that the spatial dimensions handled by the different processors be somewhat uneven, so that they all have a similar number of dynamic molecules.

At any given time in the simulation, each processor has a list of local molecules for which it has to calculate its new positions and velocities. In order to do this, the processor needs to know with which pseudoatoms its own pseudoatoms interact, whether they are in the same processor or in a neighboring one. If each processor wanted to calculate which pseudoatoms in the neighboring processors are within the cutoff distance of its own particles, then it would need all the positions of all the atoms in those processors. Each processor has 26 neighbors, and transmitting all this information to each of the processors at every time step would not be efficient at all if one is dealing with 100,000 pseudoatoms split into 64 processors.

The way we circumvent this problem, is for each processor to have a list of atoms located within a $r_{boundary}$ of the boundary with the other processors, and only send the positions of these atoms. This list of atoms in neighboring processors can be updated after a certain amount of time steps. One way to do it is to send this information after

a fixed number of steps, for instance after every 8 time steps. It has the disadvantage, that if in that time interval one of the particles moves a large distance it could fall within a r_{cutoff} distance of a particle in another processor. We don't use a fixed time interval, but instead modify this neighbor list whenever it is needed. At each time step, each processor calculates the individual displacement of all its molecules and then their maximum value. Only this value is sent to all processors, from which the maximum displacement of the molecules of the computational cell is obtained. If this value is greater than a chosen value, in our case 1.1Å, then the local neighboring lists are created again. In our equilibrated runs, the remaking of the neighboring lists happens less than 10,000 times in a 200,000 step run, which comes to an average of 1 every 20 steps.

To estimate how much a single segment moves in 20 steps or 60 fs, we can assume brownian motion and estimate that

$$\begin{aligned}
\frac{1}{2}mv^2 &= \frac{1}{2}k_B T \\
v &= \sqrt{\frac{k_B T}{m}} \\
&= \sqrt{\frac{1.380 \times 10^{-23} \text{ J/K} * 315 \text{ K}}{15 * (1.6605 \times 10^{-27})}} \\
&= \sqrt{17.46 * 10^4 \text{ m}^2/\text{s}^2} \\
v &= 417 \text{ m/s}
\end{aligned} \tag{19}$$

With an approximate speed of 400 m/s, the displacement on 60 fs is approximately $\Delta r = (400 \text{ m/s}) * 60 * 10^{-15} = 0.24 \text{ Å}$. The neighboring lists are redone every time one atom has a displacement larger than 1.1Å. This is possible because the velocity distribution is a gaussian, so even though the mean speed is approximately 400 m/s there are atoms with a speed several times larger, as well as atoms with smaller speeds.

To facilitate the studies of the properties of the confined alkane thin films, which

are in equilibrium with a surrounding bulk liquid, the solid blocks are arranged to create two regions of the alkane fluid. Inside the gap, between the two solid surfaces, the alkanes are confined as a thin film with a thickness D ranging between 6\AA and 37\AA . The size of the cell in the x direction is taken to be sufficiently large so that the alkanes in the regions outside the confinement can exhibit bulk liquid behavior. The size of the computational cell in the z direction is varied to give the desired film thickness in the gap. In our simulations the extent of the solid blocks in the x direction is 200.5\AA and the height of each block is $d_z = 17.67\text{\AA}$; the size of the cell in the z direction H_z is thus given by $H_z = 2d_z + D$, and the size of the cell in the y direction is the same as the gold blocks and is kept constant, $H_y = 199.88\text{\AA}$. The size of the cell is allowed to vary dynamically, using constant pressure MD, from approximately 400\AA to 600\AA , depending on the gap width and the system. The hydrostatic pressure, determining the magnitude of H_x , is taken to be one atmosphere; on the scale of all other stresses in the system this represents a vanishingly low pressure.

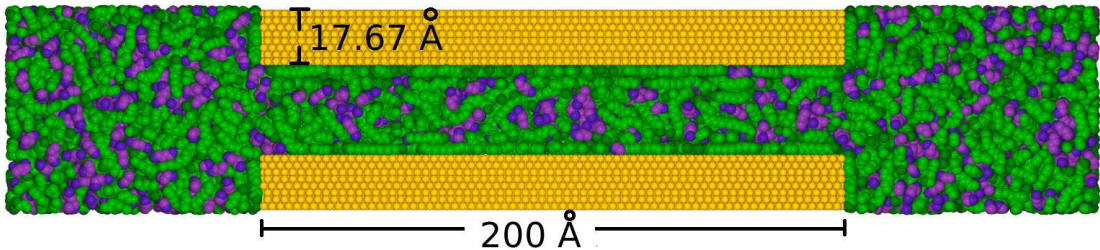


Figure 5: Dimensions of the gold blocks:

The temperature of these simulations is 315K which allows the systems to equilibrate in a reasonable amount of time. At this temperature, the 3 pure systems are in the liquid phase, given that the boiling point of hexane is 343K , 560K for hexadecane and it is unknown for phytane but it should be higher given its complexity.

The initial configuration of the system is set up with a large value of the gap width at 36.7\AA , to allow the chains to move freely. The system was heated up to 450K to promote the mixing in the equimolar case. Once the energy, force and number of

atoms in the confined space reached an equilibrium, the system was cooled down to 315K at a speed of $8.33K/ns$ and left to equilibrate more than $17ns$.

Originally we had compressed at a rate of $0.17m/s$ with a timestep of $3.05fs$ from 36.7\AA down to 6\AA while saving a configuration every 2\AA for the first 20\AA compressed and then every 1\AA . Each configuration was later evolved at a fixed gap size for extended periods of time some even as long as $38ns$, but in general the system didn't seem to reach equilibrium. For the smallest gaps, some hexane molecules seemed to be trapped in the middle of the gap unable to leave the confinement. We hypothesize that perhaps the system had reached a glassy state and even longer evolution times wouldn't reach equilibrium, or perhaps the compression had been done too fast for the molecules to escape the confinement.

It was decided that we would compress the system at a slower speed of $0.01m/s$ and a configuration would be saved every 0.1\AA allowing for a more detailed understanding of the system. This speed of compression means that the compression of 1\AA is done in $9ns$. Some configurations were evolved for extended periods of time ranging from $10ns$ to $26ns$, depending on whether they reached equilibrium or not. Some gap sizes didn't reach a clear equilibrium but after analyzing all the data it was deemed not necessary. This will be further explained in the results section. A similar process was done for all the systems, pure and mixed.

CHAPTER IV

STRUCTURE OF PURE SYSTEMS

Some pure alkanes under compression, such as hexadecane and squalane, have been modeled at a different temperature and rate of compression. Pure hexadecane, $C_{16}H_{34}$, and pure squalane, $C_{30}H_{62}$, had been modeled by Gao et al. with the same Grand Canonical Molecular Dynamics at 350K and a speed of approach of $0.17m/s$. They observed oscillations in the solvation force and layering. We originally wanted to do the compression of a simple model for a lubricant as a equimolar mixture of hexane and hexadecane under the same conditions, but at a temperature of 350K, hexadecane and squalane are liquids, but our small molecule hexane was in gas state at that temperature. So it was decided that for completeness, we would do all the simulations at 315K, at which point all our components would be in fluid form when in the bulk. We wanted to know if their properties persists when compressed until only a handful of molecular layers remain inside the confinement. This meant that we could no longer compare directly our results with J.Gao's because of the difference in temperature. We decided to do similar molecular dynamics simulations of the pure components, hexane and hexadecane, with a computational box of similar dimensions. This is how we came to decide to model 8000 hexadecane molecules, 16000 hexane molecules and an equimolar mixture of 5334 hexane molecules and 5333 hexadecane molecules.

We started by running the computer simulation for the mixture because we wanted to find out if it behaved solid-like or liquid like, at the same speed of $0.17m/s$, and we would later compare these results with the ones for the pure systems. We choose about 20 gap sizes to evolve them longer and let them reach equilibrium, but several

gap sizes wouldn't reach equilibrium after a extended amount of computational time. Some were left to evolve for as much as 50ns. Considering that we were simulating 10,667 molecules, with a combined number of 117,332 segments, a simulation for 50ns is very heavy computationally, and having to do it for 20 configurations is too expensive. We observed that the system had reached a state in which some molecules were stuck in the middle of the confinement but wanted to get out, and were taking a very long time trying to reach the bulk. We decided then to start over at the gap size of 36.7Å and do the compression at a speed 17 times slower, 0.01m/s. This a speed that is very small compared to the speed of compression done in molecular dynamics. Our compression simulations running on 64 processors took between 30 to 45 days, and afterwards we ran between 30 and 40 equilibration runs for each of our systems. The length of the equilibrations varied between 7 to 45 ns, and it depended on whether the system was more fluid or not, or whether it was going through a transition. I will explain this further when I show the results for solvation force and number of confined molecules.

After having a good understanding of how short and long molecules behaved under compression both pure and mixed, we wanted to know how would these results change if we mixed 2 alkanes of the same backbone length, but one with branches and one without, hexadecane and pythane, respectively. For this reason, it was important to simulate three pure systems, hexane, hexadecane and phytane, under exactly the same circumstances.

In summary, we modeled one-component samples of 16000 hexane molecules, 8000 hexadecane molecules and 7400 phytane molecules. In each case, part of the fluid resides in the reservoir region, and the other part confined by the 2 smooth gold surfaces. Our initial configuration started at 315K, but to make sure that the system was mobile, and not stuck in some unfavorable configuration, we heat it up to 450K. This was specially important for the mixed systems. At this elevated temperature,

hexane is in its gas phase. We allowed all the system to reach equilibrium. We checked that the force, energy and number of the confined molecules reached a point where oscillations were small around a constant value. Subsequently, we slowly cooled it down to 315K, and let it equilibrate again.

Once it had reached equilibrium at a gap size of 36.7Å, we proceeded to compress the computational box, decreasing the spacing in between the gold surfaces. At every 0.1Å intervals, the information of the system was saved. This gave us a very detailed view into the compression of an alkane system. As I mentioned before, the experiments done with a Surface Force Aparatus on the compression on pure alkane fluids had a precision of 2Å. We achived an order of magnitude more in precision that allowed us to understand some features in the force curve which would be mentioned later.

We will first take a look at how the molecules present themselves inside the confinement. We will look at several profile plots: segmental and molecular density, average length, and intralayer and inlayer orientation. Then we will see how some properties change as the system is compressed, in particular the number of molecules inside the confinement, their inlayer orientation, the solvation force and the coefficient of diffusion.

4.1 *Density Profile*

To produce these molecular density plots, we split the thickness of the gap into bins, of width 0.2\AA , and then we count the number of molecules whose center of mass falls into these bins and divide by the bin volume, $(H_y * H_x * \text{Bin}_{thickness} = (199.88\text{\AA}) * (200.5\text{\AA}) * (0.2\text{\AA}) = 8150\text{\AA}^3)$.

In Figures 6, 7 and 8, we can see side by side configuration plots for hexane, hexadecane and phytane next to the corresponding molecular densities. For each of the three fluids, I present a different gap thickness because I want to show a brief overview of how the 3 fluids behave. For hexane and phytane, I show a gap thickness where there are 3 layers. The hexane layers can be seen somewhat separated, but in the case of the phytane molecules, I had to decrease the radius of the balls that represent each segment and show a smaller region to make it clearer that there were 3 layers. While in the case of hexadecane the layers are evident, even when there are several more layers than in the other fluids. Hexane and phytane don't show the level of layering at such a large gap of 26\AA that hexadecane does. Hexane is a very small molecule with an average length of 6\AA , phytane is approximately 20\AA long with 4 branches on one side, while hexadecane is also 20\AA but without any branches. This allows the long and linear molecules to pack nicely.

On the left, we can see the film of alkane fluids compressed by the gold surfaces, and in contact with the reservoirs, on top and bottom in these pictures. With the periodic boundaries, the system extends infinitely into and out of the page. In the molecular density plots on the right, the center of mass of the gold atoms are located at the start of the yellow regions. The horizontal axis is the distance from one of the surfaces. As we can see, each peak corresponds to a layer of an alkane molecules lying with backbone parallel to the surface. In the case of hexadecane, the density in between each peak is close to zero, meaning that very few molecules are in between the layers, which is not the case for hexane or phytane. In the case of hexane, some

molecules can be oriented at an angle, and the center of mass might fall in between layers. Since phytane molecules are longer and have branches, they can be located across several layers.

The radius of a CH_2 or CH_3 can be associated with $\sigma/2$. From Eq.1, we know that σ is the same for both CH_2 and CH_3 , $\sigma_{CH_2,CH_2} = \sigma_{CH_3,CH_3} = 3.93\text{\AA}$. We can calculate the distance between 2 atoms at which the force is zero, $r_m = 1.12 * \sigma$. For segment-segment this corresponds to a center-center distance of $r_m = 4.4\text{\AA}$ between carbon segments, which gives us an estimated segmental radius of 2.2\AA . The distance between the alkane molecules and the center of the gold molecules is smaller, because $\sigma_{Au,CH_2} = \sigma_{Au,CH_3} = 3.28350$, which makes the distance from the alkane to the gold smaller, $r_m = 3.68\text{\AA}$. This would be the distance if the 2 atoms were isolated, but since they are immersed in a fluid of atoms interacting with them, the value can be slightly smaller.

When we analyze Fig.7, we observe in the configuration plot that the hexadecane molecules are layered along two directions. In the direction perpendicular to the plane of the paper, we can see hexagonal ordering of the molecules, which is confirmed if we look at the distances between the molecules and between the layers. The distance between the hexadecane peak and the gold surface layer is 3.4\AA which is smaller than value for the isolated carbon-gold interaction, as expected. The distance between the density peaks is 3.8\AA which is the distance between layers.

In a hexagonal ordering, the centers of 3 neighboring cylindrical molecules lie at the corners of an equilateral triangle. The height H of such triangle gives us the vertical distance between the layers of cylindrical molecules. If the radius of the cylinders is l , then the sides of the triangle measure $2l$, and the height is given by $h = \sqrt{(2l)^2 - l^2} = \sqrt{3}l$. In our case, where the radius of our segments is 2.2\AA , then $H=3.81\text{\AA}$, which is the distance between the layers seen in our simulations for pure hexadecane.

By looking at the interaction *epsilon* between the different types of segments in Eq. eq:epsilon, we can see the different interaction strengths depending on the interacting atoms. It is noteworthy to mention that the strength of interaction between the carbon atoms and the gold atoms is 2 or 3 times stronger than the interaction among the segments of the fluid. This leads us to presume that a surface layer of alkanes will be present on the gold surface. Several experiments have observed this long range order 2D crystallization of long linear alkane chains on smooth metal surfaces[31, 11, 29, 17, 28, 23].

Velsely theoretically calculated the potential between Lennard-Jones sticks, and arrived at which configurations were more favorable between long molecules whose segments interacting through this potential. He found that the longer the molecules, the stronger the interaction and that the most stable configuration was side-to-side, followed by perpendicular, and next by end-to-end. Which confirms, Christenson hypothesis that once a surface layer forms on the surface, subsequent layers are formed through the confinement[2]. This packing minimizes the energy of the system. In the case of hexane, this intermolecular interaction is weaker because of its short size; and in the case of phytane the presence of the branches hinders its ability to pack tightly with other molecules.

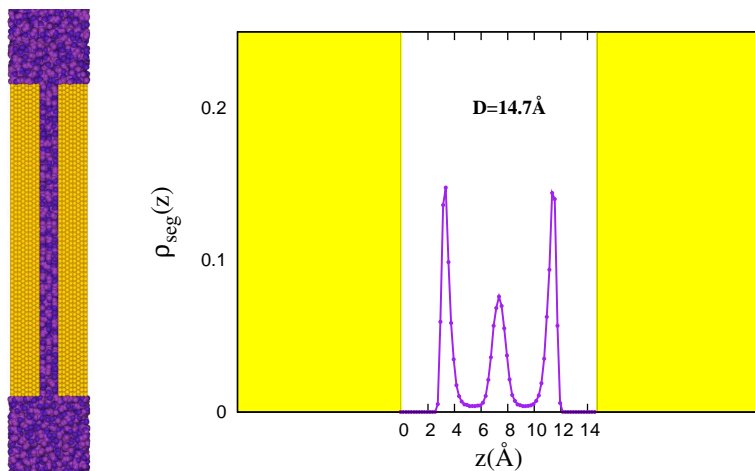


Figure 6: Hexane: Side view of gap size 14.7Å , and its segmental density profile.

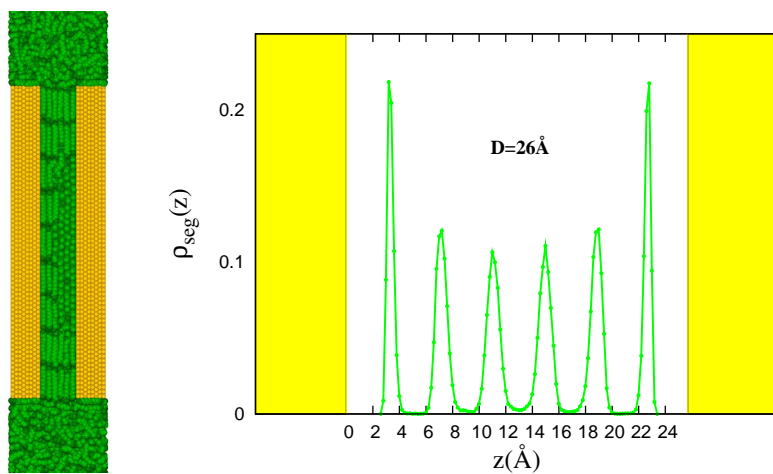


Figure 7: Hexadecane: Side view of gap size 26Å , and its segmental density profile.

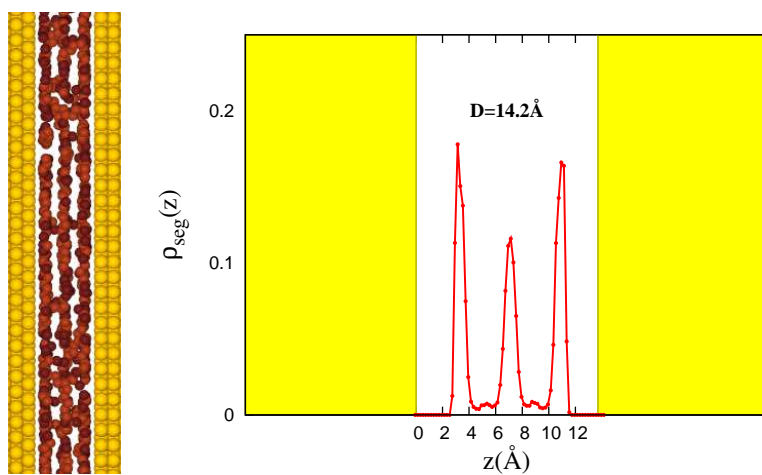


Figure 8: Phytane: Side view of gap size 14.2Å , and its segmental density profile.

After examining the segmental and molecular density plots for all the equilibrated gaps, we observed that there were some gaps that presented sharper peaks and lower valleys in between the peaks. We interpret this as being gaps where the systems has attained its best possible layering, even though in hexane and phytane this layering is not as visually evident as in hexadecane. They occur every 4 or 5 Å, depending on the system. In the following plots, we will present the largest gap we have 36.7 Å, the best 6 well-formed gaps for each system, and then the smallest gap that we reached, for a total of 8 plots showing the transformation of the systems during the slow compression. The largest gaps appears on the top right, and the thickness of the gap decreases down the right column, then it continues on the left column, until the plot in the bottom left corner represents our smallest equilibrated gap for that particular system. For each pure system, the gaps with the best formed layers are

<i>No.Layers</i>	<i>Hexane</i>	<i>Hexadecane</i>	<i>Phytane</i>
7		30 Å	34.2 Å
6	29.7 Å	26 Å	30.2 Å
5	24.7 Å	22 Å	24.2 Å
4	19.7 Å	18 Å	19.2 Å
3	14.7 Å	14.2 Å	14.2 Å
2	9.7 Å	9.4 Å	9.9 Å

(20)

In the sections where we discuss the effects of the compression on the different fluids and plot average properties versus gap size, these distances will appear as markers at the bottom of the plot next to the number of layers present at that gap size.

4.1.1 Molecular Density

For the molecular densities, we calculated the center of mass of each molecule, being careful to take into account periodic boundaries, then counted each molecule in the 0.2 Å bin where their center of mass was located. Afterwards, the number of molecules

in each bin, gave us the distribution of molecules inside the confinement. We also divide by the volumen of each bin, $V = 8150\text{\AA}^3$, just as it was calculated previously. Since the peaks are so sharp, the densities are much higher than the real densities, in which case the dimensions of the molecules are taken into account. Even though this density depends on the bin thickness, it gives us information on the relative distribution of the molecules along the width of the confinement. The horizontal axis in the density plots denotes the distance from the middle of the gap. For example, after finishing the compression, the gap has a width of 6\AA , so the horizontal axis shows a gold surface at -3\AA and the other one at $+3\text{\AA}$. The units for this molecular density are \AA^{-3} , because it is the number of molecules per volume. Since the value is dependent on the bin size, the thinner the bin, the sharper the peaks. We choose a bin size of 0.2\AA to be able to compare with previous results obtained by J.Gao.

In the molecular density profile plots, Fig.9, 10, 11, we can see how the alkane fluid is distributed in the surface and inner regions. In the molecular density plots at the larger gaps, we see well defined surface layers and very little ordering order in the middle region of the gap. Down the right column, we see how the system is being compressed down. In the case of hexane and phytane, there are some peaks in the middle region but the valleys in between the peaks are not zero meaning that there several molecules that are positioned across the layers. This is in contrast with the great layering exhibited by hexadecane, where nice layers are seen at gap distances of 30\AA and the distinction of the layers improves as it is further compressed. By 26\AA , there are 6 well formed layers with few molecules lying in between layers. As hexadecane is further compressed the system goes through gaps that are able to attain very good ordering. On the other hand, the best layering for hexane is seen at gaps smaller than 15\AA where the layers seem to be better defined.

We studied phytane to compare how the presence of branches modified the structure and dynamics observed for confined unbranched hexadecane. Phytane has 4

branches on one side of the backbone, it can twist and turn to adopt a great number of configurations. We have seen how hexadecane molecules arrange themselves in several layers inside the confinement with their backbones parallel to the gold surface, so we wondered how would phytane’s branches arrange themselves. By looking at the molecular density plots in Fig.reffig:dendenC20 we see a well defined phytane surface layer close to gold. At gap size of 14Å, a middle peak shows the emergence of a middle layer of phytane molecules, but besides that there seems to not be much order inside the gap. We expected this to happen because the branches might hinder any type of order, but just to be sure of this lack of order we checked the segmental density profile plots.

4.1.2 Segmental Density

The segmental density will tell us about the distribution of the pseudoatoms inside the confinement, remembering that hexane has 6 segments, hexadecane 16 segments and phytane 20 segments, 16 in the backbone and 4 in the branches. From now on the term pseudoatoms, atoms and segments will all refer to CH , CH_2 , CH_3 and Au . The molecular density gives us information about the average position of the center of mass of the molecules. If we had a molecule with just one segment, then the segmental and molecular densities would be the same, but in our case where our molecules are elongated, both density profiles are not necessarily the same.

In general, when the system is compressed the number of layers decreases in number and, we will later confirm, the layers that seem to change through the process are the inner layers. The segmental density shows us the average location of the segments of the alkane chains. Let us remember that hexane has 6 segments, hexadecane has 16 segments and phytane has 20 segments. In the case of the C6 and C16 chains close to the surface layer, the molecules are, on average, lying mostly parallel to the surface, and we will later see that this is not the case for phytane.

C₆ Molecular Density

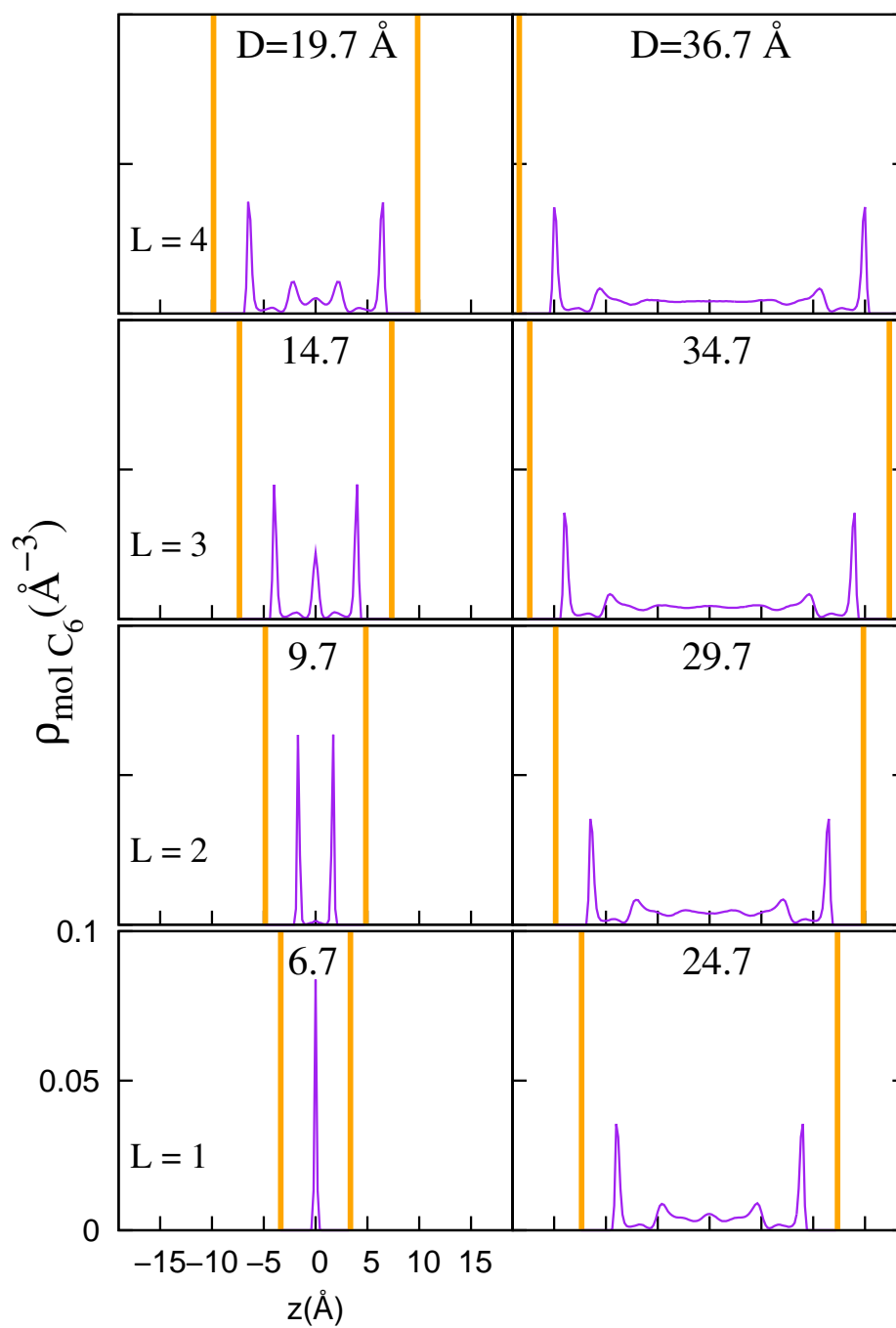


Figure 9: Hexane molecular density for well-formed gaps versus the distance from the center of the confinement

C₁₆ Molecular Density

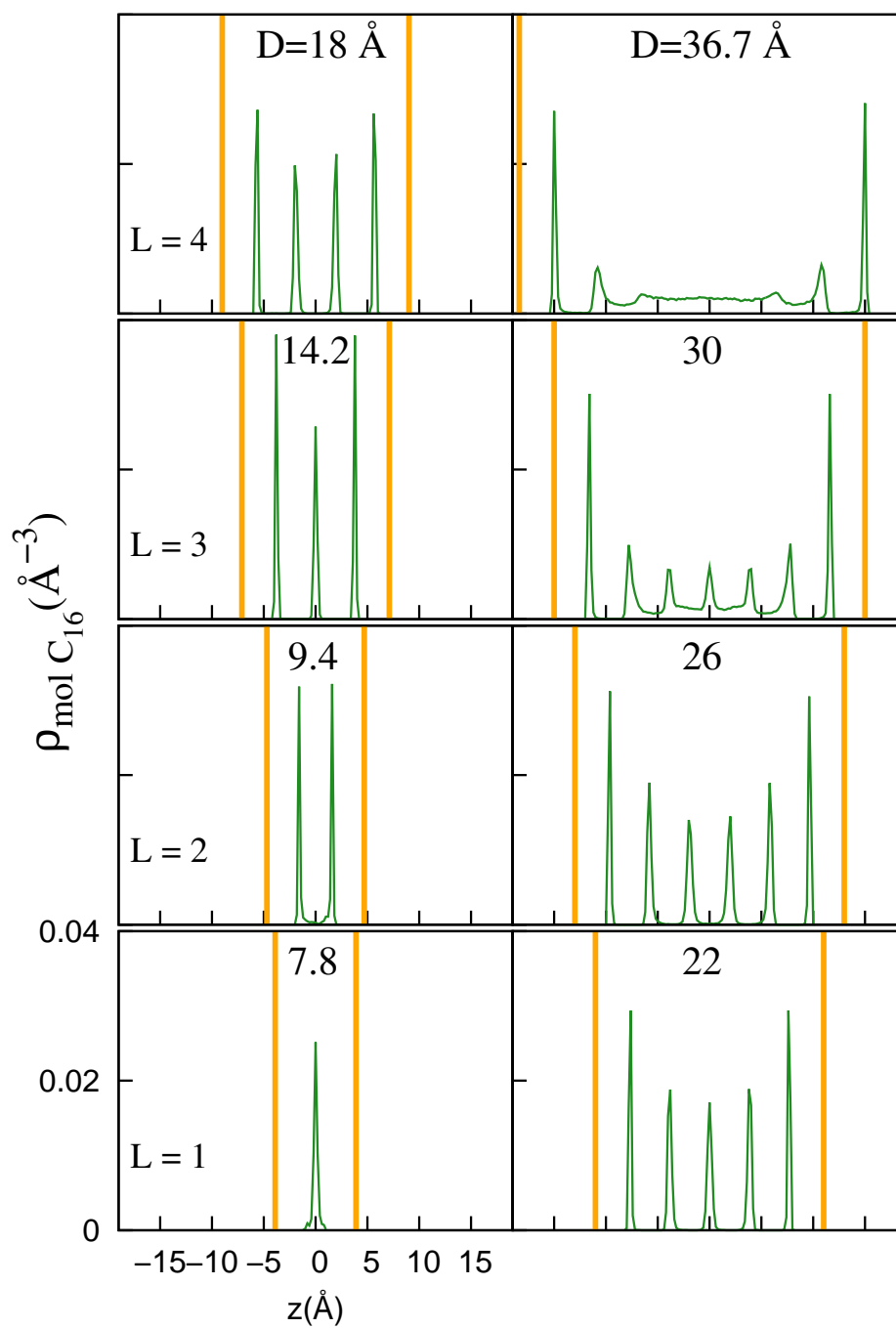


Figure 10: Hexadecane molecular density for well-formed gaps versus the distance from the center of the confinement

C₂₀ Molecular Density

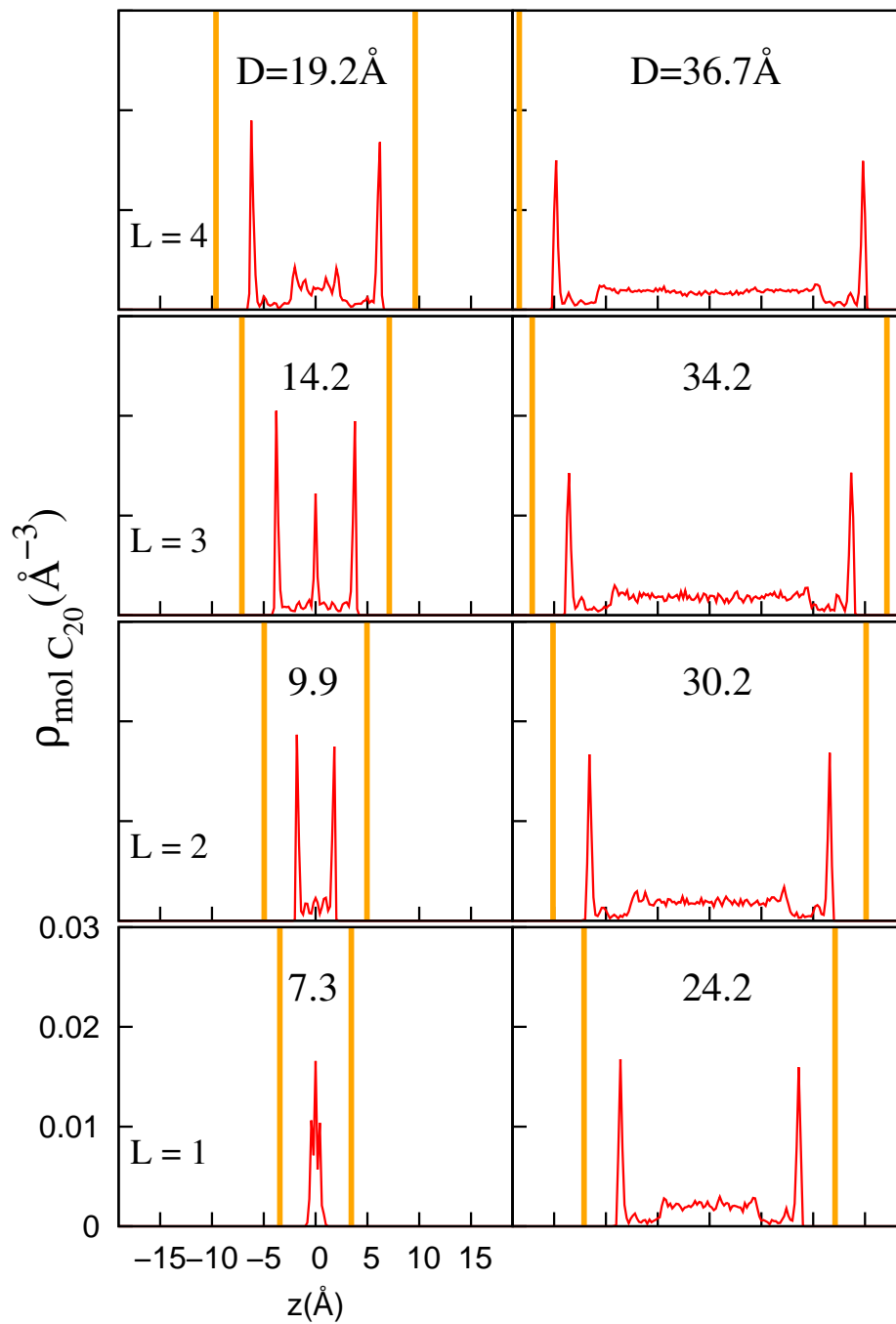


Figure 11: Phytane molecular density for well-formed gaps versus the distance from the center of the confinement

If several linear alkane molecules were packed perpendicular to a surface, the molecular density would show a peak at half their length, around 3Å for hexane, and 10Å for hexadecane and phytane; and the segmental density would show several peaks closer together next to the surface corresponding to the segments. But this is not the case, in our systems the average segmental and molecular densities have peaks in similar places inside the gap, confirming that the molecules are, on average, parallel to the confining surface.

In the segmental density plots for hexane, Fig.12, for hexadecane Fig. 13 and for phytane, Fig.14, we see layering at larger gaps than observed when looking at the center of mass of the molecules in the molecular density plots. The appearance of peaks is particularly dramatic when comparing the segmental density Fig.14 and molecular densities Fig.11 for phytane, and on a lesser extent for hexane Fig.12 and Fig.9.

Let us remember that phytane has 20 segments, 16 in the backbone and 4 branches. These profiles are showing us that even though the center of mass of the molecules are not neatly aligned in layers, the molecules can twist and bend in such a way that the different parts of a molecule can be part of different layers. This can be seen even at gaps as thick as 30Å, where phytane’s segmental density shows several peaks. Some phytane molecules can extend through the confinement and be distributed through several layers.

C₆ Segmental Density

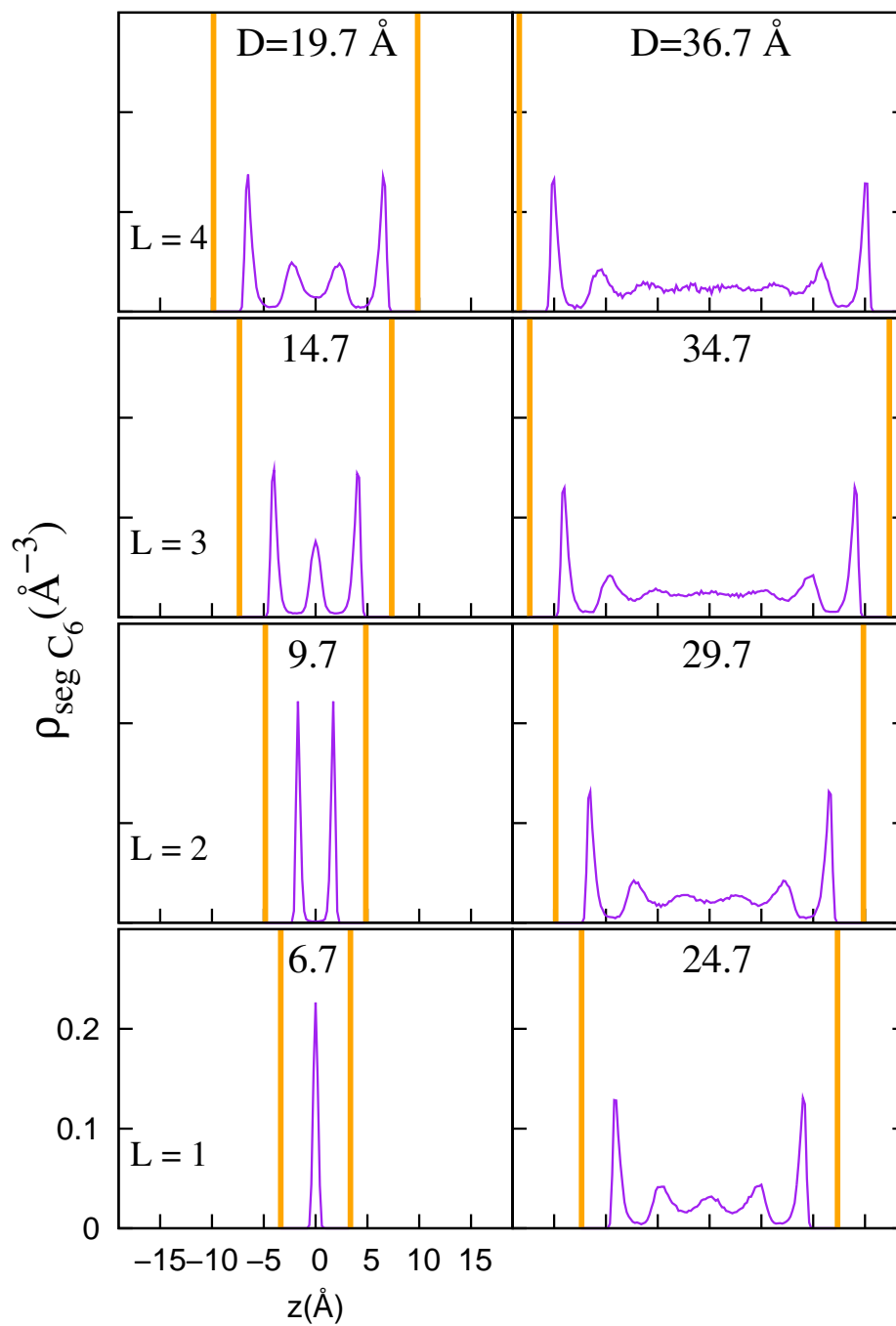


Figure 12: Hexane segmental density for well-formed gaps versus the distance from the center of the confinement

C₁₆ Segmental Density

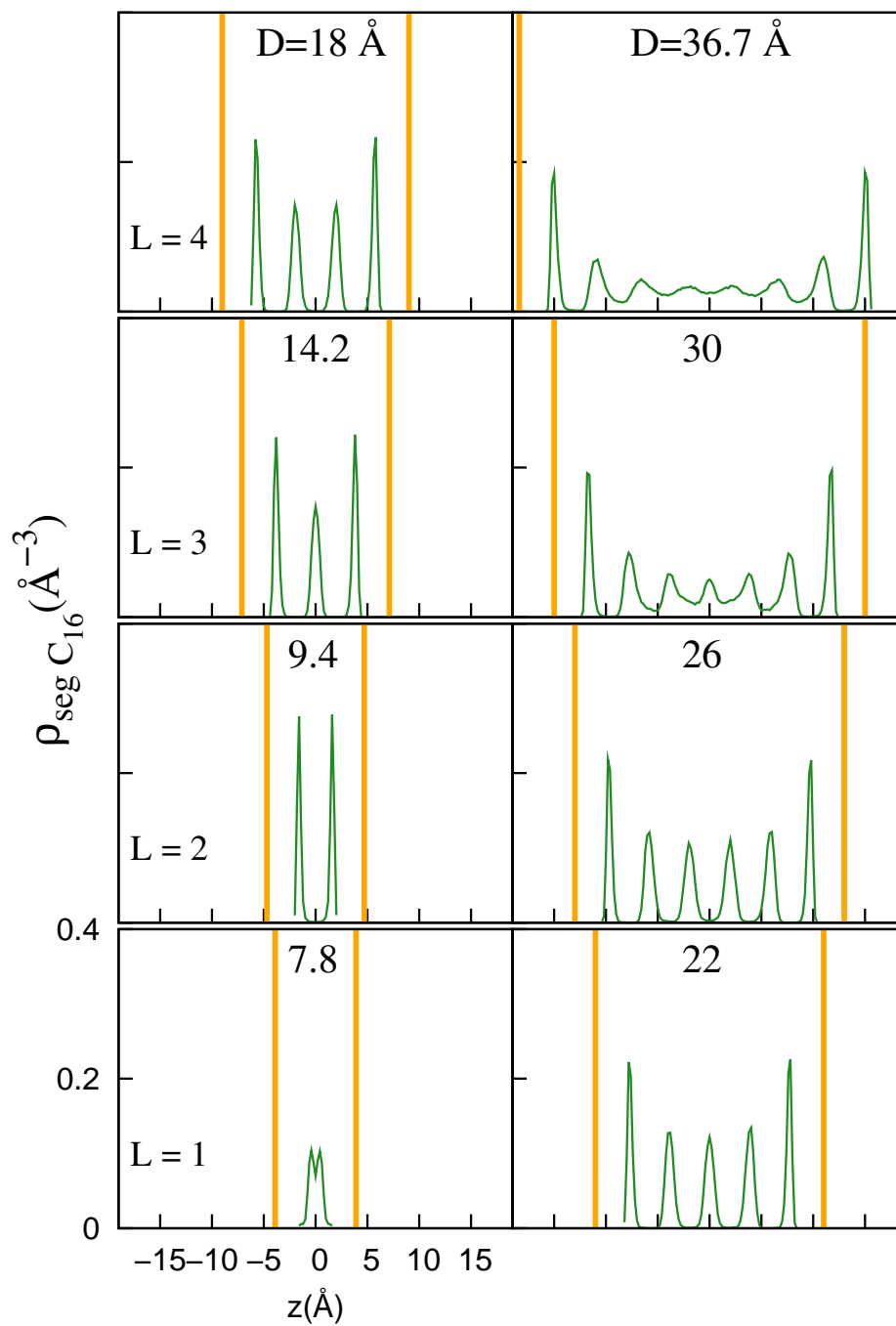


Figure 13: Hexadecane segmental density for well-formed gaps versus the distance from the center of the confinement

C₂₀ Segmental Density

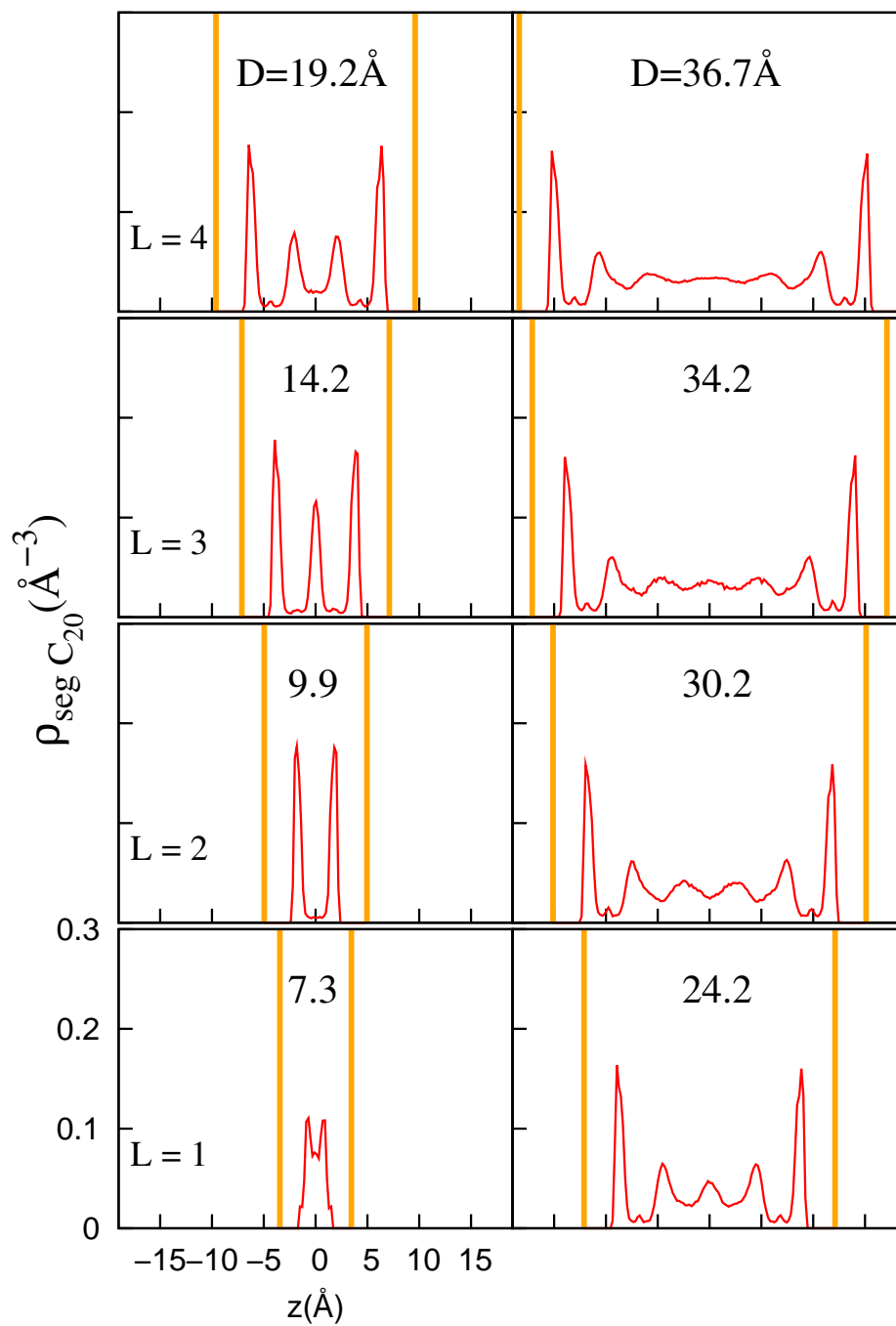


Figure 14: Phytane segmental density for well-formed gaps versus the distance from the center of the confinement

4.1.3 Densities during transition from 4 to 3 layers, and from 3 to 2 layers

In the previous section, we saw the different well-formed gaps for the three pure systems. But what happens in the transition from one ordered state to the next? While some molecules are expelled from the confinement, do the remaining molecules spread through out the gap and form the new layers, or do only some of them participate in the process of forming the new layers?. Are the molecules expelled at a uniform rate, or do they leave in groups?

We will show the pair of segmental and molecular density plots for each system during the transition from almost 4 layers down to 2 layers. In the right column of Figs. 15, 17, 19 we can see the transition from a gap slightly thinner than the one that has 4 layers, $L \sim 4$, to the gap that has 3 well formed layers, $L = 3$. The left column starts at almost 3 layers ($L \sim 3$) and compressed further to end on the bottom left corner with 2 layers ($L = 2$).

Remembering that the density is number of molecules divided by the bin volume, in the following plots, it can be seen how the number of molecules changes in the surface and inner regions, as the system is compressed. The surface layers remains almost unchanged, while the middle region holds the responsibility for the transformation from 2 middle layers to a single middle layer.

This transition in hexane and phytane is a smooth transformation as seen in the segmental density plots. The 2 middle peaks merge to form one broad peak and then it becomes thinner, as can be seen in the segmental density for C6 between 18.7Å and 17.7Å in Fig. 15; and in phytane between 18.2Å and 17.2Å in Fig. 19.

In the case of hexadecane, we don't see this intermediate step. In hexadecane, it goes suddenly from 2 middle peaks to 1 single peak while the gap thickness was only compressed 0.2Å, while in the other 2 fluids, after a compression of 1Å we could still see the middle broad peak in the compression that takes 2Å to go from 4 layers to 3 layers of either pure hexane or pure phytane. This is one of the first indications that

pure hexadecane behaves as solid-like for nanoscale confinements, while hexane and phytane behave mostly as liquid-like.

The process in the left column from almost 3 layers $L \sim 3$ to 2 layers, $L = 2$, is different for phytane. We observe phytane's transformation by analyzing Fig. 15, the system has 3 peaks as 14.2\AA and after compression shows 4 peaks at 13.1\AA . But if we look at the average distribution of the center of mass of phytane molecules, we don't see these peaks very well, so it has to do with segments. Phytane, instead of going from 3 layers to 2 layers, goes through an intermediate step in which it has 2 surface layers and 2 small inner layers.

Upon further inspection, one notices that 2 small peaks also appear in the transition between 4 layers to 3 layers as well, but smaller in magnitude, when the gap size is 17.2\AA .

This begs the question of where are the methyl branches located in these layers. In particular because, by observing the transition from 3 layers to 2 layers, there are these 2 peaks that hadn't been seen in the case of hexadecane. The other difference with the hexadecane profiles is that for larger gaps, the hexadecane system could accomodate more layers than phytane. For example for a gap distance of 26\AA , there were 6 well defined hexadecane layers with almost no segments in between layers, whilst for the same surface separation there were only 5 phytane layers with plenty of segments in between because the density is non zero. This is understandable since phytane is a molecule that on average has a larger diameter than hexadecane, unless they are laying down with all the branches on one side, which seems to be case when it goes down to 3 layers, where both phytane and hexadecane have 3 sharp peaks in the segmental densities and molecular densities for gaps sizes of 14.2\AA . We can see the evolution of the center of mass of the molecules during the transition in the molecular density plots for hexane in Fig. 16, for hexadecane in Fig.18 and for phytane in Fig.20.

C_6 Segmental Density during transition
from 4 to 3 layers, and from 3 to 2 layers

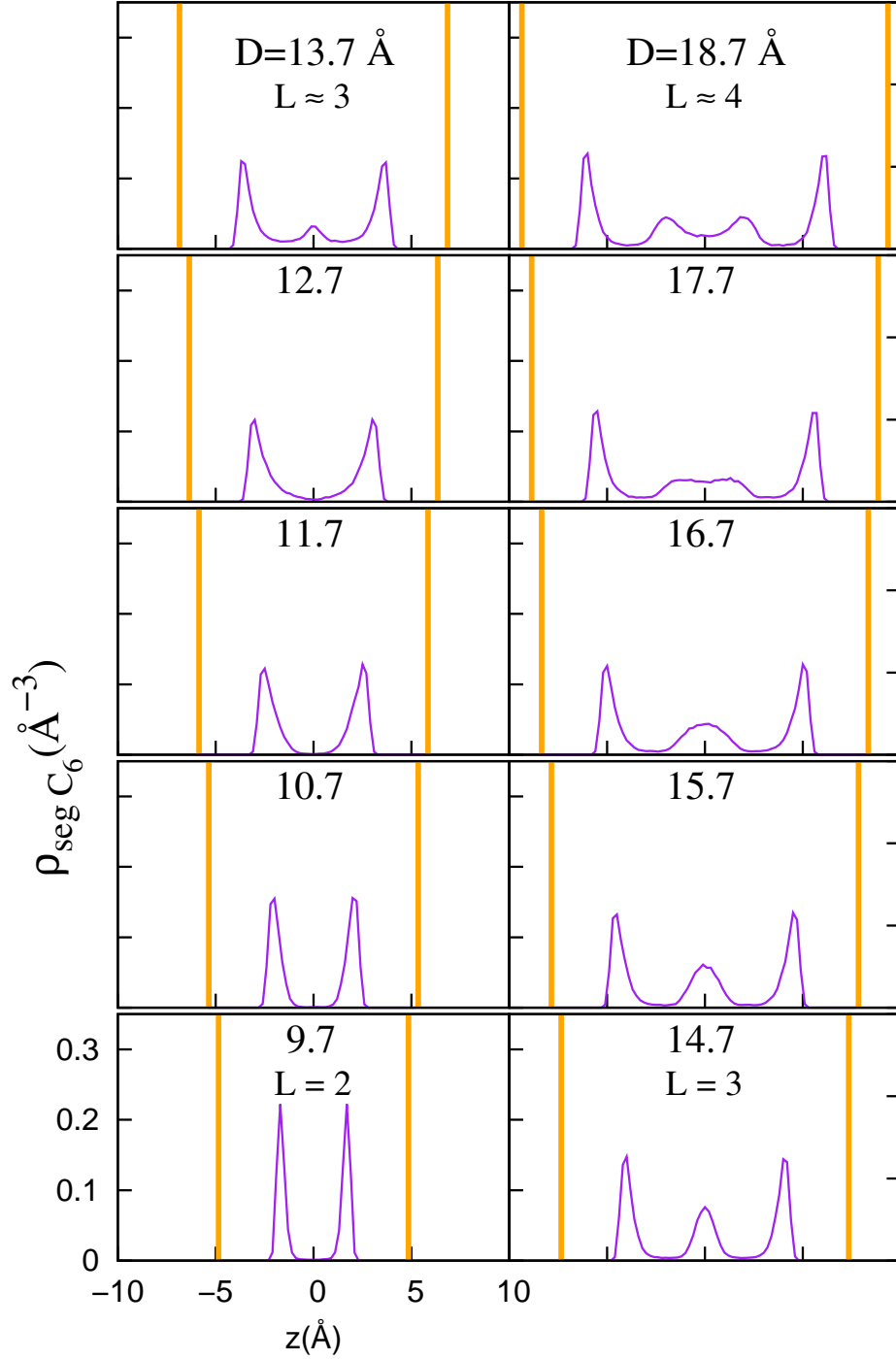


Figure 15: Hexane segmental density during transition between well-formed gaps

C_6 Molecular Density during transition
from 4 to 3 layers, and from 3 to 2 layers

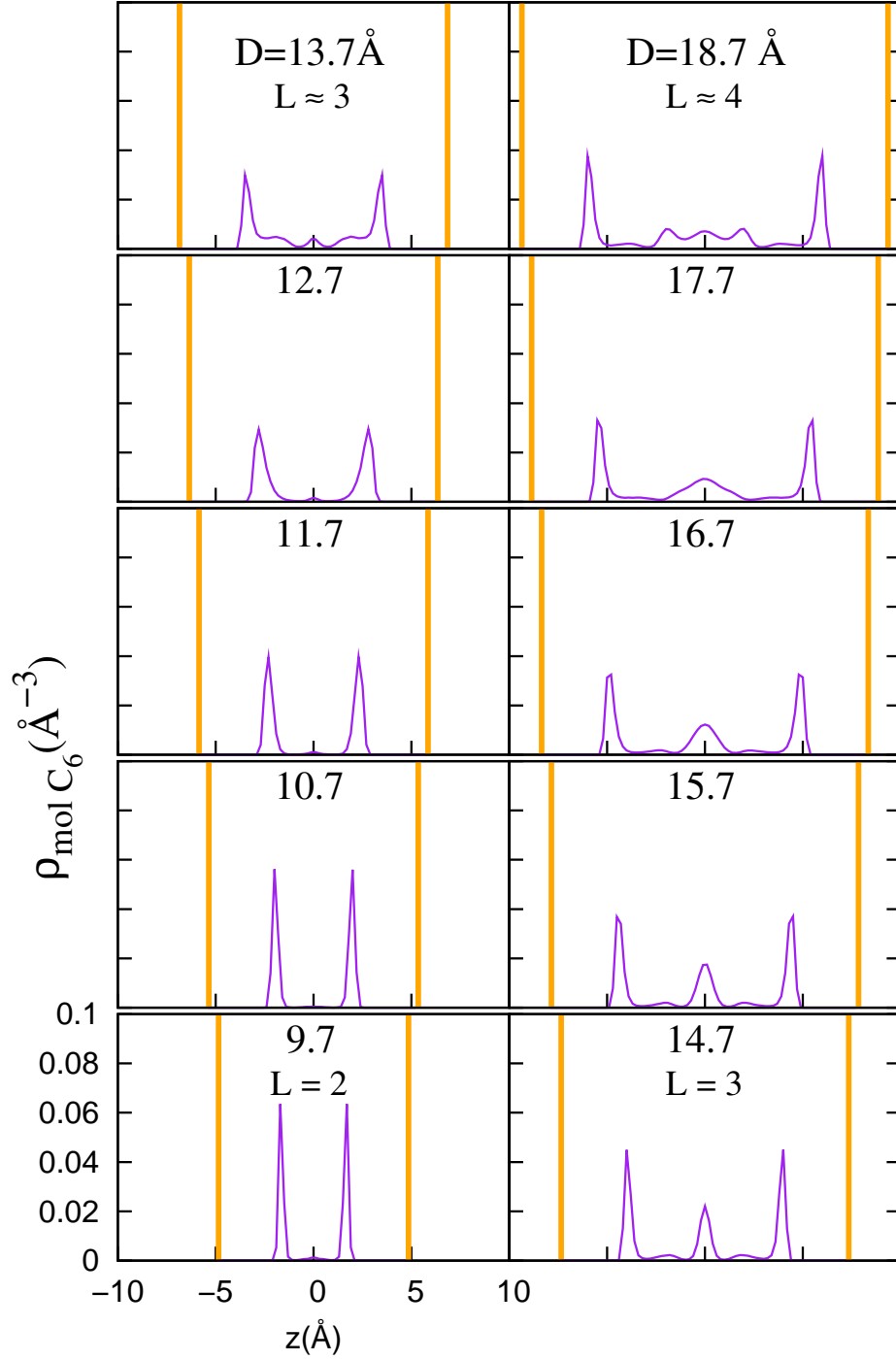


Figure 16: Hexane molecular density during transition between well-formed gaps

C_{16} Segmental Density during transition
from 4 to 3 layers, and from 3 to 2 layers

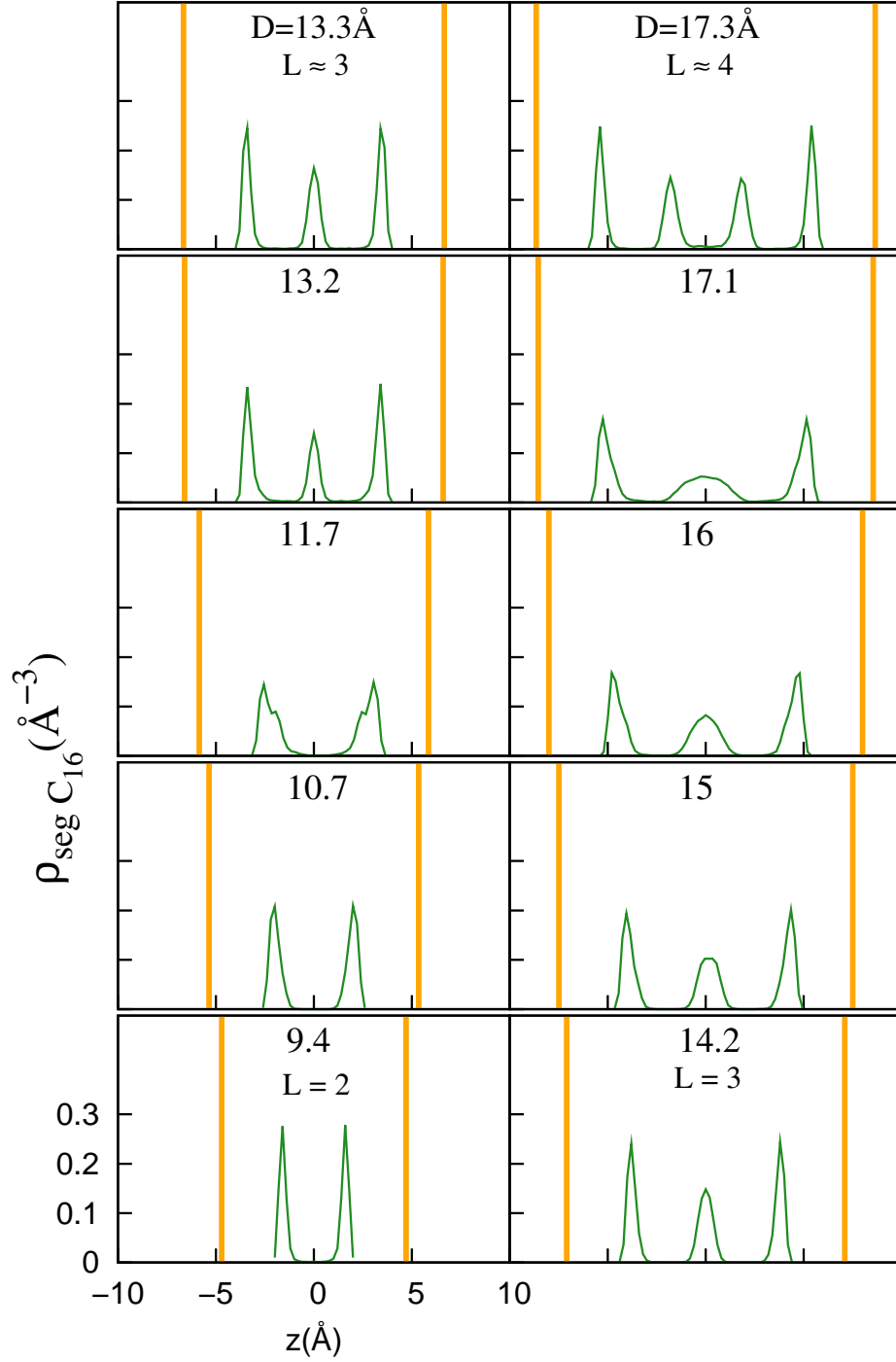


Figure 17: Hexadecane segmental density during transition between well-formed gaps

C_{16} Molecular Density during transition
from 4 to 3 layers, and from 3 to 2 layers

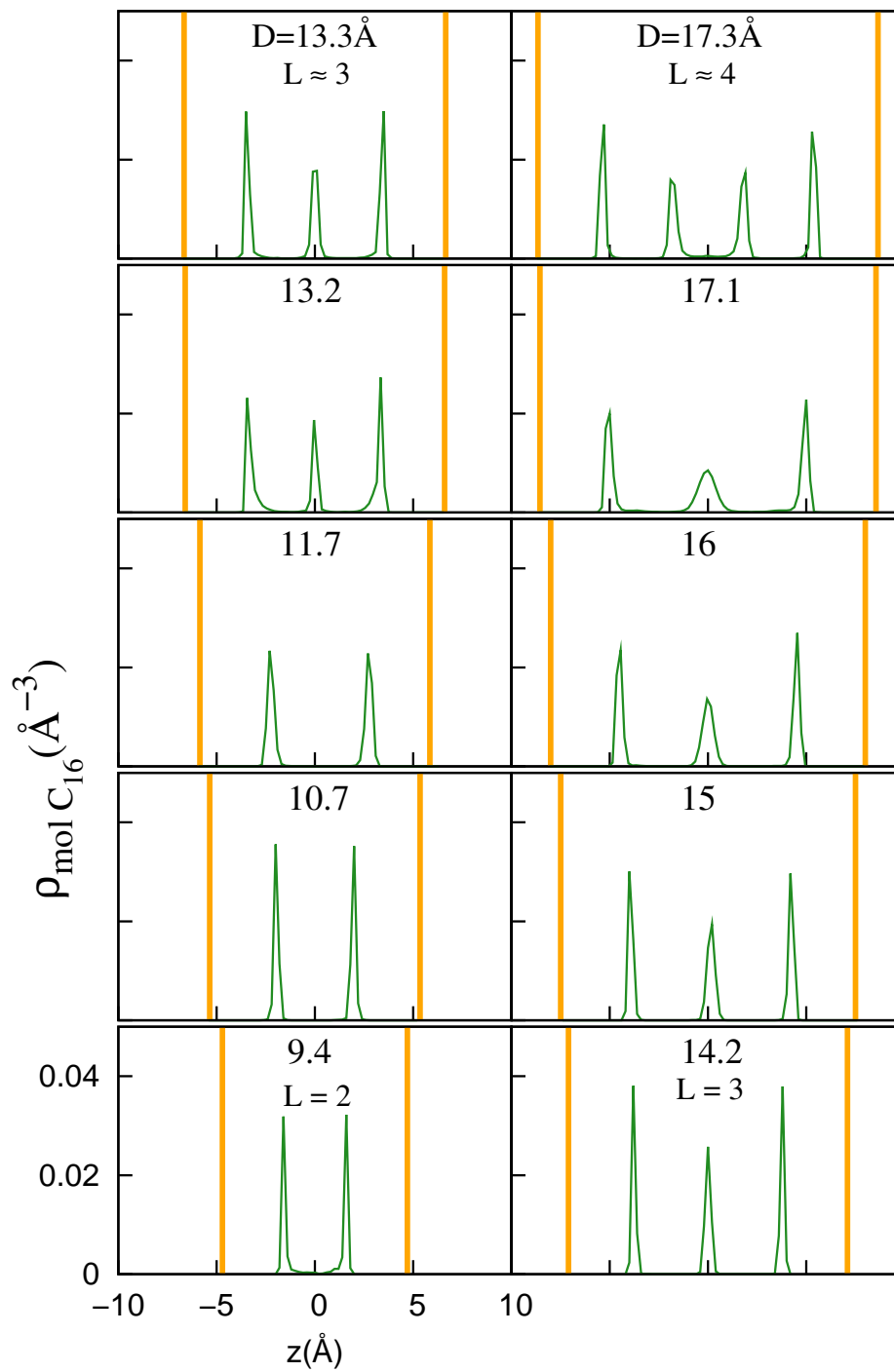


Figure 18: Hexadecane molecular density during transition from 4 to 2 layers

C_{20} Segmental Density during transition
from 4 to 3 layers, and from 3 to 2 layers

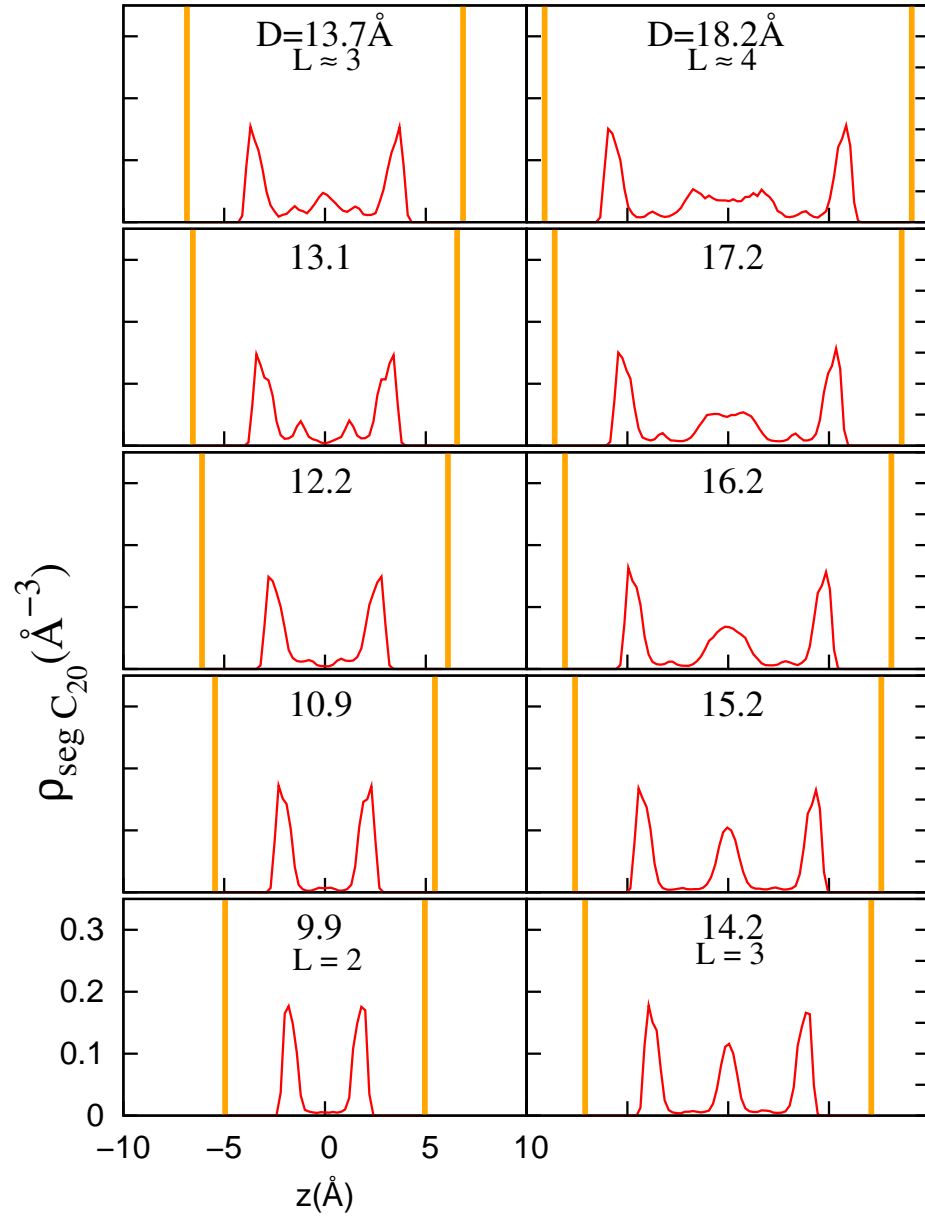


Figure 19: Phytane segmental density during transition from 4 to 2 layers

C_{20} Molecular Density during transition
from 4 to 3 layers, and from 3 to 2 layers

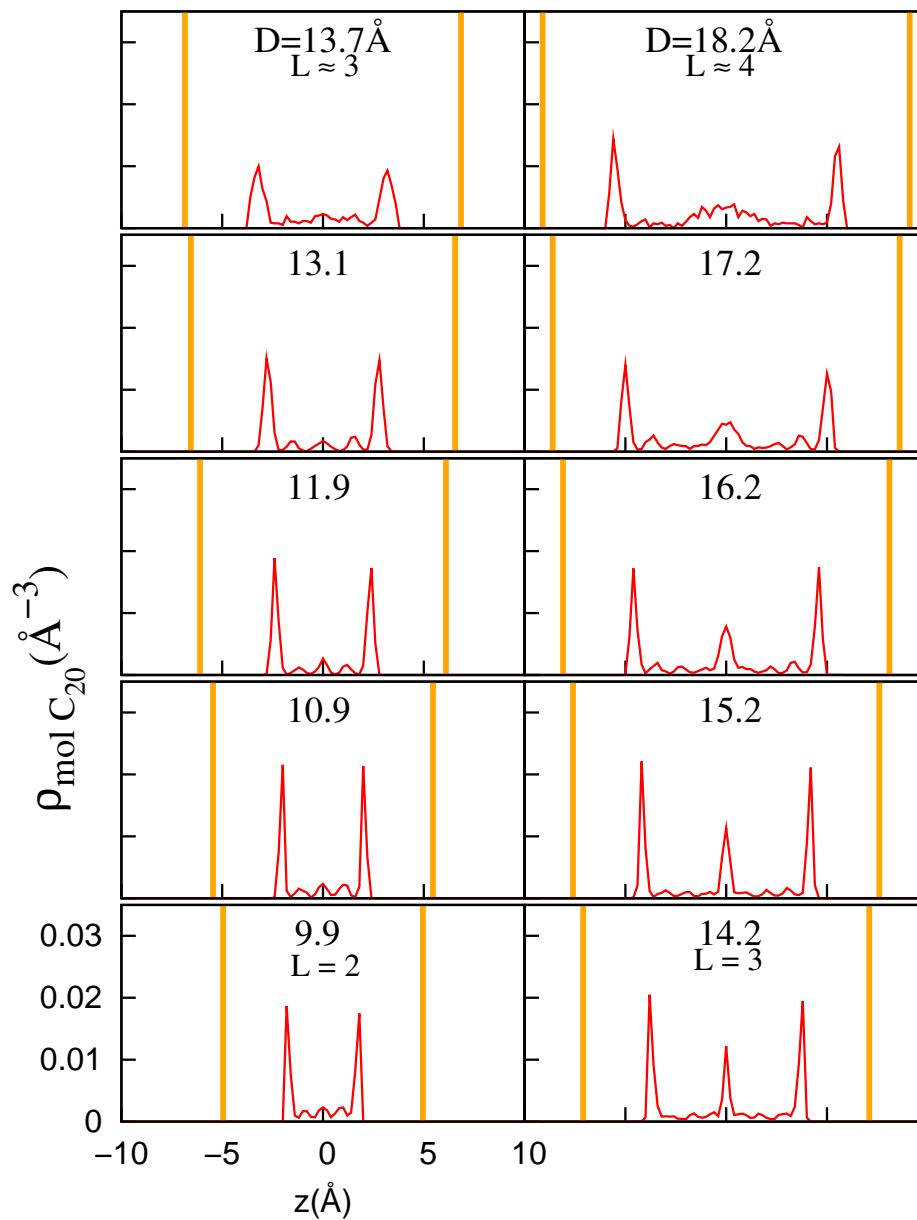


Figure 20: Phytane molecular density during transition from 4 to 2 layers

4.1.4 Phytane's Branched Density

To better understand the presence of these extra little peaks when transitioning from 4 to 3 layers, we plotted the density of branch segments in the same plot as the normal segmental densities. Using the standard chemical numbering protocol, the branches in a phytane molecules are carbon atoms with numbers 17, 18, 19 and 20th. These are the branch segments. The segments included in the previous segmental densities are all the segments, regardless of whether they were branches or non-branches.

In Fig.21, we see the distribution of branches through out the confinement and relative to the position of the segmental layers, in the gap sizes that have well formed layers. The red lines are segmental density, while the blue lines represent the branched density. There are only 4 branches for every 20 segments in a phytane molecule, which explains the difference in magnitude. To account for this difference, we present the branched density in a scale 5 times smaller than the segmental density. For the well-formed layers, the position of the branches corresponded to the position of the layers which means that the backbone and the branches were in the same plane, parallel to the gold.

To understand better the position of the branches during the transition from 4 to 3 layers, we plotted Fig. 22 with the same scale. The gap separation 17.2\AA is an intermediate point where can see some very small but still noticeable peaks in between the large segmental layers. This is also seen in the transition from 3 layers to 2, in gap sizes 13.1\AA . These smaller peaks correspond to the molecules that have rotated and their branches are facing each other. The backbones are close to the gold surface and the branches are pointing away from the surface.

We have seen that in terms of arrangement of the branched molecules versus the unbranched, the molecules rearrange themselves so that the segments organize layers inside the confinement. They want to maximize the number of molecules inside the gap, because when the system is transitioning from 4 to 3 and from 3 to 2 layers, the

molecules rotate to have their plane perpendicular to the gold because for some gaps this allows for better packing.

To quantify this phenomenon a little better, we divided the branch density by the total number of segments in each bin, and arrived at the percentage of branches at each height in the confinement, seen in Fig.23. When the system is transitioning from one layered state to the next, a good proportion of the molecules rotate to an intermediate state.

For well ordered layers as in Fig.21, the branched density is less than a quarter of the segmental density, as it is expected since there are only 4 branches out of 20 segments. When we look at the percentages of branched segments through the confinement during transition, Fig.23, at $L = 3$ the branched density oscillates around 20%. But for the other gaps during the transition process, we can see that this percentage can reach up to 60% in the location of the small inner density peaks, which confirms that they are mostly branches. The ratio in the surface layers is close to 20%, meaning that there are also branches in the surface layer.

C₂₀ Branched and Segmental Densities

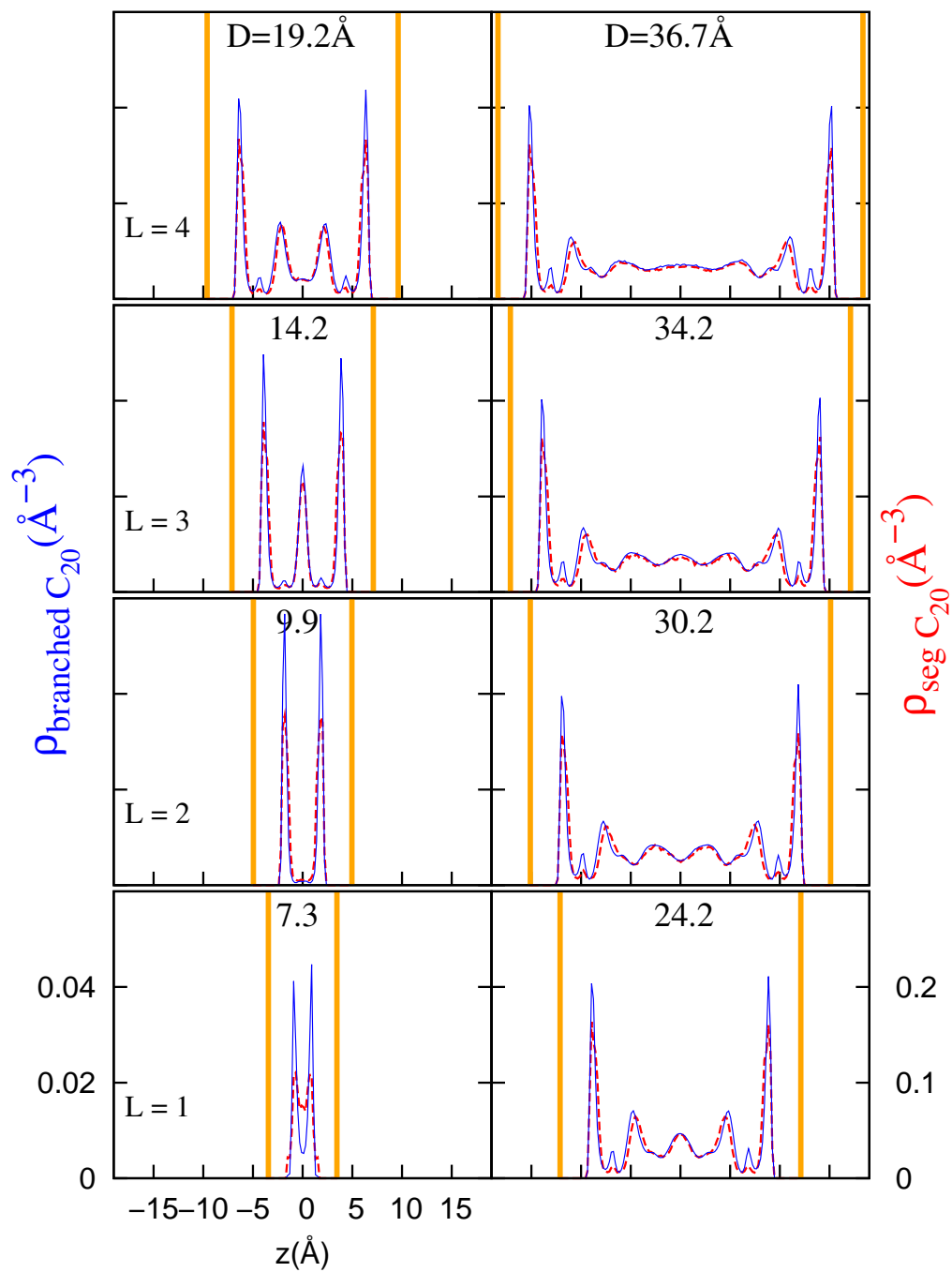


Figure 21: Phytane Segmental and branched densities for well-formed gaps versus the distance from the middle of the confinement.

C_{20} Branched Density during transition
from 4 to 3 layers, and from 3 to 2 layers

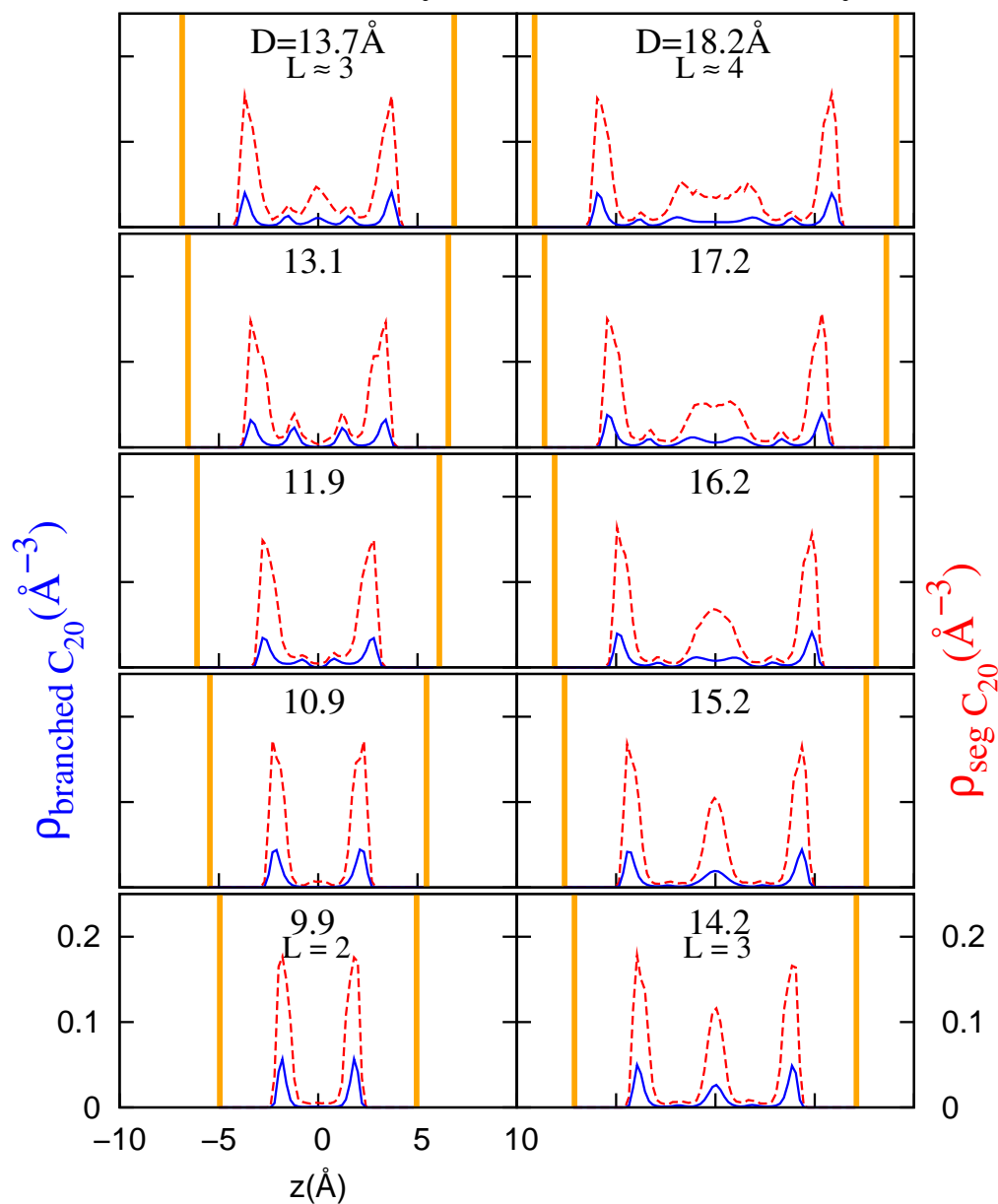


Figure 22: Phytane Segmental and branched densities during transition from 4 to 2 layers.

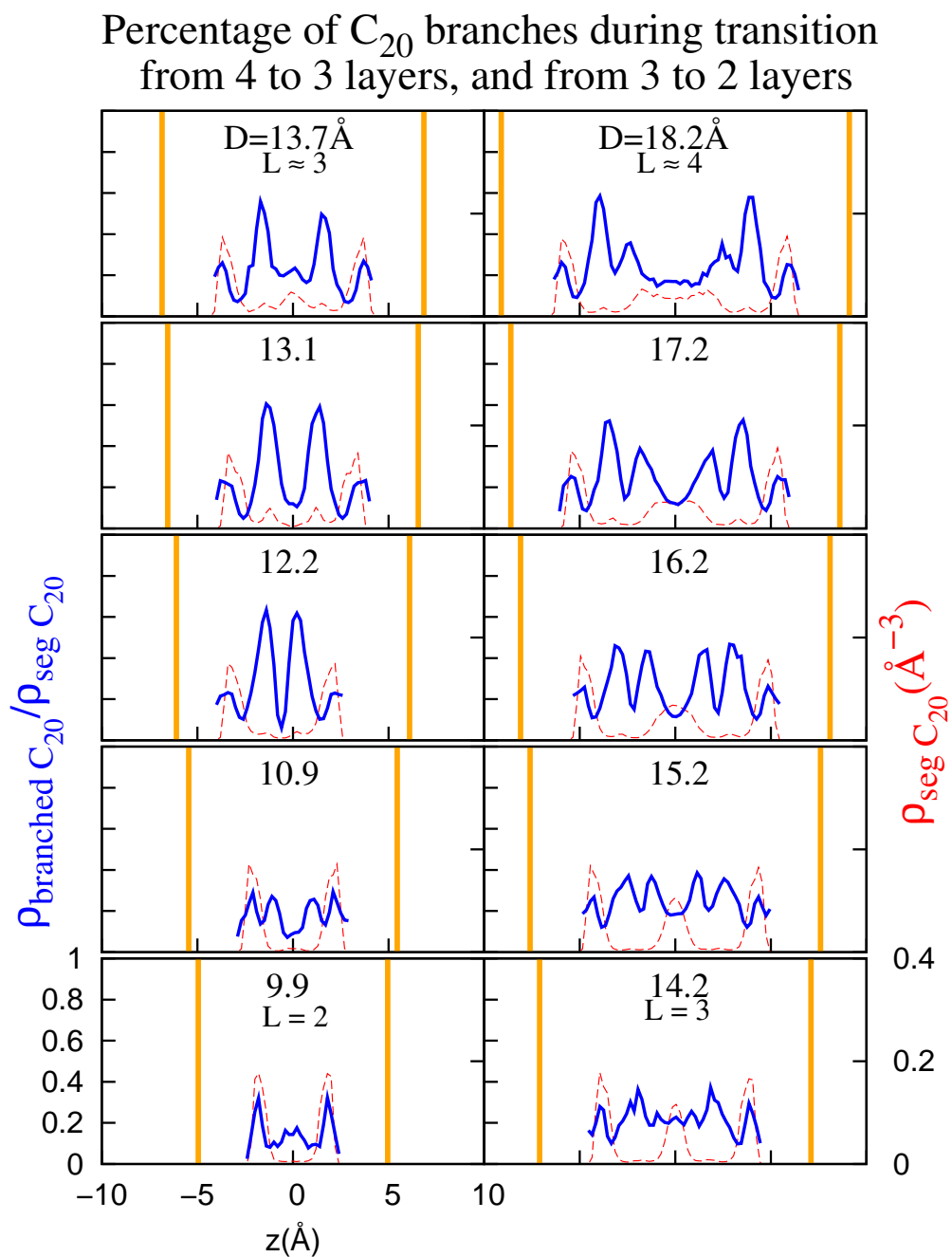


Figure 23: Percentage of phytane branches inside the confinement during the transition from 4 to 2 layers.

4.2 End-to-end distance

By examining the distribution of the average end-to-end distance versus position inside the gap, we can infer where most of the molecules are stretched, and where they are not. The expected bond length for alkanes is 1.54\AA and the bond angle is

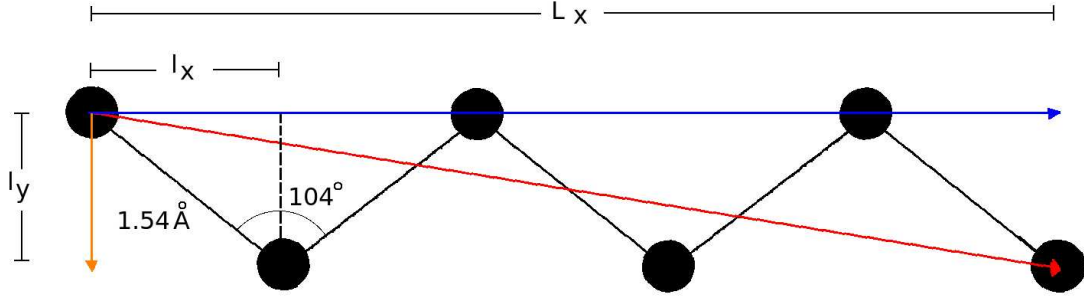


Figure 24: Diagram showing the dimensions of the backbone of an alkane molecule with n segments.

104° , and with this information we can estimate the theoretical length of an alkane chain with n segments.

$$\begin{aligned}
 L &= \sqrt{l_y^2 + ((n-1)l_x)^2} \\
 l_x &= 1.54 \cos(33^\circ) = 1.29\text{\AA} \\
 l_y &= 1.54 \sin(33^\circ) = 0.84\text{\AA}
 \end{aligned} \tag{21}$$

From Eq.??, we know that the theoretical length of hexane is 6.45\AA , and it is 19.37\AA for both hexadecane and phytane because they have same number of segments in the backbone.

From Figs.25, 26 and 27, it is evident that the alkane molecules have their full length close to the surface. The length of hexane varies between 80% and 100% of its ideal length of 6.45\AA . Most of hexadecane molecules are fully extended inside the layers, but there are some few molecules that can have an end-to-end distance of short as 5\AA . In these cases, the hexadecane molecule has colied to a point where the

ends are very close together . Phytane's end-to-end distance varies between 60% and 85% because the presence of the branches allows the molecule more freedom to bend and twist.

For the longer *C*16 and *C*20, the location of the peaks of elongated molecules correspond to the location of the density peaks through out the compression, but this is not the case for the shorter molecules. For the larger gaps, the peaks in the length don't correspond exactly with the density peaks, but as the hexane is compressed down to 3 layers the position of the stretched molecules lies in the well formed layers.

The end-to-end distance plots give us indication of the center of mass of the molecules, but the extended hexane molecules can lay either in the well-defined layers or in between layers. Even if the center of mass of a molecule lies in a layer, the molecule could be at an angle with the gold surface. This is possible because the hexane molecules are very short. We need to study the orientation that the molecules make with respect to the gold surface to understand better the arrangement of the different types of molecules.

C_6 Relative end-to-end distance and Segmental density

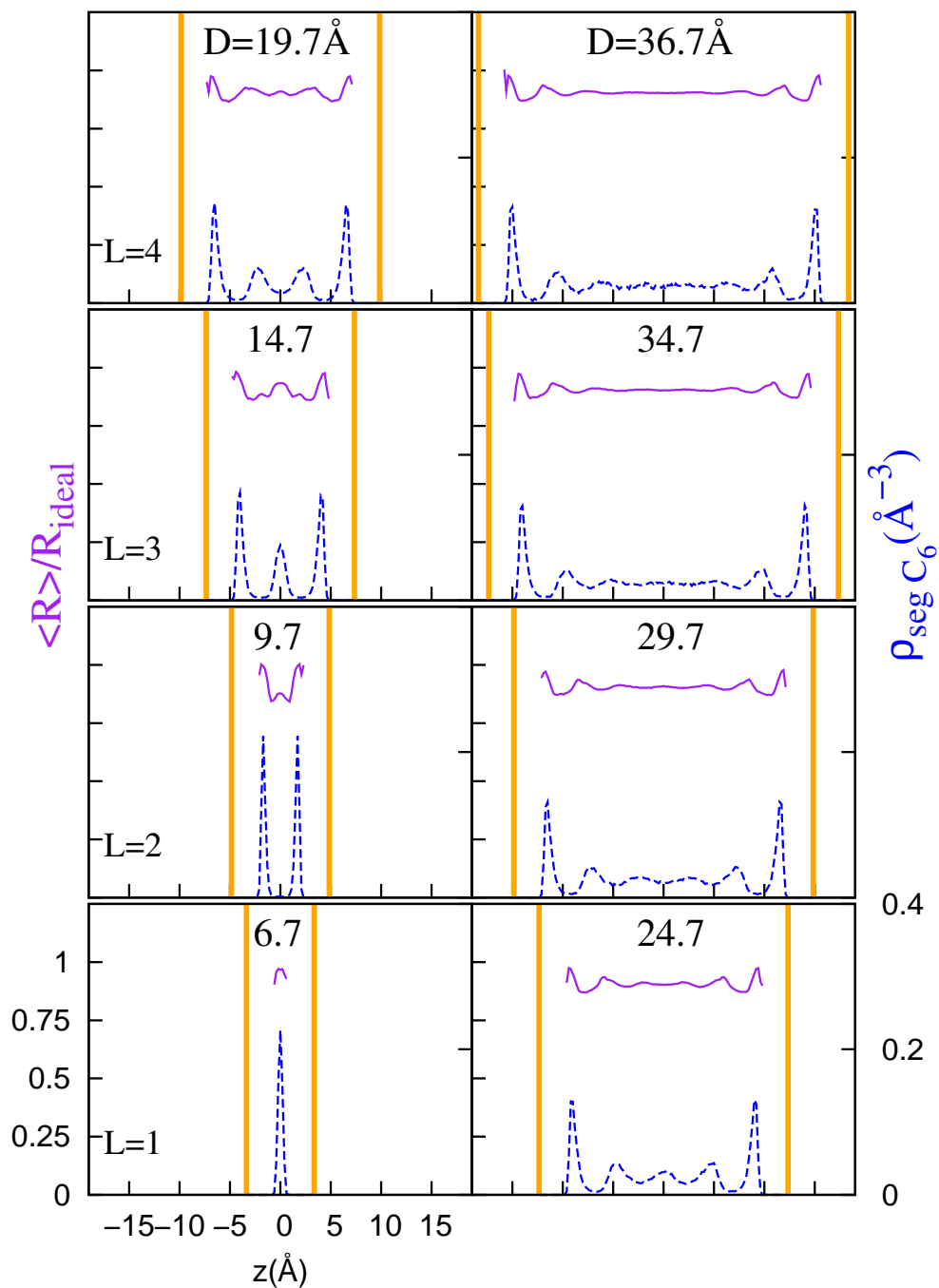


Figure 25: Comparison between the average end-to-end distance and the segmental density for hexane molecules inside well-formed gaps where $R_{ideal} = 6.45 \text{ Å}$.

C_{16} Relative end-to-end distance and Segmental density

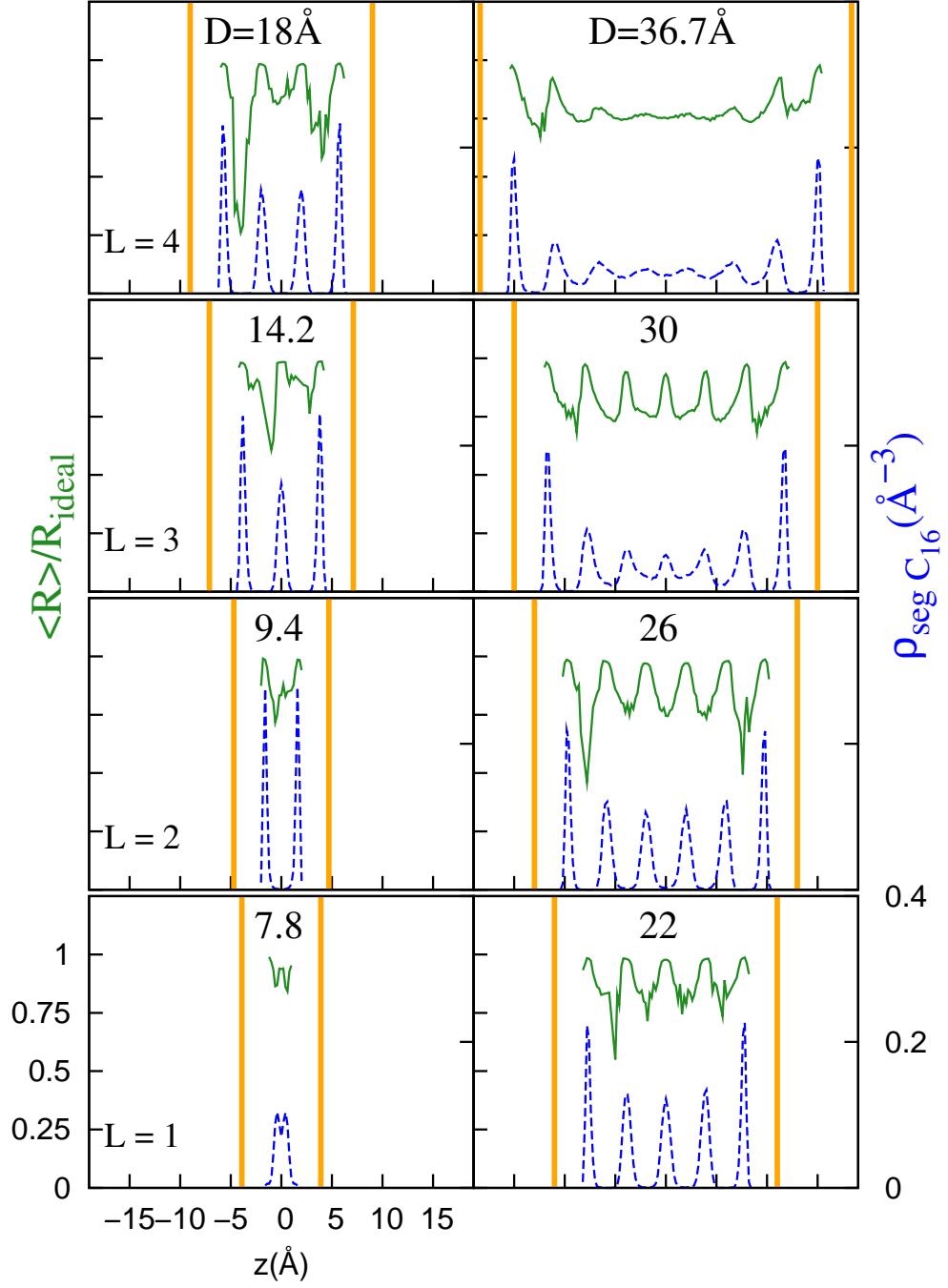


Figure 26: Comparison between the average end-to-end distance and the segmental density for hexadecane molecules inside well-formed gaps where $R_{ideal} = 19.37 \text{\AA}$.

C_{20} Relative end-to-end distance and Segmental density

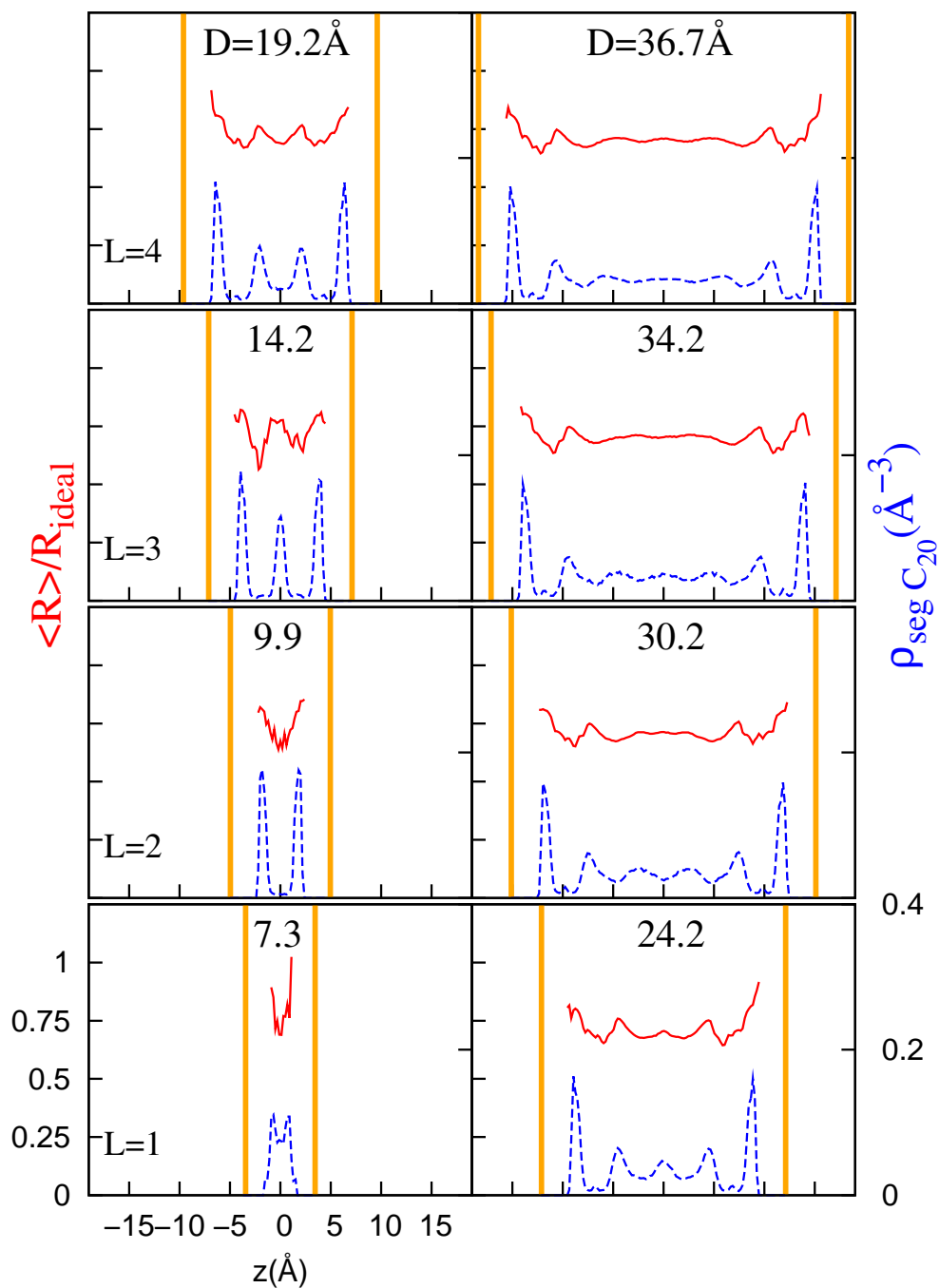


Figure 27: Comparison between the average end-to-end distance and the segmental density for Phytane molecules inside well-formed gaps where $R_{ideal} = 19.37 \text{ Å}$.

4.3 Molecule Orientation

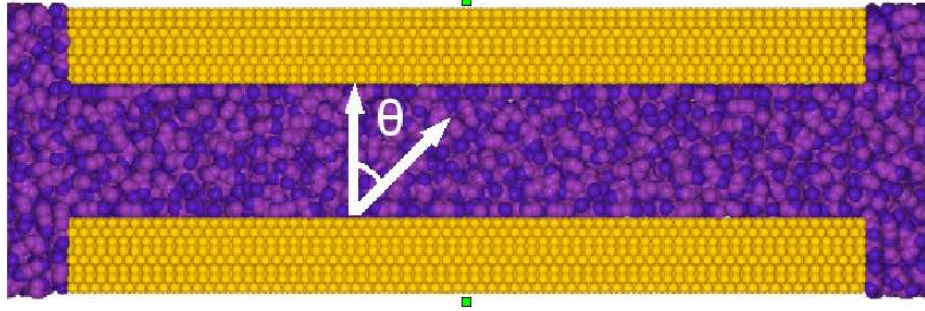


Figure 28: Intralayer ordering measured with angle θ

To study the orientation of the alkane molecules, we calculated $\sin^2(\theta)$, where θ denotes the angle the end-to-end vector for the molecules makes with an axis perpendicular to the gold surface. If $\theta = 0$, then the molecule is perpendicular to the gold surface and if $\theta = 90$ the molecule is parallel to the confining surfaces. So $\sin^2(\theta)$ varies from 0 for molecules standing up, to 1 for molecules lying down. The average value of $\sin^2(\theta)$ for molecules whose ends are undistinguishable is $2/3$.

$$\left[\begin{array}{cc} \theta & \sin^2(\theta) \\ \text{Parallel to the gold } (\theta = 90) & 1 \\ \text{Random orintation} & 0.66 \\ \text{Standing up } (\theta = 0) & 0 \end{array} \right] \quad (22)$$

For the largest gap in Fig.29, at 36.7\AA , the molecules in the middle of the confinement seem to on average have a random orientation because the average $\sin^2(\theta)$ is close to 0.66, and this value oscillates through smaller and larger values as it gets close to the surface.

In the orientation profiles, we can see that the value of peaks is close to 1 at the surface, and the lowest value it attains is close to 0.25, which corresponds to 30° with respect to a vector in between the confining surfaces. We can also see that in the case of comparing orientation with density, the peaks of the 2 properties do correspond.

The molecules in the first 3 layers close to the surface are mostly lying down parallel to it.

It is interesting to observe that in the segmental and molecular densities clear layering would start at 5 layers for hexane, but in the orientation plots even 8 peaks are clearly visibly at 36.7\AA , top right panel of Fig.29. In Fig.30, we can see a comparison of the average end-to-end distance with the segmental density. Pure Hexadecane is parallel to the confining surfaces, in all the layers up to gap thickness of 30\AA where 7 hexadecane layers have formed. In the case of Pure phytane, seen in Fig.31, the 2 closest layers to the gold are mostly parallel to it, but the inner region is not.

C₆ Orientation and Segmental density

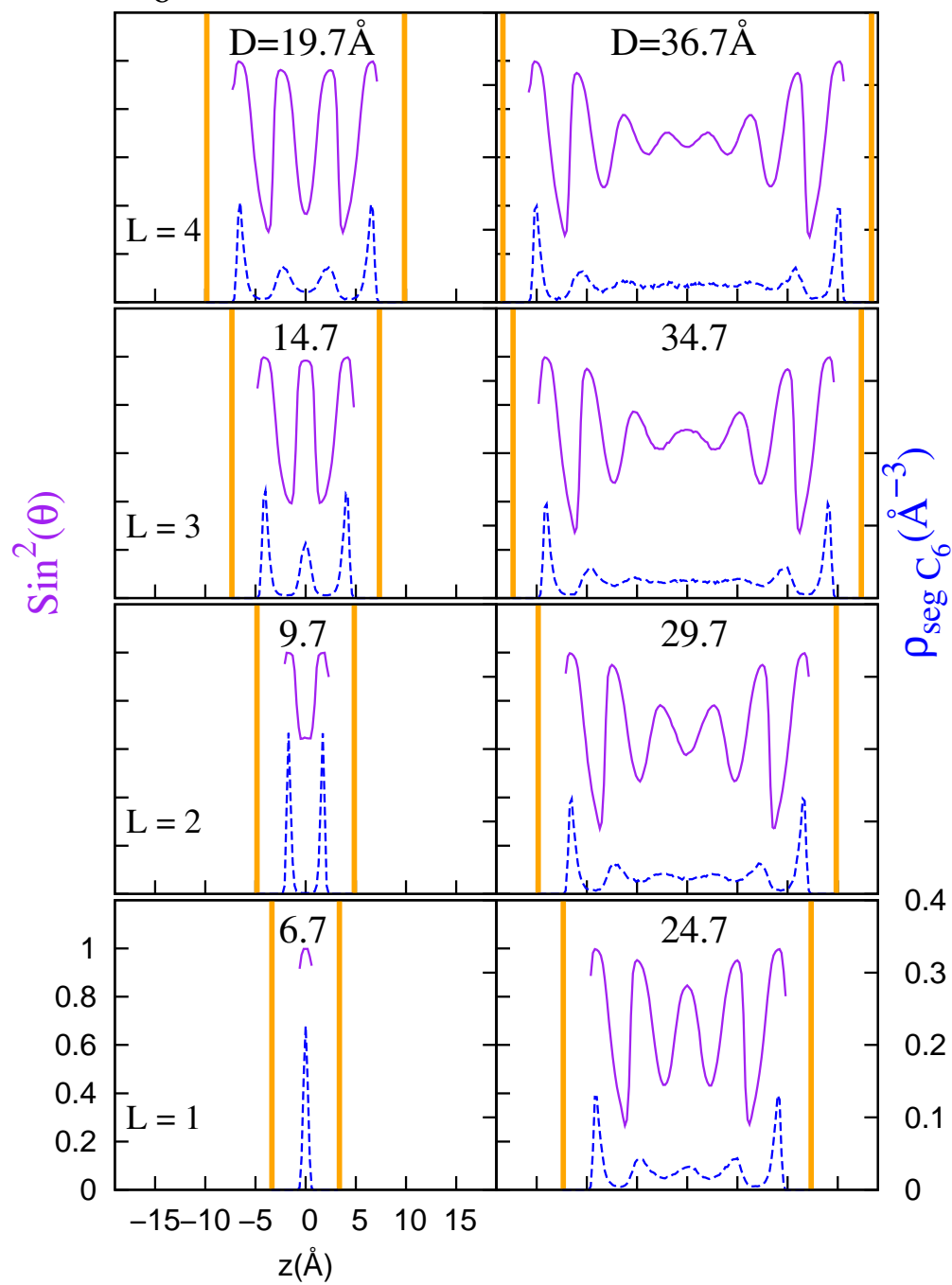


Figure 29: Comparison between the intralayer orientation and the segmental density for hexane molecules inside well-formed gaps.

C_{16} Orientation and Segmental density

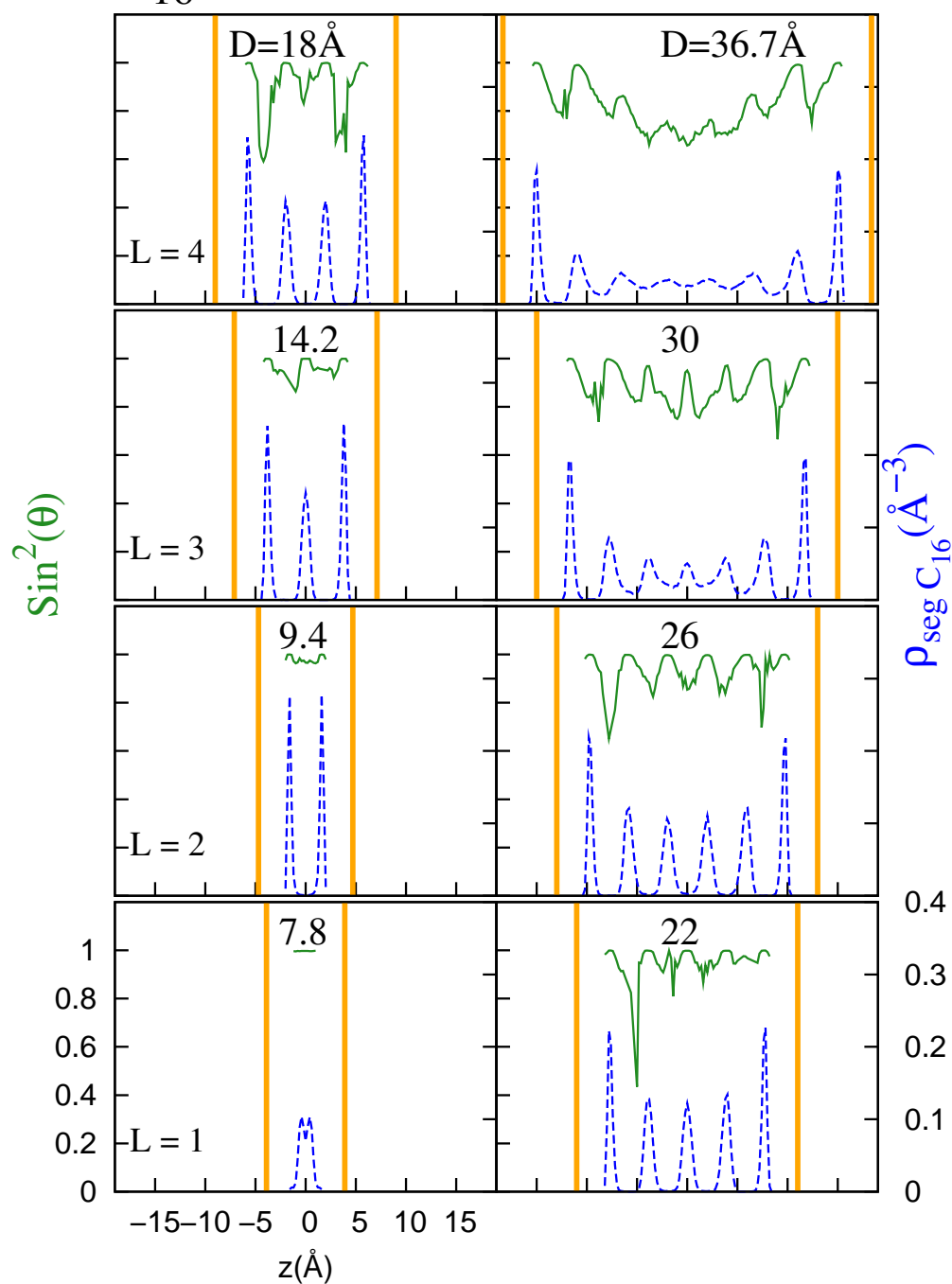


Figure 30: Comparison between the average end-to-end distance and the intralayer orientation for hexadecane molecules inside well-formed gaps.

C₂₀ Orientation and Segmental density

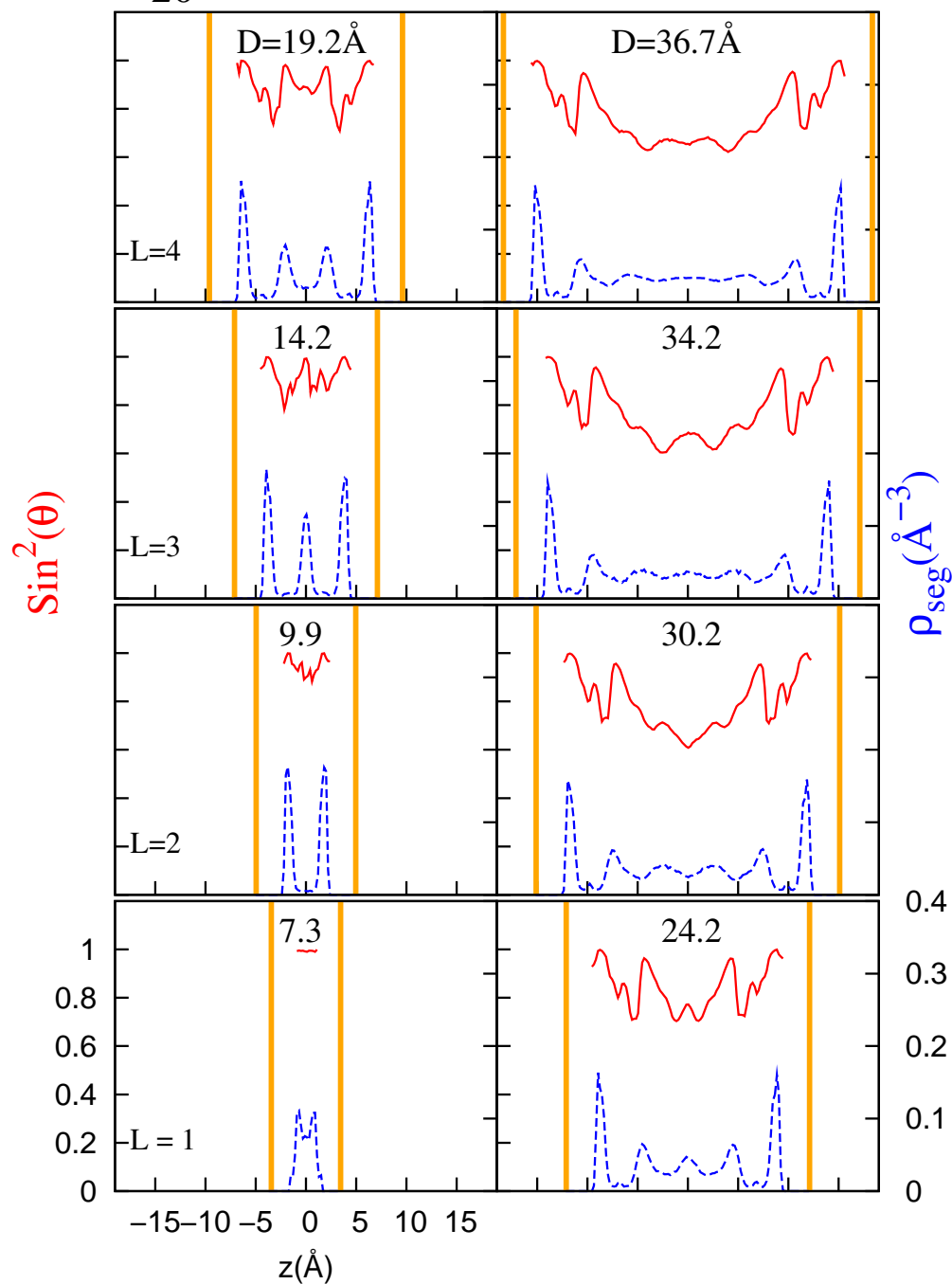


Figure 31: Comparison between the average end-to-end distance and the intralayer orientation for phytane molecules inside well-formed gaps.

4.4 *Configuration plots during compression*

In order to clarify more our compression process, in Figs. 32, 33 and 34, we present a side view of our pure systems as they are compressed from 36.7Å down to 9.7Å. The purple system is hexane, the green system is hexadecane and the red system is phytane. Our computational box becomes thinner along the z – *axis*, the gold blocks remain the same and hence the spacing in between the gold surfaces decreases. We can see how the confined fluid is in contact with the reservoir on both sides. Even though it is not shown here, the computational box grows along the x – *axis* because of the outflux of alkane molecules.

The computational box starts at approximately 400Å and grows to more than 600Å in our pure systems. Let’s remember that during the compression of all our fluids, we are saving the state of the system every 0.1Å. This consists of particle positions, velocities and accelerations, as well as temperature, box dimensions, pressure, among other parameters. For each system, we choose some particular gaps and let them equilibrate longer. During our analysis, we will refer to the ”During Compression” and the ”After equilibration” sets of data. Hexane is a particular case in which both sets of data correspond very well throughout the compression process, indicating that the fluid was very close to equilibrium, if not in it, the whole time.

The smaller gaps had a longer computational box along x , so we cut the computational box along the x – *axis* for all the gaps so all of them would start the equilibration process with the same x length. The smaller gaps tend to take longer to equilibrate because of the lack of space, so having less molecules makes the equilibration time similar to the one of larger gaps.

By observing Fig. 32 for gaps larger than 14Å, we can see how hexane, whose average molecule length is 6Å, can move around around in the confinement and not form any type of layers. When the confinement is 9.7Å thick there are there are 2 layers and they are somewhat visible.

In Fig. 33, we can see side views of how hexadecane molecules arrange themselves inside the confinement. The combination of a stronger interaction to the gold than with other molecules results in a good surface layer seen even in the initial configuration of 36.6\AA . From then on, the tendency of long linear alkanes to pack together, fosters the formation of subsequent layers. One noteworthy feature seen in the side view plots of the computational box, Fig.33 is that the horizontal alignment of the long molecules with respect to the confining surfaces starts at the edge of the gap towards the bulk. When the system is compressed, some hexadecane molecules leave the confinement, and the ones close to the reservoir align horizontally. As we can see in the progression, this alignment seems to propagate towards the middle of the gap.

In pure phytane, Fig.34, it is very hard to see the layering because the molecules tend to spread across several layers. The layers are not separated, as could be noted from the molecular densities, where there was a non-zero density in between the high-density peaks. The largest gap at 36.7\AA is shown with a smaller radius to show the surface layer present through out the compression. During the compression from 36.7\AA to 15\AA the layers were not separated, until it reached a gap size of 14.2\AA where 3 good layers can be seen. Again for the gap with $D = 14.2\text{\AA}$, we also make the representation of the segments smaller to show the layering attained by phytane.

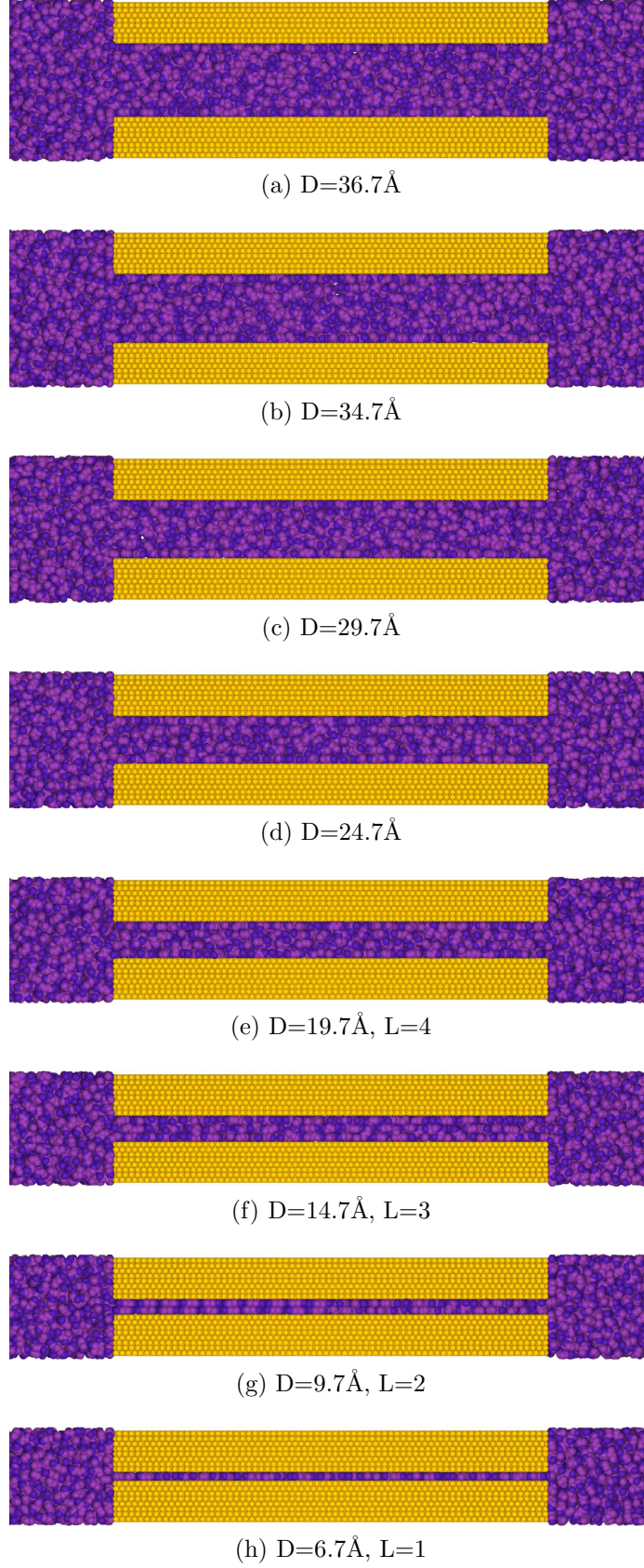


Figure 32: C6: Side view of the confinement for various well formed gaps. D denotes the thickness of the gap and L indicates the number of layers inside the gap, either independent or intertwined.

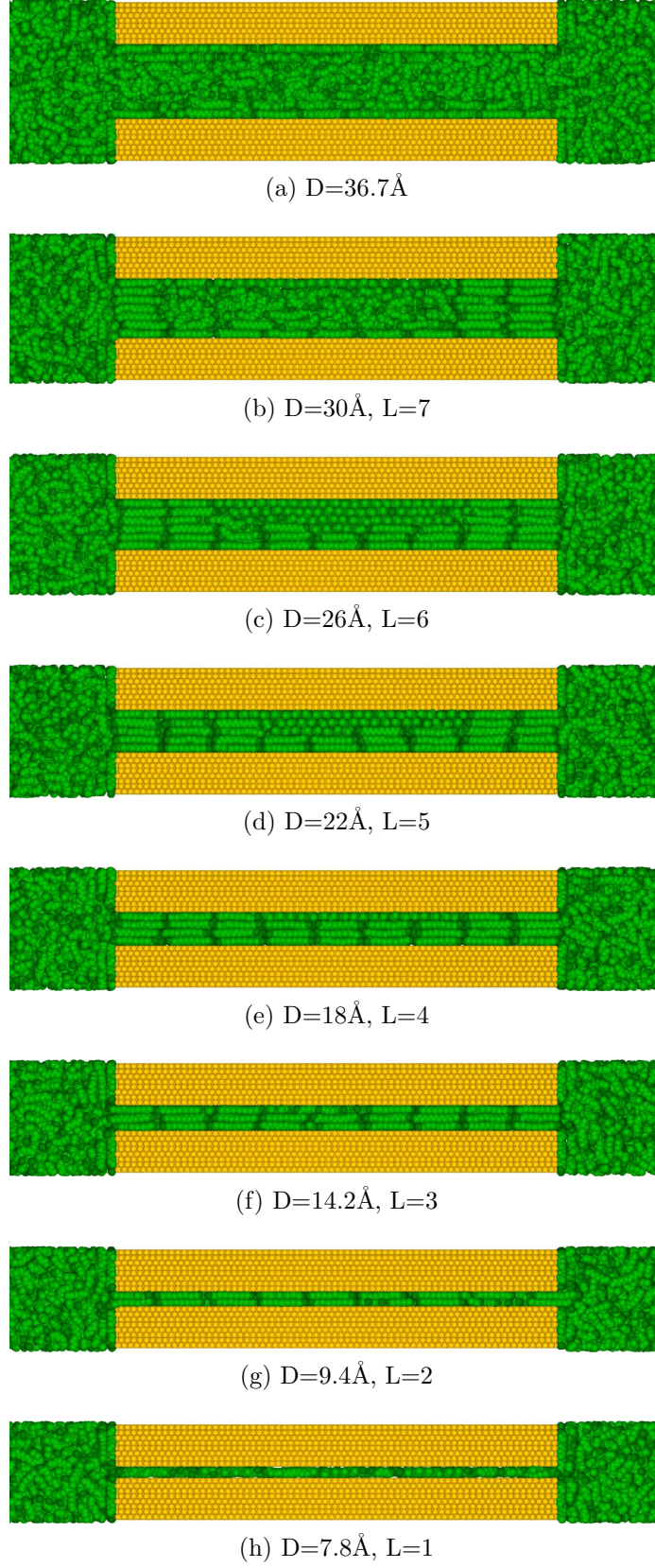
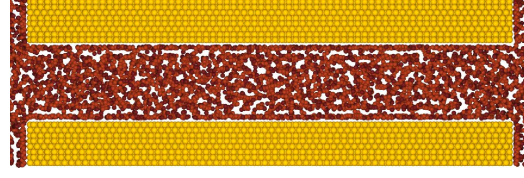
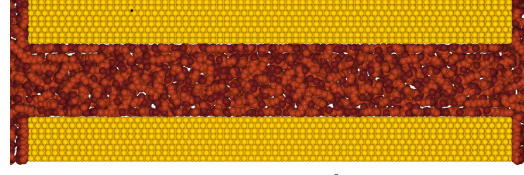


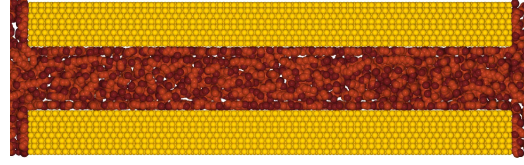
Figure 33: C16: Side view of the confinement for various well formed gaps. D denotes the thickness of the gap and L indicates the number of layers inside the gap, either independent or intertwined.



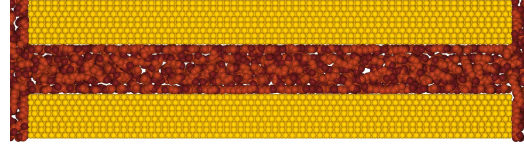
(a) $D=36.7\text{\AA}$



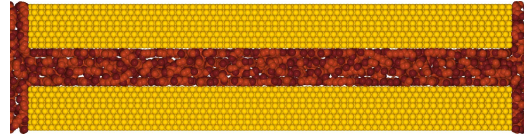
(b) $D=34.2\text{\AA}$



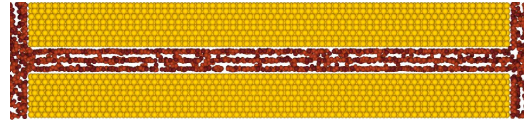
(c) $D=30.2\text{\AA}$



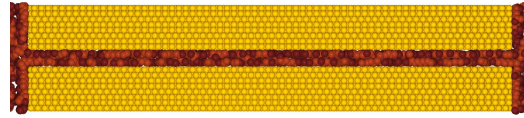
(d) $D=24.2\text{\AA}$



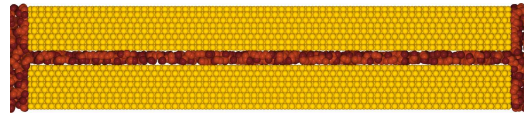
(e) $D=19.2\text{\AA}$, $L=4$



(f) $D=14.2\text{\AA}$, $L=3$



(g) $D=9.9\text{\AA}$, $L=2$



(h) $D=7.3\text{\AA}$, $L=1$

Figure 34: C20: Side view of the confinement for various well formed gaps. In Fig.34a, we present the phytane segments smaller to make evident the surface layer, it is similarly done in Fig.34f to show the 3 well formed layers

4.5 *Number of confined molecules during compression*

4.5.1 Hexane

Up to this point we have looked at individual quantities measured inside the confinement of some specific gaps, and we have observed that hexadecane has more structure than hexane and phytane. We have also looked at side views of the three systems while they underwent compression. From now on, we will plot quantities obtained as averages over all the confined molecules inside a gap, and plot them against the corresponding gap thickness. We will look at the number of confined molecules, the inlayer ordering, the solvation force and the coefficient of diffusion, all of them as a function of the gap size.

When we look at the complete evolution in the number of confined hexane molecules from a large gap of 36.7\AA to a gap 6.7\AA , in the top section of Fig. 35, we can see that the number of confined molecules presents a smooth decrease down to 3 layers, at which point we see a small step from 3 to 2 layers, and then a larger one from 2 to 1 layer. This may indicate that the hexane fluid is mostly liquid-like except for gaps less than 15\AA thick. At a gap size close to 14\AA , a considerable number of hexane molecules leave the confinement, then it slowly drains while it is compressed. Around 9\AA , a larger number of molecules leave suddenly before reorganizing as a single layer.

A solid-like fluid, instead of having a continuous outward flow of molecules, expels only large groups of molecules from the confinement, and otherwise doesn't expel any molecules. Hexane is not quite solid-like for small gaps, but shows some level of order. We will see this effect also in our other systems, to a higher or lesser degree.

The second section of Fig. 35, presents the number of hexane molecules inside the confinement but not on the surfaces, as the system is compressed from 36.7\AA down to 6.7\AA . We chose these molecules to be the ones whose center of mass was farther than 6\AA from the center of mass of the gold atoms. This distance was decided after careful inspection of the density profiles for all equilibrated systems, Figs. 12, 13 and

14, and it was observed that the second layer started after the 6Å from the surface.

This middle region shows a rather soft incline as the molecules are leaving the confinement from 4 to 3 layers. The last drop is when the middle region transforms from 3 to 2 layers, at which point there are no more non-surface molecules.

The third section shows the evolution of the hexane surface layer. The number of molecules in the surface layers remains unchanged until there are 3 well formed layers at 14.7Å. From that point, as the system is compressed the surface layers suffer dramatic changes to accomodate to the new gap thickness. When we see a drop in the number of molecules in the middle region, around 14Å, we see a spike in the number of molecules in the surface region coming from the middle region. Upon further compression, the surface layers are able to expell some molecules and then the system tries to return to their previous number of molecules per layer.

4.5.2 Hexadecane

When we observe the variation on the total confined hexadecane molecules during compression, we see a solid-like behavior on a much greater magnitude. For gap sizes greater than 30Å, there is continous drain of molecules towards the bulk. For thinner gaps, the total number of confined molecules decreases in sharp steps of approximately 400 molecules which is the number of molecules that fit in a layer. Otherwise, the system doesn't let any molecule leave the confinement, until it expells a whole layer in a few nanosecs. The time it takes to go from one step to the next is 1.8 ns, while it is compressed 0.2Å

A similar behavior is seen for the molecules in the middle of the confinement, the non-surface molecules. The layer that is expelled is part of the inner region of the gap. Upon inspection of the plot of number of surface hexadecane molecules versus gap size, we can see that when a whole layer is expelled the surface layer is somewhat disturbed but on a much smaller scale, only losing a few molecules each time. The

number of surface molecules lost in this process is larger when there are only 3 layers or less inside the gap. When there is only one layer inside the gap, the density is larger than compared to the usual surface layer.

4.5.3 Phytane

In the previous properties, we saw that both hexane and phytane lacked the level of structure seen in hexadecane. In the number of confined phytane molecules versus gap size, the behaviour observed in phytane resembles the one seen in hexane. While the system was compressed at gap sizes larger than 15Å there was a slow drain of molecules leaving towards the bulk. At a gap size of about 14Å, a group of molecules were expelled from the confinement, then there was a slow outflow of molecules, and approximately at 9Å a larger group of molecules left the confinement. The molecules in the inner region behaved in a similar way. The phytane surface molecules showed no change during the process of compression a slight disturbance at 14Å when the system transitioned from 3 to 2 layers. When there were only 2 layers, the number of phytane molecules in the surface layer increased slowly until it reached a point where it managed to expelled a small number of molecules to become a much denser surface layer than at any point in the compression. We can mention here that phytane molecules tend to lie across several layers, so leaving the confinement when the gap size is less than 9Å is extremely hard.

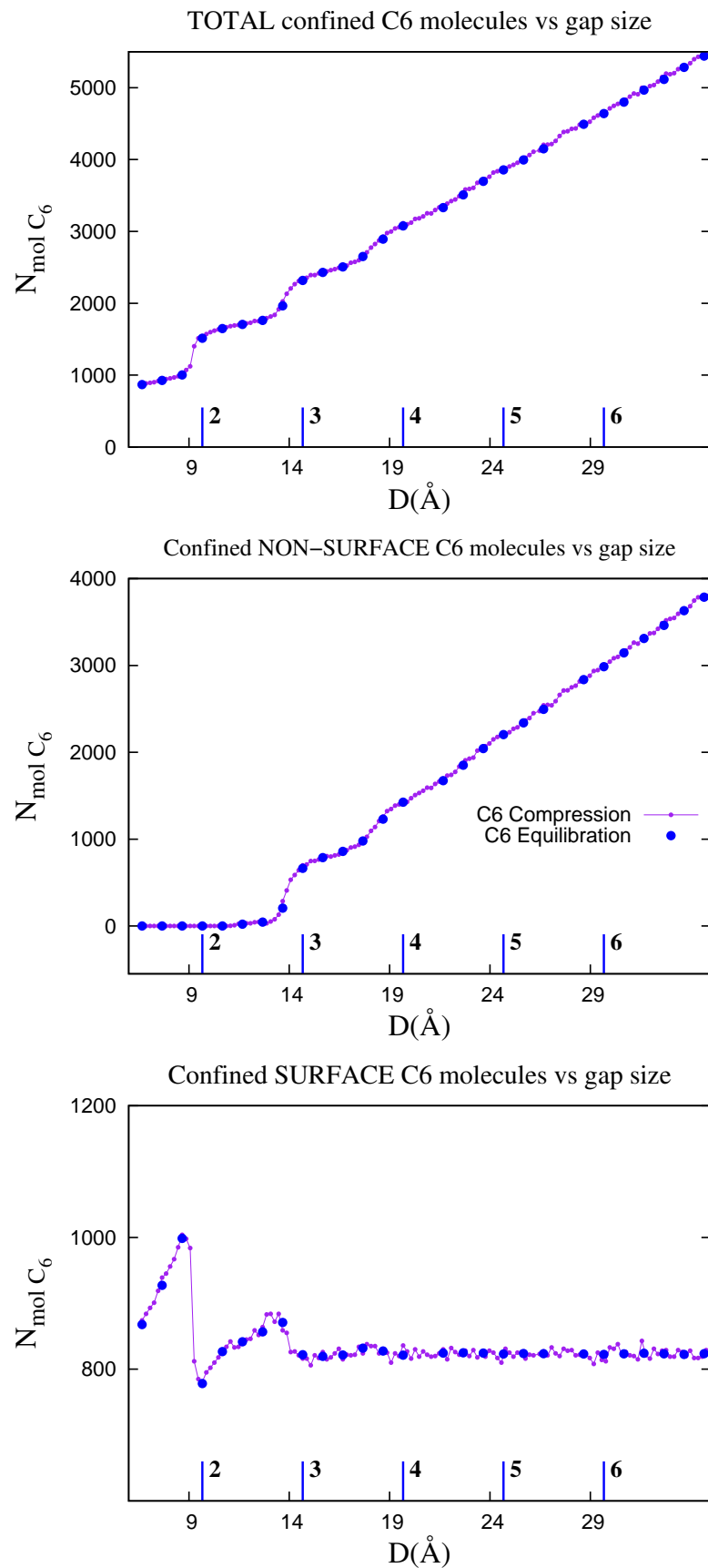


Figure 35: Number of confined hexane molecules versus gap size

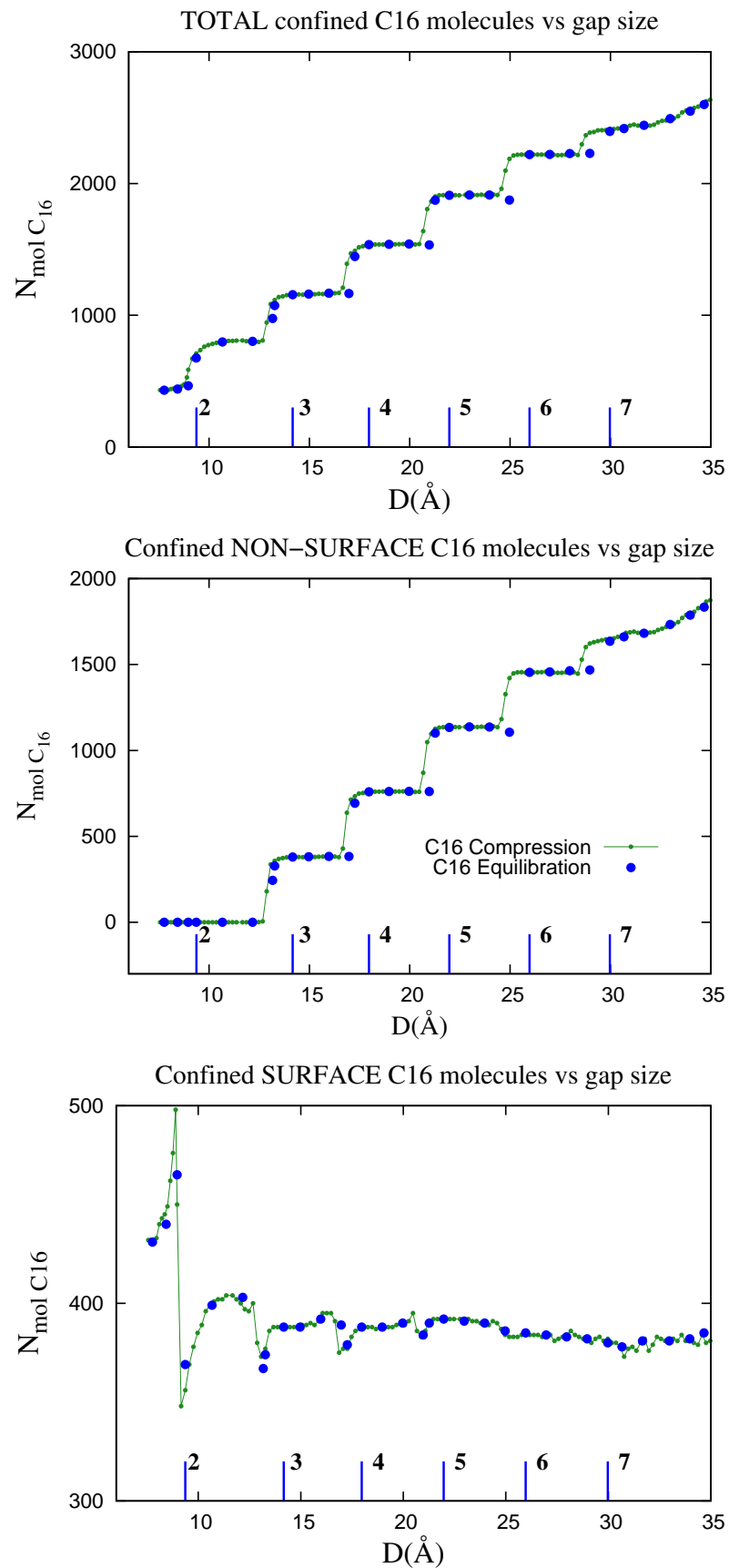


Figure 36: Number of confined hexadecane molecules versus gap size

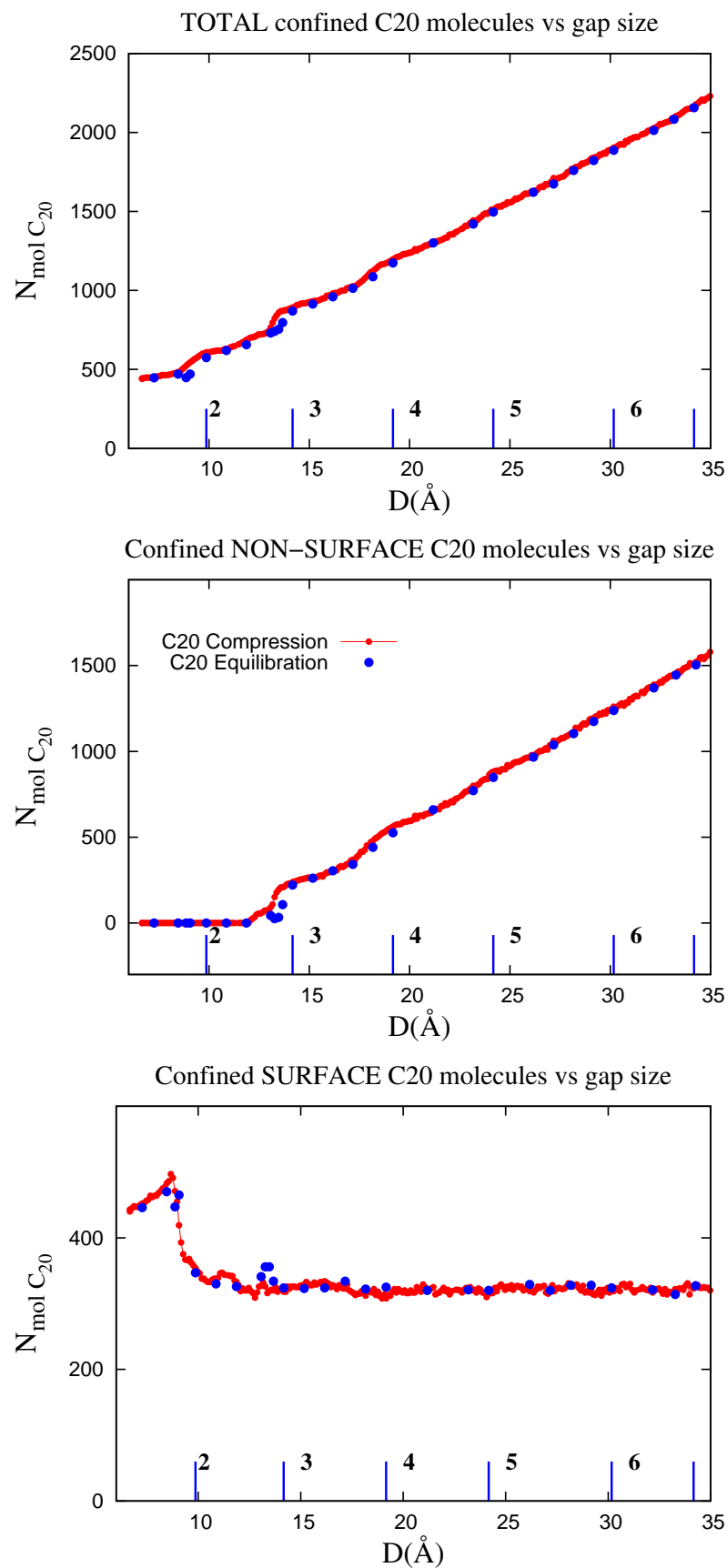


Figure 37: Number of confined phytane molecules versus gap size

4.6 Distribution of surface molecules during compression

4.6.1 Hexane

In Fig.39, we will see how hexane molecules arrange inside on the surface. Hexane molecules don't tend to aggregate in patches, or show any particular ordering on the surface, or the inner layers. Remember that we previously said that from the step-like phenomena shown in the number of confined molecules versus gap size, we inferred a solid-like behaviour where groups of molecules are expelled simultaneously. In Fig. 35, we saw that the jump in the number of molecules inside the confinement from 2 layers to 1 layer is larger than from 3 to 2 layers. Hexane does show some tendency to pack in domains when there are 2 layers inside the confinement. The steps in the number of confined molecules can be explained by the larger extensions of the agglomeration of hexane molecules in the surface layers when there are only 2 layers as compared to when there are 3 layers, as seen in Fig.38.

In Fig. 39, we can see a top view of the hexane molecules in the bottom surface for the gaps that show well ordered layers. In all the gaps, except where $D = 9.7\text{\AA}$, the hexane molecules don't show any particular orientation.

4.6.2 Hexadecane

When we look at Fig.40 we can see how the hexadecane molecules in the bottom surface are arranged during the compression. The top right figure is the initial configuration with our largest gap thickness of 36.7\AA . We already see a tendency of the hexadecane molecules to orient in the same direction as several of the molecules around them forming domains with a certain predominant alignment. Between the initial gap size of 36.7\AA and the next shown a 30\AA a steady outward flow of hexadecane molecules has left the confinement and joined the reservoir, as seen in Fig.36. As we go down the right column, we see that some domains have merged and become larger. In the configuration plot at 30\AA , we see 2 directions competing, towards the

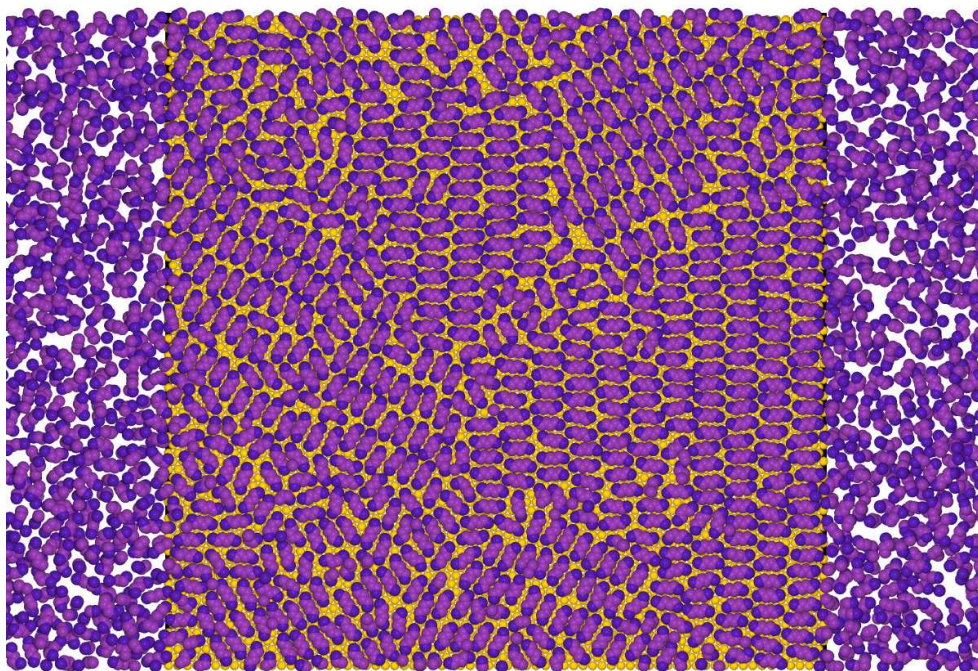


Figure 38: Some alignment of the hexane molecules is evident when there are only 2 confined layers, $D = 9.7\text{\AA}$ and $L=2$.

bulk and perpendicular to it.

Let's remember that our use of periodic boundaries makes our system effectively infinite along the y – axis, which means that each of the plots can be replicated towards the top and bottom of the page forming a infinitely long slab, with a reservoir to the left and right. The extension of the slab along y , added to the tendency of the linear molecules to pack together, explains the vertical ordering in the middle of the gap. The presence of a slow drain of molecules at the beginning of the compression, reoriented some molecules towards the bulk.

In hexadecane, the molecules leave the confinement as a whole layer and disrupt the surface layer in the process very little except at 4 layers, as we previously saw in the bottom picture of Fig.36. In this Fig.40, we can see that virtually no change happened to the surface layer when the system was compressed from 6 to 4 layers. When the system had 4 layers and expelled one middle layer to become 3 layers,

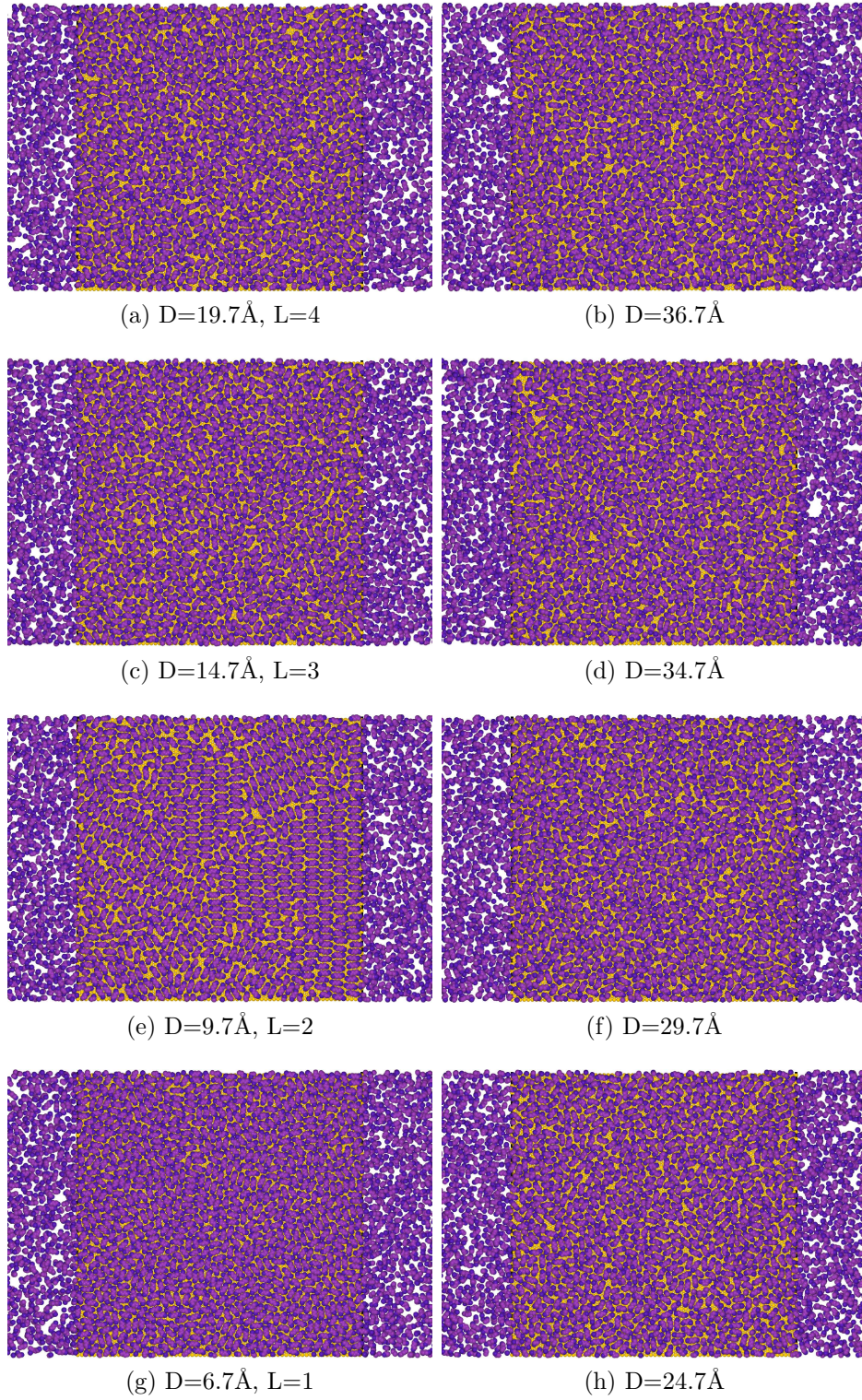


Figure 39: Top view of the bottom surface layer for hexane in well formed gaps. D denotes the thickness of the gap and L indicates the number of layers inside the gap, either independent or intertwined.

the surfaces were perturbed enough to break some domains. At 3 layers, we can see smaller domains and a competition between the 2 orientations. Some molecules are reorienting themselves towards the bulk. When observing the rearrangement of molecules during the compression, we can see that the order seems to abruptly end when there are 2 layers inside the confinement. We had seen that for larger gaps, the hexadecane molecules on the surfaces had formed large domains either towards the bulk or perpendicular to it. When there were only 2 layers, each layer interacted strongly with the gold surface but at the same time the hexadecane molecules tend to pack tightly with other molecules and form domains. By careful observation of both surfaces in Fig.41, we can see that there is intralayer ordering because molecules are forming smaller domains but with molecules belonging to both surfaces.

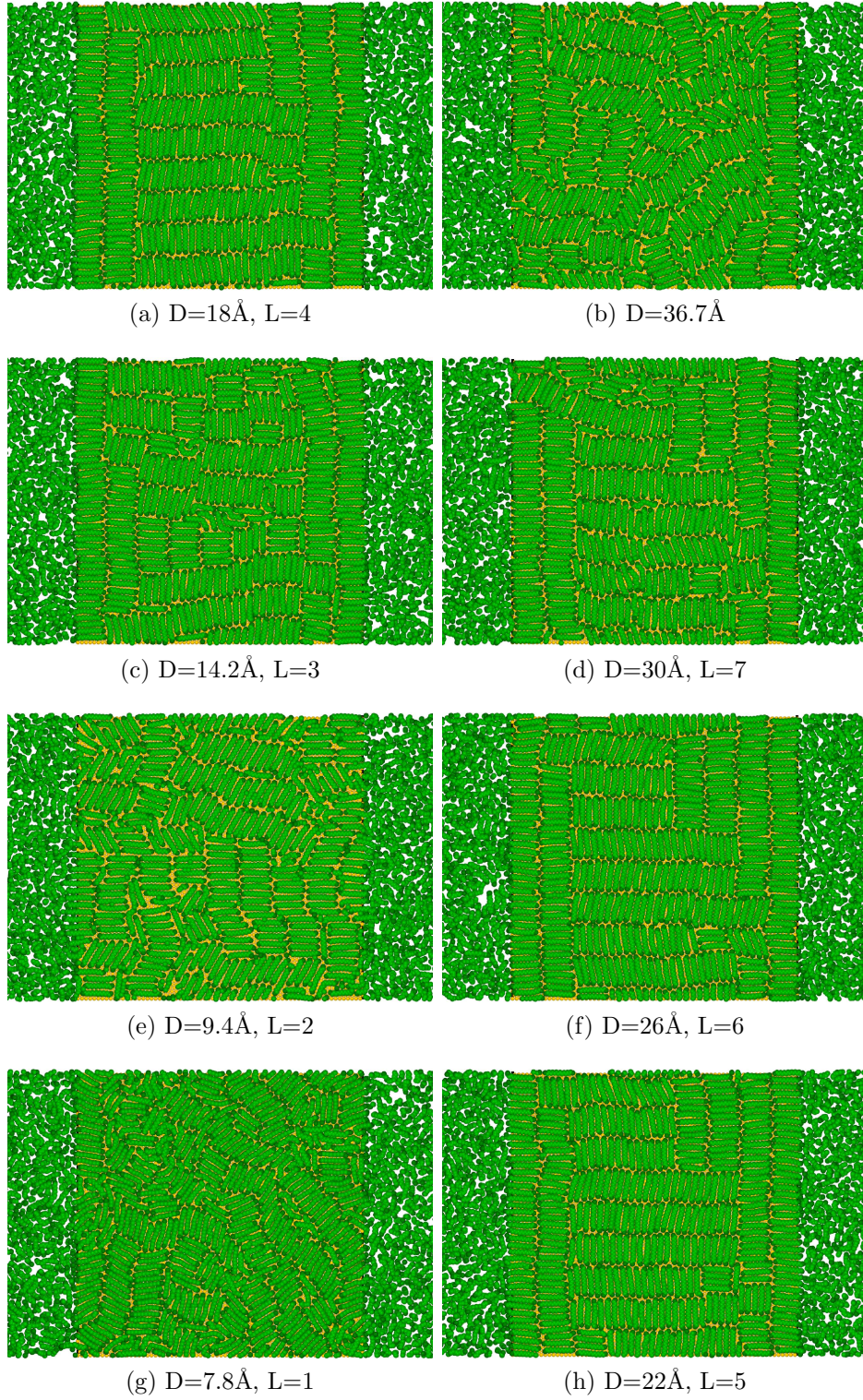


Figure 40: Top view of the bottom surface layer for hexadecane in well formed gaps. D denotes the thickness of the gap and L indicates the number of layers inside the gap, either independent or intertwined.

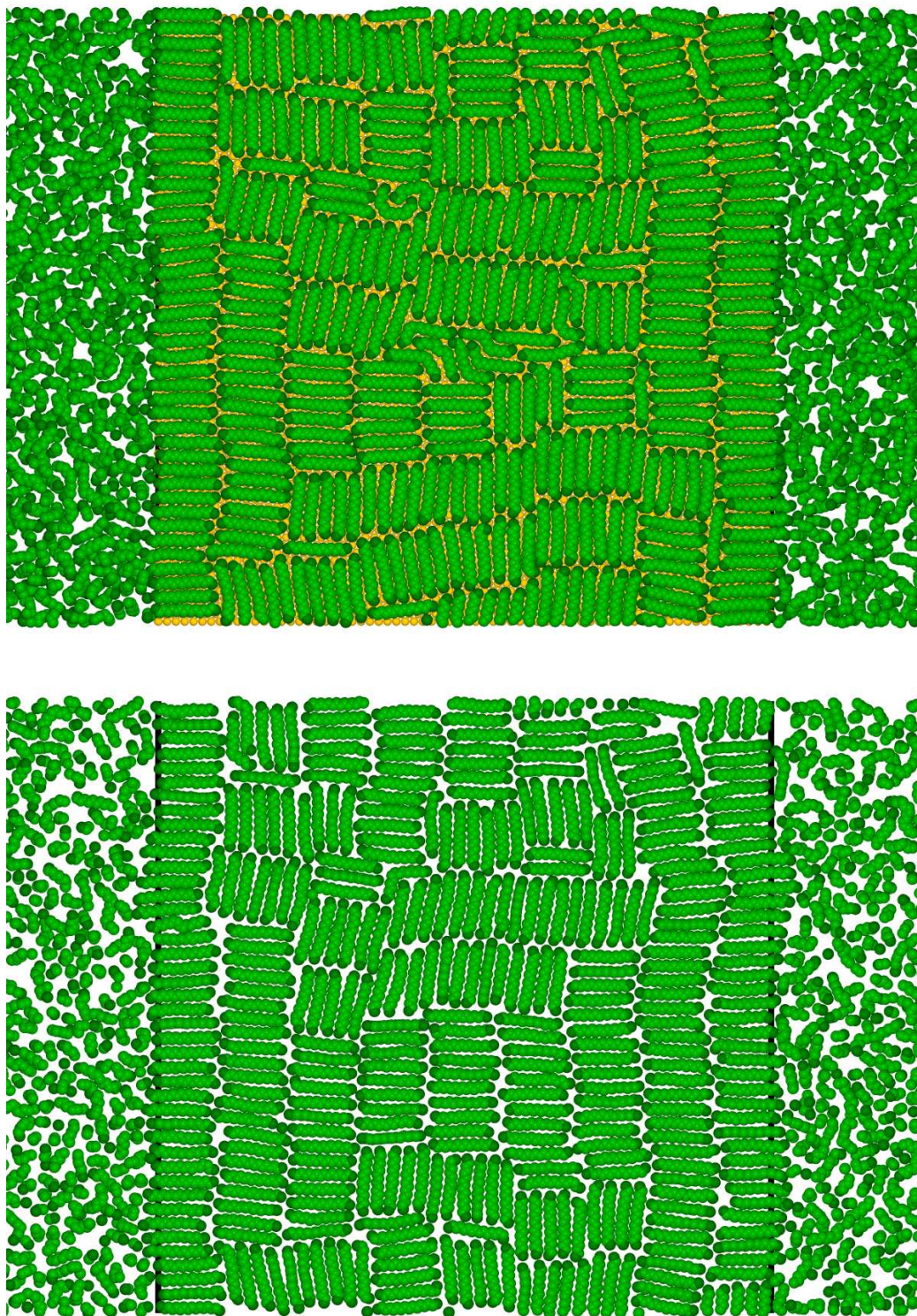


Figure 41: The hexadecane molecules in first (top image) and second layer (bottom image) have a similar distribution, showing some intra-layer ordering.

4.6.3 Phytane

Phytane's branches give it a larger degree of freedom to attain various conformations not easily reached for hexadecane. These branches on the other hand, don't allow phytane to form large domains with other molecules, as seen in Fig.42. In Fig.43, we can

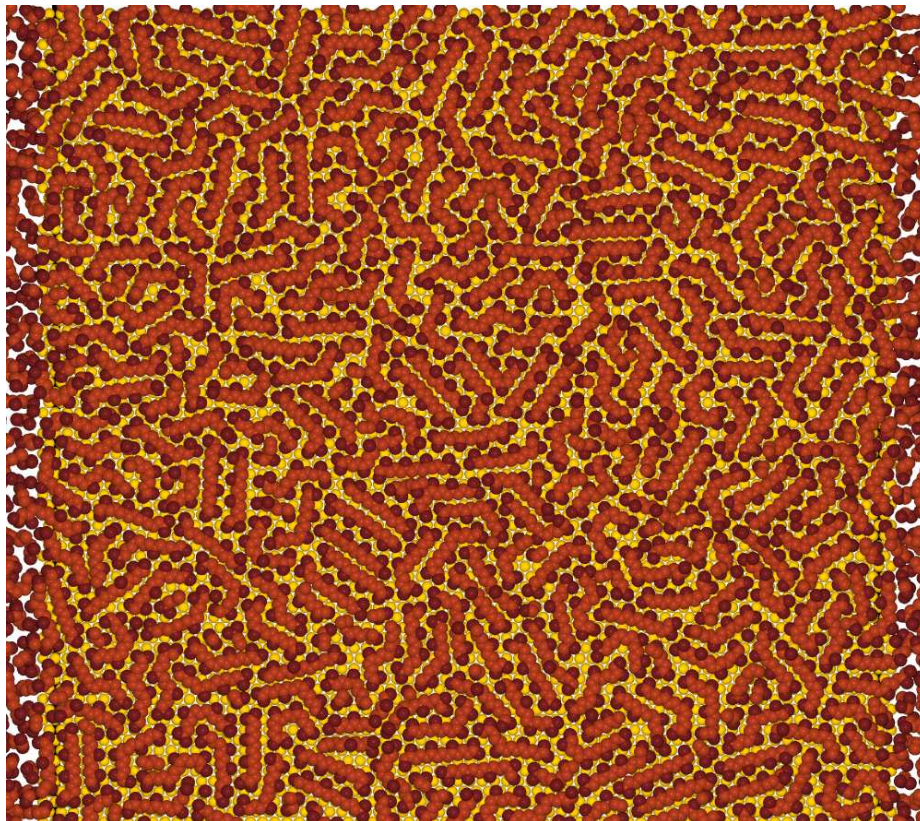


Figure 42: Top view of surface layer when there are 3 layers inside a gap with thickness of 14.2\AA . At this gap spacing, the 3 layers are mostly separated one from the other, and most of the phytane molecules are completely laying parallel to the gold surface.

see the evolution of the bottom layer during slow compression. The molecules don't seem to aligned any particular direction or form clear domains of several molecules.

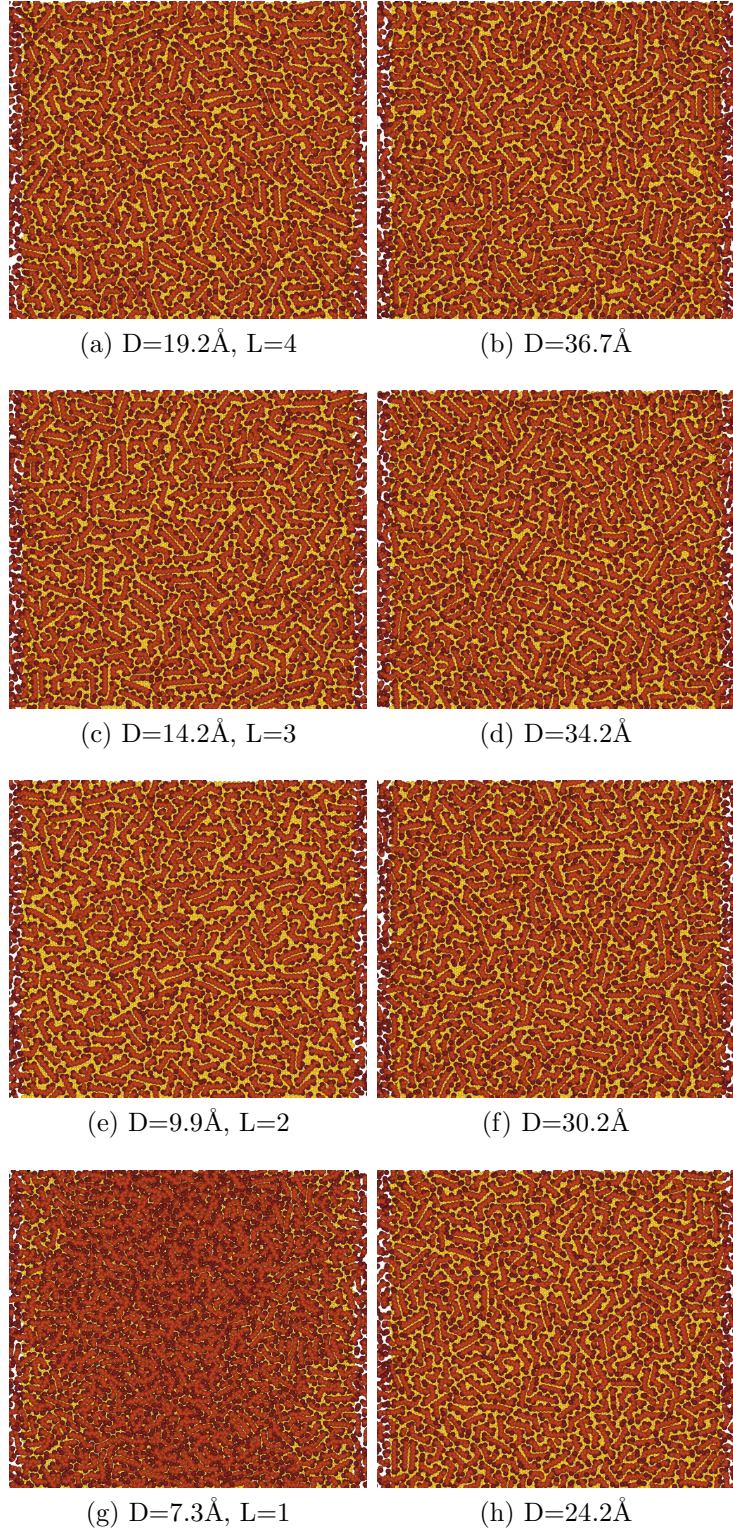


Figure 43: Top view of the bottom surface layer for phytane in well formed gaps. D denotes the thickness of the gap and L indicates the number of layers inside the gap, either independent or intertwined.

4.7 *In-layer alignment during compression*

To quantify the degree of alignment of the alkane molecules, we can calculate the average $\cos^2(\phi)$ for the molecules in the whole confinement, as well as in the surface region and in the middle region. The surface molecules are those whose center of mass is 6\AA from the center of mass of the gold atoms. We can see in both Figs. 46

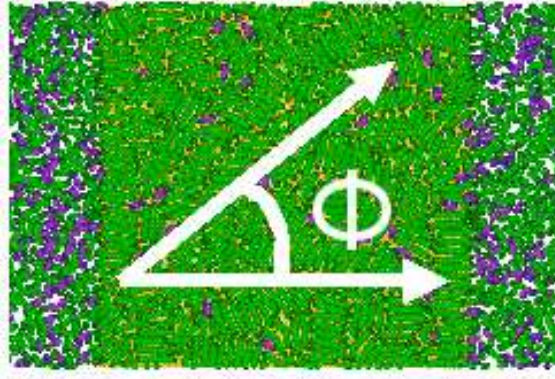


Figure 44: ϕ is the angle, on a plane parallel to the gold surface, with respect to a line connecting the reservoirs. The line at $\phi = 0$ is known as the director.

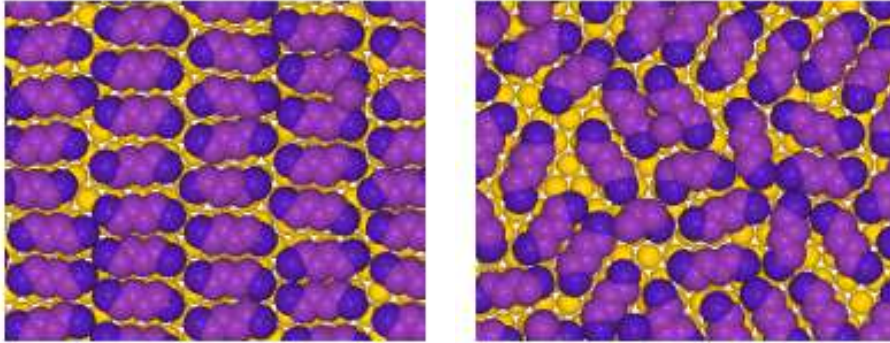
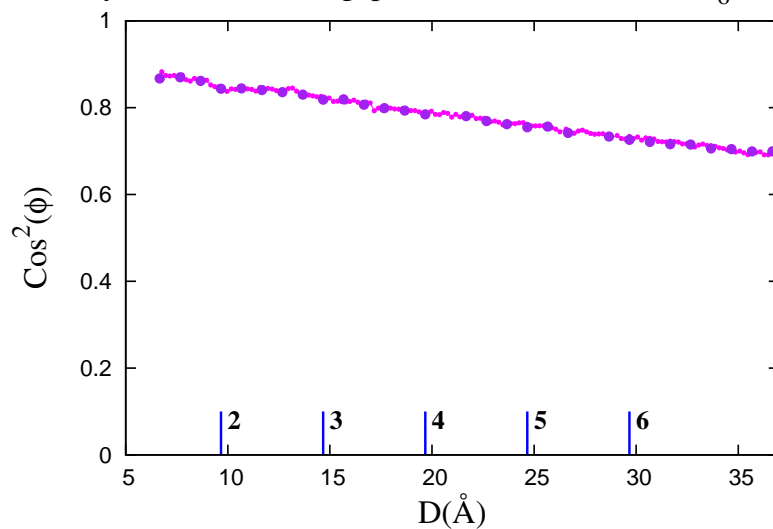


Figure 45: $\cos^2(\phi)$ for molecules along the direction is equal to 1, while it is $1/3$ for molecules with an isotropic distribution

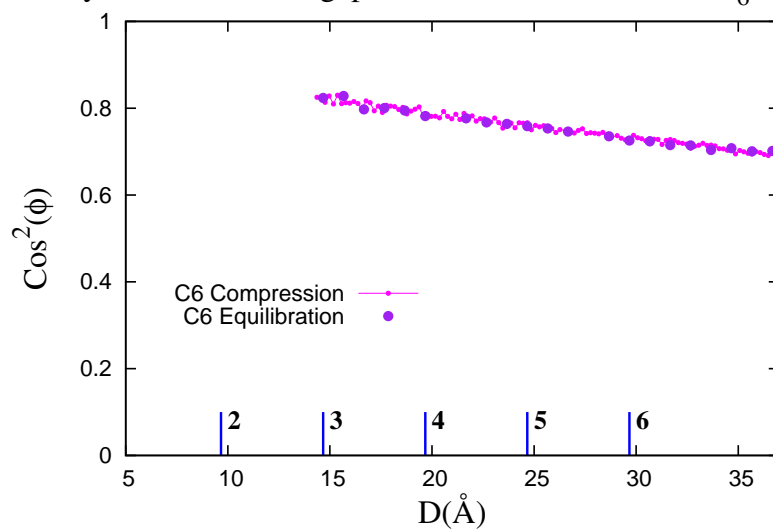
and 48, that the average orientation for hexane and phytane, increases as the system is compressed, perhaps due to the smooth outward flow of molecules. In the pure

hexadecane case, there is no increase in the alignment of the molecules due to the large domains. The surface and inner region behave in a similar way, with perhaps slightly higher values for the non-surface region.

In-layer orientation vs gap size for ALL confined C_6 molecules



In-layer orientation vs gap size for NON SURFACE C_6 molecules



In-layer orientation vs gap size for SURFACE C_6 molecules

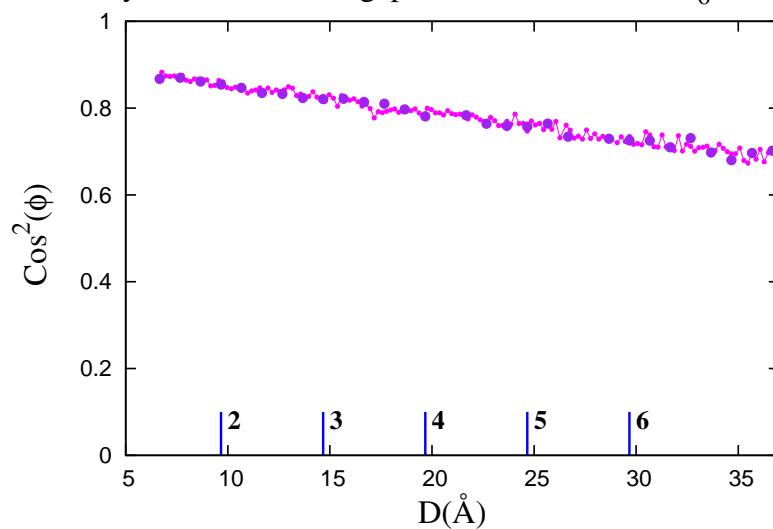
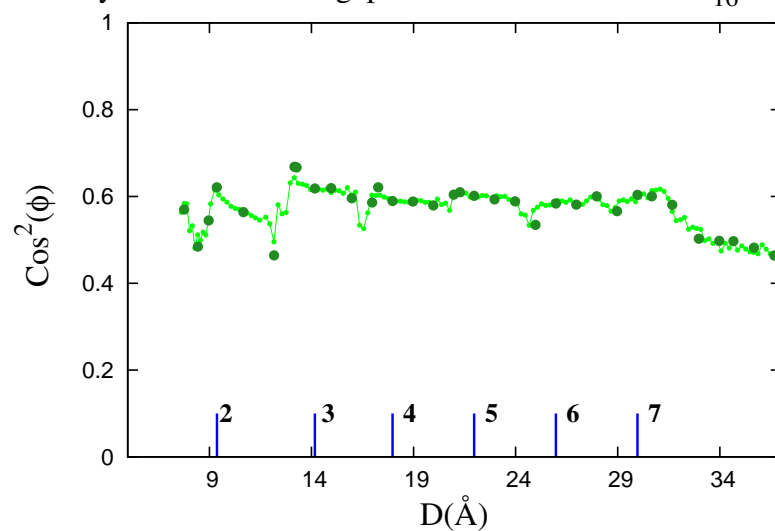
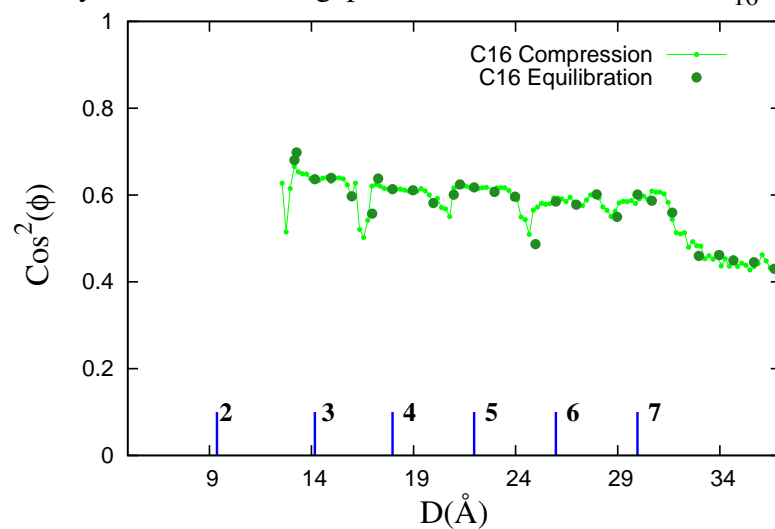


Figure 46: Inlayer orientation in pure hexane: $\cos^2(\phi)$ versus gap size.

In-layer orientation vs gap size for ALL confined C₁₆ molecules



In-layer orientation vs gap size for NON SURFACE C₁₆ molecules



In-layer orientation vs gap size for SURFACE C₁₆ molecules

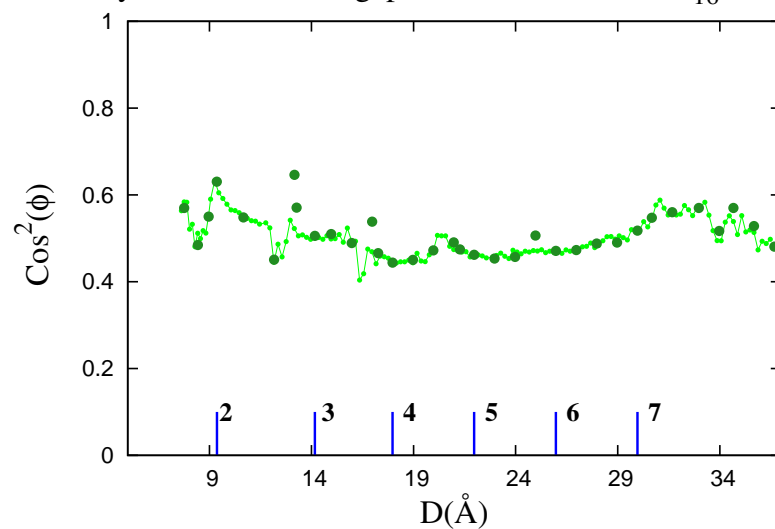
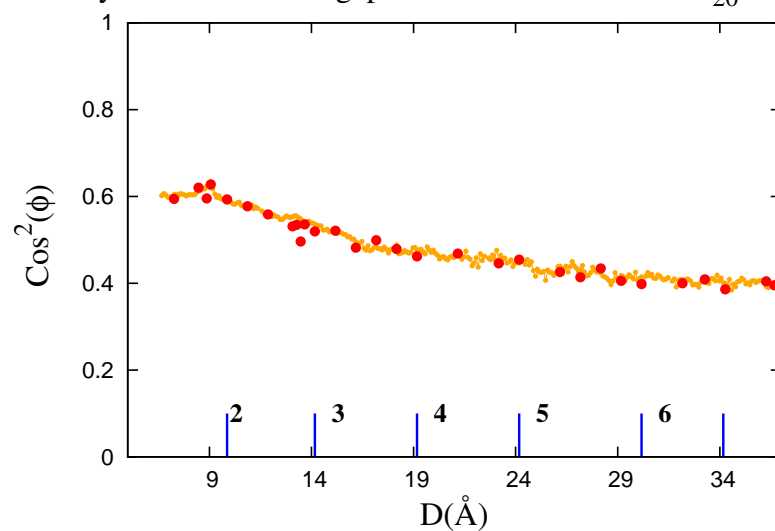
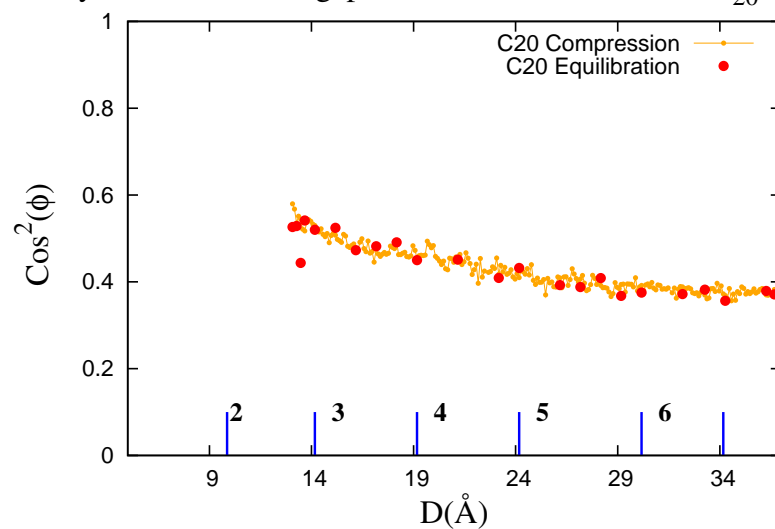


Figure 47: Inlayer orientation in pure hexadecane: $\cos^2(\phi)$ versus gap size.

In-layer orientation vs gap size for ALL confined C₂₀ molecules



In-layer orientation vs gap size for NON SURFACE C₂₀ molecules



In-layer orientation vs gap size for SURFACE C₂₀ molecules

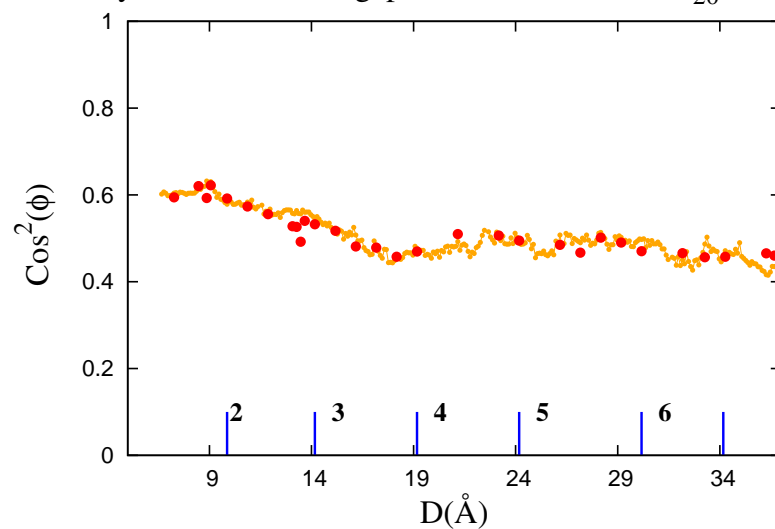


Figure 48: Inlayer orientation in pure hexane: $\cos^2(\phi)$ versus gap size.

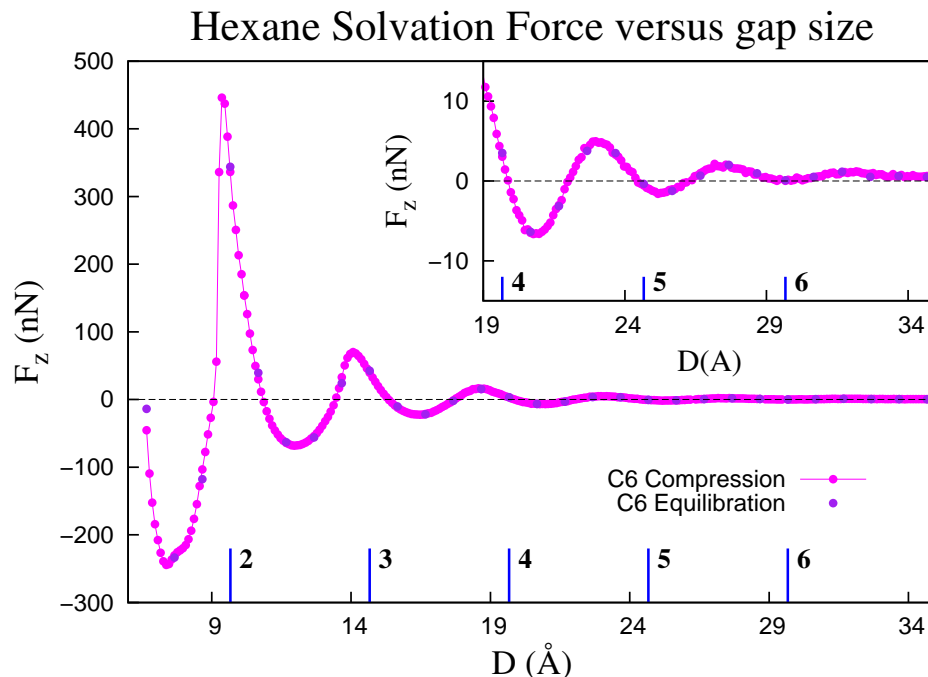


Figure 49: Solvation force for pure hexane. Top inset: Vertical zoom after 18Å.

4.8 Solvation Force during compression

During the compression process, we save configurations of the system every 0.1\AA , as I have mentioned before. From these configurations, we choose some gap sizes to let them evolve longer in separate processes until they reached equilibrium. In the case of hexane, we evolved configurations 1\AA apart, which means that we equilibrated 30 configurations, starting at 36.7\AA down to 6.7\AA . If the features in the curve are 2 nanometers in size, then evolving configurations every 1\AA would be fine. In the case of hexane, an interval of 1\AA was sufficient, but in hexadecane and phytane the behaviour of the fluid changes in a matter of 1\AA , so configurations have to be evolved fractions of angstroms apart to be able to detect small changes in the system. Let's remember that our rate of compression is 1\AA in 9ns , or approximately $0.1\text{\AA}/\text{ns}$. The solvation force is the force experienced by the confining surfaces and exerted by the fluid. For large separation of the surfaces, the force is equal to the pressure in the fluid times the area of the surfaces. In our particular case, our fluid is in contact

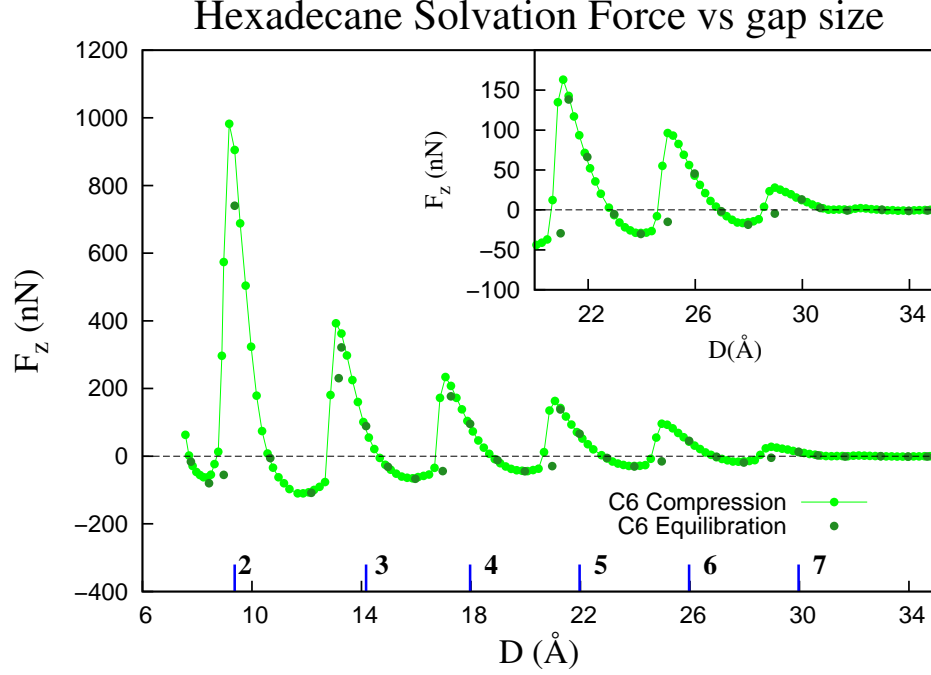


Figure 50: Solvation force for hexadecane. Top inset: Vertical zoom after 20Å.

with a reservoir kept at $P = 1\text{atm}$, maintained through variations of the size of the computational box. The dimensions of the gold block are 200.5\AA along x -axis and 200\AA along y -axis, for a total area of 40100\AA^2 . Since $1\text{atm} = 101325\text{Pa}$, the force for large separations is close to $0.04nN$, but as the system is compressed down to a few molecular layers this force oscillates with strengths as high as $1000nN$ and as low as $-250nN$. This values depend on the system being compressed.

In the same plot, we present the force obtained during compression, smaller dots every 0.1\AA , as well as the ones obtained from configurations that were further equilibrated, smaller dots at larger intervals. In Fig. 49, the purple dots denote the solvation force during compression, while the blue dots denote the force experienced after further equilibration. Each of these equilibrated points were made to run approximately between 5 and 7ns. As you can see in the force curve, the equilibrated points follow the curve obtained during compression, which means that during the equilibration process the number of molecules oscillated around a value very close to

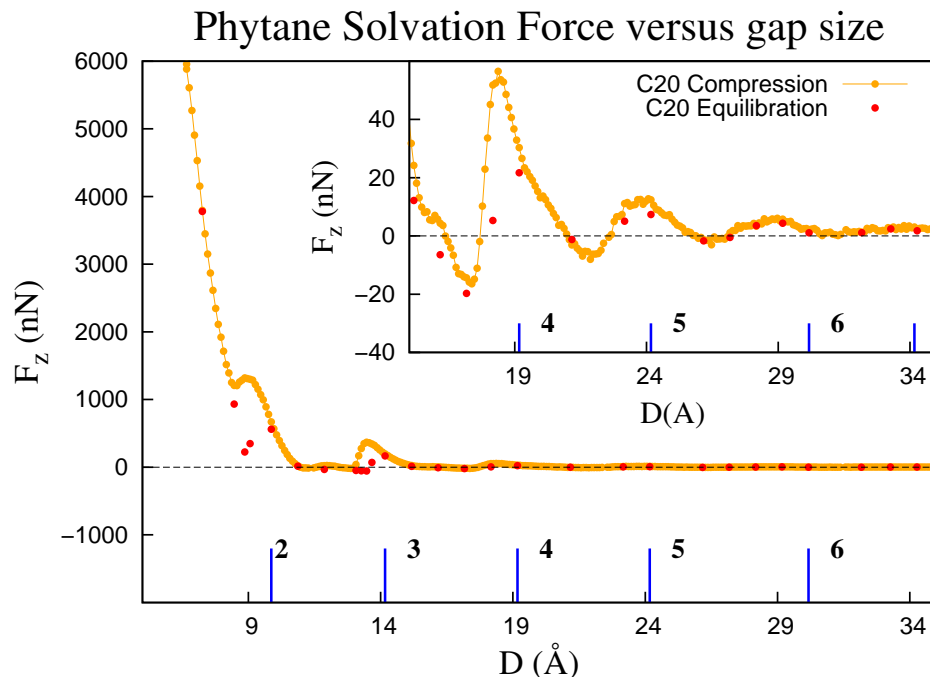


Figure 51: Solvation force for phytane. Top inset: Vertical zoom after 15Å.

the value during compression. This suggests that the system was in equilibrium as it was being compressed, hexadecane and phytane are mostly in equilibrium except for nanosecond intervals in which a group of molecules leave the confinement. The solvation force for hexane shows oscillations whose peaks increase as the gap size is decreased. The valleys also become deeper as the system is compressed. The shape of the peaks is symmetrical.

The inset of the curve shows a vertical zoom to show more detail about the force oscillations at larger gaps. Pay special attention to the difference in scale for the force curve, between the main plot and the inset.

In Fig.50, we can see the solvation force versus gap distance for hexadecane, and when compared with the shorter hexane the oscillations are higher in strength and appear at larger gaps. The oscillations seem to have a consistent period, which is approximately $4.0 \pm 0.1 \text{ Å}$. This distance is similar to the diameter of the hexadecane molecule. The peaks in hexane's force curve are spaced farther apart because its

layers are not as well defined as hexadecane where almost all the molecules are laying parallel to the surface.

In the hexadecane case, we observe that some equilibrated points don't correspond to the points obtained during compression, namely some force points to the left of the peaks, which indicates that those gap sizes are mechanically unstable. These unstable configurations start with a certain number of confined molecules exerting a force on the surface, but after they are left to equilibrate at a fixed gap size several hundred molecules leave the confinement, the force drops sharply. They are allowed to run until the solvation force and number of confined molecules versus time reaches a plateau. This unstable change can be seen in Fig.50 to the left of the peaks, the equilibrated points have considerably lower values than the points obtained during compression. This instability is also seen in Atomic Force Microscope experiments, when the gradient of the attractive force exceeds the elastic force constant of the measuring device only allowing to record the right side of the force peaks.

How does the presence of branches modify the force exerted on the confining surfaces? If we compare the solvation force for phytane with the solvation force for pure hexadecane, there are several similarities and some differences. Hexadecane shows a very uniform behaviour, with peaks 4\AA spaced apart, the strength of the peaks increasing slowly, as well as the depth of the valleys, the shape of all the peaks is asymmetrical, further enhanced after equilibration. The pure phytane system also shows oscillations, but they don't have a uniform spacing between the peaks. For large surface separations, the strength of the peaks is very small, in the order of a few nanoNewtons, and increases sharply to the point where the force at 6\AA is close to 4000\AA , not shown in the plot to be able to show smaller features. This is due to the size of the branched molecules and the inability of some of them to rotate to accommodate the confining space inside the gap.

The peaks in the solvation force for pure phytane after 20\AA , seem symmetric in

shape as we previously saw in Fig. 51, but as the system is compressed the shape of the peaks becomes greatly asymmetric. The peaks corresponding to the transition between 4 to 3 layers, and 3 to 2 layers, have a very shallow valley, as compared to the valley in hexadecane. After inspection of the branched density in Fig.22, we noticed that they happen when the system is transitioning from layers with phytane molecules whose plane is parallel to the gold, to layers with some molecules whose branches are perpendicular to the surfaces.

Another element that is different in both cases is the discrepancy between the force during compression and the force obtained after further equilibration. In the hexadecane case, after equilibration the highest point in the peak dropped to zero or below, implying that configuration was unstable, and the point 0.2\AA to the right of the peak became the highest point after equilibration; but in the case of pure phytane the point 0.2\AA to the right of the peak was also unstable making the highest point after equilibration to be further down the slope, which might suggest that during compression more configurations are unstable compared to the pure hexadecane fluid.

At the end of the compression, at 6\AA there is one layer of hexadecane and the force is close to zero. For the branched alkane confined to separations below 8.5\AA when the fluid is trying to transition to one layer, the force increases up to 6000nN at 6\AA . This has to do with the fact that the diameter of the phytane molecule is close to 4.4 on the side with no branches, but it can measure close 8.5\AA along the other dimension because of the branches. If some molecules were not able to turn, so that their plane is parallel to the gold surface, then it will take a great force to bring the surfaces together. The whole scale is shown in Fig. 51.

The height of the peaks in the pure phytane case increases as the gap size decreases, and this increase is higher than the decrease of the valleys. The magnitude of the solvation force for phytane, for comparable gap sizes larger than 10\AA , is in between the strength seen in hexane and hexadecane. The hexane fluid is composed of small

molecules and behaves mostly liquid-like opposing the compressing surfaces with little pressure compared to the other 2 pure fluids. Phytane, which has showed liquid-like features, is able to exert a large force against the surfaces for gaps less than 9\AA because some of its molecules are stuck. We could have stopped the compression at 9\AA for the branched systems, but we wanted to check whether they were able to rearrange themselves.

All 3 fluids present 2 layers at gaps 10\AA thick because the diameter of the segments is approximately 4.4\AA . When the gaps are compressed to 9\AA hexane and hexadecane after expelling a group of molecules are able to convert to a single layer. Phytane, even after expelling some molecules, is not able to transform to a single thin layer because of its branches, so it exerts a extremely large force in the order of 5000nN . After compression, some branched molecules leave the confinement and the force drops when the molecules are reorganizing into one layer. The force increases once more for the final equilibrated value indicating that the gap size was too thin for the system.

4.9 Diffusion during compression

Another property, besides the solvation force and the number of confined molecules, that can give us an indication on whether the system is solid-like or fluid like is an indicator of the mobility of the particles. It can either be the calculation of the viscosity of the system or the diffusion of the molecules. The viscosity of the system can be calculated through a Green-Kubo relation, which requires an integration over the stress autocorrelation function. From inspection of the other parameters of the system, it is evident that our system transitions through solid-like and liquid-like states as it is compressed, which means that the ability of different gaps to recover from an outside perturbation would vary with the gap size. This would translate into the need for time integration limits that would be orders of magnitude different from one gap to the other, because the stress correlation function would decrease almost to zero much faster in the liquid-like state than in a solid-like state where the time for a perturbation to dissipate completely would take time intervals several order of magnitude because of the level of crystallization of the fluid.

For this reason, we chose to calculate the coefficient of diffusion for the molecules of the system. The self-diffusion coefficient is given by

$$D = \lim_{t \rightarrow \infty} \frac{\langle |r^2(t + t') - r^2(t)| \rangle}{2dt} \quad (23)$$

where d is the number of dimensions. In our case, $d=2$ because we will only be interested in the diffusion of the molecules in the inner region, in a plane parallel to the confining surfaces. The molecules on the surface have a slower diffusion than the ones freely moving in the inner region. Since our surface layers combined have a thickness of approximately 10\AA , our inner region goes from less than 27\AA for our largest gap, to 4\AA when the gap is 14\AA thick. The vertical spacing is quite small so we will not focus on the vertical displacement, but only on the diffusion on the xy plane.

For comparison purposes, we calculated the displacement in the reservoir regions to make sure than the diffusion coefficient along the 3 directions were similar. In order for the displacement along the x - *axis* to be symmetrical, we couldn't include in our calculations the molecules in the reservoir that were close to the gold surfaces or the gap, because their displacement to the right wouldn't be the same as towards the left. Since we can actually look at the reservoir, as the fluid from the right of the confinement until the next image block appears, the reservoir region can be 200Å wide.

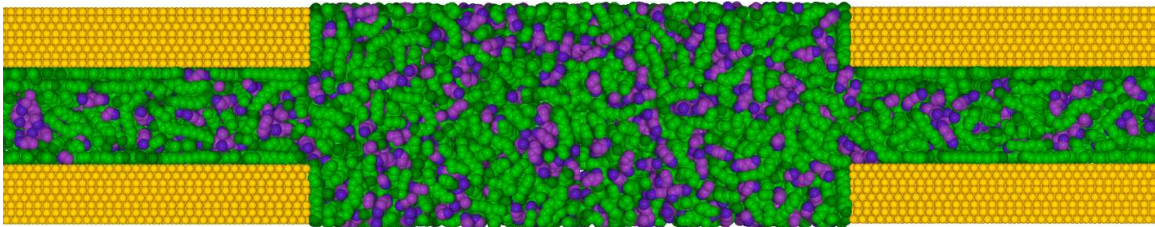


Figure 52: Side view of the reservoir region in between two consecutive confinements.

The diffusion can be calculated over several time origins, which ideally are not correlated. For each time origin, the displacement squared versus time averaged over all the chosen molecules should give a linear line, after a short transient. If the system is indeed in equilibrium, then the slope of the lines starting at different time origins should be very similar. We average the displacement squared for different time intervals, over all the time origins, which gives us one plot for the displacement squared versus time interval.

For the molecules in the reservoir, we've chosen molecules whose center of mass are located inside a infinite vertical 50Å slab in the middle of the reservoir. All the molecules can move 50Å in all directions with the same probability. The time range used to calculate the displacement squared was such that the molecules wouldn't get closer to the gold surfaces, and would behave as in the bulk.

To calculate the diffusion inside the confinement, we chose the molecules whose center of mass was in a horizontal slab in the middle of the confinement that would

extend from -50\AA to 50\AA , and 6\AA away from the gold surfaces. This way, all the molecules would be able to move 50\AA to the right or left with the same probability. The time used in the computations was such that the molecules wouldn't be able to leave the confinement in that time. The diffusion was calculated only for the gaps that were further evolved because we could check if they were close to equilibrium.

4.9.1 Hexane

The coefficient of diffusion for the hexane molecules decreases rather smoothly while the system is compressed. There is a small drop when the system goes from 4 to 3 layers. This step is enhanced when we plot the diffusion in logarithmic scale.

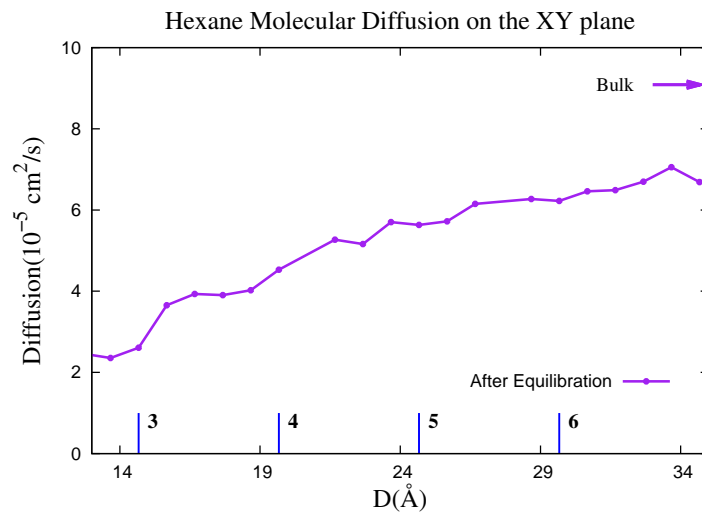


Figure 53: Hexane coefficient of Diffusion versus gap size

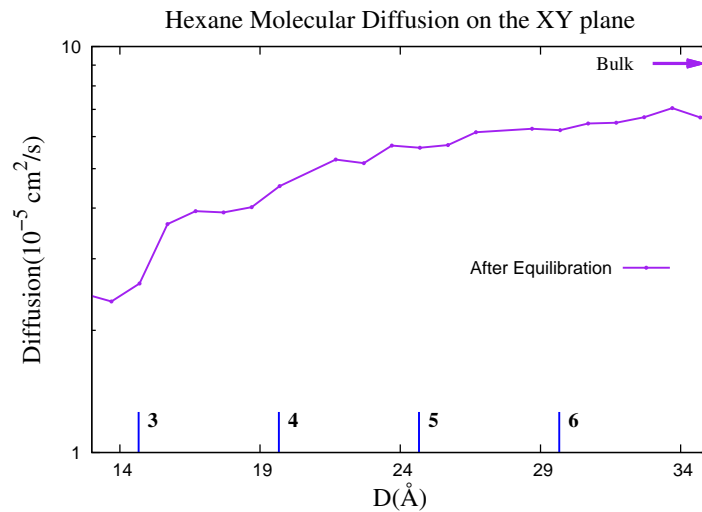


Figure 54: Hexane coefficient of Diffusion versus gap size in logarithmic scale

4.9.2 Hexadecane

The long linear unbranched hexadecane chains show a very different behavior than the one exhibited by the short hexane molecules. For gaps wider than 30 Å, as the system is compressed and molecules continuously flow out of the confinement, the coefficient of diffusion decreases. When a layer is expelled between 29 Å and 30 Å, the diffusion peaks to a value of 0.8. The fluid then compacts itself into rigid layers with almost no mobility and a coefficient of diffusion close to zero. As the system is further compressed, whenever the system reaches a well-formed layer, the molecules form large domains and are virtually static with a very small coefficient of diffusion. The coefficient of diffusion peaks when a layer of hexadecane is expelled, and the fluid becomes liquid-like momentarily before being compacted and becoming rigid again. In the logarithmic scale, the difference in the coefficient

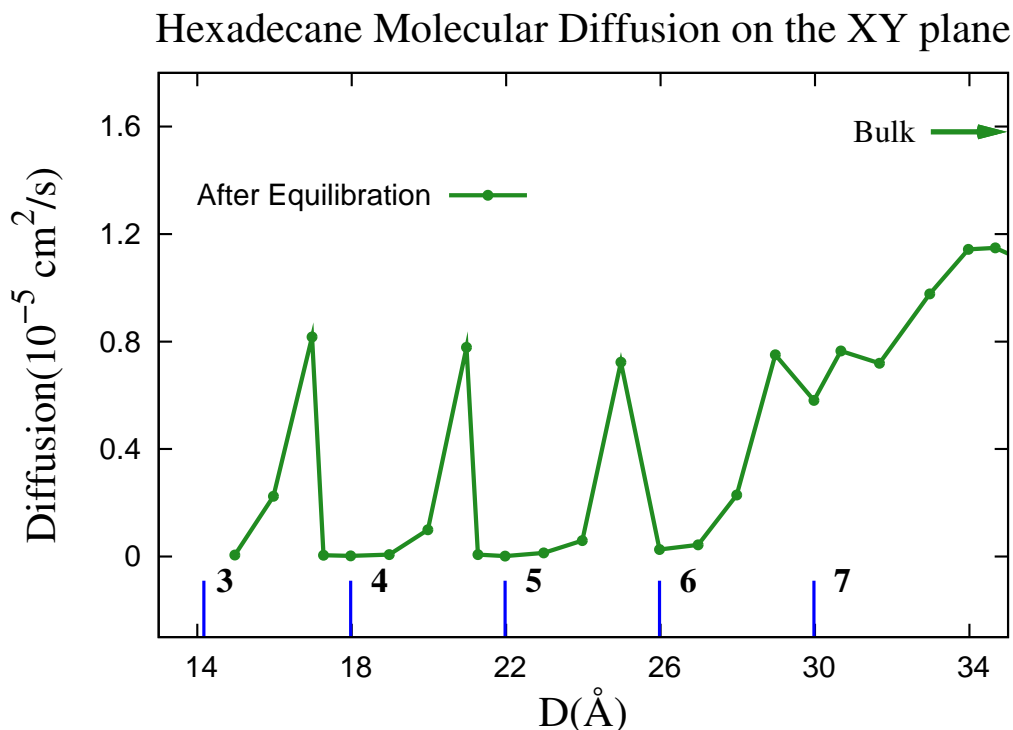


Figure 55: Hexadecane coefficient of diffusion versus gap size

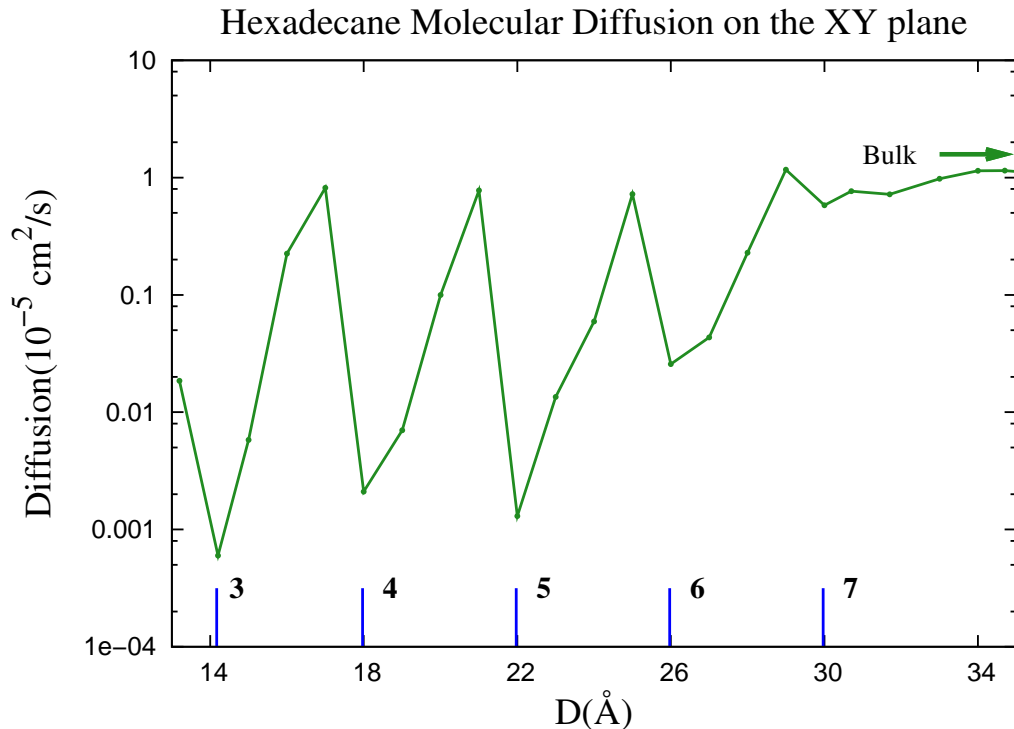


Figure 56: Hexadecane coefficient of diffusion versus gap size, in logarithmic scale.

of diffusion between a solid-like state and a liquid-like state is several orders of magnitude. Remembering that this diffusion is along a plane parallel to the gold surface, the inner molecules are tightly packed to their neighbors. In this calculation, we haven't included the displacement of the surface molecules. As we saw in the surface configuration plots, the molecules had no displacement for several nanoseconds that took to compress from 6 to 4 layers. Even in the middle region, hexadecane shows a high level of crystallization both in-layer and intralayer for some gaps, and for others it behaves more fluid.

4.9.3 Phytane

Phytane had a similar behavior as hexane when we had compared the number of molecules through the compression process, Figs.35 and 37. They both has a small slope through out the compression, a slight steps from 3 to 2 layers, and a larger step went expelling a larger number of molecules to transition to a single layer. In the coefficient of diffusion for phytane, there are some similarities and differences with hexane. The coefficient of diffusion for the branched fluid slowly decreases as the confinement is compressed as it did in the case of the short molecules.

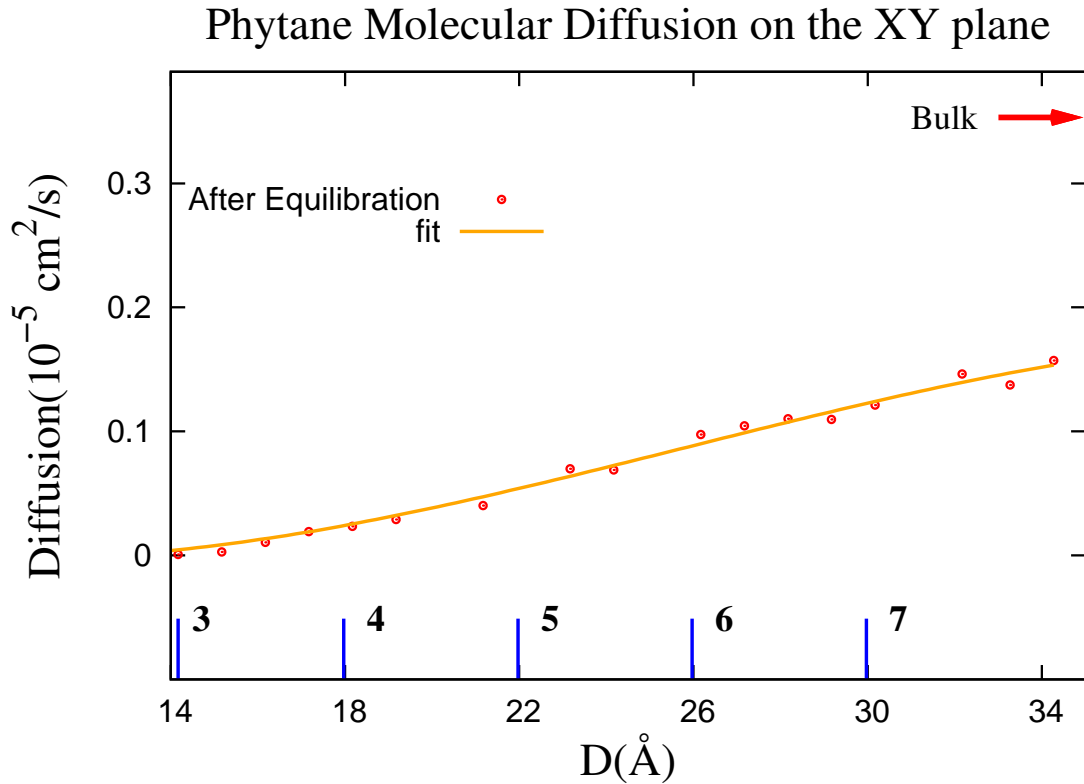


Figure 57: Phytane coefficient of diffusion versus gap size.

But when observed in a logarithmic scale, the drop in the coefficient of diffusion when the fluid is transitioning from 4 to 3 layers, is considerably larger than in the hexane case. When the group of molecules is expelled, the mobility of the molecules increases as well as the liquidity of the system.

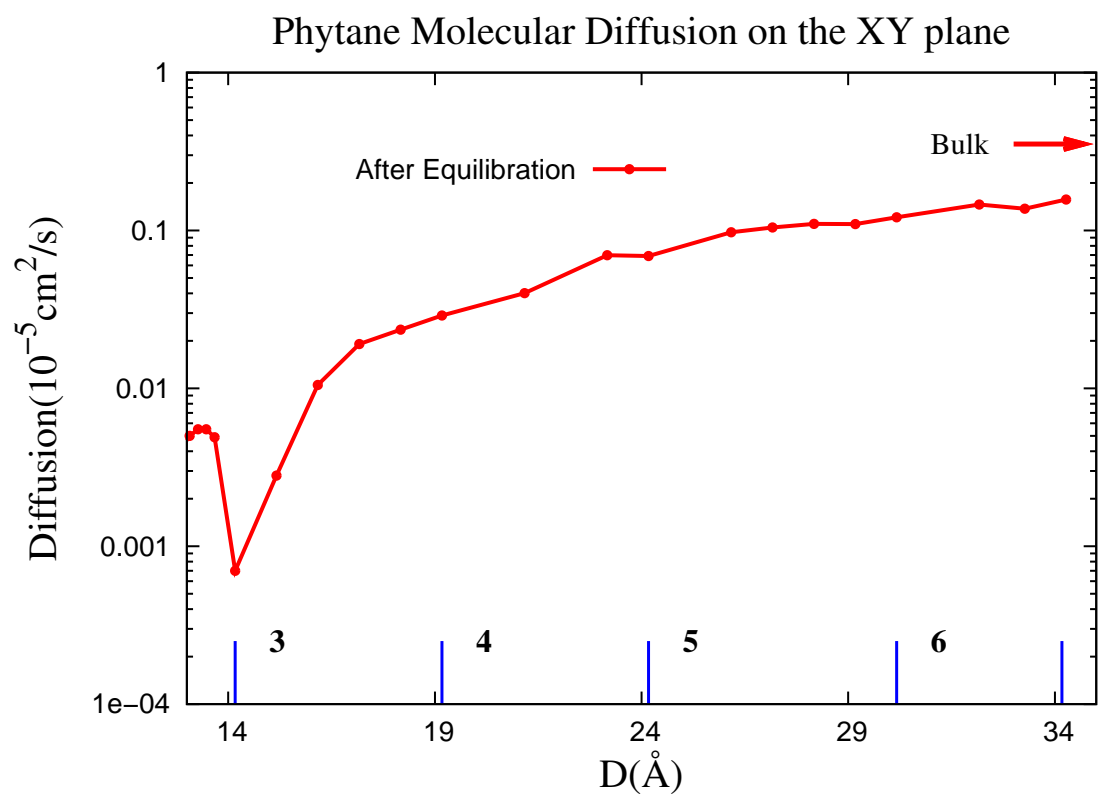


Figure 58: Phytane coefficient of diffusion versus gap size, in logarithmic scale.

4.10 *Comparison on the three pure systems*

By observing the evolution of the number of confined molecules, the oscillations in the solvation force and the changes in the coefficient of diffusion, we have seen solid-like and liquid-like properties in the 3 pure alkane fluids. In this section, we will compare the steps in the number of molecules, with the location of the peaks in the force, and the oscillations in the diffusion.

In the Fig.59, the top row shows the solvation force, the middle row shows the number of confined segments, and the bottom row shows the coefficient of diffusion in logarithmic scale. The columns show the corresponding property for each pure system: hexane, hexadecane and phytane. When this 3 plots are compared, it is evident that the oscillations in the 3 graphs are related. The hexane system started with a certain number of confined molecules and it decreases as it was compressed until around a gap size of 19\AA when undulations start to appear. As the system was compressed to 15\AA , the solvation force increased, while some molecules left the confinement, and the system compacts itself with less mobility of the molecules, seen as a small dip in the coefficient of diffusion. At 14.7\AA , the fluid yields and a group of molecules are expelled, so we can detect a slight step in the plot of number of confined molecules versus gap size. Simultaneously, the diffusion of confined molecules levels. The system was compressed again, the force rises up to 500nN and at 9.7\AA the system yields and expels a larger number of molecules in a short amount of time, approximately 1ns . For gaps smaller than 13\AA , we no longer show the coefficient of diffusion because we are interested in the molecules in the inner region, not directly in contact with the surfaces. In the case of the small molecule with 6 carbons, the mobility of the molecules smoothly decreases as it is compressed, which is expected.

In the case of the longer hexadecane with 16 carbons, the behavior during compression is somewhat different, we see cycles of plateaus and sharp steps. In the case of hexane, there is a low slope in between the steps which indicates a small flow of

hexane molecules out of the confinement, but in the hexadecane case, there is almost no outward flow except for the abrupt expulsion of a layer of hexadecane at certain gap sizes. At the gaps that correspond to plateaus in the number of confined molecules, the gap size is decreasing, so the density increases up to the point where a layer is expelled, and the density in the confinement drops.

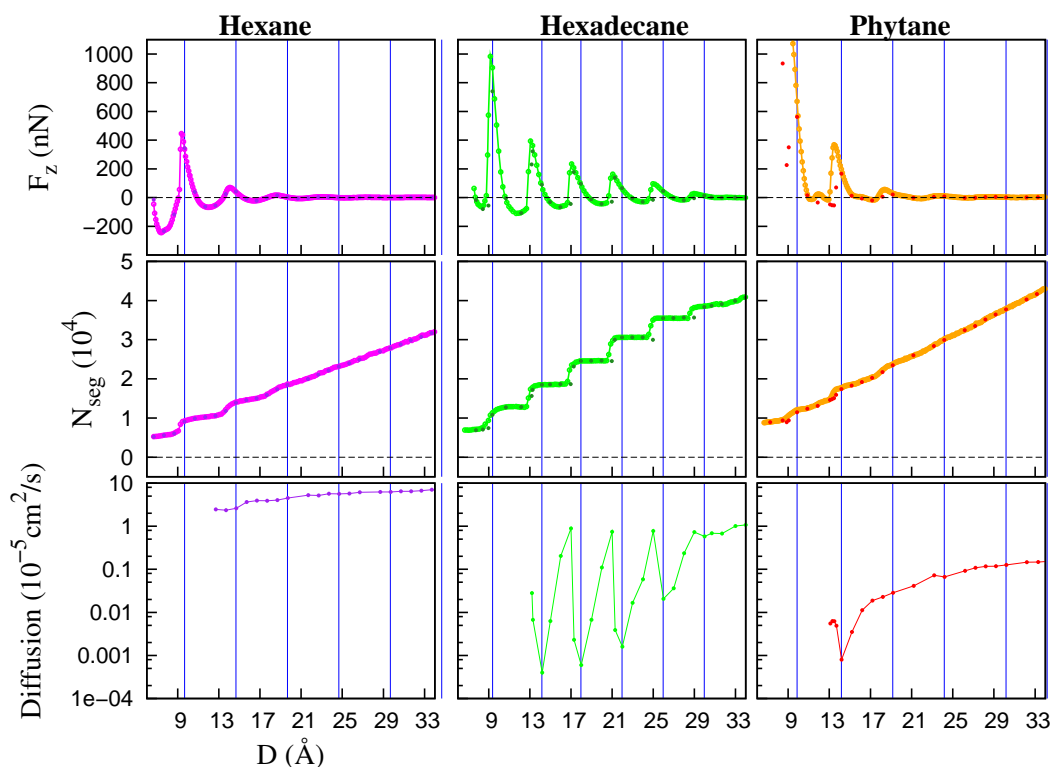


Figure 59: Comparison of solvation force, number of confined molecules and diffusion for C6, C16 and C20.

We can clearly see how hexadecane shows solid-like behavior through the compression starting at 30\AA . For thinner gaps, while the system is compressed no molecules leave the confinement but become compacted, the diffusion decreases sharply, the force increases up to a point where the system yields, and expels a whole layer, approximately 400 molecules at which point the diffusion peaks to $0.8 \times 10^{-5} \text{cm}^2/\text{s}$.

Hexane and phytane have some similarities because they both behave mostly liquid-like. The molecules in both cases slowly drain from the confinement into the bulk at a slow rate, and only for very small gaps, do they expell groups of molecules. The oscillations in the solvation force are very small for large gaps, and the strength increases considerably when distance between the surfaces decreases to less than 20\AA . This increase is especially high for phytane when there is only one layer in the confinement and the branch molecules are under a high level of stress.

In the diffusion coefficient plots for hexane and phytane, we see that they drop slowly except when doing the transition from 4 to 3 layers. This phenomena is enhanced when looked at the logarithmic of the diffusion coefficient, where we see a sharp drop when phytane has compacted itself to 3 layers parallel to the confining surfaces.

In the next chapter we will see how the solid-like or liquid-like properties of these pure alkanes persist or are damped by the mixing of another alkane. In particular, we will compare the results for pure hexane, hexadecane and phytane, with a mixture of small and long alkanes by studying an equimolar mixture of hexane and hexadecane; and by studying a mixture of branched and unbrached alkanes by looking at the behaviour of an equimolar mixture of hexadecane and phytane.

CHAPTER V

STRUCTURE OF MIXED SYSTEMS

In the previous chapter, we showed the structure and behaviour of three pure systems: hexane, hexadecane and phytane. The first alkane fluid made of small molecules, is very liquid and presents little ordering, except when compressed to 2 layers. The second system, made of flexible rods, showed a tendency to aggregate in small ordered domains, but not very mobile in general. The branched system, shows very little inlayer or intralayer order, and tends to be somewhat fluid. In summary, when these alkane fluids were compressed down to the nanoscale, hexadecane showed solid-like features by forming rigid layers and only expelling one layer at a time when compressed, on the other hand, hexane and phytane showed liquid-like behavior in that there was an outward flow while being compressed down to 3 layers. For thicknesses smaller than 3 layers, the difference in molecular shape is evident and hexane shows better structure than phytane.

From previous work done by Landman and Gao, although at a higher compression rate, hexadecane showed similar solid-like features. We wanted to compare these properties when it was mixed with a shorter alkane. This would help us understand how a lubricant composed of alkanes of different lengths behaves when compressed down to a few molecular layers. Since we used a different temperature and our speed of approach was much smaller, we will compare the results from our most recent simulations on pure systems described in the previous chapter, with our simulations of a short and long molecule mixture.

Once we studied the effect on mixing short molecules with hexadecane, we decided that for completeness, we should also analyze what happens when we mix branched

molecules with hexadecane. To isolate the effect of the branches, we choose an alkane with a backbone the same length as hexadecane, 16 carbons. Even though, there are other alkanes with the same backbone length and with a symmetrical distribution of the branched segments on both sides of the backbone, we chose phytane because it naturally appears in nature as a component of crude oil. Phytane has 4 branches on the same side of the backbone. If we number the carbons on the backbone from 1 to 16, the branches are connected to carbons 2, 6, 10, 14. To understand the combination of branched and unbranched alkane chains, we model an equimolar mixture of phytane and hexadecane.

The procedure to study the mixtures was very similar to the study of the pure systems. The system was prepared at $315K\text{\AA}$, then warmed up to $450K$ to assure well mixing, allowed to equilibrate before slowly cooling it down to $315K$. At 315\AA , both systems were made to run until the molar fraction and the solvation force had small oscillations around a constant value. Our largest gap was 36.7\AA , and chosen such that the inner region would behave as much as possible as in the bulk. In these simulations, the confinement is in contact with a reservoir maintained at an equimolar composition. The confining surfaces are the same as described in Chapter 3.

In each mixture, one type of molecule had a higher tendency to adhere to the gold surface, but since the gap was in contact with a equimolar reservoir, the other species was forced to leave the confinement so that the inner region of the confinement would also be an equimolar mixture. This phenomenon slightly changed the composition of the reservoir. We wanted to assure that the bulk section of the computational box resembled a thermodynamic reservoir where the composition is not affected by the behaviour of the confinement. Every 900 ps, we corrected the molarity of the bulk by randomly eliminating a few molecules that were in excess of a 50:50 composition. The number of deleted molecules each time were in the order of 20 to 40 molecules, which is less than a fraction of a percent of the total number of molecules in the

computational box, 10667 molecules in the hexane-hexadecane mixture and 7400 in the phytane-hexadecane case. After eliminating the few molecules, we compressed with a higher pressure for 60 ps to restore the original density.

We verified that the number of confined molecules were not affected by this correction to the bulk molarity. Modifying the molarity of the bulk allowed the confinement to have the same probability of interacting with either type of molecule when interacting with the reservoir. This correction only decreased slightly the number of molecules in the reservoir, but since we are using periodic boundaries, the fact that the real number of molecules in the reservoir changes does not in fact modify the system which is being replicated by image molecules in neighboring computational cells.

Every time the system was compressed 0.1\AA , every 900ps, the state of the system was saved, and of these configurations some were chosen to evolve longer and reach equilibrium. In these cases, all the configurations were set to a computational box size of 400\AA along the x axis for uniformity. During the equilibration process, to maintain the 50:50 bulk molarity, some molecules were eliminated such that the remaining computational box measured 400\AA . During the process of correcting the molarity of the bulk, the number of confined molecules remained the same because it was done fast enough to not perturb any of the molecules inside the gap.

When observing the differences between the pure and mixed systems, we will see that depending on the constituents of the mixture, the mixture can be strickenly different or similar to one of its component in pure form. We are interested in the structure of the confinement as it is compressed. We will look at the same properties as in the previous chapter, plus the molar fraction inside the well ordered gaps, as well, as how does this parameter evolves during compression.

5.1 Density Profile

We model an equimolar mixture of hexane and hexadecane, with 5334 and 5333, respectively; and phytane and hexadecane, with 3600 molecules of each species. Both mixtures occupy a similar computational box, the first mixture has 117,332 segments and the second mixture has 129,600. The segmental and molecular densities give us information on the relative distribution of the molecules through out the confinement.

We have previously mentioned that in our model, the interaction between the segments and the gold is stronger than between the segments, but at the same time the range of this interaction is approximately 7.5\AA from the center of the gold atoms because the $r_{cutoff} = 2.5\sigma$. This increases the possibility of alkane chains forming a layer on the gold surface. Several experiments have observed 2D crystallization of long linear alkane chains on smooth metal surfaces.

We saw in Fig.10 that pure hexadecane forms large domains of tightly packed molecules on the molecularly smooth gold surfaces. Hexane and phytane don't tend to pack as well. From the density plots we see how the molecules organize at the largest confinement and how does this evolve as the system is compressed. After examining the segmental and molecular densities for all the equilibrated gaps, approximately 40 configurations for each mixed system, we observed that there were some particular gaps that showed better layering than others. For the mixed systems, these well-formed gaps are

No. Layers	Hexane & Hexadecane	Hexadecane & Phytane
7	32.7 \AA	33.4 \AA
6	27.7 \AA	28.4 \AA
5	21.7 \AA	23.4 \AA
4	17.7 \AA	18.7 \AA
3	13.3 \AA	14.0 \AA
2	9.7 \AA	10.2 \AA

(24)

5.1.1 Molecular density

The molecules in the pure systems distributed themselves in a high-density surface layer and a more fluid middle region for the largest gap thicknesses. As they were compressed, they all showed a tendency to form layers inside the confinement, hexadecane at larger gaps than the other systems. We observed two types of layers, independent layers, identified by high density peaks separated by regions of almost no molecules; and intertwined layers, represented by medium density peaks separated by a non-zero density. In the pure systems, hexadecane showed independent layers starting at 26\AA , with 6 layers, while hexane and phytane only showed somewhat independent layers starting at 14\AA , with only 3 layers.

In Fig.60, we can see the distribution of hexane and hexadecane in the mixture. The purple lines represent hexane and the green lines show hexadecane. The hexadecane density is several times larger than the hexane density, as can be noted by the difference in scale. At the largest gap of 36.7\AA , we can see how hexadecane has formed high density surface layers, while the middle region starts as an equimolar mixture. As the mixture is compressed, hexadecane starts showing 5 independent layers at 21.7\AA , with a small proportion of hexane molecules remaining in the gap. From the C6&C16 molecular density plots, there doesn't seem to be much order for larger gaps.

In the molecular density profile plots for branched-unbranched equimolar mixture, Fig.61, we can see a very similar scenario as in the pure phytane case, for larger confinements there is no layering except in the surface. Contrary to the short-long mixture, both components here have a similar density. The red lines represent the branched molecules while hexadecane is represented by green lines. The surface peaks corresponding to phytane are considerable higher than the ones for hexadecane. The ability of this mixed system to form layers, follows pure phytane's behavior because the system only forms independent layers when there are 3 layers inside the gap.

In general alkane fluids compressed down to 1 or 2 layers become sluggish and have difficulty reaching equilibrium. This is particularly so for phytane, both pure and mixed, because the width of the molecule is between 8 and 9 Å.

C₆&C₁₆ Molecular Density

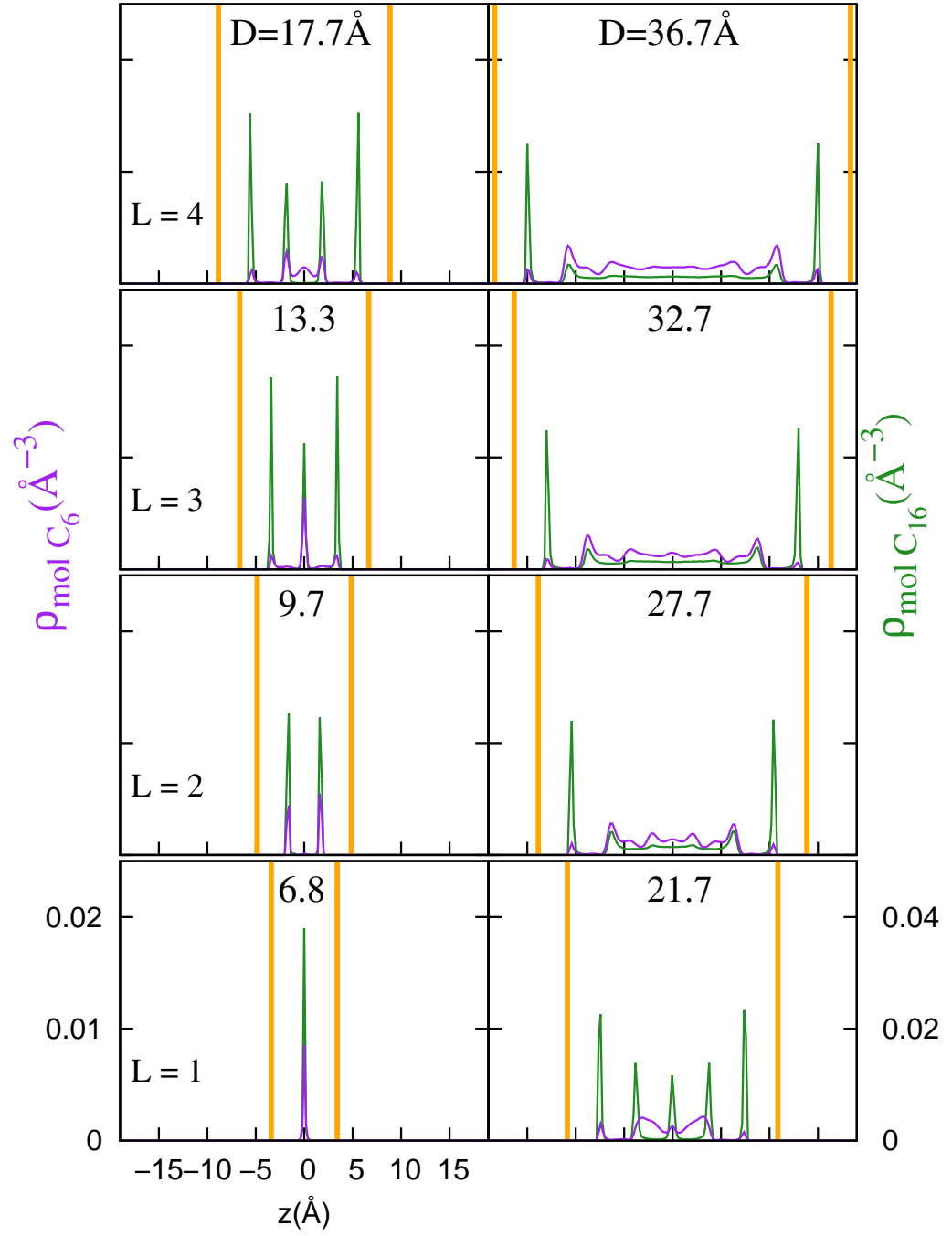


Figure 60: Molecular density inside well-formed gaps for C₆&C₁₆ mixture.

C₂₀&C₁₆ Molecular Density

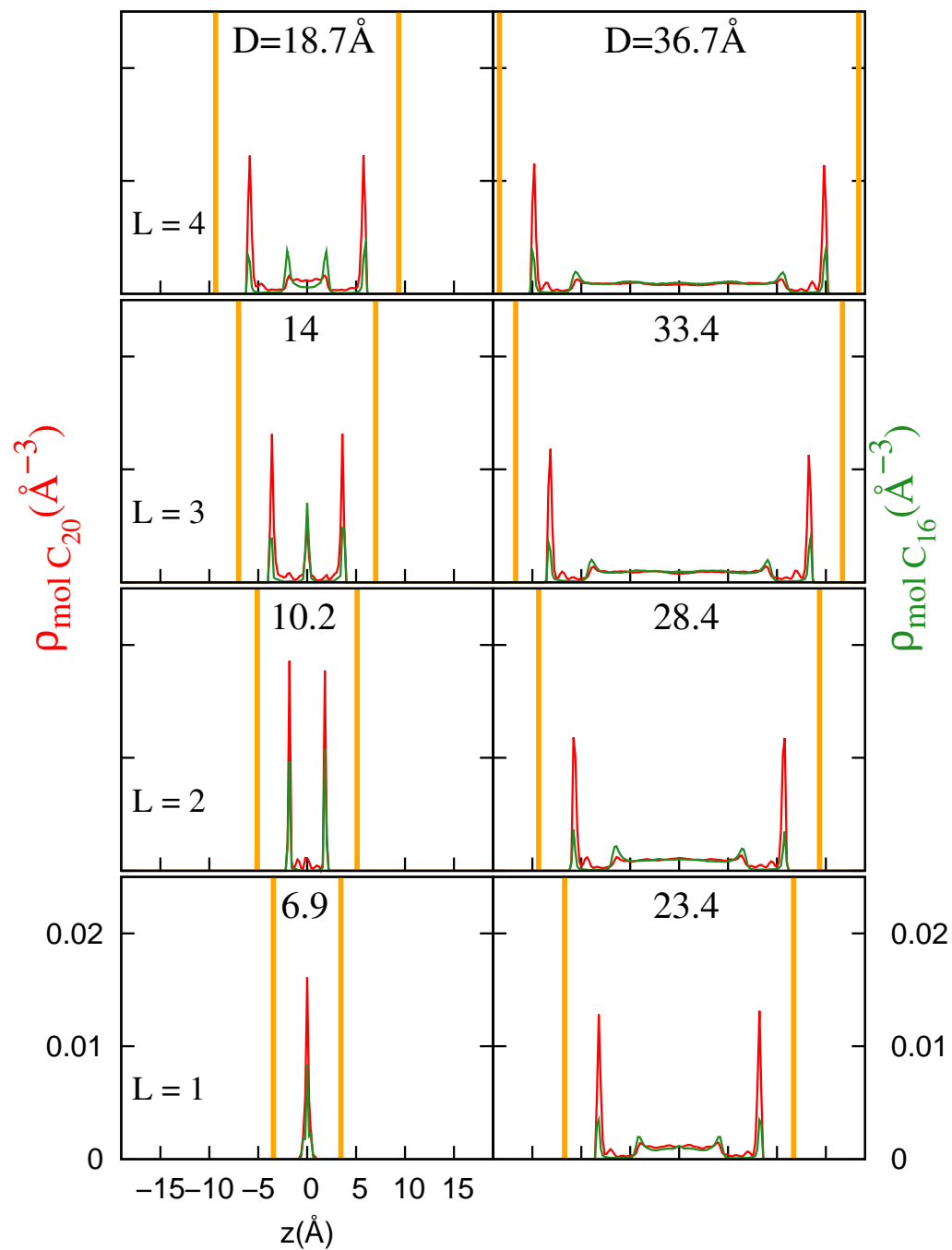


Figure 61: Molecular density inside well-formed gaps for C₂₀&C₁₆ mixture.

5.1.2 Segmental density

Let us remember that hexane has 6 segments, hexadecane has 16 segments and phytane has 20 segments. In the segmental density plots for hexane, Fig.12, for hexadecane Fig. 13 and for phytane, Fig.14, we see layering at larger gaps where molecular density plots do not show clear layers. This means that at larger gaps, we see intertwined layers, the center of mass are not organized in layers, but the segments are ordering themselves in layers, even though they are not independent from each other.

When we look at the segmental densities for C6&C16 and C20&C16, the intertwined layering starts at gaps as thick as 33Å in both systems. The hexadecane layers in the C6&C16 start to separate and form 5 layers, even though hexane is still showing a rather uniform distribution in the inner region of the confinement. Notice that the segmental densities for hexane and hexadecane are shown with different scales in order for the small peaks of hexane to be visible. At 4 layers, both long and short molecules are forming independent layers.

In the branched-unbranched mixture, phytane lags behind hexadecane in the transition from the intertwined to independent layers. In this case, true independent layers are observed at 14Å. We can see the presence of small phytane peaks in between the main layers. We will discuss this later. At a gap size of 6.9Å, the phytane-hexadecane mixture had shown a single peak in the molecular density plot, Fig.61, but in the segmental density is a double peak. This indicates that some phytane molecules were not able to lie sideways.

C₆&C₁₆ Segmental Density

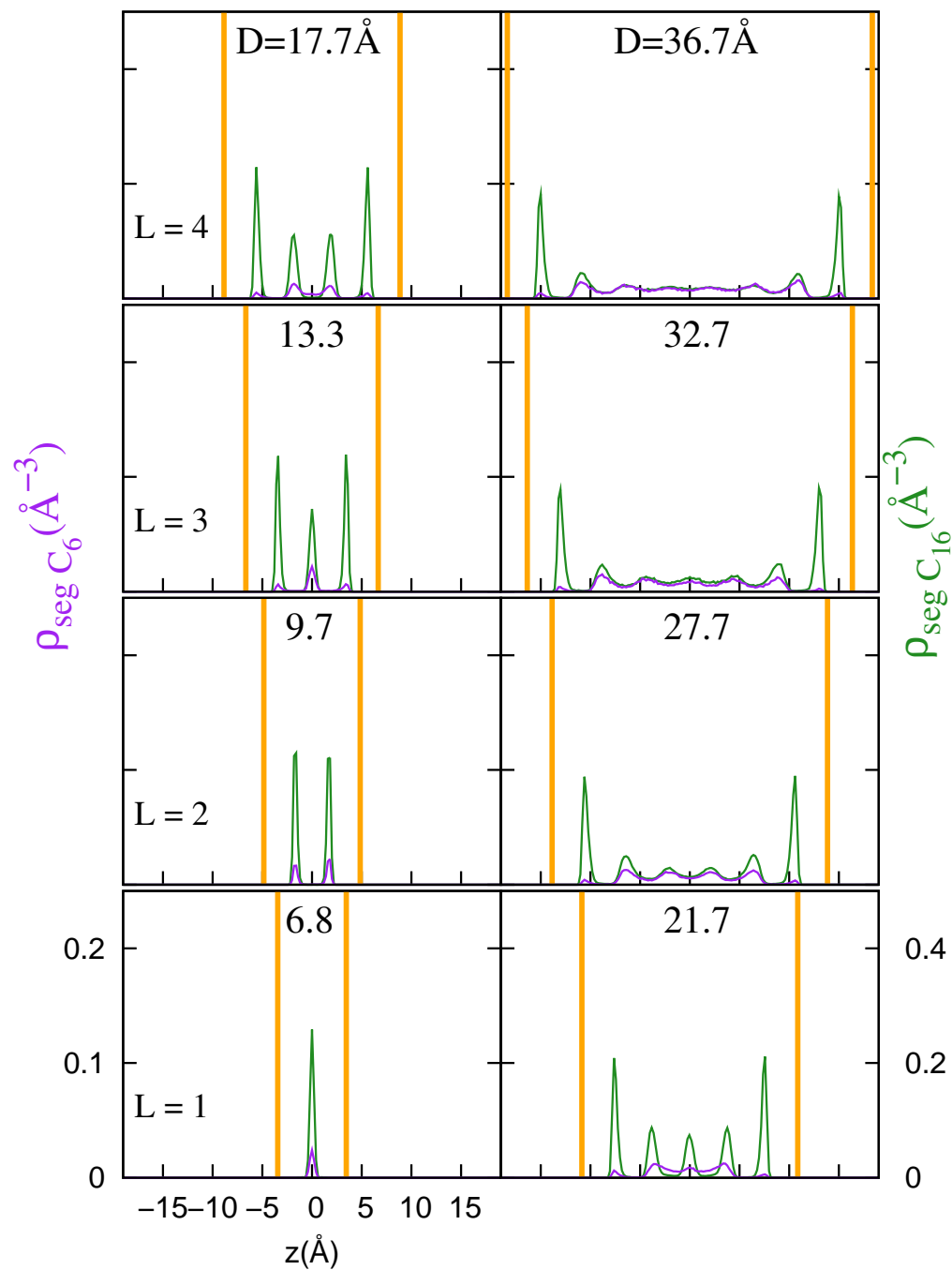


Figure 62: Segmental density inside well-formed gaps C20&C16

C₂₀&C₁₆ Segmental Density

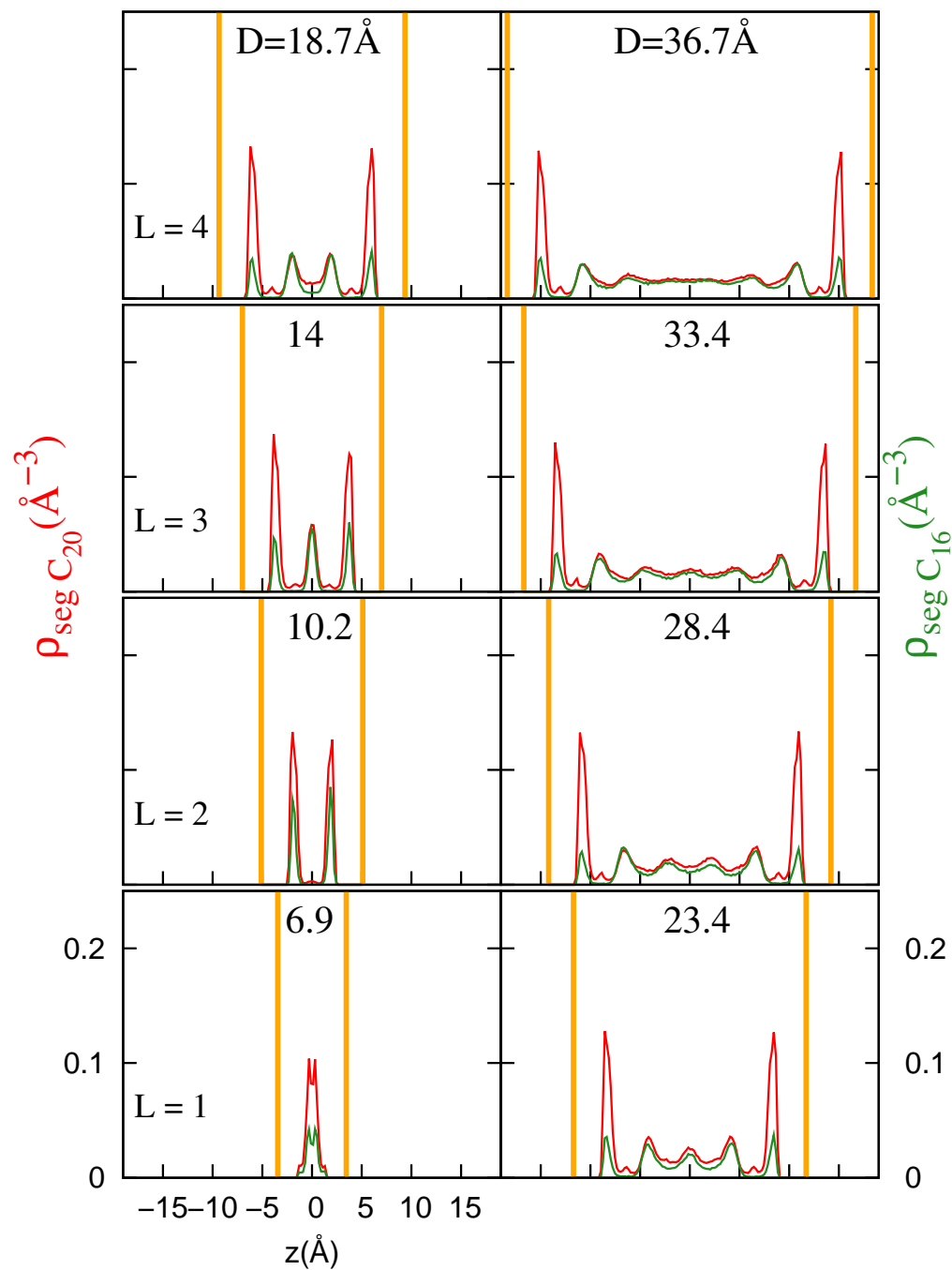


Figure 63: Segmental density inside well-formed gaps for C₂₀&C₁₆ mixture.

5.1.3 Molar fraction

A new and important property unique to mixtures is the molar fraction in the confinement. In Fig.64, we show the molar fraction of the short-long mixture, Γ_6 and Γ_{16} , while in Fig. 65 we present the molar fraction for the branched-unbranched mixture, Γ_{20} and Γ_{16} . In each plot, we present the molar fraction of each component, as it is expected their sum is 1, and when one peaks, the other one dips.

In the Fig.64 for hexane and hexadecane molar fraction, at a gap thickness of 21.7Å, we see 5 hexadecane peaks separated by 4 hexane peaks. This doesn't mean there are 9 layers, but gives information on the relative composition of the different regions in the confinement. As I had noted before, at this thickness hexadecane had managed to form 5 independent layers, while hexane was still distributed through the confinement, not necessarily uniformly, which means that at the location of the peaks, there was a high proportion of long chains, therefore the high C16 molar fraction peaks; while in the hexadecane valleys there are few short molecules making hexane's molar fraction larger. This corresponds to the layering observed in the corresponding segmental plots. So the layering process in this mixture showed a trend of molecular selection in which hexane molecules are forced to leave the confined gap as the gap size is reduced. This phenomenon continues as the system is compressed.

In the case of branched-unbranched molecules, molar fraction peaks do not show close relation to the peaks in segmental density profiles. For example, the segmental density of C20&C16 shows 4 layers at a gap of 19.6Å, but the molar fraction at this gap shows 3 phytane peaks and 4 hexadecane peaks. When the segmental density shows 3 layers or less inside the confinement, the molar fraction only shows that there is a larger proportion of hexadecane, but not how they are layered. This has to do with the fact that neither one of the components is dominant, contrasting to the case of hexane-hexadecane where the layers are mostly composed of long chains.

C₆&C₁₆ Molar Fraction

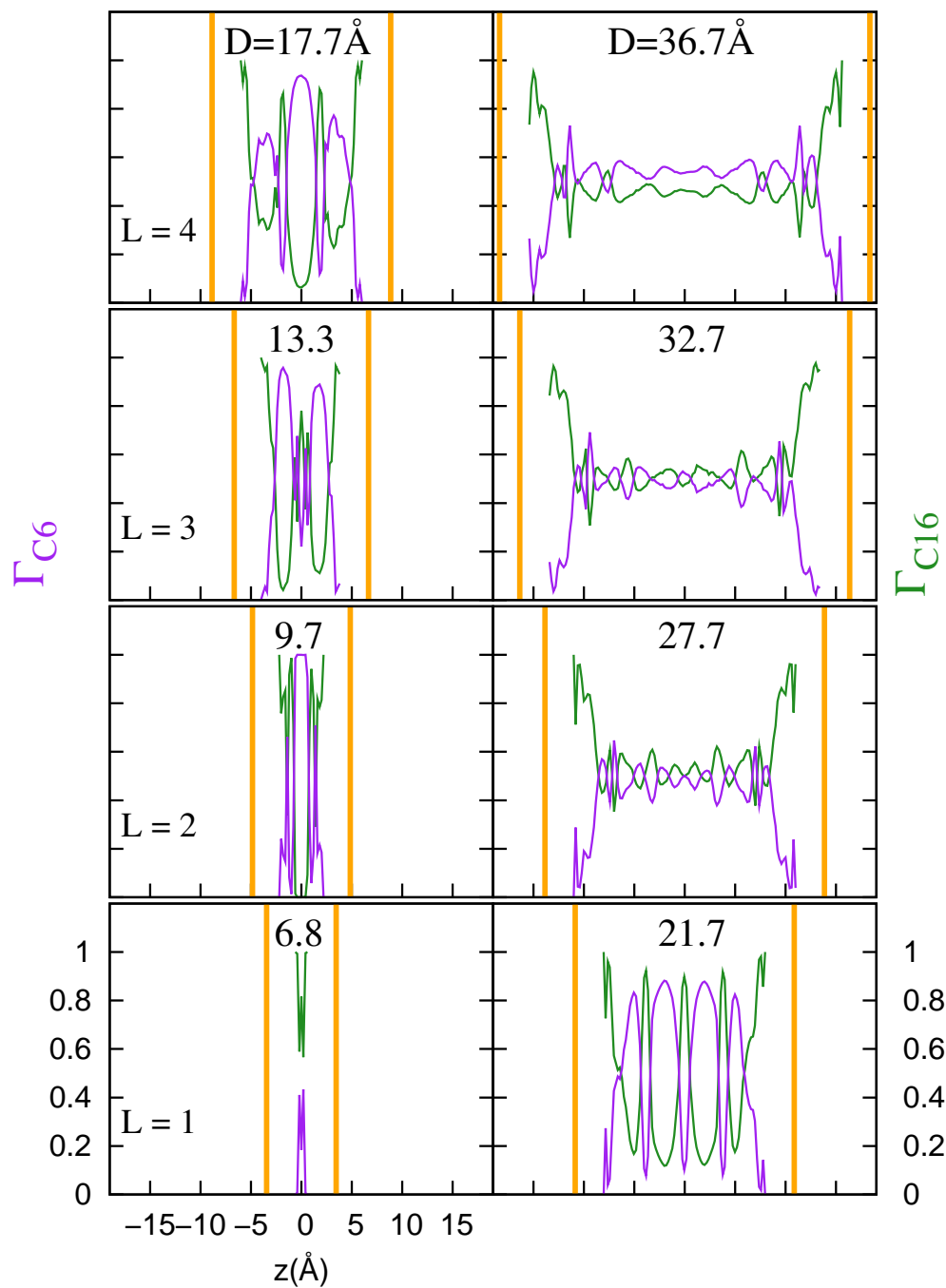


Figure 64: Molar fraction inside well-formed gaps for C₆&C₁₆ mixture.

C₂₀&C₁₆ Molar fraction

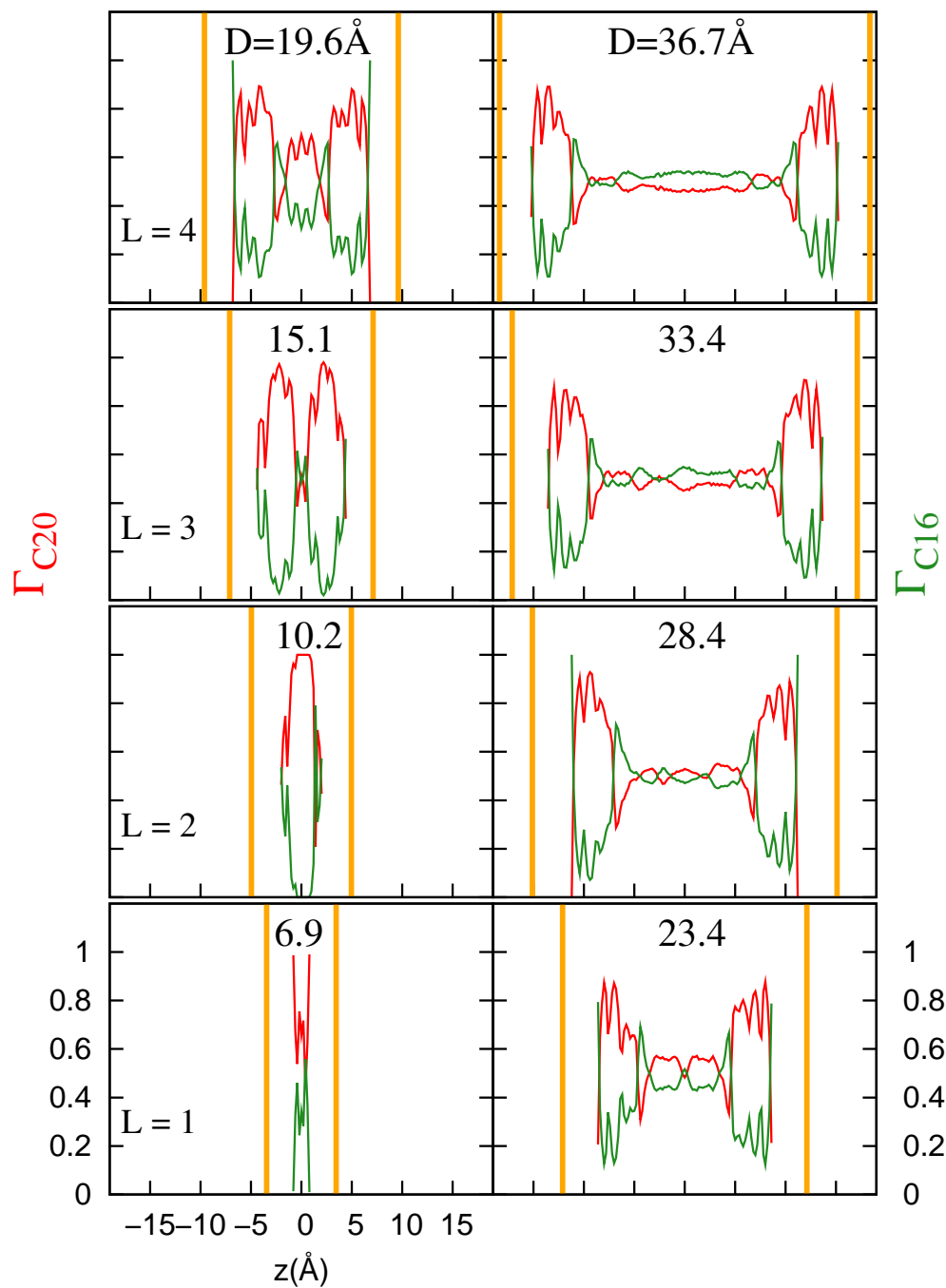


Figure 65: Molar fraction inside well-formed gaps for C₂₀&C₁₆ mixture.

5.1.4 Densities during transition from 4 to 3 layers, and from 3 to 2 layers

When we looked at the transition from 4 to 2 layers in the pure systems, we saw that hexadecane had an abrupt transition from 4 to 3 layers and from 3 to 2 layers, happening when the system was compressed 0.2\AA or less. On the other hand, hexane and phytane underwent a smooth transition from 4 to 3 layers and then to 2 layers. After hexane and phytane had being compressed 1\AA , we could still see the intermediate product of merged layers. Hexane's transformation took place while the system was compressed approximately 2\AA , while phytane took the compression of almost 4\AA to go from 4 well-formed layers to 3 layers because of the reordering of the branches.

In the case of the mixture of hexane and hexadecane, both processes happen simultaneously; Hexadecane transforms, during the compression of 0.6\AA , from having 4 layers to suddenly 3 layers, while hexane shows an intermediate step where the 2 middle layers at 17.3\AA start merging to form the middle layer at 16.7\AA . Which implies that hexadecane still possesses some solid-like qualities seen in its pure form, while hexane still remains liquid-like. This is partially due to the confinement induced molecular selection process which reduces the number of hexane molecules significantly inside the gap allowing hexadecane to dominate the behavior of the confined mixture.

Hexadecane's behavior is quiet different when it is mixed with phytane. Both molecules remain mixed in the gap throughout the process of reducing gap size. When the C20&C16 mixture is transitioning from 4 to 3 layers, it undergoes a smooth transition, but when transitioning to 2 layers it manages to do it as fast as when it is mixed with hexane, during the compression of 0.5\AA .

In the left column of Fig.68, we can see the three layers of phytane and hexadecane. There are more segments of phytane on the gold surface than there are hexadecane segments. We could say that the layers are almost independent, because the density is very low in between the peaks. While decreasing the separation of the gold surfaces,

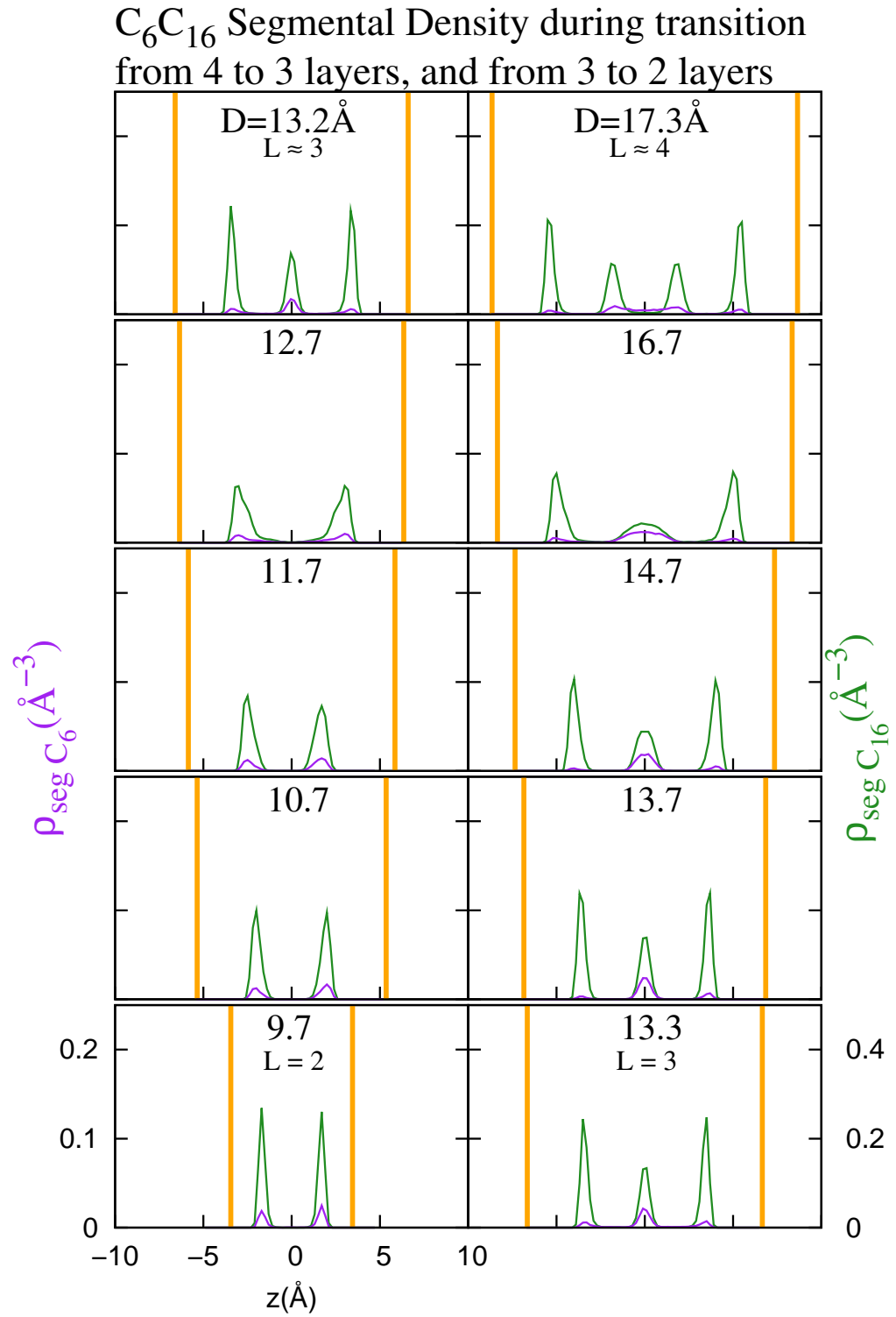


Figure 66: C_6 & C_{16} : Segmental density inside well-formed gaps during transition from 4 to 3 layers on the right column, and transition from 3 to 2 layers on the left column.

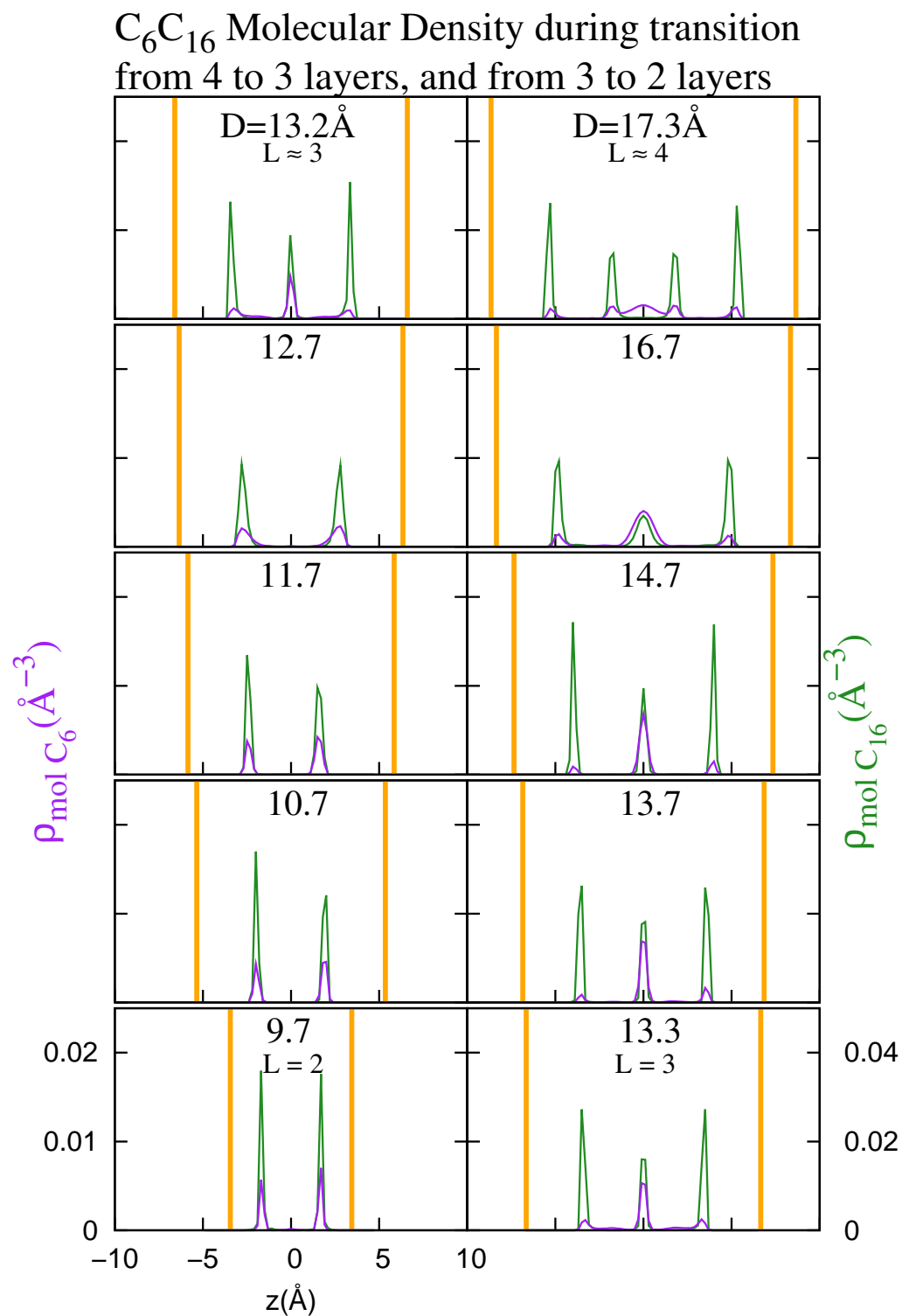


Figure 67: C_6 & C_{16} : Molecular density inside well-formed gaps during transition from 4 to 3 layers on the right column, and transition from 3 to 2 layers on the left column.

$C_{20}C_{16}$ Segmental Density during transition
from 4 to 3 layers, and from 3 to 2 layers

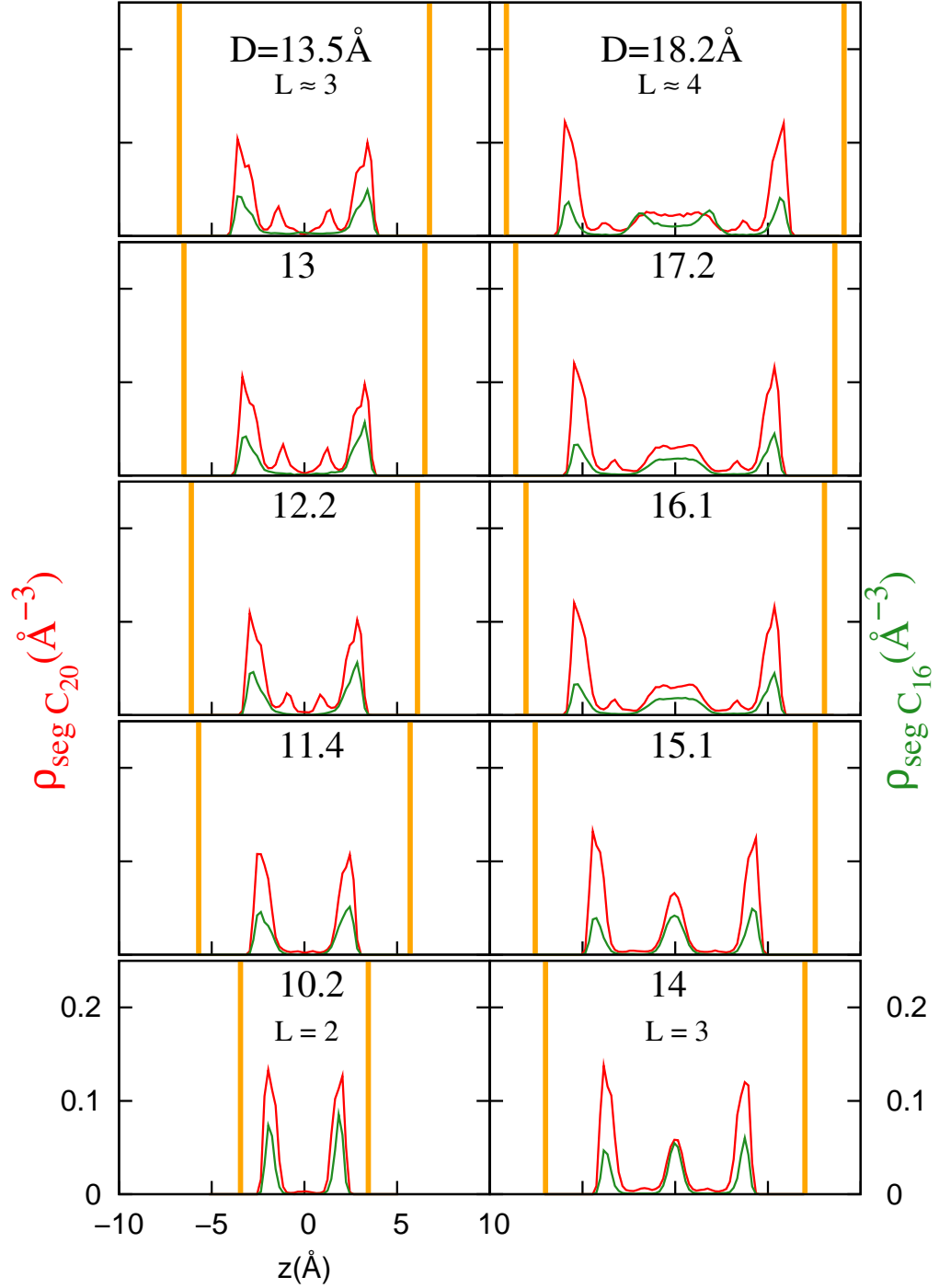


Figure 68: C_{20} & C_{16} : Segmental density inside well-formed gaps during transition from 4 to 3 layers on the right column, and transition from 3 to 2 layers on the left column.

$C_{20}C_{16}$ Molecular Density during transition
from 4 to 3 layers, and from 3 to 2 layers

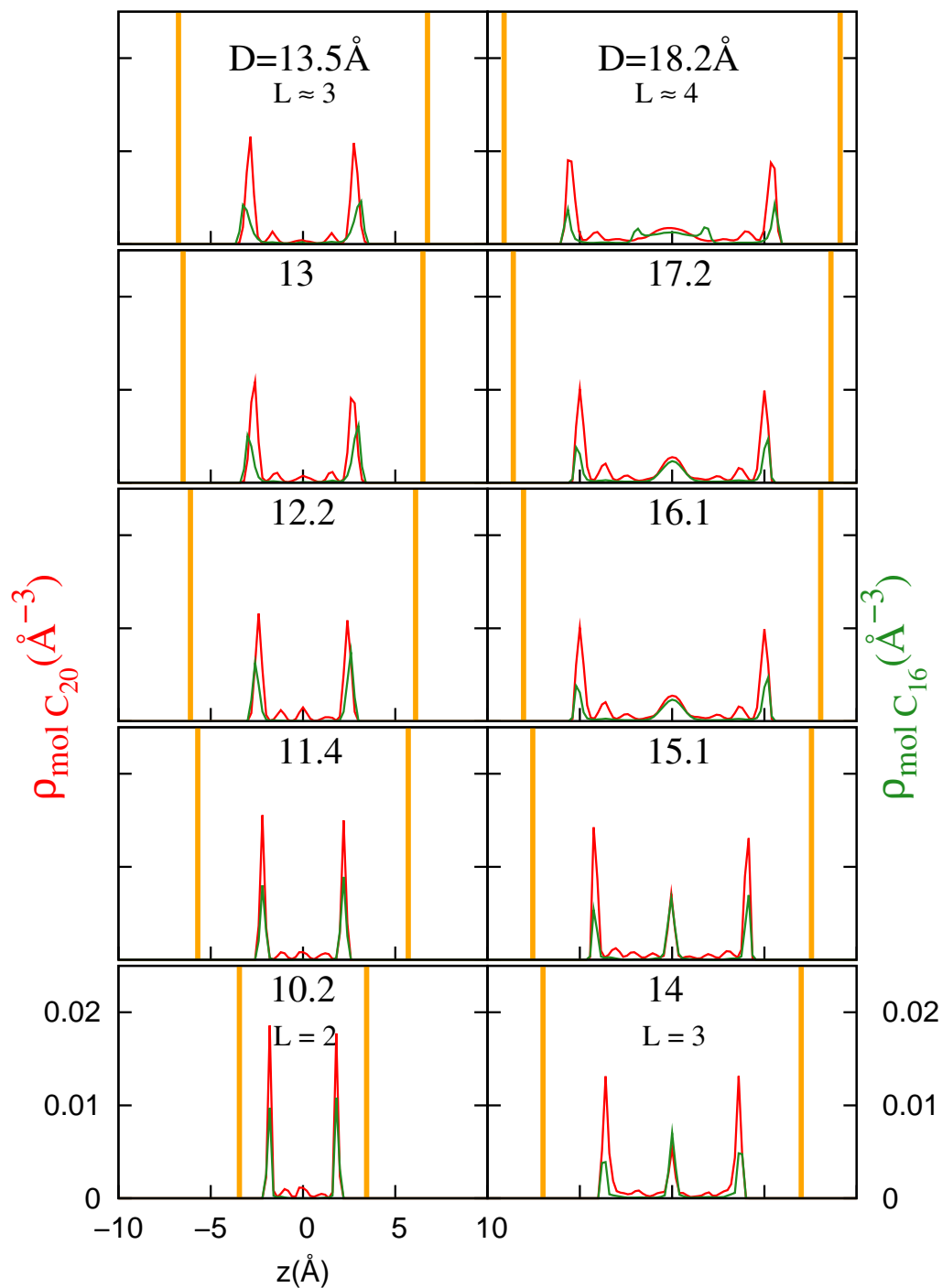


Figure 69: C_{20} & C_{16} : Molecular density inside well-formed gaps during transition from 4 to 3 layers on the right column, and transition from 3 to 2 layers on the left column.

the middle layer decreased in size. The middle hexadecane layer abruptly dissapeared, while the phytane middle layer split into 2 small peaks. The presence of the 2 surface peaks, and the 2 inner layers, appears from 13.5Å down to 11.47Å, not shown, where at that point the system is composed of 2 well defined layers.

In the following section, we will see that these small peaks correspond to branches from phytane molecules whose backbones are on the surface. We also see these extra peaks, when the system was transitioning from 4 to 3 layers but smaller. To see this phenomenon in more detail, we will present the branched density inside well formed gaps as well as during the transition.

5.1.5 Phytane's Branched Density in the C20&C16 mixture

To better understand the presence of these extra little peaks when transitioning from 4 to 3 layers, we plot the density of branch segments in the same plot as the normal segmental densities. Using the standard chemical numbering protocol, the branch-segments in a phytane molecule are number 17, 18, 19 and 20th. The segments included in the previous segmental densities are all the segments, regardless of whether they were branches or non-branches. The red lines are segmental density, while the blue lines represent the branched density. There are only 4 branches for every 20 segments in a molecule, which explains the difference in magnitude.

Even though the gap sizes that were equilibrated for the pure and mixed system are slightly different, if we compare phytane's branched density when pure in Fig.21, with its branched density when mixed with hexadecane, in Fig.70, we can see that the relative position of phytane's branches and segments is virtually the same regardless of the presence of hexadecane in the second case.

For the well-formed layers, the position of the branches corresponded to the position of the layers, which means that the backbone and the branches are in the same plane, parallel to the gold. When it is compressed further some molecules leave the confinement, and the remaining phytane rearrange to 3 layers and then 2 layers.

From the segmental and molecular densities, we know that when the phytane fluid is 18.7Å thick it has 4 layers, and at 14Å has 3 layers. To understand better the position of the branches during the transition from 4 to 3 layers, we plotted in Fig. 71 the branched density next to the segmental density.

On a layer with whole molecules, the branched density should be similar to 20% of the segmental density. For intermediate gaps in between well-formed layers, we see that the proportion of branched density is particularly high in between the peaks of segmental layers. This effect is more noticeable when the system is transitioning from 3 to 2 layers, on the left column of Fig.71, where there are 4 branched density peaks,

C_{20} Branched and Segmental Densities in the C_{20} & C_{16} mixture

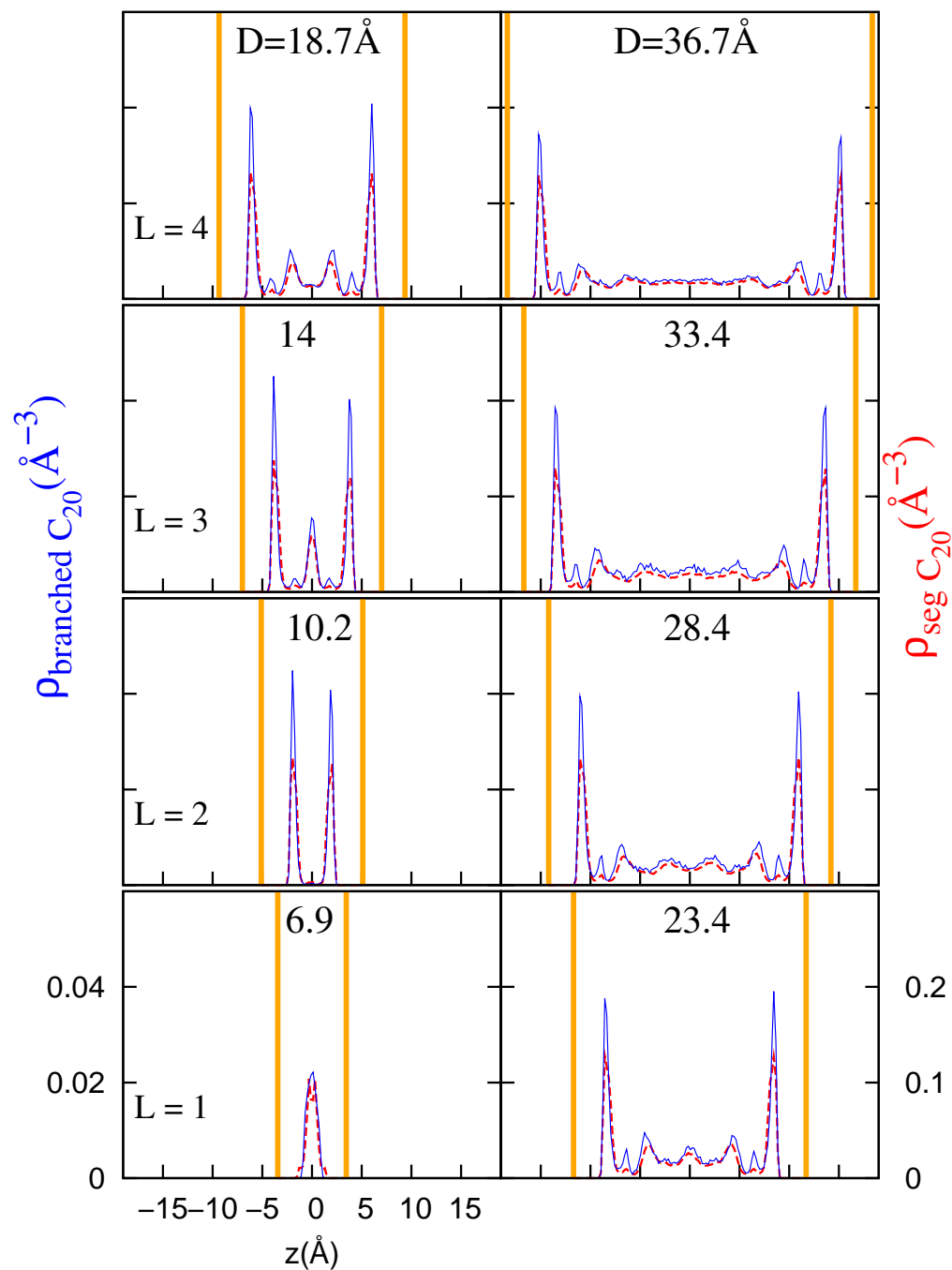


Figure 70: Phytane's Branched density inside well formed gaps when part of the C_{20} & C_{16} mixture.

Phytane Segmental and Branched densities
in mixture $C_{20}C_{16}$ during transition
from 4 to 3 layers, and from 3 to 2 layers

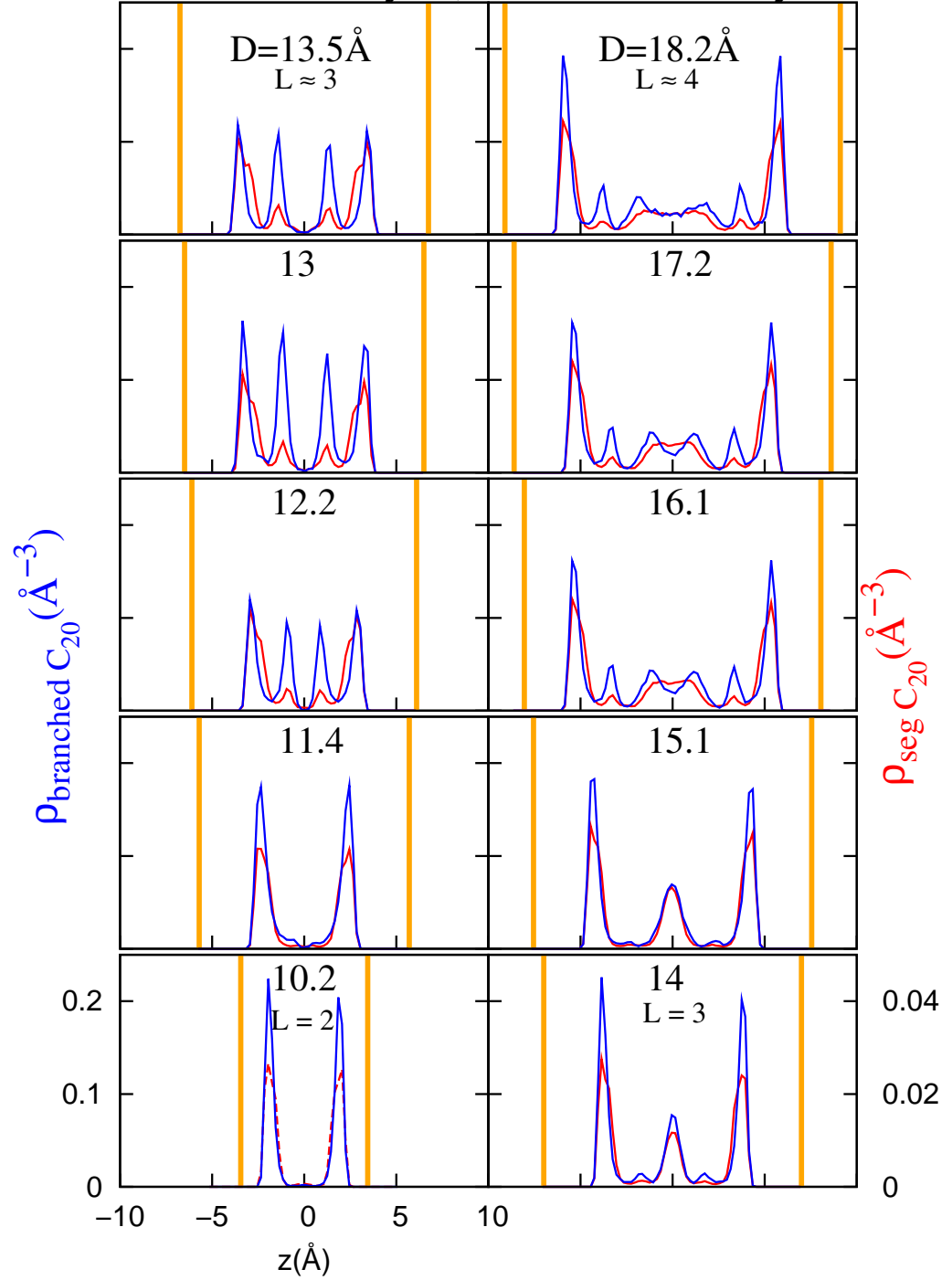


Figure 71: Phytane's Branched density inside well formed gaps when part of the C_{20} & C_{16} mixture during transition from 4 to 2 layers.

but only 2 predominant segmental peaks. These middle peaks have a high proportion of branches, suggesting that several molecules have their branches pointing towards the middle of the gap, instead of parallel to the surface, as in the case of well formed layers. This means some molecules throughout the system have rotated and their backbones are close to the gold surfaces while the branches are pointing away from the surfaces.

5.2 *End-to-end distance*

Since the segmental density has wider defined peaks than the molecular density, we can infer that the phytane molecules are rearranging themselves in layers even though some molecules may be part of one or two layers. As we saw in the branched density plots, the backbone might be in one layer, while the branches might be part of another layer. By plotting the average end-to-end distance versus the distance from the middle of the gap, we can see the distribution of the stretched or coiled molecules through the thickness of the confinement.

In both mixtures, as it was the case in the pure systems, the alkane chains attain their longest extension on the surfaces. Hexane in the C6&C16 mixture, shows its extended length in the well-formed layers, starting at 5 layers, oscillating around 90% of its 6.5Å ideal length, evident from Fig.72. Phytane in the C20&C16 mixture, seen in Fig.74, oscillates around 65% of its ideal length, while in pure form it oscillates around 70%.

Even though phytane has the same backbone as hexadecane, the end-to-end distance for pure phytane oscillates around smaller value of 12.5Å compared to the ideal value of 19.47Å, because its branches allow the backbone to bend with more freedom. When mixed with hexadecane, the phytane end-to-end distance oscillates around 15.6Å. The presence of the long linear hexadecane promotes phytane to stretch more than when it is by itself.

In the case of hexadecane, its length oscillates around 80% of their theoretical value when mixed with hexane, as seen in Fig.73, but when it is mixed with phytane its length oscillates at only 75% of their ideal length as evidenced in Fig.75.

This means that the presence of branches hinders hexadecane from fully stretching like it does when it is mixed with linear chains.

C_6 Relative end-to-end distance and Segmental density in the C_6 & C_{16} mixture

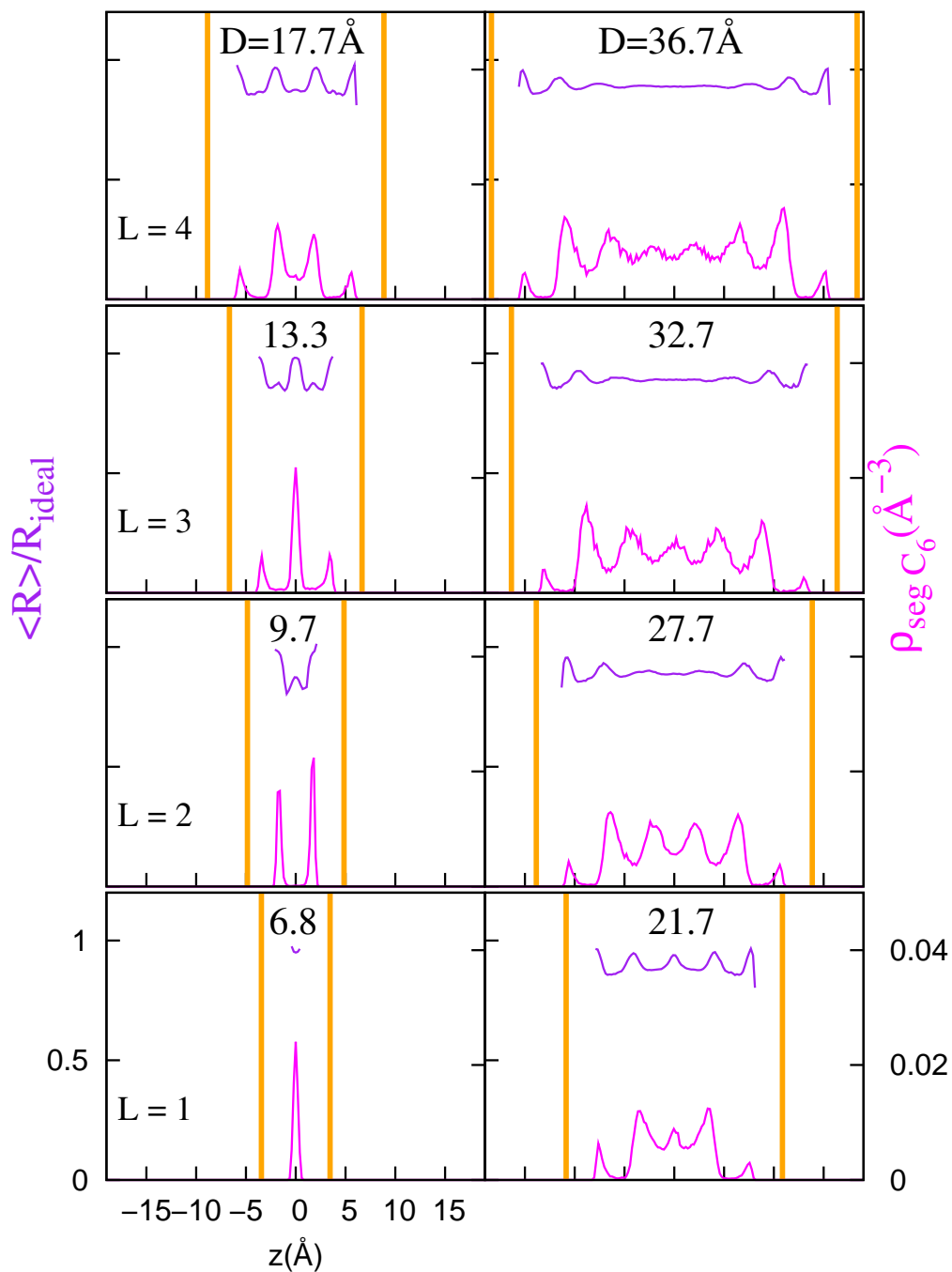


Figure 72: C_6 Relative end-to-end distance and density inside well ordered gaps in the mixture C_6 & C_{16} .

C_{16} Relative end-to-end distance and
Segmental density in the C_6 & C_{16} mixture

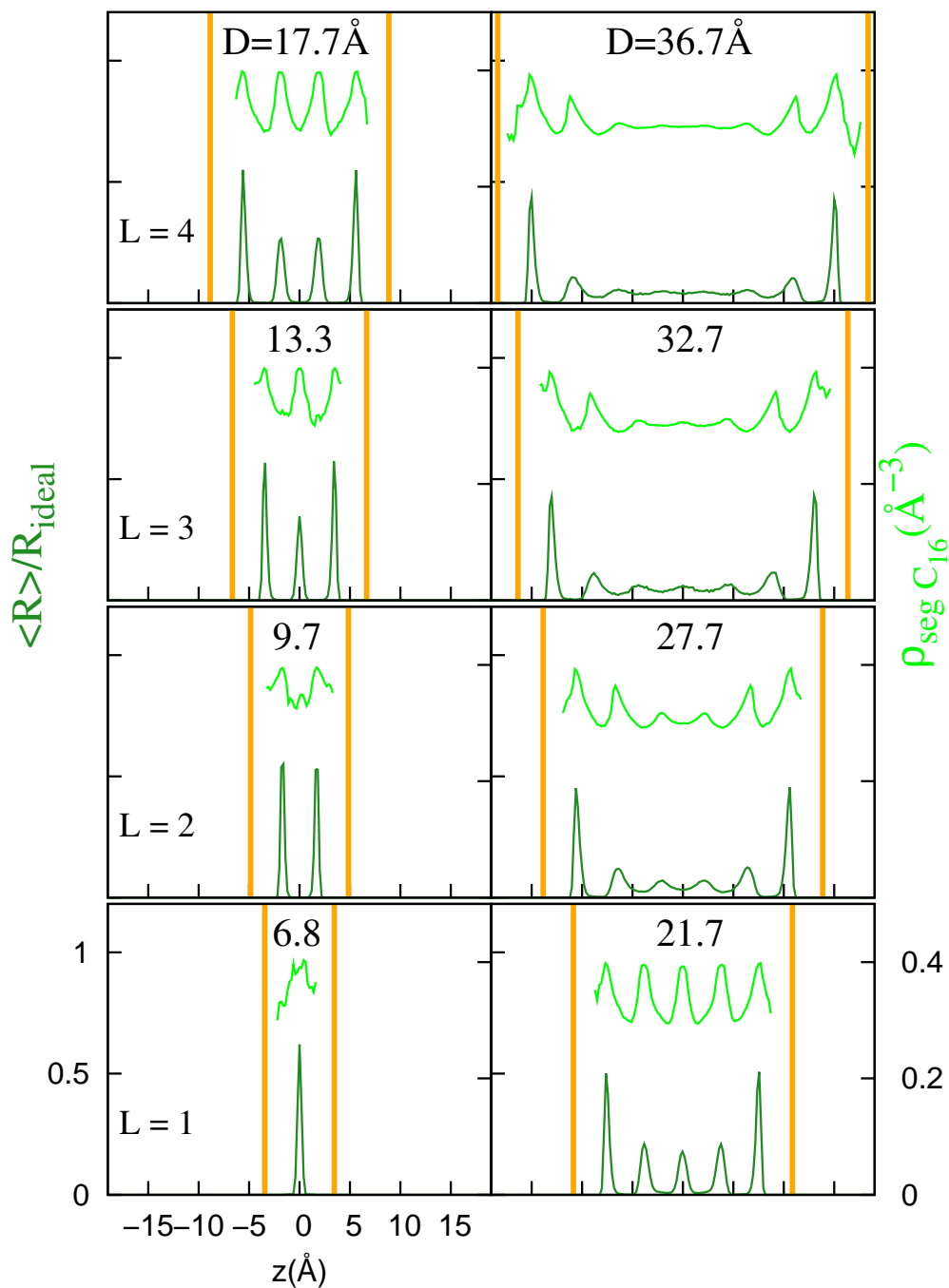


Figure 73: C_{16} Relative end-to-end distance and density inside well ordered gaps in the mixture C_6 & C_{16} .

C_{20} Relative end-to-end distance and
Segmental density in the C_{20} & C_{16} mixture

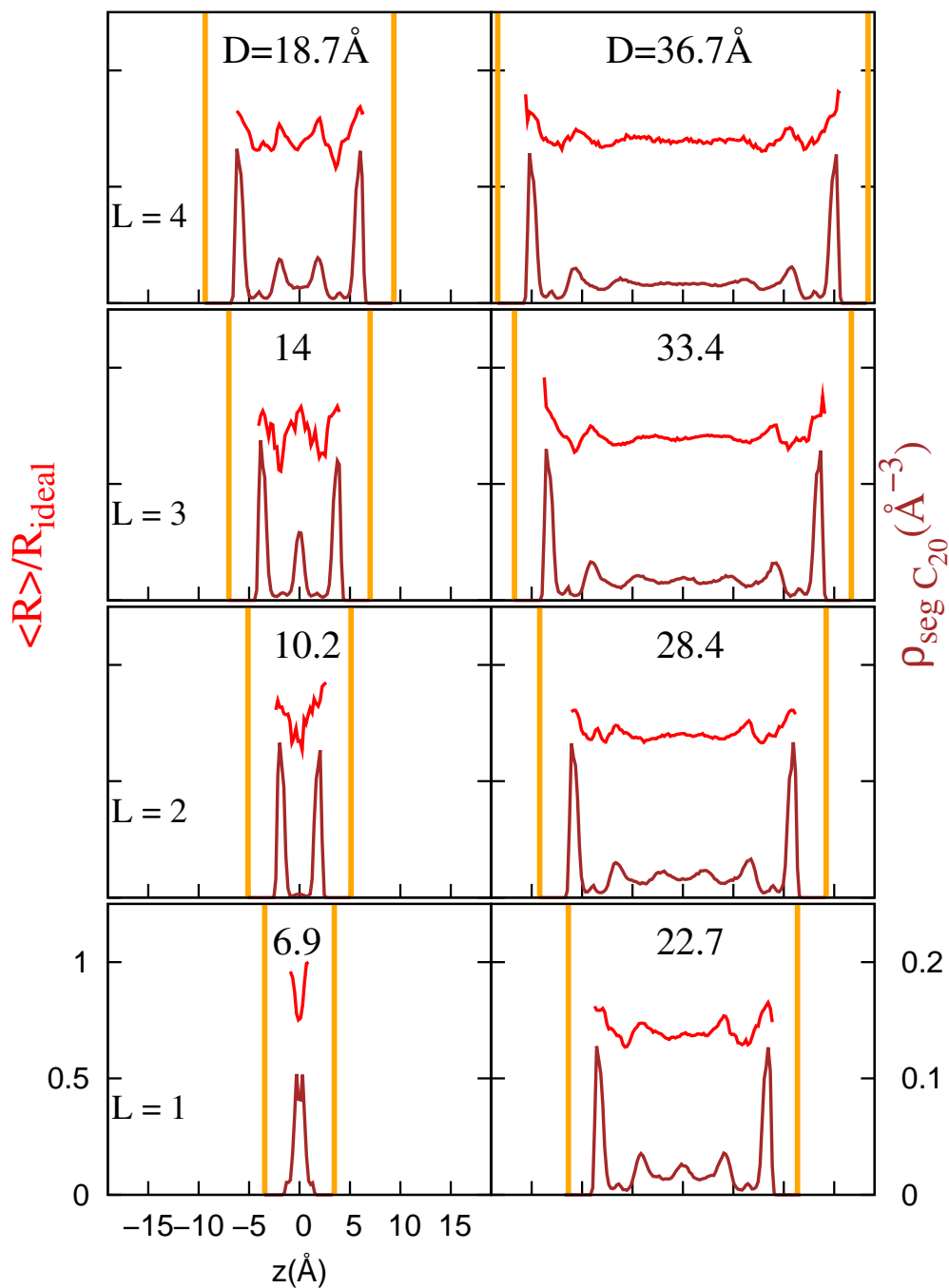


Figure 74: C_{20} Relative end-to-end distance and density inside well ordered gaps in the mixture C_{20} & C_{16} .

C_{16} Relative end-to-end distance and
Segmental density in the C_{20} & C_{16} mixture

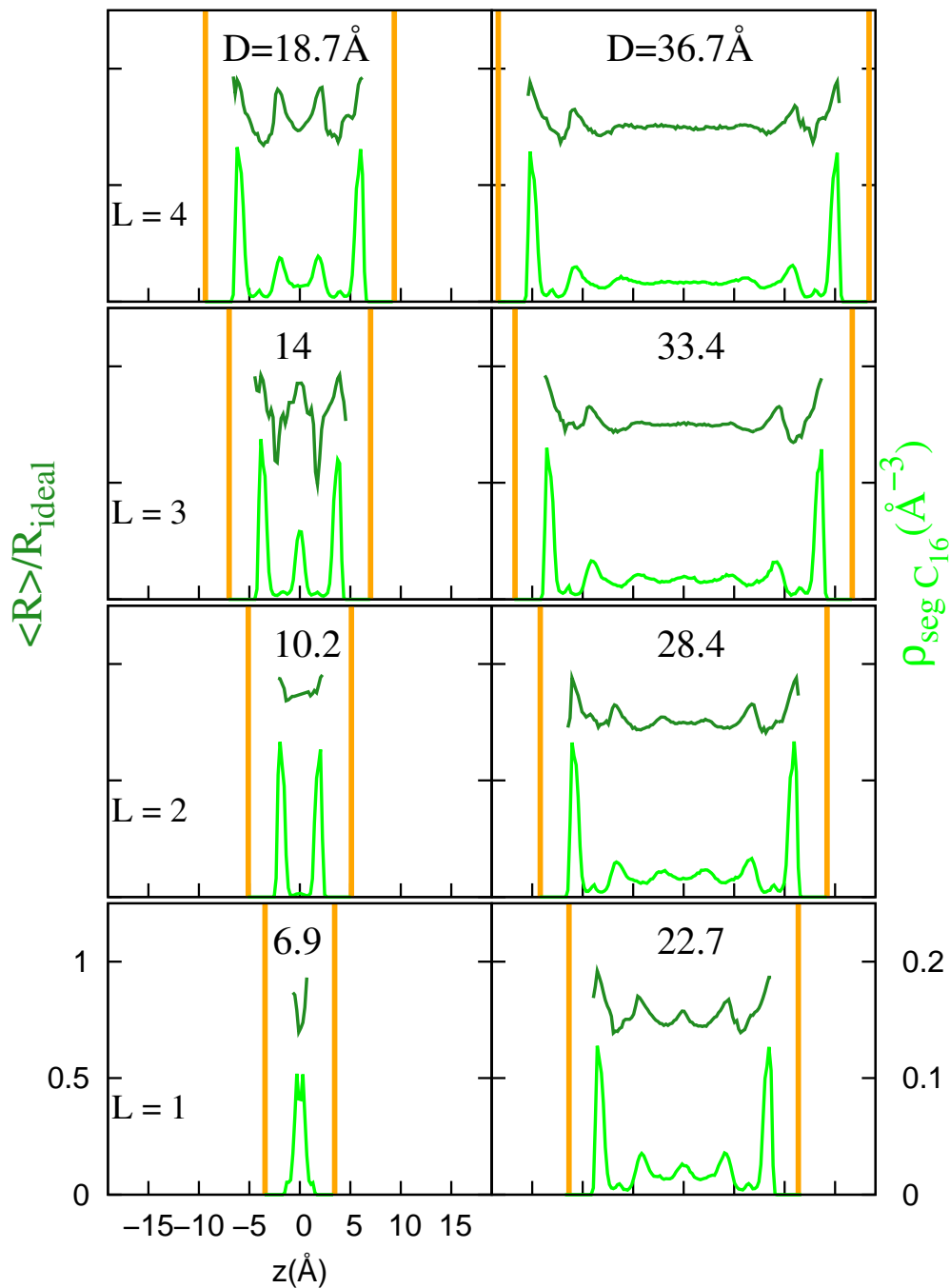


Figure 75: C_{20} Relative end-to-end distance and density inside well ordered gaps in the mixture C_{20} & C_{16} .

5.3 Molecular Orientation

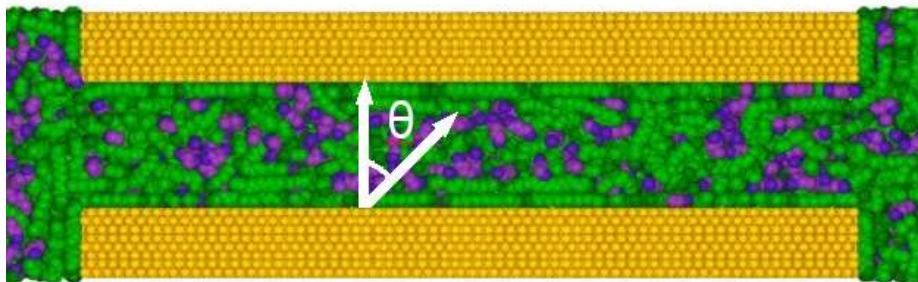


Figure 76: Intralayer ordering measured with angle θ

By studying the molecular density profile, we obtained information about the position of the center of mass of our molecules, and the average end-to-end distance gave us an indication of where were the molecules extended or compressed. Now, by calculating the average distribution of $\sin^2(\theta)$ through out the confinement, we get a better understanding of how the molecules are arranged inside the gap. θ is the angle the end-to-end vector of the molecules do with the z axis, an axis perpendicular to the confining surfaces. If all the molecules were parallel to the gold surface, the value of the function would be 1. On the other hand, if all the molecules are randomly distributed inside the confinement, then the value would be $2/3$. We chose $\sin^2(\theta)$, instead of $\cos^2(\theta)$, because the $\sin(\theta)$ function has the maximum value for molecules parallel to the gold surface.

To calculate this average, we calculate the end-to-end distance of a molecule and the location of its center of mass. We calculate this property as a function of z , in bins of 0.2\AA , through the thickness of the gap. We calculate $\sin^2(\theta) = 1 - (L_z/L)^2$, where L_z is the z-component of the end-to-end distance for a molecule. We add $\sin^2(\theta)$ over all the molecules whose center of mass is located in a particular bin, and then we divide by the number of molecules in that bin.

Fig.77 shows the orientation of hexane molecules in the C6&C16 mixture, Fig.78 shows the orientation of hexadecane in the C6&C16 mixture, while Fig.79 shows

the orientation of phytane in the C6&C16 mixture and Fig.80 shows the orientation of hexadecane in the C20&C16 mixture. For the largest gap 36.7Å in all cases, the molecules in the middle of the confinement seem to have a random orientation because the average $\sin^2(\theta)$ is close to 0.66. From this random orientation, $\sin^2(\theta)$ value oscillates through smaller and larger values as it gets close to the surface, where it is close to 1. A value of 1, indicates molecules lying parallel to the confining surfaces.

We can also see that in the case of comparing orientation with density, the peaks of the 2 properties do correspond. It is interesting to observe that in the segmental density for pure hexane layering would start at 25Å, but in the orientation plots for mixed hexane clear peaks are visibly at 36.7Å. This is evident by comparing length and orientation for pure hexane in Fig.29 with the density and orientation for mixed hexane in Fig.77. This means that even though hexane showed liquid-like features in its pure form, being in the presence of hexadecane, which tends to form layers, has induced it to attain a higher degree of layering. We can see that the hexane chains are extended and parallel to the substrate inside the well defined layers, and bent and tilted in between layers. We see 8 peaks in the orientation plot of hexane in the mixture, Fig.77, with a smaller angle against the surface as it gets closer to it.

In the case of hexadecane, how does the orientation inside the confinement change from when it was in pure form as to being mixed with short molecules and also with branched molecules? In pure form, the hexadecane chains are stretched and mostly parallel to the surface, even at gap sizes as thick as 30Å when there are 7 layers. When hexadecane is combined with hexane, it forms only 5 horizontal layers. This ordering decreases even further when mixed with branched molecules. The first 2 layers close to each surface are parallel to the confinement through the whole compression, but this order doesn't extend any further into the middle of the gap. There are on average 4 horizontal layers at most, compared to the 7 layers seen in its pure form, and 5 when combined with hexane. The orientation of phytane in the mixture is very similar as

in pure form. At most the 2 closest layers to the surface align with it. There is no horizontal alignment for molecules in the inner region of the gap.

C_6 Intra-layer ordering and Segmental density in the C_6 & C_{16} mixture

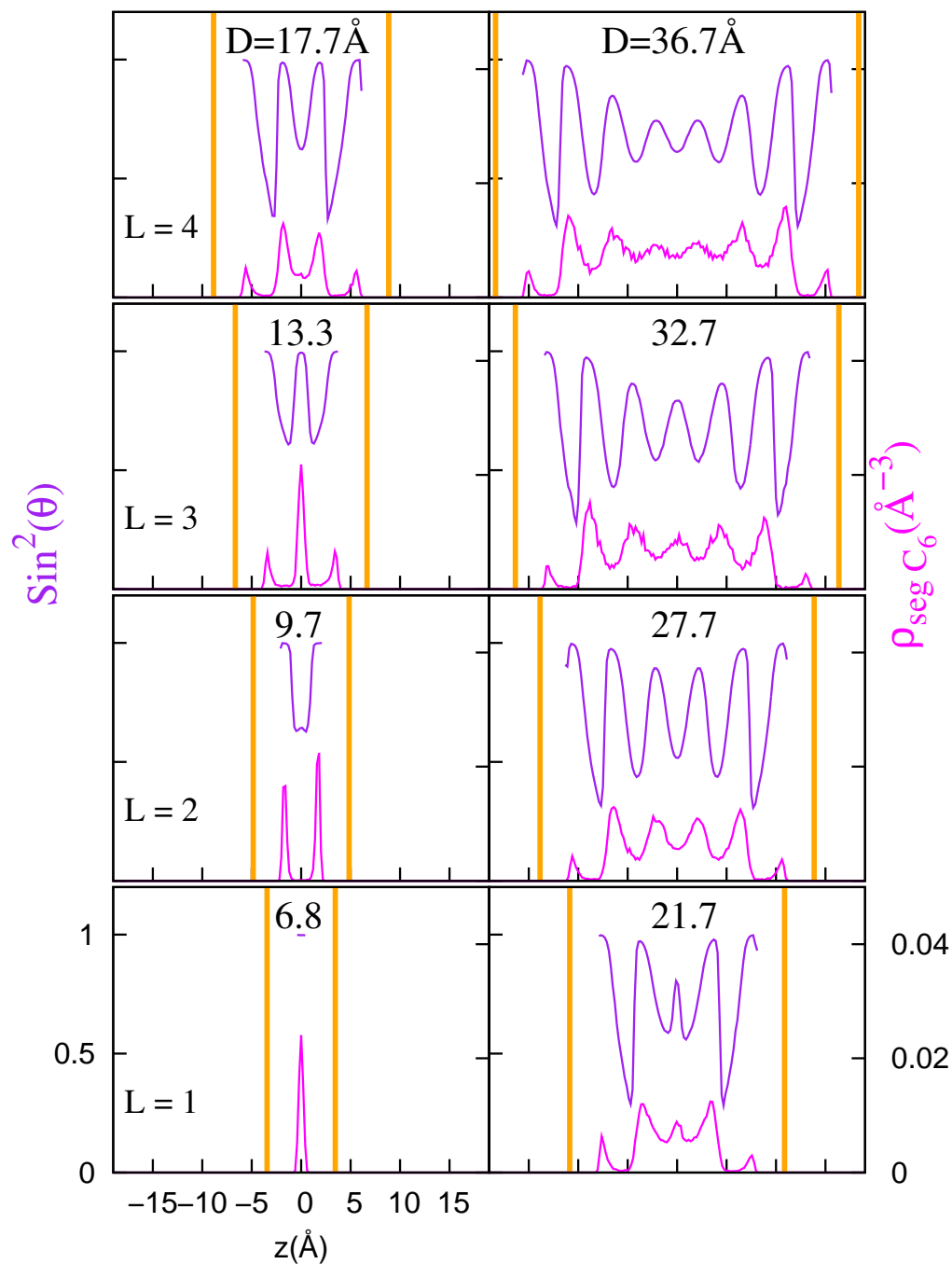


Figure 77: Comparison between the segmental density and the intralayer orientation for hexane molecules inside well-formed gaps of C_6 & C_{16} mixture.

C_{16} Intra-layer ordering and Segmental density in the C_6 & C_{16} mixture

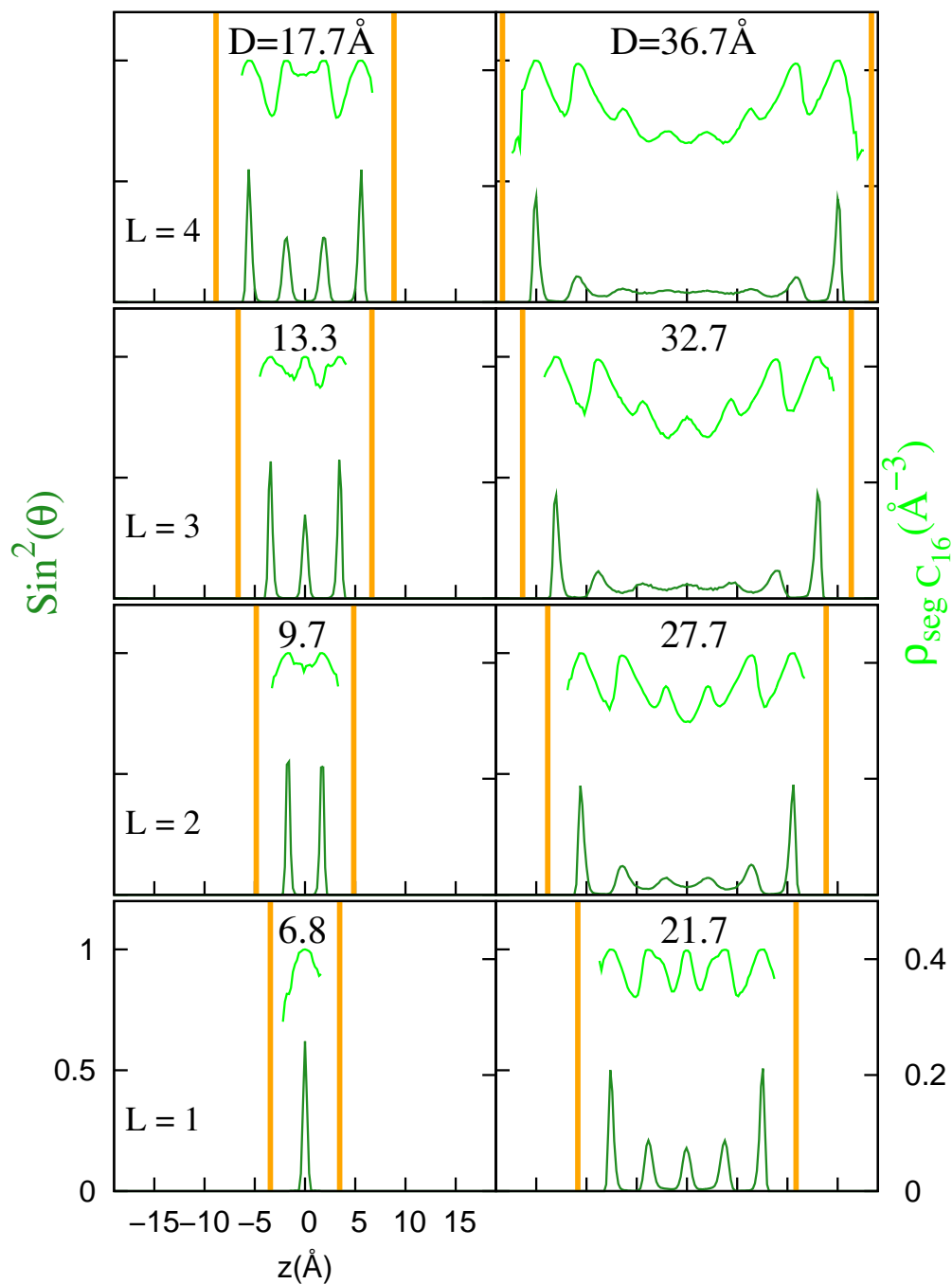


Figure 78: Comparison between the segmental density and the intralayer orientation for hexadecane molecules inside well-formed gaps of C_6 & C_{16} mixture.

C_{20} Intra-layer ordering and Segmental density in the C_{20} & C_{16} mixture

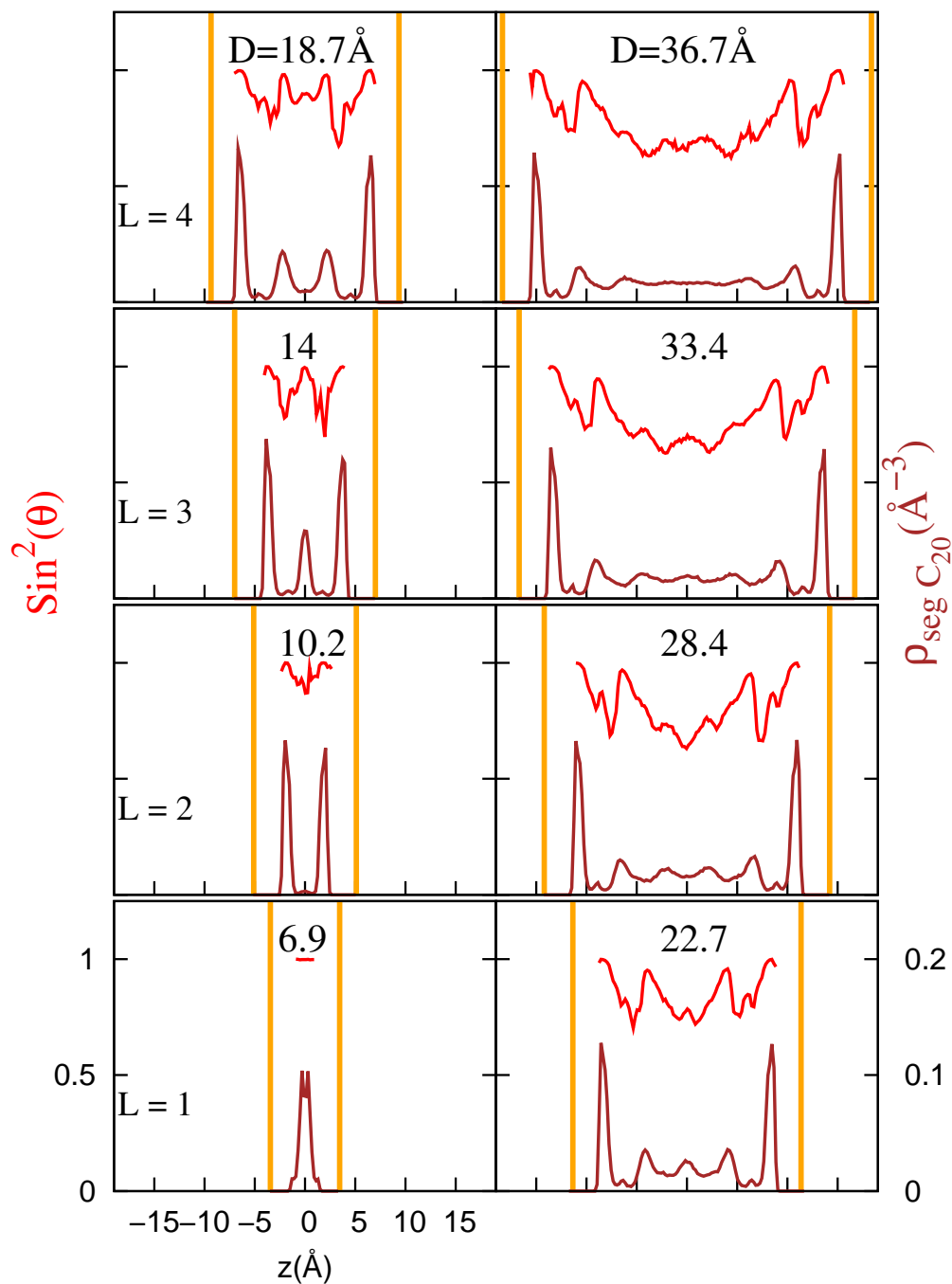


Figure 79: Comparison between the segmental density and the intralayer orientation for phytane molecules inside well-formed gaps of C_{20} & C_{16} mixture.

C_{16} Intra-layer ordering and Segmental density in the C_{20} & C_{16} mixture

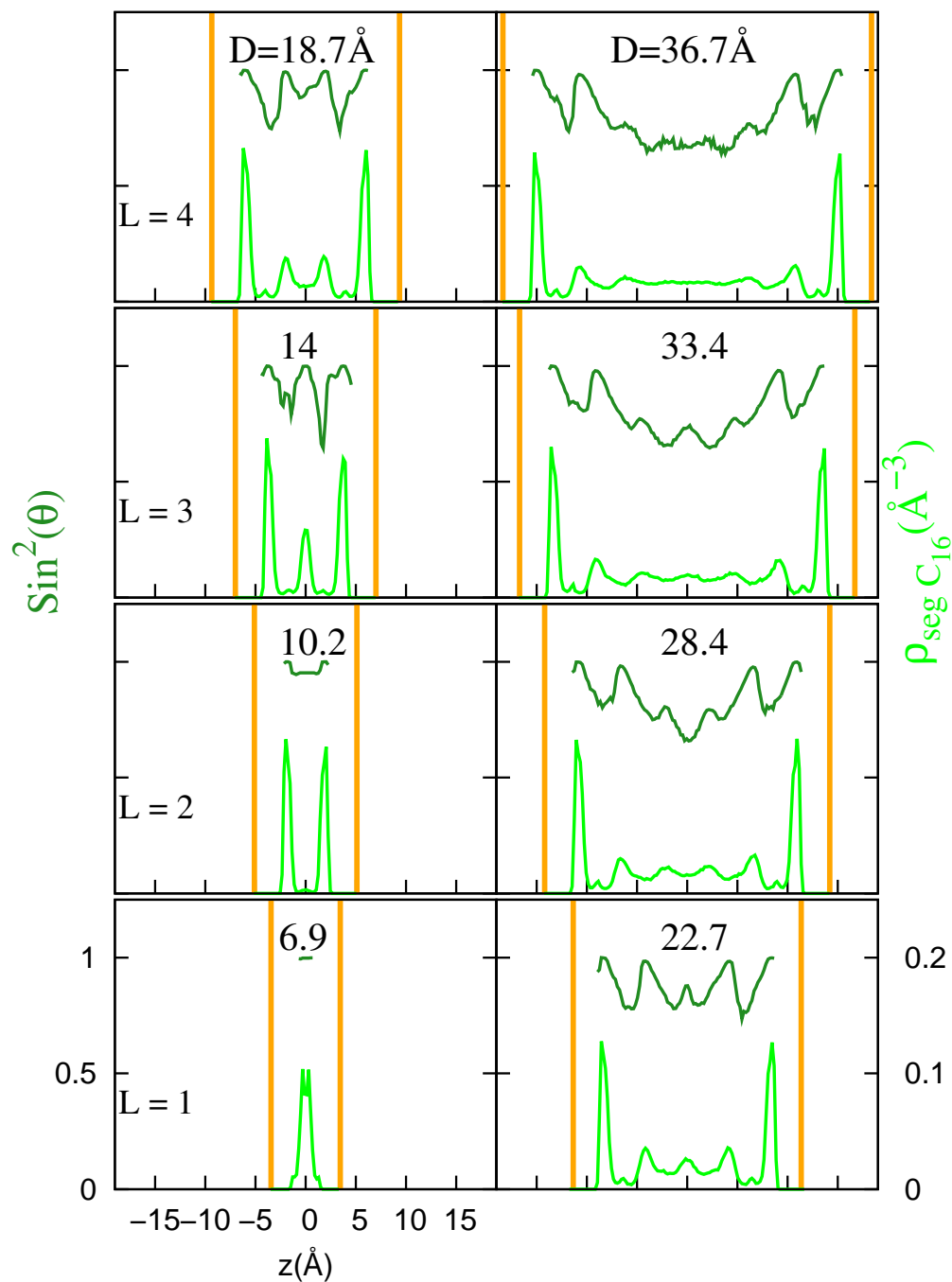


Figure 80: Comparison between the segmental density and the intralayer orientation for hexadecane molecules inside well-formed gaps of C_6 & C_{16} mixture.

5.4 *Configuration plots during compression*

In Fig.81, we see a side view of the computational cell when the system being modeled is an equimolar mixture of hexane and hexadecane. Just as we had seen in Fig.33, the horizontal alignment of the hexadecane molecules starts at the edge of the confinement and propagates into the middle of the confinement. We also see a tendency for the hexadecane molecules to form intralayer ordering, as can be seen from the different layers having a similar ordering along the height of the gap, especially when there are 5, 4 and 3 layers inside the confinement.

Hexadecane managed to be able to maintain some degree of layering when mixed with a shorter linear alkane, but was not possible when mixed with phytane. In the previous section on molecular orientation, we talk about 4 layers of hexadecane when it was mixed with phytane, but upon closer inspection, it is evident from Fig.?? that the magnitude of the 2 middle peaks is less than half of the surface density peaks, and that they are not fully independent as there is still a non-zero density in between the peaks.

Another interesting phenomenon, is the purification process in which the small hexane molecules are being expelled from the confinement in the C6&C16 mixture. We will later see that the alignment of the hexadecane in the C6&C16 mixture is related to the outward flow of hexane as they leave the confinement. During the compression of the C20&C16 mixture, Fig.82, neither species leaves the confinement at a predominant rate, and no particular ordering or layering is evident. In the next section we will see how the total number of molecules inside the confinement evolves as the system is compressed.

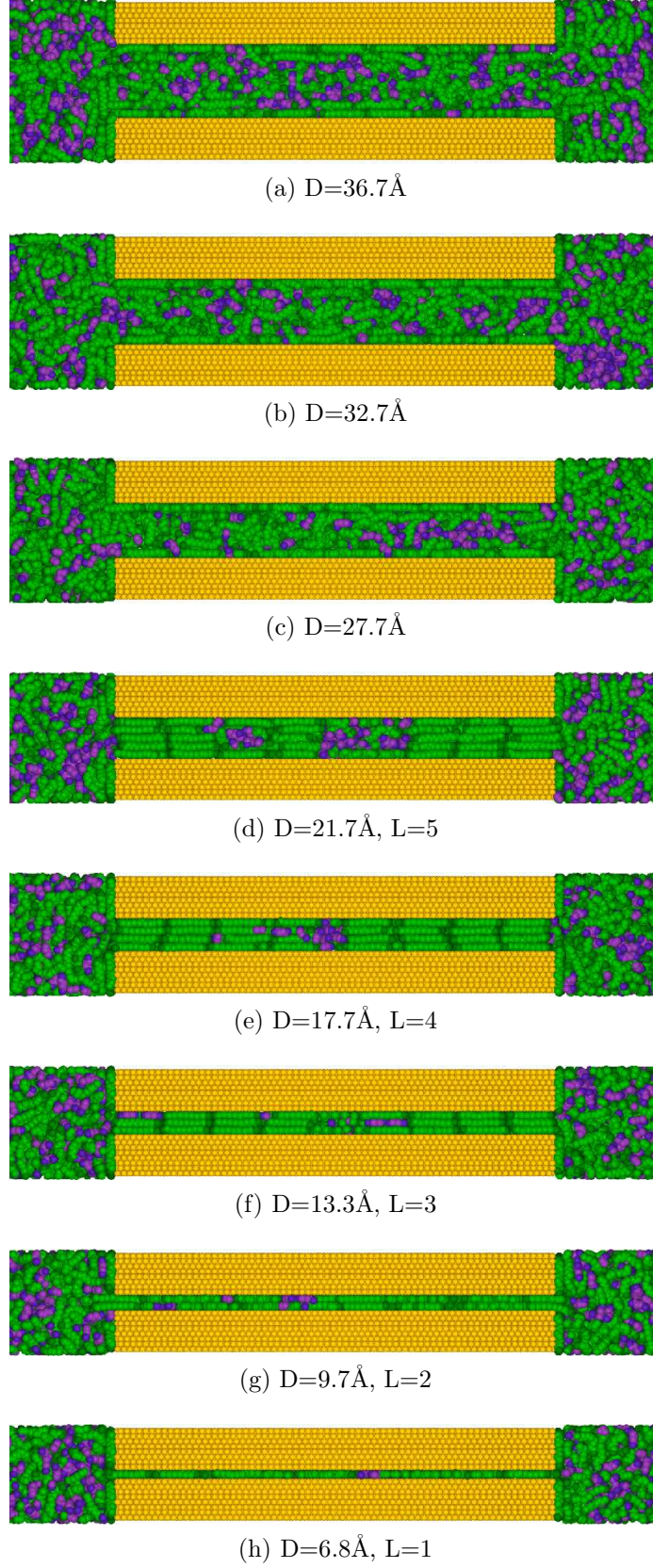
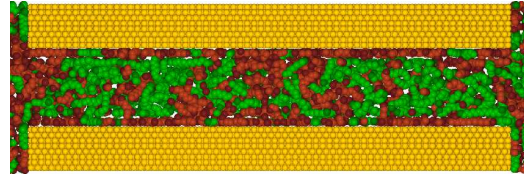
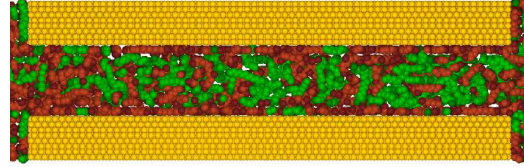


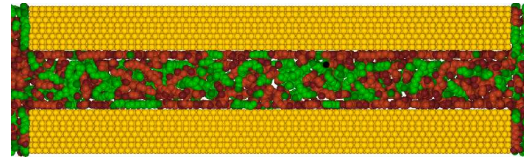
Figure 81: C20&C16: Side view of the confinement for various well formed gaps.



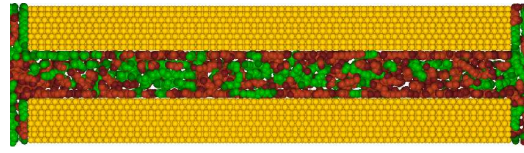
(a) $D=36.7\text{\AA}$



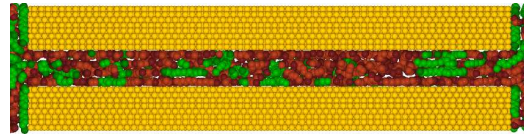
(b) $D=33.4\text{\AA}$



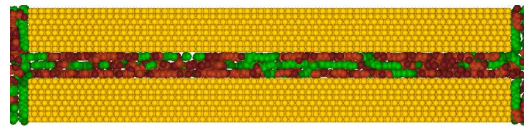
(c) $D=28.4\text{\AA}$



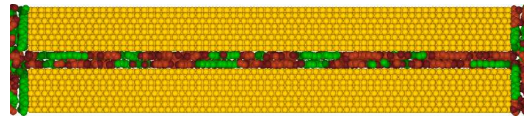
(d) $D=22.7\text{\AA}$



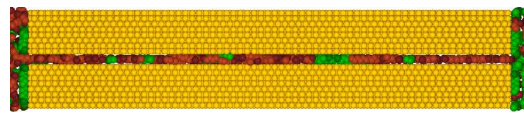
(e) $D=18.7\text{\AA}$, $L=4$



(f) $D=14\text{\AA}$, $L=3$



(g) $D=10.2\text{\AA}$, $L=2$



(h) $D=6.9\text{\AA}$, $L=1$

Figure 82: C20&C16: Side view of the confinement for various well formed gaps.

5.5 *Number of confined molecules during compression*

When we saw the evolution of the number of confined molecules during the compression for the pure systems, we concluded that pure hexadecane showed solid-like features either expelling no molecules or expelling a whole layer of hexadecane (Fig.36); on the other hand, both hexane and phytane expelled molecules through the whole compression process, and expelled a small group of molecules when transitioning from 3 to 2 layers, and a larger group when transitioning to a single layer (Fig.35 and 37).

When hexadecane is mixed with hexane, it shows the steps in the number of confined molecules but it start occurring at a thinner gap than it did when hexane was not present. When it was pure, the first sudden drop in number of molecules occurred when transitioning from 7 to 6 layers, at a gap size of 28Å; when mixed with hexane there was a smooth slope until there were 5 layers, and a large group of approximately 250 hexadecane molecules leave the confinement when it was 21Å thick. From this point, hexadecane expells large number of molecules equivalent to a whole layer, at compression intervals of 4Å. During this time, the number of confined hexane molecules decreases slowly as the system is compressed. This translates into a slow outward flow of small linear hexane molecules towards the bulk.

Another similar feature between the pure and mixed cases, is that the molecules that leave the confinement belong to the inner region, as can be seen in the middle panel of Fig.83 for the C6&C16 mixture, while the surface layer is only slightly perturbed when the molecules leave. Down to 3 confined layers, the surface layer only loses a few molecules. In the lower panel of Fig.83, we see that the number of hexadecane molecules doesn't change much even at 2 layers, but the number of hexane molecules in the surface layer does increase considerably. This transfer of middle region molecules towards the surface increases the combined density of molecules inside the confinement when there is only one layer inside the gap.

The behaviour of the branched-unbranched mixture is different in several ways

from the short-long mixture. Both phytane and hexadecane flow smoothly out of the gap as the gold surfaces move together up to a distance of 23\AA , where there are 5 intertwined layers. The transition from 5 to 4 intertwined layers was more abrupt in the previous mixture than in this one. In the branched-unbranched there is a slight step at 23\AA in the total number of hexadecane molecules inside the confinement. This transition is more evident if we look at the middle panel of Fig.84 where we see a large drop in the number of molecules in the middle region, but no change in the surface layer, lower panel of the same figure. A similar effect can be seen during the transition from 4 to 3 layers. Again, the step in this transition is much smaller than when hexadecane was mixed with hexane. The number of molecules that left the confinement in both cases was approximately 100, compared to 350 in the other mixture. This has to do with the fact that in the previous mixture the confinement was between 75% to 80% hexadecane, while in this mixture the composition of linear molecules is only 35% to 40%. It should be noted that at these gap sizes, there is a small plateau in between the steps of the number of confined hexadecane molecules. Phytane on the other hand, either pure or mixed, doesn't present these plateaus because there is a constant outflow of branched molecules towards the bulk.

By observing the middle panel of Fig.84, we can see that middle region conserves very well its initial equimolar composition, while the composition of the surface layer is mostly phytane but it changes as the gap size is reduced. The proportion of species in surface layer on the other hand changes for smaller gaps, where we can see that there are hexadecane molecules going into the surface layer when the confinement transforms for having 3 layers down to 1 single layer. In the following section, we will look more closely at the relative composition of the species when the short-long and branched-unbranched mixtures are compressed.

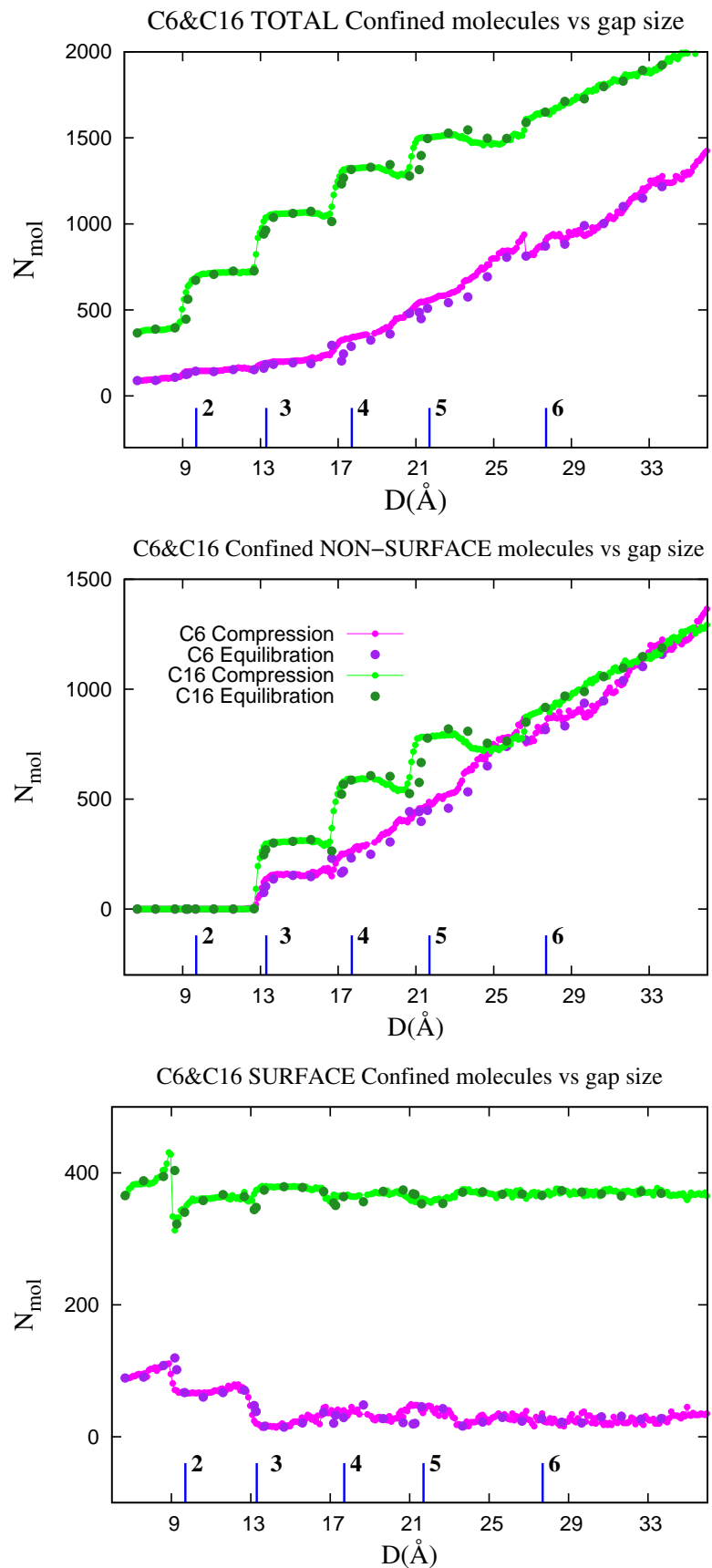


Figure 83: Number of confined hexane and hexadecane molecules versus gap size

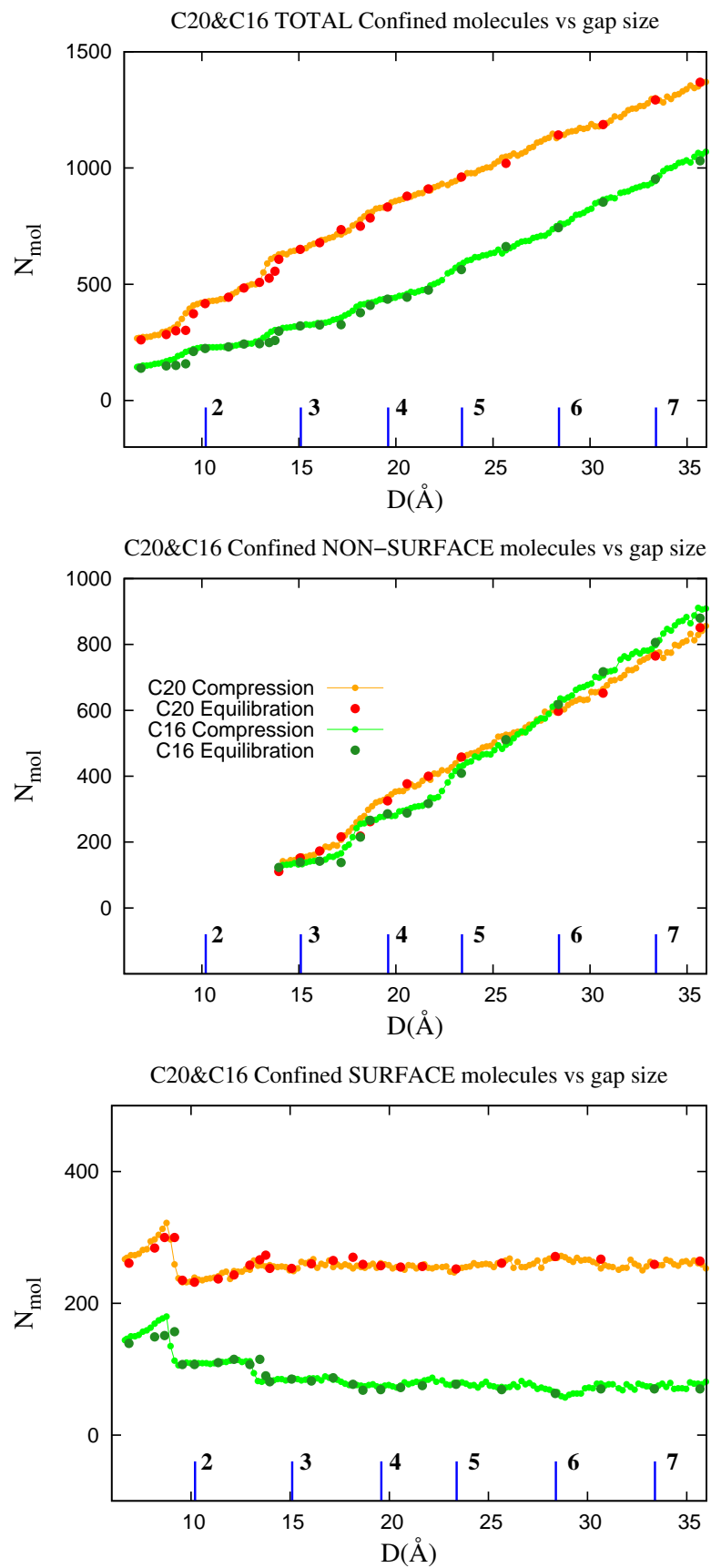


Figure 84: Number of confined phytane and hexadecane molecules versus gap size

5.6 *Molar fraction during compression*

The molar fraction is defined as the number of molecules of one species divided by the total number of molecules in the system. In a two-species mixture, as the composition of one species increases, there is a decrease in the other one.

In this section, we will compare the relative composition of each species inside the C6&C16 and the C20&C16 mixtures, in the whole gap, on the surfaces and in the middle region.

In the hexane-hexadecane mixture, the longer alkane formed a surface layer even before the compression started. This surface layer was 90% hexadecane and only 10% hexane. The strength of the interaction between the CH_3 segments and the gold atoms is 2 or 3 times stronger than the interaction with other segments, and is 50% stronger than the interaction of CH_2 with gold. In the case of hexane and hexadecane where they both have the same number of CH_3 segments this doesn't seem to affect the system and the effect that seems prevalent in the surface layer is hexadecane's ability to pack tightly maximizing the number of molecules in the surface.

In the other mixture, the surface has a larger proportion of phytane than of hexadecane. This occurs possibly because phytane has a larger proportion of CH_3 segments per molecule, 6 segments out of the 20, interacting strongly with the gold surface than hexadecane, only 2 of the 16 segments are CH_3 . The proportion of phytane on the surface, 80:20, is smaller in the C20&C16 mixture, compared to 90:10 in the C6&C16 fluid.

Another phenomenon occurring during the slow compression is the purification of the C6&C16 mixture, because a greater number of the molecules leaving the confinement are hexane. The system starts as an equimolar mixture and reaches a 82:18 composition in the total gap when there are 3 layers in the confinement. This proportion drops slightly when there is only one confined layer. The purification effect is not as pronounced in the branched-unbranched system. The mixture C20&C16

starts as an equimolar system and after being compressed down to 3 layers, its relative composition is 67:33, dropping down to 60:40 for the smallest gap.

The middle region, from where the molecules were expelled, oscillates between different compositions. In the case of hexane-hexadecane, the oscillations are larger than in the phytane-hexadecane mixture.

The surface layers in the C6&C16 mixture is mostly hexadecane with a composition of 90% long chains and only 10% short chains. While the phytane-hexadecane mixture has a 80:20 composition. In both cases, this composition changes.

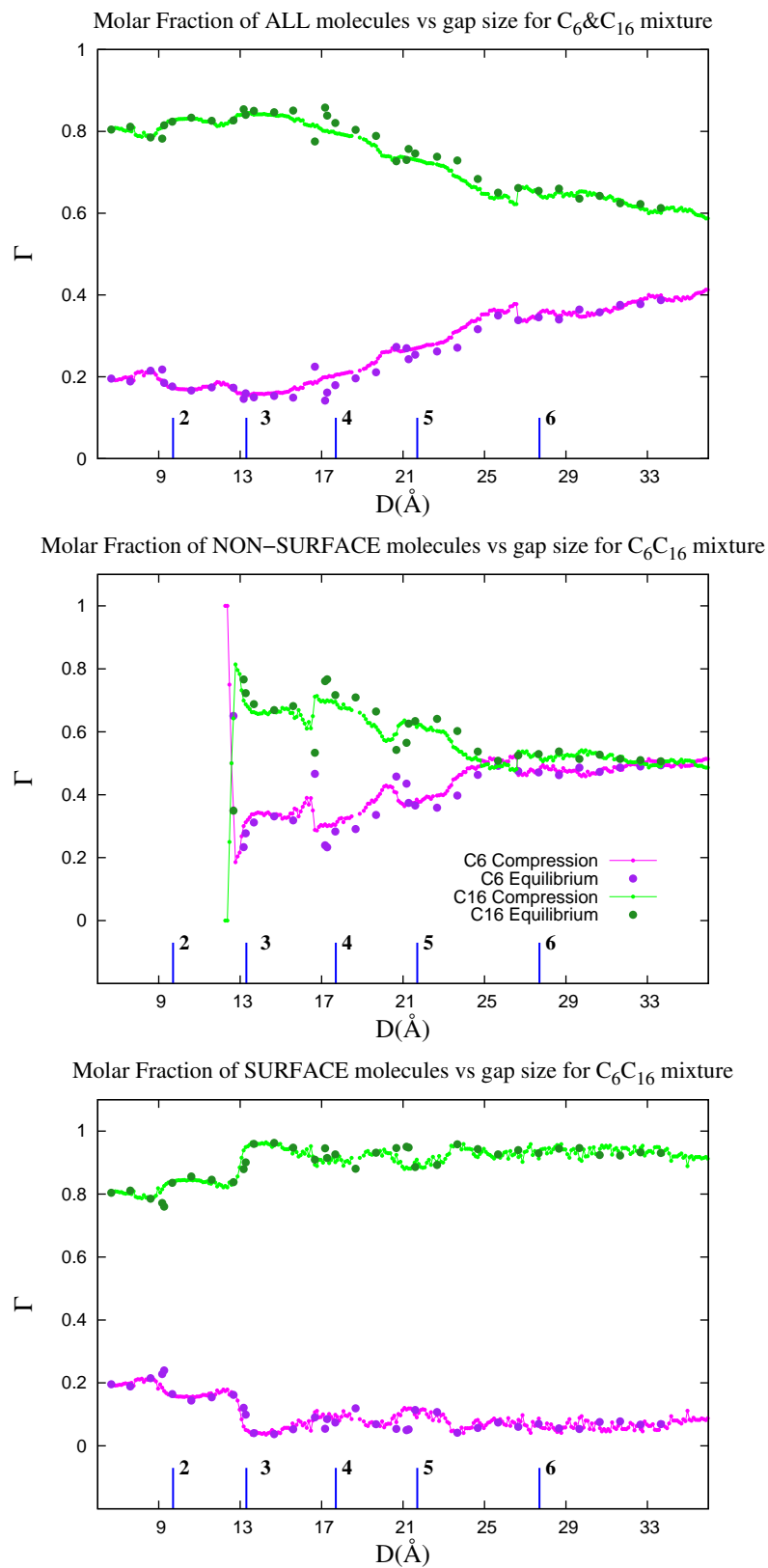


Figure 85: Molar fraction versus gap size, for molecules in the whole gap (top), in the inner region (middle) and the surface layer (bottom)

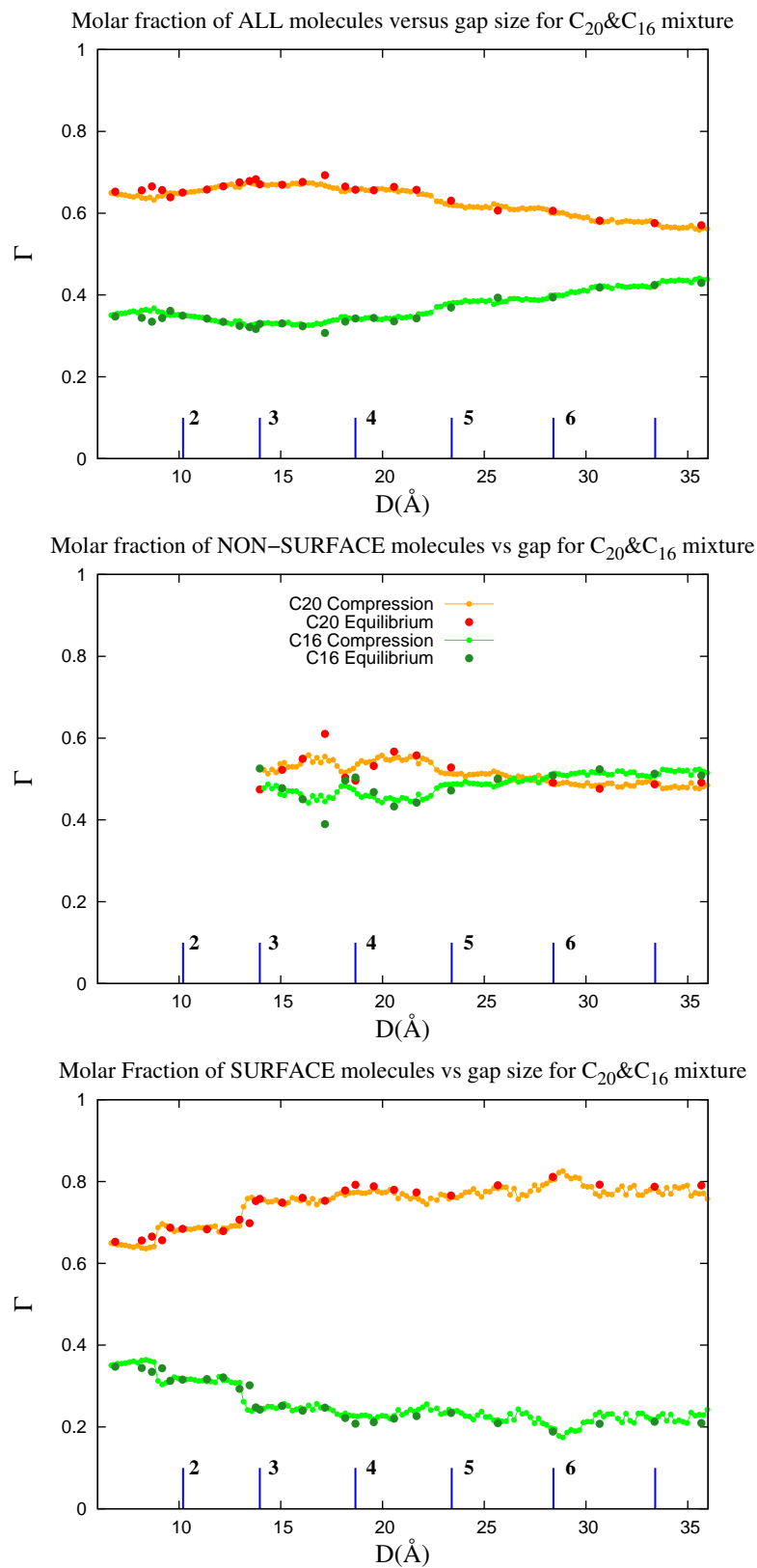


Figure 86: Molar fraction versus gap size, for molecules in the whole gap (top), in the inner region (middle) and the surface layer (bottom)

5.7 *Distribution of surface molecules during compression*

In this section, we will discuss the degree of ordering that hexadecane attains when mixed with hexane and with phytane compared to its ordering when it was in pure form.

5.7.1 Hexane-Hexadecane

The surface layer at the largest gap for pure hexadecane, left panel of Fig.89, shows several groups of molecules aligned next to each other, but there is no prevalent order inside the confinement. A similar scenario occurs at the largest gap when hexadecane is mixed with hexane in equal proportions. As we had mentioned previously, the proportion of hexadecane is 90% in the C6&C16 mixture. The small hexane molecules arranged themselves in between the hexadecane domains. While the system is slowly

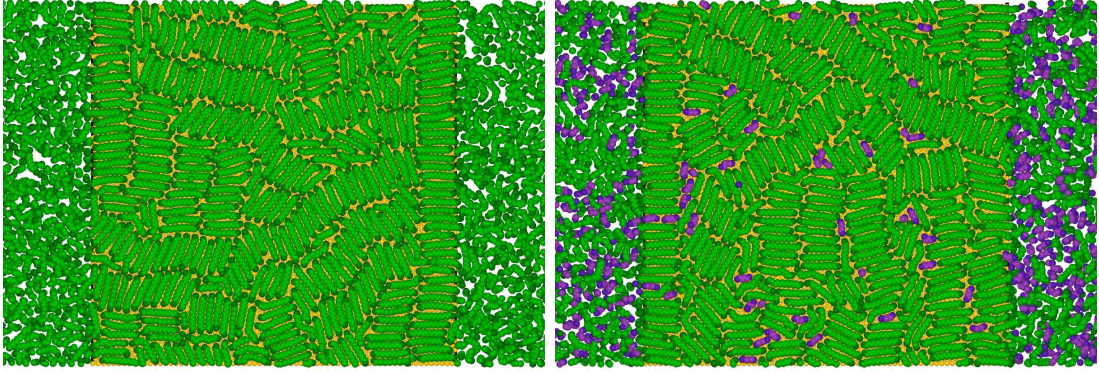


Figure 87: Initial surface layer for pure hexadecane (left) and when mixed with hexane(right)

compressed at a rate of $1\text{\AA}/9ns$, pure hexadecane leaves the confinement as whole layers, barely disturbing the surface layer, while in the C6&16 system there is a continuous flow of small linear molecules towards the bulk. We can estimate the Reynolds number for this flow Q ,

$$Q = \frac{\text{Volume leaving the confinement}}{\text{Interval of time}} = \frac{1}{2} \frac{\Delta N_{C_6}}{\Delta D} \frac{1\text{\AA}}{9ns} (V_{C_6}) \quad (25)$$

where $\Delta N_{C_6}/\Delta D$ is the slope of the plot of number of confined molecules versus gap size, $1\text{\AA}/9ns$ is the time it takes to compress the computational box 1\AA , and V_{C_6} is the volume of a hexane molecule. The $1/2$ comes from the fact that the volume of molecules leave through both sides of the confinement.

The volume for a hexane molecule in the bulk can be calculated using the atomic mass $86.18g/mol$, the density $0.6548g/cm^3$ for liquid hexane, and Avogadro's number 6.022×10^{23} molecules/mol. It is 218.55\AA^3 per molecule, which is slightly more than what we've seen in terms of dimensions of a hexane molecule, less than 7\AA in length, 6\AA in height and 5\AA in width.

We estimated the slope when the gap at 25\AA , as 350 molecules leaving the confinement when the system is compressed 4\AA . This gives us an estimate for the flow of $1.06 \times 10^{-20}m^3/s$ and dividing by an area of $25 \times 200\text{\AA}^2$, we obtain an estimate for the speed of the flow as $2 \times 10^{-4}m/s$. When we compare this value with the velocity due to thermal vibrations, approximately $400m/s$, it is very small.

The Reynolds number for a fluid draining from in between 2 plates, whose length is much larger than their spacing, is $R = \frac{QD_H}{\nu A}$ where Q is the flux, D_H is the characteristic distance which in this case is twice the spacing between the plates, ν is the kinetic viscosity of hexane and A is the area of the channel. For the ν we took the value for pure hexane 4.5×10^{-7} . This gives an estimate for the Reynolds number of 1.1×10^{-6} , which tells us that the flow of hexane can be laminar and is far from turbulent. It has a very small speed and flows among the layers of hexadecane.

To understand if this small flow of hexane molecules can affect in any way the longer hexadecane molecules, we need to consider the shape of this flow. Since the molecules are leaving through both sides of the confinement, at $x = -100\text{\AA}$ and $x = 100\text{\AA}$, the flow in the middle of the gap at $x = 0$ is effectively zero. Since we are compressing slowly and the molecules are exiting towards the bulk, it is fair to assume that on average the largest horizontal component of the speed will be at the

edge of the gap. From the pure hexadecane, we know that the long molecules tend to form layers. In the density profiles for pure hexadecane, we can even see 7 layers parallel to the confining surface. In the mixture with hexane, we see 5 independent layers parallel to the gold.

When the hexadecane molecules are lying parallel to the gold surfaces, they see a flow of hexane molecules with a gradient of speed, whose horizontal component increases away from the center of the gap. In Fig.88, I present a simple representation of the speed flow seen by the hexadecane molecules lying in a plane parallel to the gold. Yellow represents the gold surface and blue the bulk. Each layer would see different magnitudes of the flow because each plane parallel to the gold would see the x component of the flow, whichever exact form it has. Since we are using a periodic boundary along y, it is fair to assume that the net flow would towards the bulk.

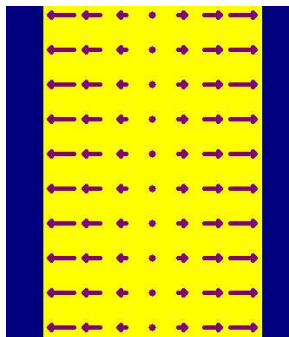


Figure 88: A simple diagram depicting the gradient in the speed of the flow.

Let's compare the surface layer when there were 3 layers, of pure hexadecane versus the mixed hexadecane has been subjected to this small flow of hexane molecules. When a hexadecane molecule is part of a layer parallel to the gold surface and is oriented at an angle with respect to a line connecting the reservoirs, the different segments of its backbone would feel a different angular momentum. The segments closer to the bulk would have a stronger angular momentum, each given by $\vec{L} = \vec{r} \times \vec{p}$, where \vec{r} would be the vector from the center of the molecule to the segment, $\vec{p} = m\vec{v}$, \vec{v} the velocity of the segments and m the mass of a segment. The angular

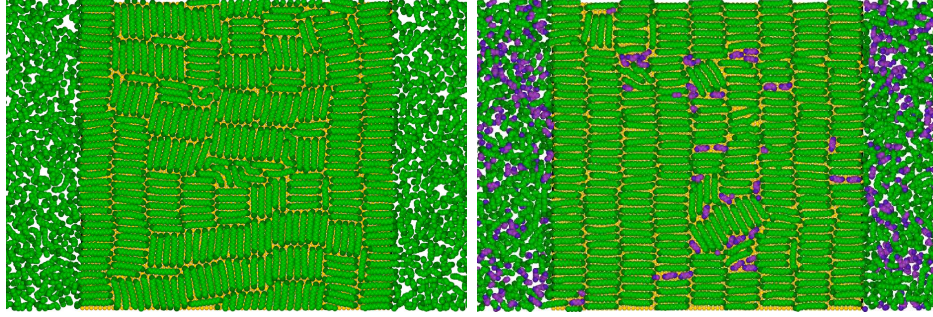


Figure 89: Surface layer when there are 3 layers in the confinement, for pure hexadecane (left) and when hexadecane is mixed with hexane(right)

momentum of the half of the molecule closer to the reservoir would counteract the angular momentum of the other half, and the molecule would rotate around its center until it aligns itself with the flow. When the molecules are aligned along the x-axis, \vec{r} is parallel to \vec{v} and the angular momentum is zero. Although the molecules would continue to move and turn due to the thermal vibrations, the gradient of the speed would guarantee that the molecules would align with the flow. The only requirement is that the compression be done at such a slow rate as to allow the molecules to reorient themselves. Before doing the compression at a speed of $0.01m/s$, we did it 17 times faster and we didn't see the level of order that we see in this case. In this case, the 30\AA took 270ns, but at the faster rate, the same compression took less than 16ns. The added time allowed the order to propagate through the confinement.

In Fig.92, we can see the evolution of the alignment of the molecules in the surface layer in some detail. The figures presented correspond to well ordered gap, which were chosen based on the quality of the density peaks. Each figure shows the gap size and the number of layers inside the confinement. Starting on the right top corner at the largest gap, we see domains but no prevalent direction. Down the right column, we see that some molecules are aligned towards the bulk. When $D = 21.7\text{\AA}$, there are 5 layers inside the gap, all parallel to the gold, as seen in the bottom right panel of Fig.78. The alignment in the surface with the outward flow continues until there are 3 layers in the confinement.

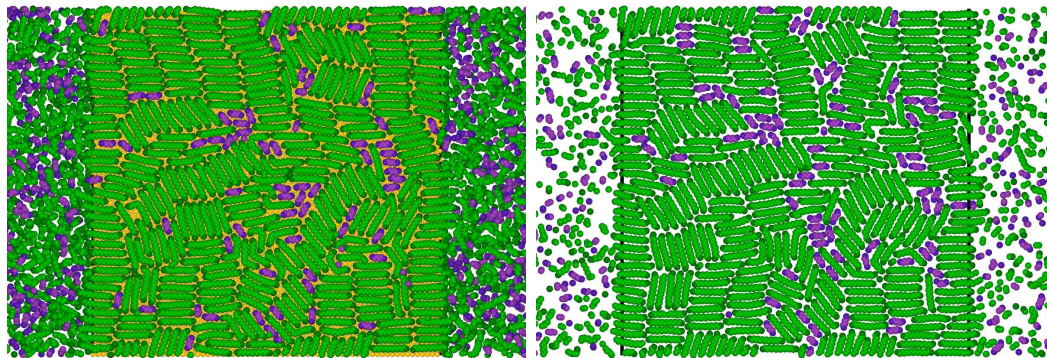


Figure 90: Top and bottom layer when there are only 2 layers inside de confinement

When there are only 2 layers inside the confinement, each layer is interacting with the surface and with the other layer. Upon closer inspection, we can see that the hexadecane molecules try to align with the molecules in their own layer and with the molecules in other layer, as in Fig.90. But because of the stronger interaction between the segments and gold, they are not as free to rearrange with the outward flow. When there were 3 layers, the middle layer worked as a lubriant between the surface layers. The alignment also exists in the middle layers, as we can see in Fig.91.

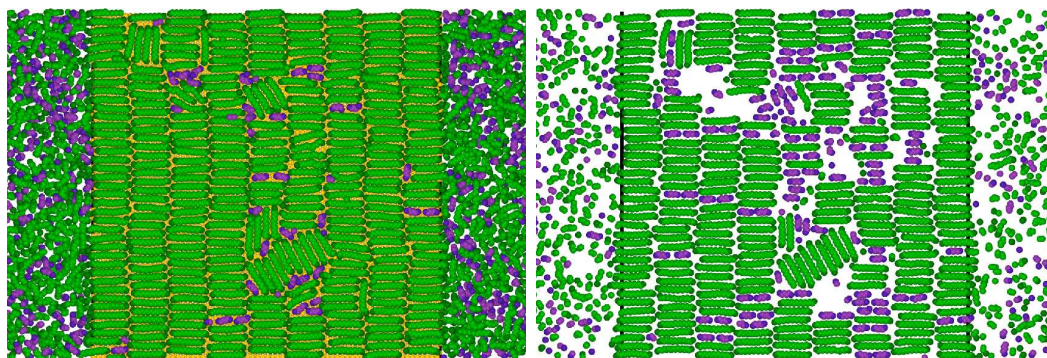


Figure 91: Top and middle layer when there are 3 layers inside de confinement

Here we also see a correspondence between the molecules in the 2 layers. There is a the group of molecules oriented at an angle in both layers. On the right panel, we can see the hexane molecules directed towards the bulk. In Fig.93, we can see the evolution of the second layer and how the level or alignment seen in the surface layer is also present in layers not touching the surface. Hexadecane's strong tendency to align

with its neighbors is coupled with the effect of the smooth hexane flow. We've seen that the addition of small linear molecules to a hexadecane system, allowed the long molecules to form smaller domains, and with the outer flow of these small molecules, gave the system the ability to orient along a particular direction. When we conceived the idea of the mixture of phytane and hexadecane to study the effect of the branches on hexadecane's solid-like properties, we wondered who would leave the confinement and who would manage a higher level of crystallization. We've already seen that the layers that are formed are mostly intertwined and the steps in the number of confined molecules are considerably smaller than in hexadecane's pure fluid.

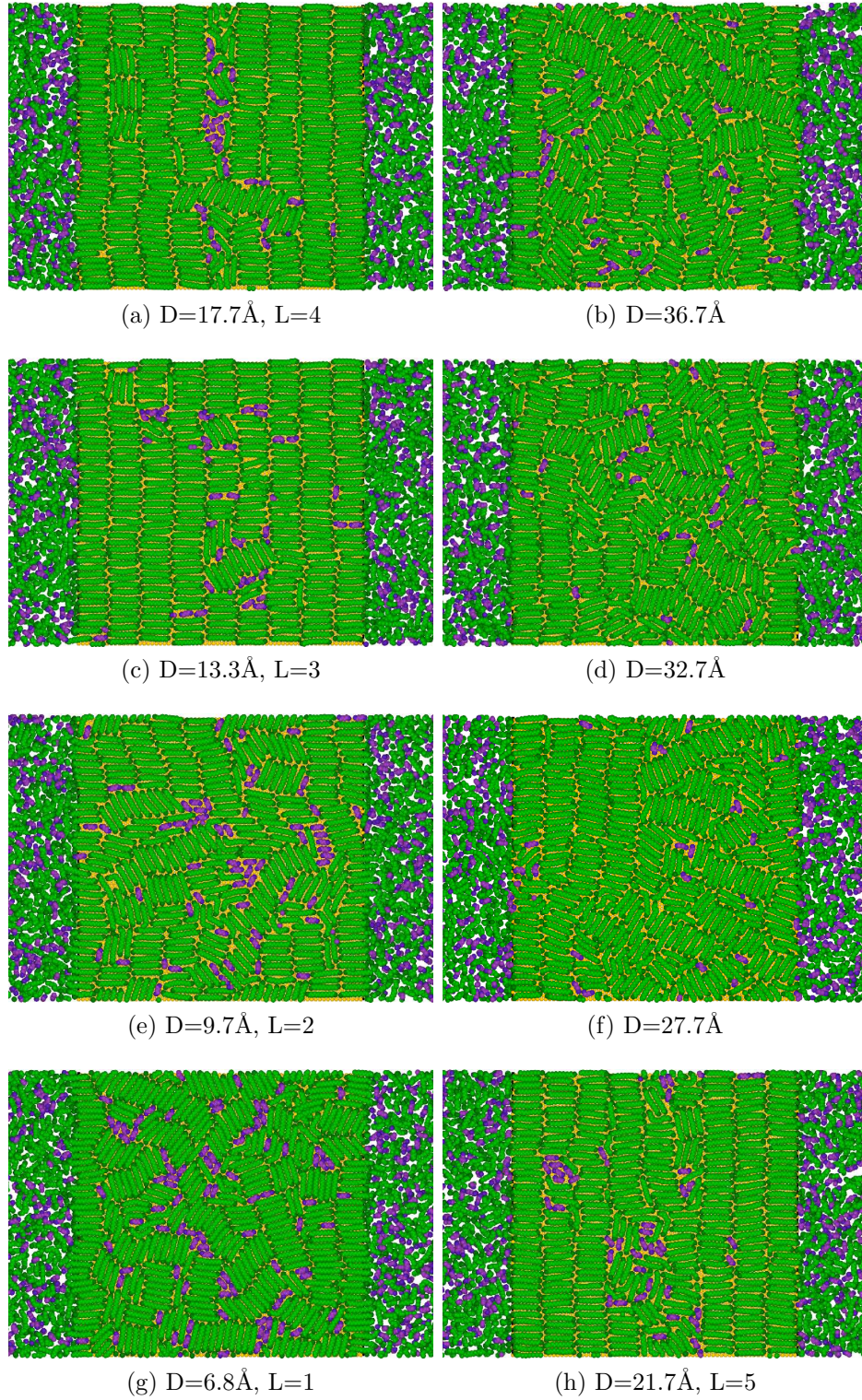


Figure 92: Top view of the surface layer for the mixture C6&16 in well formed gaps. D denotes the thickness of the gap and L indicates the number of layers inside the gap, either independent or intertwined. Note that when the appearance of well formed layers starts, for $L=5$, the increase in alignment is evident.

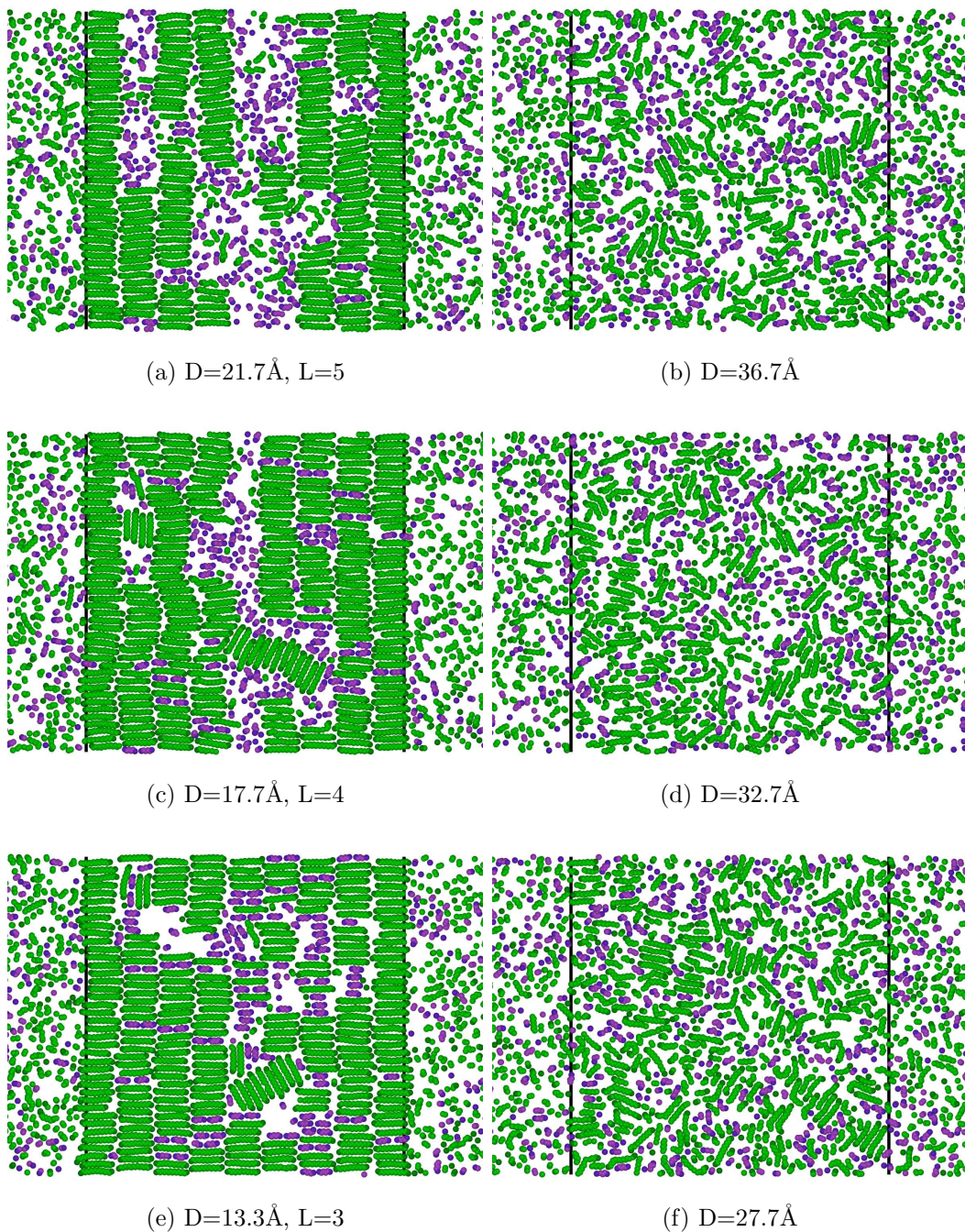


Figure 93: Top view of the second layer for the mixture C6&16 in well formed gaps. D denotes the thickness of the gap and L indicates the number of layers inside the gap, either independent or intertwined. Note that when the appearance of well formed layers starts, for $L=5$, the increase in alignment of the hexadecane molecules is dramatic.

5.7.2 Phytane-Hexadecane

The evolution of the surface and second layers in the C20&C16 mixture can be seen in Figs.95 and 96, respectively. There is no predominant order whether in the surface layer or the second. Some small domains of phytane and hexadecane can be seen when there are 3 layers inside the confinement. The hexadecane domains are larger in the middle region. To see how the surface layer changes during the compression,

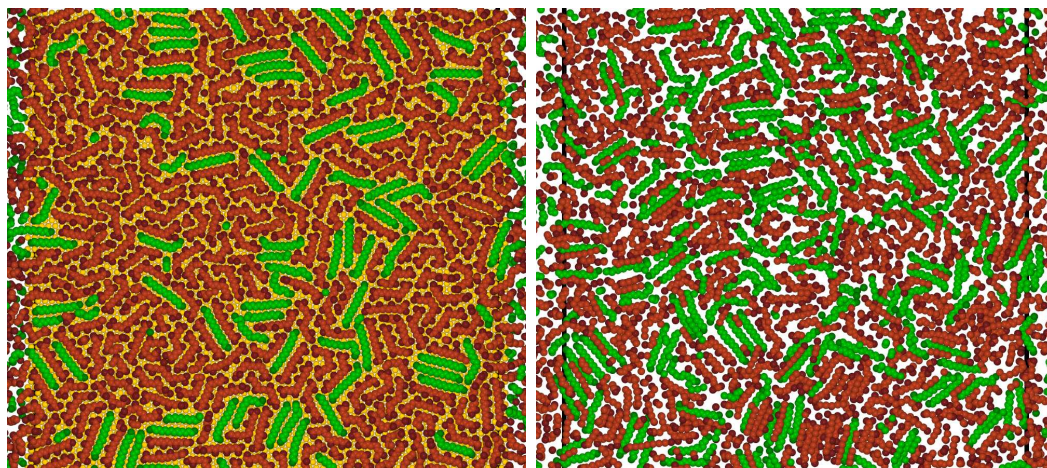


Figure 94: Top and middle layers, when there are 3 layers inside the confinement, $D=14\text{\AA}$.

let us inspect Fig.95 for any degree of ordering, and for any indication of ordering in the second layer or intralayer ordering we can look at Fig.96.

No preferred direction is easily discernible. The high proportion of phytane inside the confinement makes it hard for hexadecane to form domains of molecules pointing along one particular direction. The fact that the layers are intertwined also hinders the ability of hexadecane of forming layers parallel to the confining surfaces. The outward flow of structured molecules doesn't induce any alignment in the long linear hexadecane.

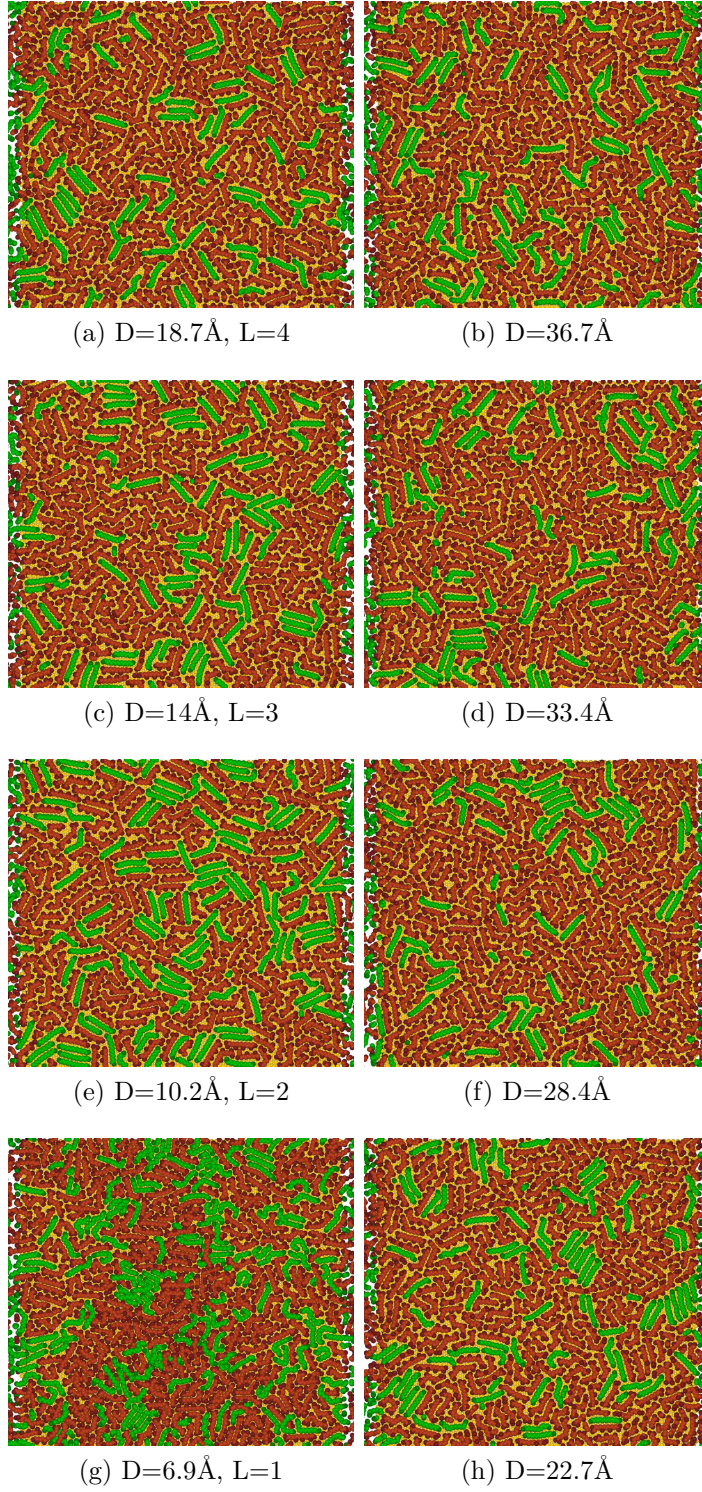


Figure 95: Top view of the second layer for the mixture C20&C16 in well formed gaps. D denotes the thickness of the gap and L indicates the number of layers inside the gap, either independent or intertwined.

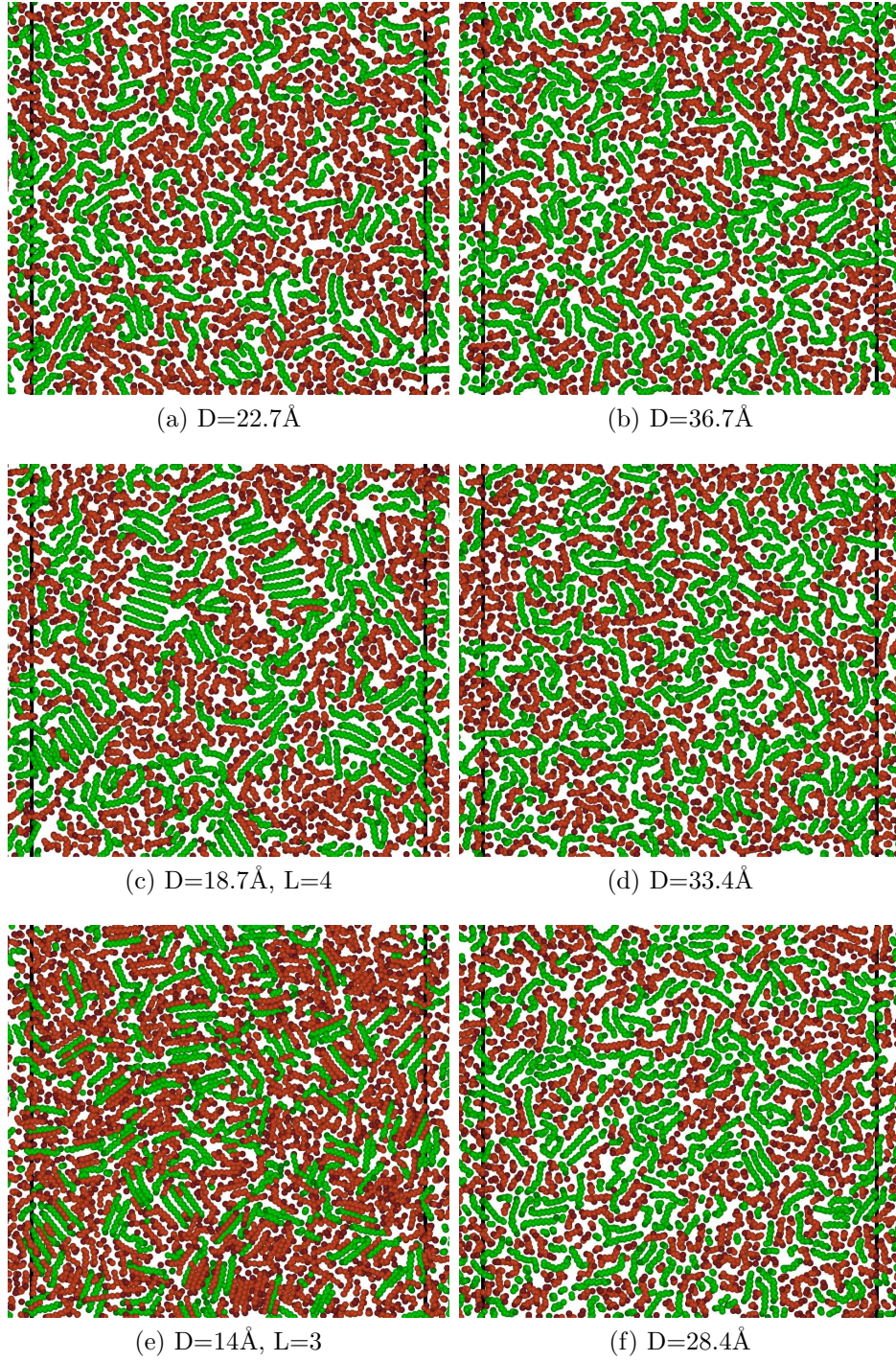


Figure 96: Top view of the second layer for the mixture C20&C16 in well formed gaps. D denotes the thickness of the gap and L indicates the number of layers inside the gap, either independent or intertwined. The black vertical lines indicate where the confinement ends.

5.8 *In-layer alignment during compression*

In the previous section, we discussed qualitatively the alignment of the molecules inside the confinement as the mixed fluids were slowly compressed. One way to quantify this phenomenon is to calculate the average of $\cos^2(\phi)$ that the end-to-end vector for the confined molecules make with the x direction. $\cos^2(\phi)$ has a value of 1 for complete alignment along the x direction, and a value of 1/3 for an isotropic distribution of the molecules. We previously saw for pure hexane in Fig.46 and for pure phytane in Fig. 48, that the average orientation $\cos^2(\phi)$ for pure hexane and pure phytane slowly increases as the system is compressed. This means that the molecules slowly tended to slightly reorient towards the bulk. In that case, the flow consisted of molecules of their own species. In the case of pure hexadecane, the orientation of the molecules didn't change much during compression. This happened because pure hexadecane had formed very rigid large domains that were not able to rotate easily.

In the mixture of hexane and hexadecane, we see a completely different behavior. In the configuration plots, Fig.92 and 92, how starting when there were 5 layers in the confinement the alignment of the molecules seemed to increase as the system was compressed until there were 2 layers. We can see this alignment quantitatively in the plot of $\cos^2(\phi)$ versus gap size for the hexane-hexadecane mixture in Fig.97. The light green line corresponds to the average orientation of hexadecane during compression, we have a value every 0.1Å, while the dark green dots correspond to the alignment after those configurations were equilibrated further. The line connecting the dots is intended to guide the eye. The orientation of hexane is shown in pink for values obtained during compression and in purple for those gathered after further equilibration.

From the initial confinement at 36.7Å down to a gap of 24Å, the rate of expelling molecules is fairly constant, as seen from the slope of the total number of confined molecules versus gap size, Fig.83, but the gap spacing is decreasing which implies that

the speed of the flow becomes larger. From gaps with thickness 26Å down to 22Å, there is no outward flow of hexadecane but only a reorientation of the molecules until on average they reach a $\cos^2(\phi) = 0.95$. This ordering occurs both on the surface and in the middle region of the confinement.

$\cos^2(\phi)$ gives a value of 1 for molecules oriented at an angle ϕ of 0° or 180° because linear molecules should be indistinguishable from both ends, giving us a measure of how well the molecules are aligned along the 0° line.

As we've seen before, when hexadecane is compressed it tends to leave in large groups usually the size of a layer. In this case, when a layer is expelled, the system momentarily loses its alignment, but the continuous outward flow of hexane, induces the alignment of the hexadecane molecules once again, until another layer is expelled. It continues oscillating between states of alignment and disalignment until there are only 2 layers. We already discuss that at this point both layers are interacting strongly with the gold surfaces and are not as free to reorient. In general, as the hexadecane molecules start arranging in horizontal layers, starting around between 23Å and 25Å, we see the increase of alignment of the hexadecane molecules with the flow. We previously discussed that once the molecules are parallel to the gold surface, they will feel a speed gradient in the hexane flow that would allow them to reorient with the flow.

Fig.98 shows for $\cos^2(\phi)$ versus gap size for the C20&C16 mixture. It doesn't show much improvement in the alignment of the hexadecane molecules during the compression of the system. The phytane molecules has a similar behavior as when it was pure, a slight increase in the orientation, as seen in Fig.48. This means that the presence of the branches disrupts hexadecane's tendency to align. In this unbranched-branched case, the outward flow is composed equally of both types of molecules and the composition inside the gap is more mixed than in the case of the short-long mixture where the gap had become mostly composed of long molecules with the short ones

aiding to align the long molecules. As we mentioned before in Ref.[14], they had done several molecular dynamics simulations on mixtures of hexane-hexadecane and had arrived to the observation that "The short chains act as a plasticizer or solvent for the long chains". In our case, the spatial arrangement of our system allowed for an outward flow of these molecules along one particular direction that helped to align the long molecules. In the phytane-hexadecane case, neither component is dominant, the flow is composed equally of both and the remaining hexadecane inside the confinement are not able to pack because of phytane's branches.

In polymer physics or liquid crystals, $3 \langle \cos^2(\phi) - 1 \rangle / 2$ is an order parameter used to measure the alignment. From our 3 pure systems and 2 mixed system, only the hexane-hexadecane mixture is able to attain a high order parameter for well-formed gaps.

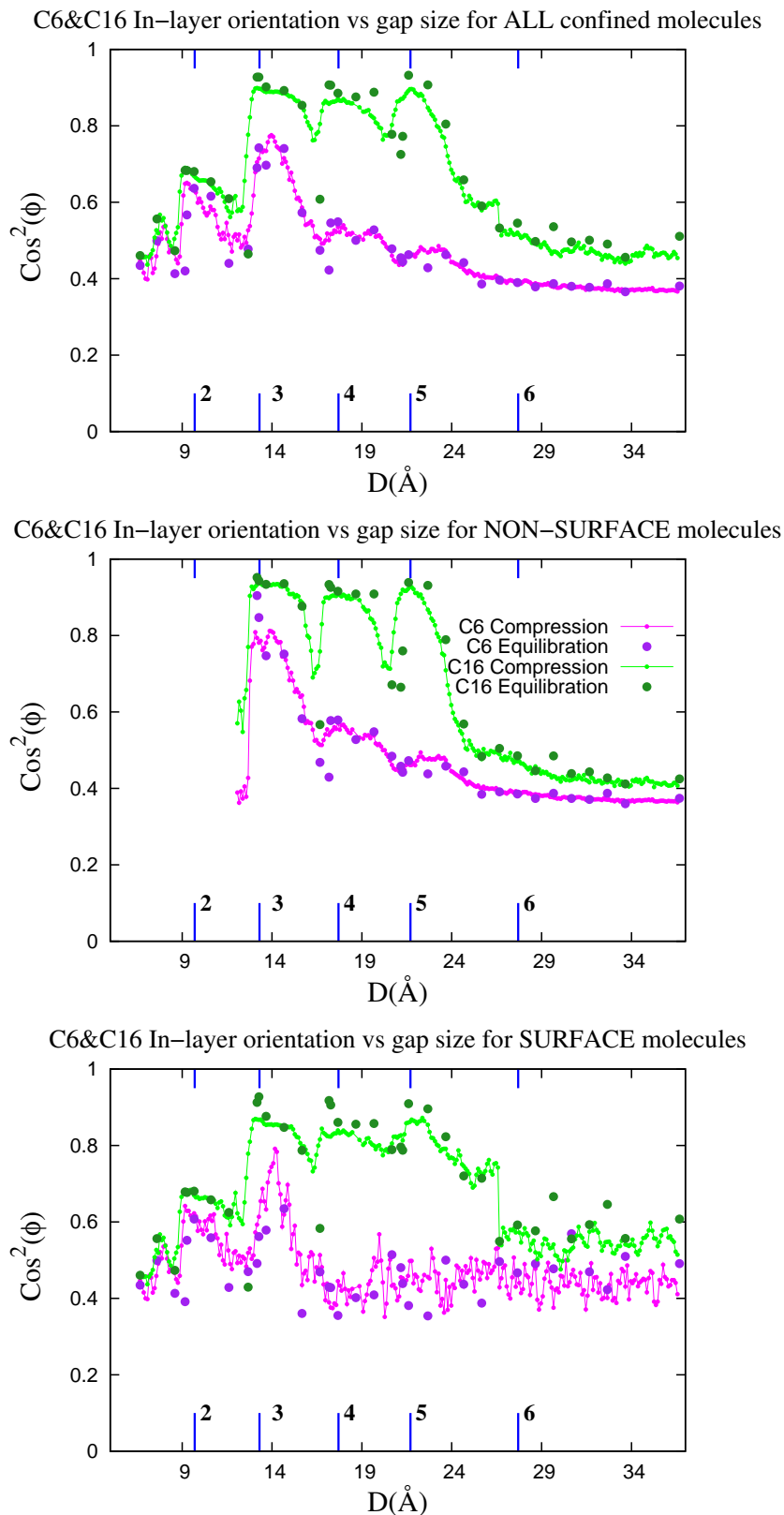


Figure 97: The average value of $\cos^2(\phi)$ versus gap size. We clearly see how the hexadecane molecules orient themselves along the direction of the flow. The hexane molecules are oriented on average along the x-axis, as explained in the text.

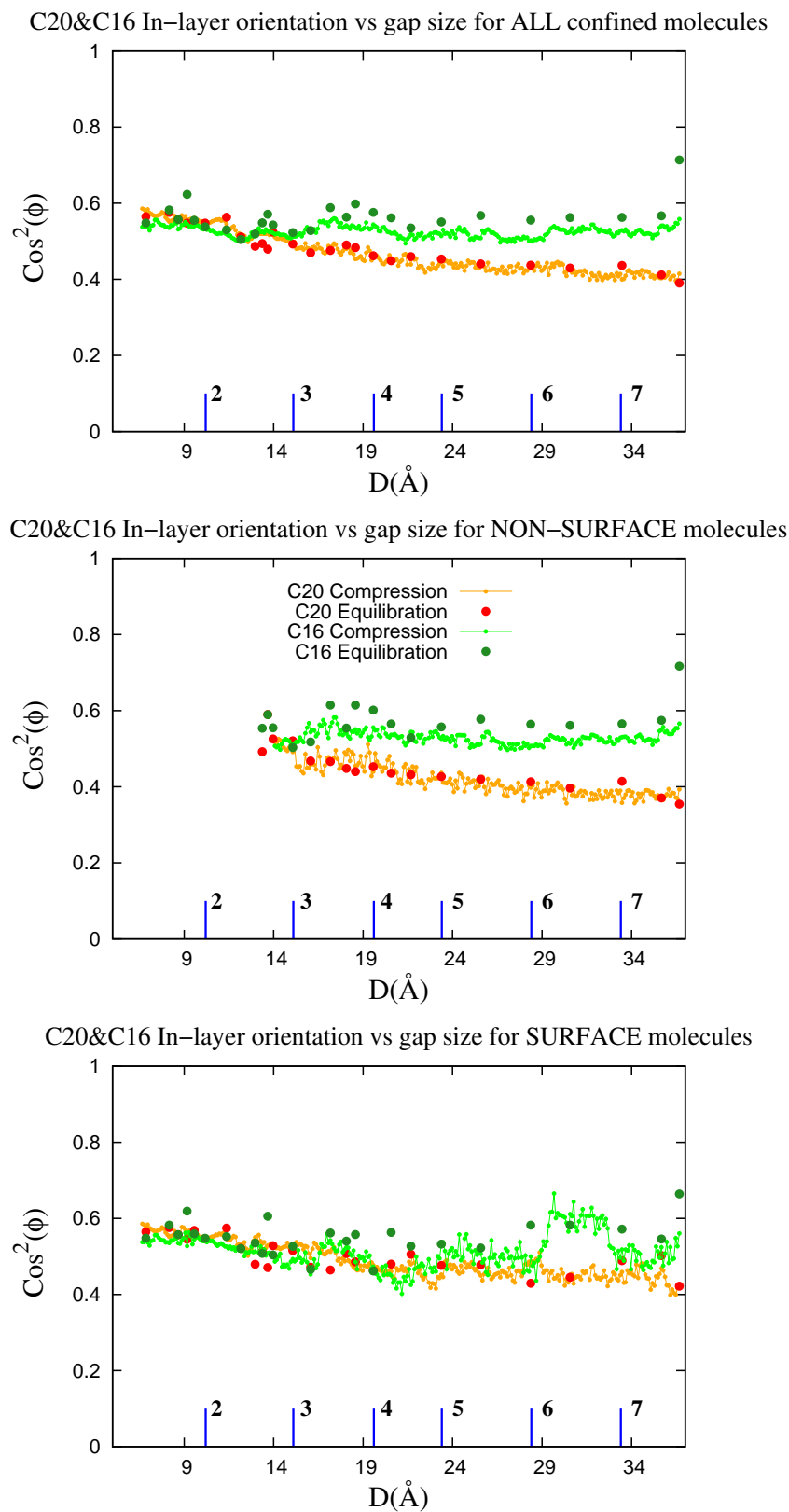


Figure 98: The average value of $\cos^2(\phi)$ versus gap size in the C6&C16 mixture. We see a very small increase in the orientation of the hexadecane molecules.

5.9 Solvation force during compression

We have discussed so far the density profiles and how the molecules organize inside the confinement in layers, the way the number of confined molecules and their orientation changes as the different systems are compressed. We have observed that the short-long mixture shows much better layering and ordering than the mixture of branched-unbranched. In this section, we will see the differences in the solvation force between the two mixtures, and between the mixtures and the solvation force of each component as they were compressed pure, as we saw in the chapter on pure systems.

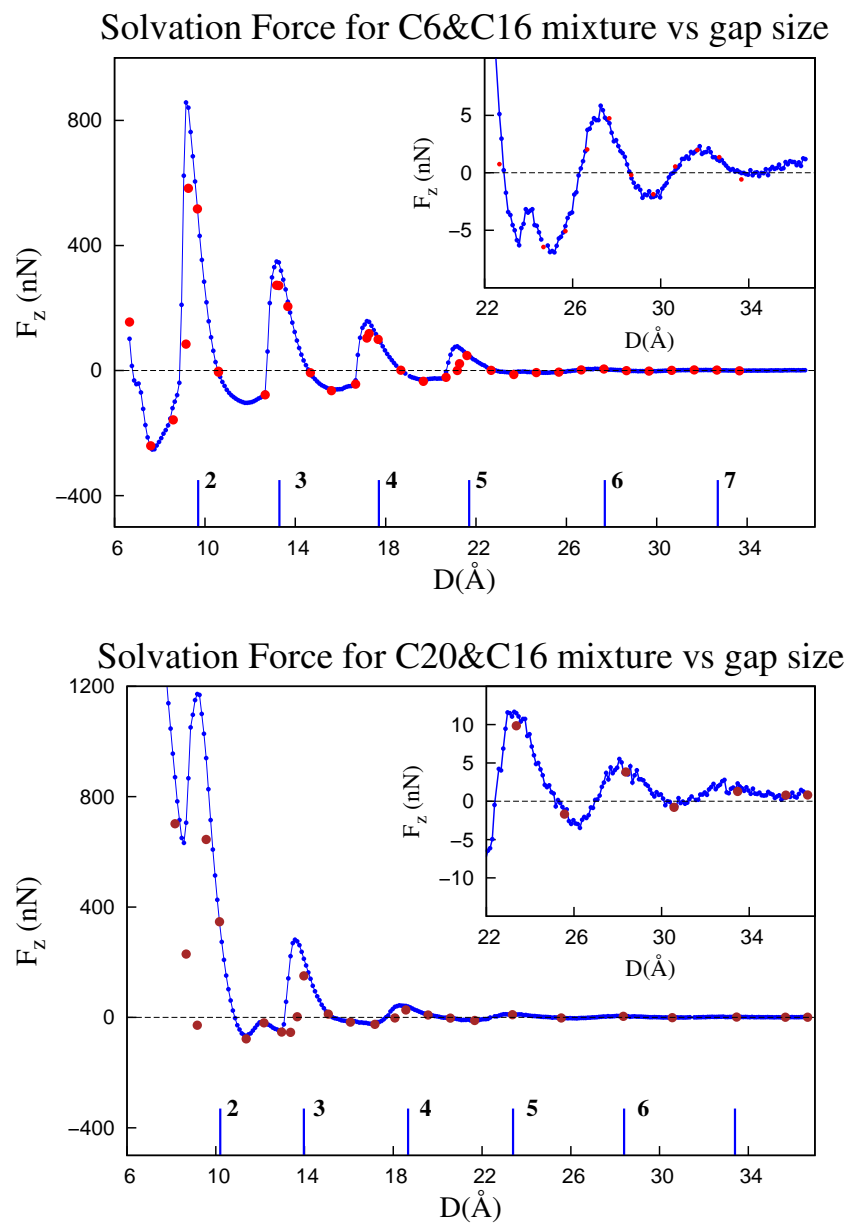


Figure 99: Solvation force versus gap size for mixtures C6&C16(top) and C20&C16 (bottom). The data taken during compression is blue, and after equilibration is red.

In Fig.99, we can see the solvation force for the mixture between short hexane and long hexadecane, and in Fig.reffig:Force-C20C16 the force for the branched-unbranched mixture. The blue values were taken during compression, while the red and brown values were taken after equilibration. For most of the compression these 2 sets of data correspond very well, but there are certain gaps at which they don't correspond very well. For hexane-hexadecane this discrepancy starts occurring when there are 5 layers inside the gap, while it starts at smaller gaps for the phytane-hexadecane system when there are 4 layers. The gap with the highest force and the gaps to the left of the peaks have varying degrees of correspondence with the values obtained during compression. The difference is higher, the thinner the gap is, but in the branched-unbranched system the discrepance is larger than in the short-long mixed system. As we discussed in the chapter on pure systems, the oscillations in the solvation force are an indication of solid-like properties for the system being compressed. When we compare the force versus gap size for both mixtures, we see that they both experience 6 peaks during the 30Å compression. The strength of the force peaks increases as the gap thickness decreases, but the rate is smaller in C6&C16 than in the C20&C16 mixture. As the fluid is compressed, the system becomes less liquid and is able to withstand pressure, hence the increase in force, but it reaches a state at which it yields to the pressure and expells some molecules. Then it is compacted once again and able to hold a pressure slightly higher than before, until it gives in and becomes liquid again. It oscillates between peaks and valleys.

In the solvation force for phytane-hexadecane, the valleys in between 4 and 3 layers, and again between 3 and 2 layers are different from the valleys of the hexane-hexadecane system. Upon close inspection of the branched density curves for the C6&16 at these gaps in Fig.71, we observed that at these gaps the branches of the phytane molecules are reorganizing themselves to accomodate for the decreased space by rotating from having their plane perpendicular to the surface to lying down with

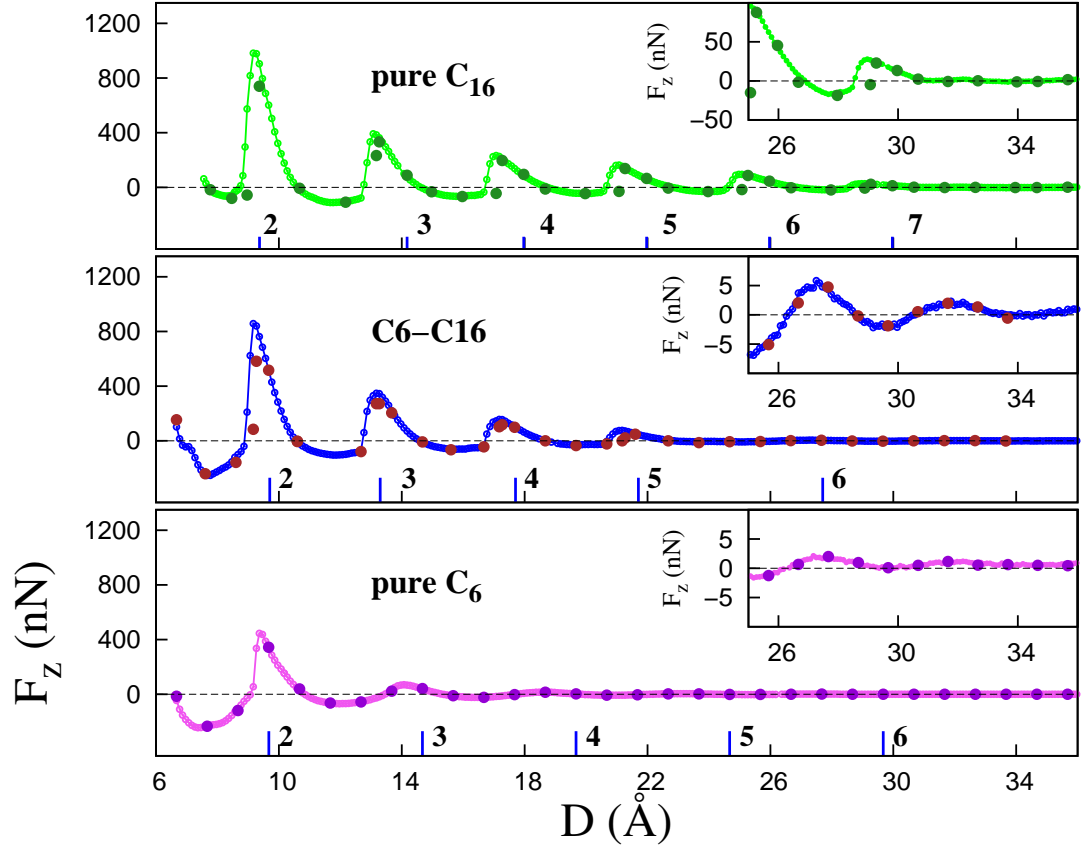


Figure 100: Comparison of solvation forces during compression for pure Hexadecane, hexane-hexadecane mixture and pure hexane versus gap size. A vertical zoom is shown in the inserts for the mixture and pure hexane.

their branches closer to the surface.

How each component of the mixture contributes to the solvation force can be understood by observing Figs.100 and ?? where we see the solvation curve for each component in their pure form compared to the solvation of the mixture. In the hexane-hexadecane system for gaps larger than 25\AA , the fluid behaves more like its liquid-like component hexane, and for smaller gaps, the oscillations resemble the behavior of its solid-like component hexadecane. Pure hexane shows very soft oscillations, while hexadecane shows strong periodic oscillations. In the case of a mixture of branched phytane and linear hexadecane, the solvation curve resembles highly the force curve for pure phytane. When we were doing the simulations, we were not aware of their

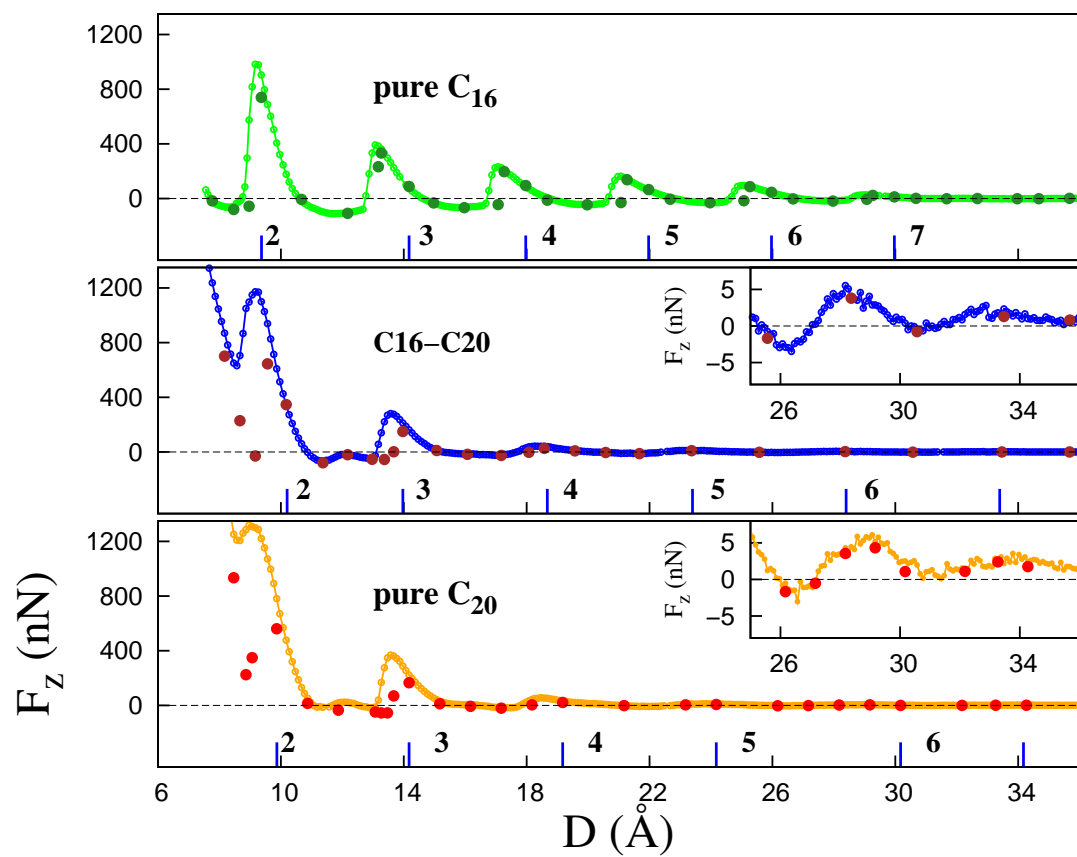


Figure 101: Comparison of solvation forces during compression for pure Hexadecane, phytane-hexadecane mixture and pure phytane versus gap size. A vertical zoom is shown in the inserts for the mixture and pure phytane.

great resemblance, so we equilibrated different gaps, but both curves taken during compression are very similar. There is some difference between the force for pure phytane and mixed phytane when there is only one layer in the confinement. In the case of the mixed system, it is somewhat able to reorganize its branches and form a thin single layer, and upon further equilibration the force does drop down as in the case of pure hexadecane. When the pure phytane system is compressed under 9\AA , the system is very sluggish and some molecules are not able to reorganize and lie down sideways. Remember that the diameter of a segment is approximately 4.5\AA , so for a system containing phytane to be compressed at a constant speed the molecules have to lie with its branches on the gold surface. After equilibration, the mixed system reorganizes itself and the force drops at 9\AA and then rises again for smaller gaps.

5.10 *Diffusion during compression*

The coefficient of diffusion for the hexane molecules decreases rather smoothly while the system is compressed. There is a small drop when the system goes from 4 to 3 layers. This step is enhanced when we plot the diffusion in logarithmic scale.

The long linear unbranched hexadecane chains show a very different behavior than the one exhibited by the short hexane molecules. When the system reaches a well-formed layer, the molecules belong to large domains and are virtually static. The coefficient of diffusion peaks when a layer of hexadecane is expelled, and the fluid becomes liquid like momentarily before being compacted and becoming rigid again. In the logarithmic scale, the difference in the coefficient of diffusion between a solid-like state and a liquid-like state is several orders of magnitude. Remembering that this diffusion is along a plane parallel to the gold surface, the inner molecules are tightly packed to their neighbors. In this calculation, we haven't included the displacement of the surface molecules. As we saw in the surface configuration plots, the molecules had no displacement for several nanoseconds that took to compress from 6 to 4 layers. Hexadecane show a high level of packing both with molecules in the same layer as the surrounding layers. Phytane had a similar behavior as hexane we had compared the number of each type of molecules through the compression process, Figs.36 and 36. They both have a small slope through out the compression, a slight steps from 3 to 2 layers, and a larger step went expelling a larger number of molecules to transition to a single layer. The coefficient of diffusion for phytane slowly decreases as the confinement is compressed.

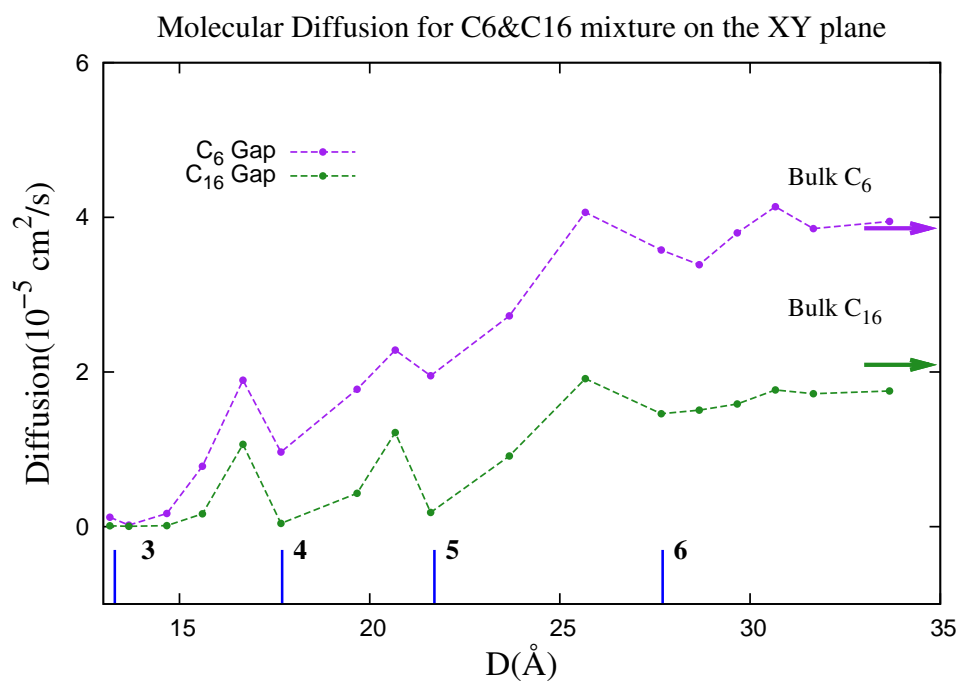


Figure 102: Diffusion coefficient for the mixture of C6&C16 versus gap size.

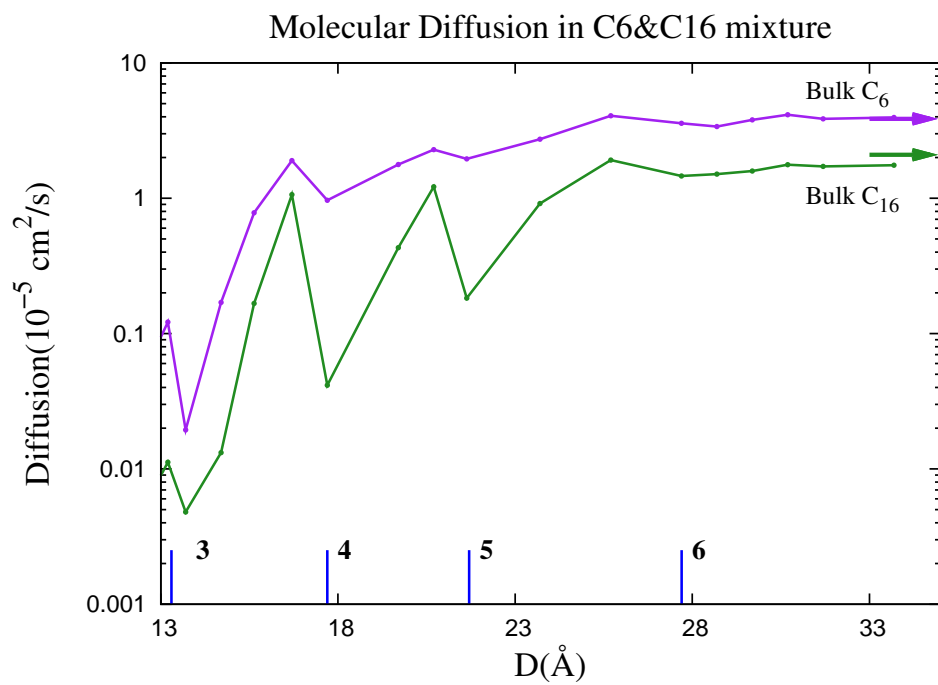


Figure 103: Diffusion coefficient for the mixture of C6&C16 versus gap size, in logarithmic scale.

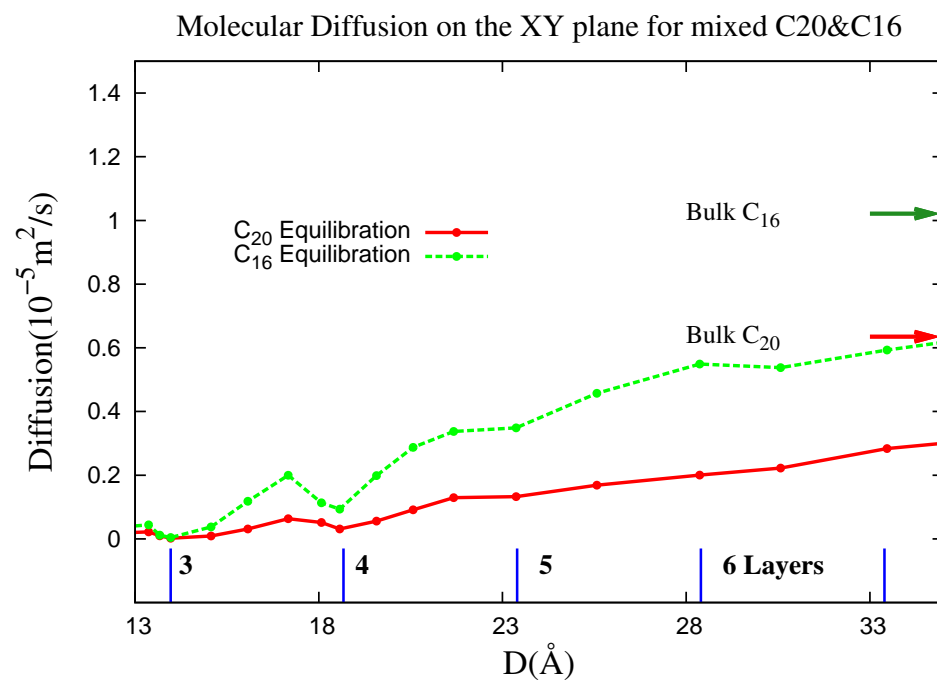


Figure 104: Diffusion coefficient for the mixture of C20&C16 versus gap size.

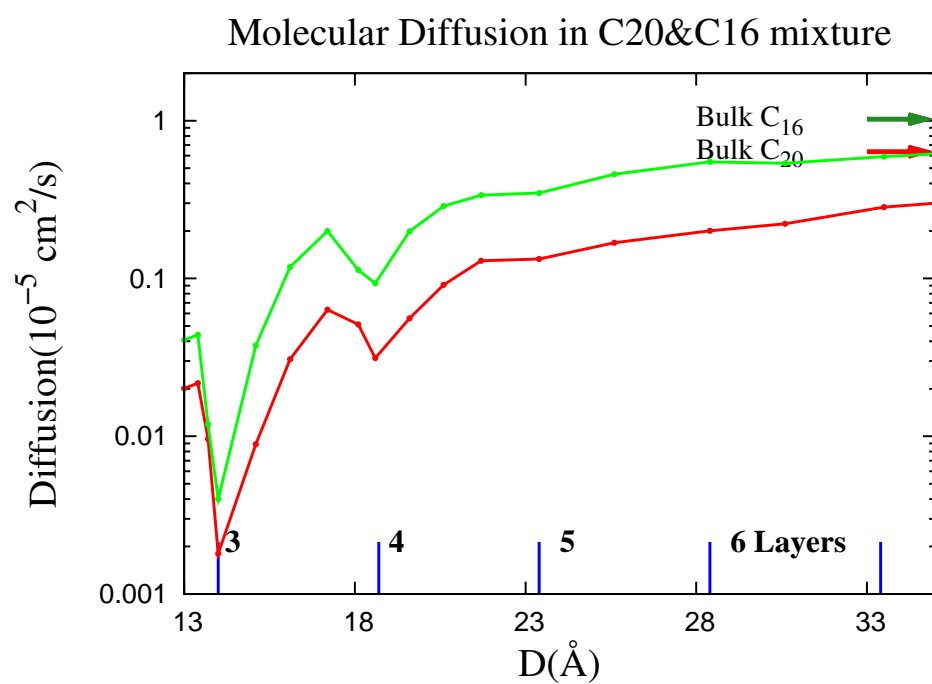


Figure 105: Diffusion coefficient for the mixture of C20&C16 versus gap size, in logarithmic scale.

5.11 *Comparison on the two mixed systems*

In Fig.106 and Fig.107, we will compare the evolution of each mixed system with each of its components. The top part row shows the solvation force, the middle row shows the number of confined segments, and the bottom row has the diffusion coefficient for the molecules not in contact with the surface. The columns are the mixture and its components.

In both plots, it is evident that the oscillations in the 3 properties are related. For solid-like systems, such as the hexane-hexadecane mixture and the pure hexadecane, during some compression intervals no molecules leave the confinement with the confined molecules being compacted into tightly packed layers, the force increases and the diffusion drops until the best layers are formed, represented by the vertical markers. After this, the system yields and expels a large group of molecules equivalent to a whole layer, the force drops and the diffusion peaks. In the liquid-like systems, such as pure hexane, pure phytane and the mixture phytane-hexadecane, the systems expell molecules continously during the compression process. They too undergo force oscillations but on a smaller magnitude, the number of confined segments decreases as the system is compressed, sometimes presenting slight steps, and the changes in the diffusion coefficient are not as dramatic as in the solid-like systems.

In the hexane-hexadecane case, as we mentioned earlier, for large gaps the system behaves liquid-like as its small component hexane, with similar oscillations in the force curve and a small slope in the number of confined segments and in the diffusion coefficient; but for smaller gaps, it resembles strongly the behavior of pure hexadecane as it is compressed. They both have sharp steps and plateaus in the number of confined segments, the period and shape of the force oscillatios are very similar, they have large drops in the coefficient of diffusion that corresponds to gaps with well formed layers, represented by the blue vertical lines; and when the system expells a layer, seen as a step in the number of confined segments and a drop in the solvation force, the

diffusion of the confined molecules peaks.

We have seen that the solvation force for the mixture phytane-hexadecane is very similar to the force for pure phytane, except at very small gap separations. In Fig.??, we can see side-by-side for the pure and mixed cases, the solvation force, the number of molecules and the diffusion coefficient versus gap separation are very similar. The decrease in the number of confined phytane molecules behaves the same in both cases, accounting for the difference in magnitude, and further more the shape for the diffusion coefficient is almost identical for pure and mixed phytane, except for an added drop at 4 layers, not seen in the pure case.

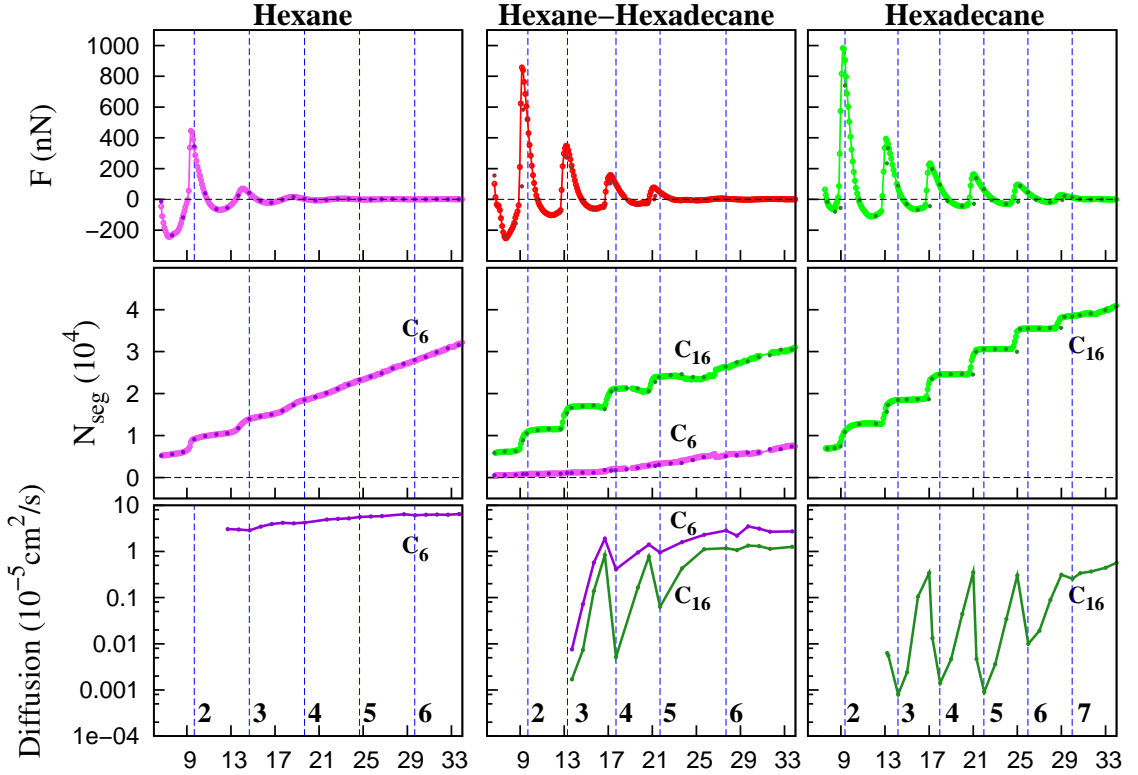


Figure 106: Comparison of solvation forces, number of confined segments and coefficient of diffusion for pure Hexadecane, hexane-hexadecane mixture and pure hexane versus gap size.

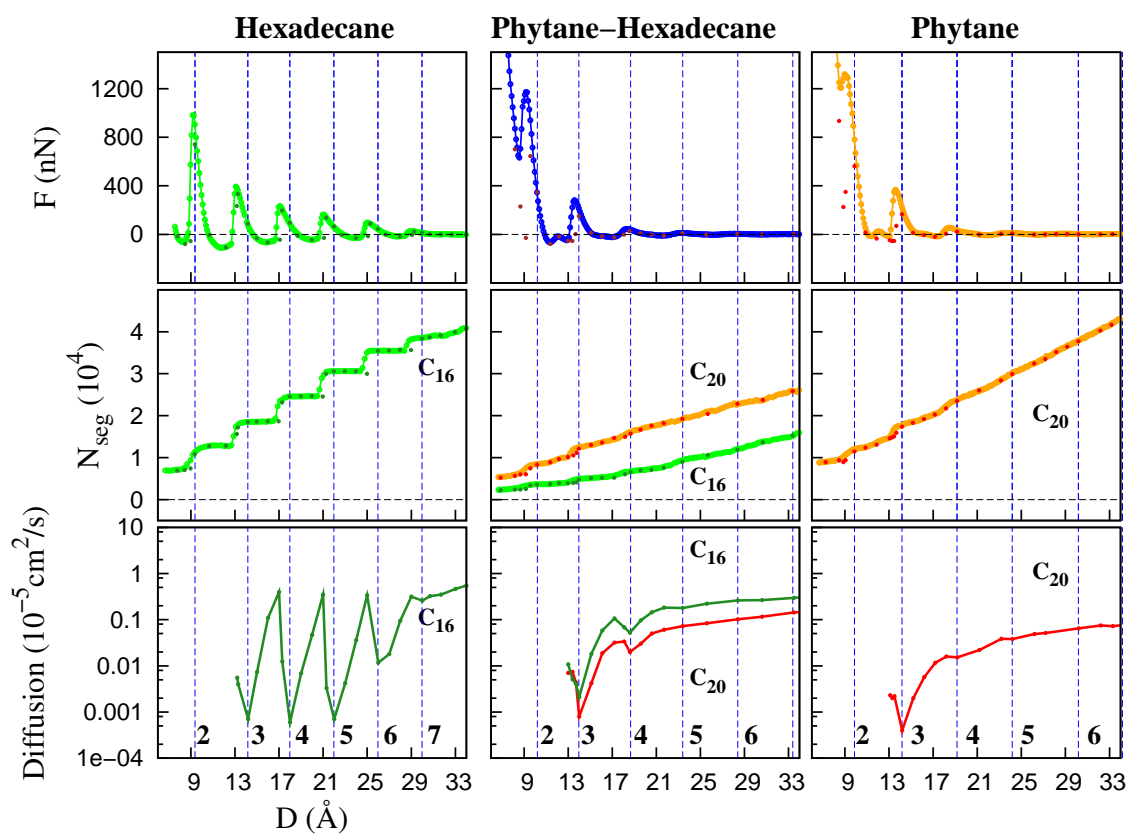


Figure 107: Comparison of solvation forces, number of confined molecules and coefficient of diffusion for pure Hexadecane, phytane-hexadecane mixture and pure phytane versus gap size.

CHAPTER VI

CONCLUSIONS

-Properties of highly confined mixtures show dependencies on: relative sizes of the molecular components, molecular architecture (e.g., linear vs branched alkanes), and molecular shape (e.g. spherical-like vs rod-like).

-Longer linear alkanes (e.g. hexadecane) segregate near the confining solid surfaces (forming well ordered layers, with intra-layer crystalline order), while the smaller alkane component of the mixture (e.g. hexane) behaves more fluid-like and is expelled upon reducing the gap, resulting in compositional separation.

-Confined branched alkane films (e.g. phytane) behave in a liquid-like manner down to relatively small gap widths (approximately 1.5 nm). An equimolar mixture with a linear alkane of similar molecular weight (e.g. hexadecane) maintains liquid like-properties (for both components). Preferential segregation is reduced in these mixtures compared to the case of long/short alkane mixtures.

-Technologically used lubricants are made of molecular mixtures. In light of a continuing trend toward machine miniaturization (that is, smaller gaps between moving parts), our findings with regard to the influence of the molecular characteristics of the mixture components on the molecular density distribution in the gap, the nature of the solvation forces, and the composition of the boundary layers, may assist in the choice of lubricants for nanotribological systems.

REFERENCES

- [1] BERENDSEN, H. J. C., POSTMA, J. P. M., VAN GUNSTEREN, W. F., DINOLA, A., and HAAK, J. R., "Molecular dynamics with coupling to an external bath," *The Journal of Chemical Physics*, vol. 81, pp. 3684–3690, Oct. 1984.
- [2] CHRISTENSON, H. K., GRUEN, D. W. R., HORN, R. G., and ISRAELACHVILI, J. N., "Structuring in liquid alkanes between solid surfaces: Forces measurements and mean-field theory," *The Journal of Chemical Physics*, vol. 87, pp. 1834–1841, Aug. 1987.
- [3] CHRISTENSON, H. K., HORN, R. G., and ISRAELACHVILI, J. N., "Measurement of forces due to structure in hydrocarbon liquids," *Journal of Colloid and Interface Science*, vol. 88, pp. 79–88, 1982.
- [4] CUI, S. T., CUMMINGS, P. T., and COCHRAN, H. D., "Effect of branches on the structure of narrowly confined alkane fluids: n-hexadecane and 2,6,11,15-tetramethylhexadecane," *The Journal of Chemical Physics*, vol. 114, pp. 6464–6471, Apr. 2001.
- [5] DEROUANE, E. G. *Chemical Physics Letters*, vol. 142, p. 200, 1987.
- [6] DEROUANE, E. G., ANDRE, J. M., and LUCAS, A. A. *Journal of Catalysis*, vol. 110, p. 58, 1988.
- [7] DERYCKE, I., VIGNERON, J. P., LAMBIN, P., LUCAS, A. A., and DEROUANE, E. G. *The Journal of Chemical Physics*, vol. 94, p. 4620, 1991.
- [8] FLORY, P. J., *Statistical Mechanics of Chain Molecules*. New York: Wiley-Interscience, 1969.
- [9] GAO, J., LUEDTKE, W. D., and LANDMAN, U., "Origins of solvation forces in confined films," *Journal of Physical Chemistry B*, vol. 101, pp. 4013–4023, May 1997.
- [10] GAO, J., LUEDTKE, W. D., and LANDMAN, U., "Structure and solvation forces in confined films: Linear and branched alkanes," *The Journal of Chemical Physics*, vol. 106, pp. 4309–4318, Mar. 1997.
- [11] HE, Y., YE, T., and BORGUET, E., "The role of hydrophobic chains in self-assembly at electrified interfaces: Observation of potential-induced transformations of two-dimensional crystals of hexadecane by in-situ scanning tunneling microscopy," *Journal of Physical Chemistry B*, vol. 106, pp. 11264–11271, Oct. 2002.

- [12] JORGENSEN, W. L., MADURA, J. D., and SWENSON, C. J. *Journal of the American Chemical Society*, vol. 106, p. 6638, 1984.
- [13] KATZ, E., YARIN, A. L., SALALHA, W., and ZUSSMAN, E., "Alignment and self-assembly of elongated micronsize rods in several flow fields," *Journal of Applied Physics*, vol. 100, pp. 1–12, Aug. 2006.
- [14] KIOUPIS, L. I. and MAGINN, E. J., "Rheology, dynamics, and structure of hydrocarbon blends: a molecular dynamics study of *n*-hexane/*n*-hexadecane mixtures," *Chemical Engineering Journal*, vol. 74, pp. 129–146, 1999.
- [15] KRISHNA, R. and VAN BATEN, J. M., "The darken relation for multicomponent diffusion in liquid mixtures of linear alkanes: an investigation using molecular dynamics (md) simulations," *Industrial and Engineering Chemistry Research*, vol. 44, pp. 6939–6947, 2005.
- [16] LI, T.-D., GAO, J., SZOSZKIEWICZ, R., LANDMAN, U., and RIEDO, E., "Structured and viscous water in subnanometer gaps," *Physical Review B*, vol. 75, p. 115415, Mar. 2007.
- [17] MARCHENKO, O. and COUSTY, J., "Molecule length-induced reentrant self-organization of alkanes in monolayers adsorbed on Au(111)," *Physical Review Letters*, vol. 84, pp. 5363–5366, June 2000.
- [18] MONDELLO, M. and GREY, G. S., "Molecular dynamics of linear and branched alkanes," *The Journal of Chemical Physics*, vol. 103, pp. 7156–7165, June 1995.
- [19] PAZZONA, F. G., BORAH, B. J., DEMONTIS, P., SUFFRITTI, G. B., and YASHONATH, S., "A comparative molecular dynamics study of diffusion of *n*-decane and 3-methyl pentane in γ zeolite," *Journal of Chemical Sciences*, vol. 121, pp. 921–927, Sept.
- [20] RYCKAERT, J. P. and BELLEMANS, A., "Molecular dynamics of liquid alkanes," *Faraday discussions*, vol. 66, pp. 95–106, 1978.
- [21] SIEPMANN, J. I., KARABORNI, S., and SMIT, B. *Nature*, vol. 365, p. 330, 1993.
- [22] SMIT, B., KARABORNI, S., and SIEPMAN, J. I. *The Journal of Chemical Physics*, vol. 102, p. 2126, 1995.
- [23] UOSAKI, K. and YAMADA, R., "Formation of two-dimensional crystals of alkanes on the Au(111) surface in neat liquid," *Journal of the American Chemistry Society*, vol. 121, pp. 4090–4091, Apr. 1999.
- [24] VESELY, F. J., "Lennard-jones sticks: A new model for linear molecules," *The Journal of Chemical Physics*, vol. 125, pp. 1–5, Dec. 2006.
- [25] XIA, T. K. and LANDMAN, U., "Molecular dynamics of adsorption and segregation from an alkane mixture," *Science*, vol. 261, pp. 1310–1312, Sept. 1993.

- [26] XIA, T. K. and LANDMAN, U., "Structure and dynamics of surface crystallization of liquid *n*-alkanes," *Physical Review B*, vol. 48, pp. 11313–11316, Oct. 1993.
- [27] XIA, T. K., OUYANG, J., RIBARSKY, M. W., and LANDMAN, U., "Interfacial alkane films," *Physical Review Letters*, vol. 69, pp. 1967–1970, Sept. 1992.
- [28] XIE, Z. X., XU, X., TANG, J., and MAO, B. W., "Reconstruction-dependent self-assembly of *n*-alkanes on Au(111) surfaces," *Journal of Physical Chemistry B*, vol. 104, pp. 11719–11722, Nov. 2000.
- [29] YAMADA, R. and UOSAKI, K., "Two dimensional crystals of alkanes formed on Au(111) surface in neat liquid: Structural investigation by scanning tunneling microscopy," *Journal of Physical Chemistry B*, vol. 104, pp. 6021–6027, June 2000.
- [30] YU, Y. X. and GAO, G. H., "Lennard-jones chain model for self-diffusion of *n*-alkanes," *International Journal of Thermophysics*, vol. 21, no. 1, pp. 57–70, 2000.
- [31] ZHANG, H.-M., XIE, Z.-X., MAO, B.-W., and XU, X., "Self-assembly of normal alkanes on the Au(111) surfaces," *Chemistry - A European Journal*, vol. 10, pp. 1415–1422, 2004.
- [32] ZHU, Y. and GRANICK, S., "Superlubricity: A paradox about confined fluids resolved," *Physical Review Letters*, vol. 93, pp. 096101(1–4), Aug. 2004.